The role of BK channel in cellular proliferation and differentiation in human osteoblast and osteoblast-like cells

By

Bo Li

A thesis presented to the Cardiff School of Pharmacy and Pharmaceutical Science of Cardiff University
For the degree of Doctor of Philosophy

July 2012

Summary

Both excitable and non-excitable cells possess plasma membrane ion channels and evidence has accumulated over the last 30 or so years that these channels perhaps play key roles in the cell life and death. This Thesis investigated the characteristics and putative functions of one class of potassium channel, the BK channel in osteoblast-like cells and primary osteoblasts from human, rat and mouse. The properties and functions were defined *in vitro* using a combination of patch-clamp, reverse transcription-polymerase chain reaction (RT-PCR) and functional assays for cell growth and mineralisation. RT-PCR showed the presence of KCNMA1, KCNMB1, KCNMB2, KCNMB3 and KCNMB4, the gene for BK channel α, β1, β2, β3 and β4 subunits respectively. The channel was voltage-dependent with a mean unitary conductance of 315 pS in cell-attached patches, a conductance of 124 pS in excised outside-out and 151 pS in inside-out patches. The channel was blocked by TEA (0.3 mM), TBuA (1 mM), TPeA (1-10 μM), THeA (1-3 μM), tetrandrine (5-30 μM) and paxilline (10 μM) and was activated by isopimaric acid (20 μM). Notably iberiotoxin (IbTX) (90 nM) only blocked a proportion of the channels tested (2/5). Osteoblast-like MG63 cell number changed in response to BK channel modulators. It increased significantly with TEA and tetrandrine at low concentrations (1 mM, 3 μM respectively), and reduced at high concentrations (>10 mM, >10 μM respectively). It was not affected by IbTX (20-300 nM) or slotoxin (300 nM). The increase in cell number by TEA was blocked by isopimaric acid. In addition, TPeA and THeA caused a decrease of osteoblast-like SaOS2 cell mineralisation at the concentrations (3 and 0.3 μM, respectively) increased MG63 cell numbers. The BK channel has a distinctive pharmacology and represents a new target for therapeutic strategies in modulating osteoblast proliferation.

Acknowledgements

First of all, I would like to show my deepest gratitude to my supervisor, Prof. K. T. Wann, without his supervision and encouragement I could never compelte the thesis. His kindness and vigorous academic observation enlightens me not only in this thesis but also in my future life.

I really appreciate Dr. Bronwen Evans for all her previous advices and support. I would also like to thank Ms. Carole Elford, Dr. Neil Henny, Dr. Pablo Reviriego and all the other members in Welsh school of Parmacy for their support and help during all these years.

Finally, I would show my love and gratitude to my parents and family for their supports and encouragement.

Abbreviations

$[Ca^{2+}]_i$	Intracellular calcium concentration
$[K^+]_i$	Intracellular potassium concentration
$[K^+]_o$	Extracellular potassium concentration
ALP	Alkaline phosphatase
α-MEM	α minimal essential medium
BK channel	Large conductance Ca-activated potassium channel
BMPs	Bone morphogenetic proteins
ChTX	charybdotoxin
DMEM	Dulbecco's modified eagle medium
DPBS	Dulbecco's phosphate buffered Saline
ED_{50}	Median effective dose
FBS	Fetal bovine serum
FGF	Fibroblast growth factor
Giga-seal	A seal between the pipette tip and the cell membrane in the patch-clamp technique that creates an electrical resistance between the pipette solution and the bathing solution of more than 1 giga-Ohm
HOB	Human primary osteoblast
IbTX	iberiotoxin
IK channel	Intermediate conductance Ca-activated potassium channel
K_{ATP} channel	ATP dependent potassium channel
K_{Ca} channel	Ca-activated potassium channel
K_{ir} channel	Inwardly rectifying potassium channel
K_v channel	Voltage-gated potassium channel
MTS	3-(4, 5-dimethylthiazol-2-yl)-5-(3-carboxymethoxyphenyl)-2-(4-sulfophenyl)-2H-tetrazolium
OD	Optical Density, absorbance
PCR	Polymerase chain reaction
PDGF	Platelet-derived growth factor
PKA	Protein kinase A
PKC	Protein kinase C
PKG	cGMP-dependent protein kinase
Po	Ion channel opening probability
PTH	Parathyroid hormone
QAs	Quaternary ammonium acids
SK channel	Small conductance Ca-activated potassium channel
Slo	BK channel α subunit
STOC	Spontaneous transient outward current
TBuA	tetrabutylammonium acid
TEA	tertraethylammonium acid
THeA	tetrahetylammonium scid
TPeA	tetrapentylammonium acid
VDCC	Voltage-dependent Ca channel
V_m	Membrane voltage

TABLE OF CONTENTS

LIST OF FIGURES

4. Expression and activity of BK channels in MG63 and HOB cells

5. BK channels in osteoblasts show neuronal-type features

6. BK channels have roles in osteoblast cell function

SECTION 1: INTRODUCTION

1.1 Overview

Non excitable cells express ion channels which play key roles in the growth and differentiation of these cells. For example in osteoblasts, bone forming cells, both single cell patch-clamp and RT-PCR show that a number of ion channels are present. These include large conductance Ca^{2+}-activated K^{+} channels (BK) which are amongst the most prevalent channels observed in cell lines (e.g. MG63 cell). The precise subunit composition of the native BK channel and its role remain however unknown. BK channels normally exist as a tetramer of 4 α subunits associated with β subunits. The subunit composition, specifically the type of β subunit co-assembled with the α subunits, modifies both the voltage- and Ca^{2+}-sensitivity and the pharmacological characteristics (e.g. sensitivity to iberiotoxin) of BK channels (Orio et al., 2002). This channel is the focus of this Thesis and the work presented here attempts to delineate a preliminary pharmacology of the channel, to investigate its role in proliferation and differentiation and try to specify the subunit composition of BK channels in both a human cell line (MG63) and primary human osteoblasts HOB cells.

1.2 Ion channels

There is a voltage gradient across the plasma membrane of all living cells. It is also called the cell membrane potential which is caused by the different permeabilities to charged ions on either side of the membrane. Ion channels, ion pumps and ion transporters in the membrane are the functional proteins that exist to generate the relevant permeabilities or to maintain these different ionic concentrations inside and outside of the cell (Shieh et al., 2000). Ion channels are different from ion pumps and ion transporters. Ion pumps and ion transporters move ions against their concentration gradient. Ion channels allow ions to flow following their electrochemical gradient (Hille, 2001). To enable them to carry out their functions, ion channels are built of an assembly of several proteins including the pore forming subunits and regulatory subunits (Hille, 2001). The pore forming subunits have a selectivity filter to select and conduct the specific type of ion. The gating mechanism are able to open and close the channel in response to given cues, such as voltage, ATP and intracellular calcium (Doyle et al., 1998; Zhou et al., 2001; Jiang et al., 2003). Ion channels can be classified by the selected ions, the gating system and the pore number. The ion channels in question are potassium channels, sodium channels, calcium channels, chloride channels, proton channels and general (non-specific) ion channels. According to the gating system, ion channels are classified as voltage-gated, ligand-gated and “other” gated channels. There are also other classifications and naming based on other characteristics such as potassium channels and two-pore channels. Large numbers of ion channels

have various functions and the disruption of the normal function of ion channels could lead in principle to a range of diseases (Ashcroft, 1999). Ion channels have been appealing as an already frequent target for new drugs, and new ion channels continue to generate extra tremendous excitement as therapeutic targets. The study of ion channels involves a range of powerful scientific techniques such as electrophysiology (particularly patch clamp), molecular biology (e.g. RT-PCR) and immunolocalisation (e.g. Western-blot).

1.2.1 Potassium channels

There is a large super family of ion channels that are potassium channels, widely expressed in many tissues and organisms. Potassium channels are classified into subfamilies in different ways as shown on table 1.1. (Chandy et al.,1991; Gutman and Chandy, 1993; Goldstein et al., 1996 and 2001; Lesage et al.,1996; Orias et al., 1997; Lesage et al., 2000; Dworetzky et al., 1994; Kohler et al., 1996 and Papazian et al., 1987).

Table1.1 subfamilies of K channel

	Families
Structure	Six transmembrane, one pore channel (6 TM, 1P), Two transmembrane, one pore channel (2 TM, 1P), Four transmembrane, two pore channel (4 TM, 1P)
Gating system	Calcium-activated K channel, Voltage-gated K channel

The large numbers of different types of potassium channels map out their wide expression and various functions. Briefly, potassium channels (e.g. voltage-

gated potassium channel) have a role in setting the resting membrane potential and regulate action potential of excitable cells (e.g. neurons) and processes such as cellular proliferation in non-excitable cells (e.g. glioma) (Wonderlin et al., 1996; Huang and Rane, 1994). Therefore the location, structure and regulatory mechanisms of these channels remain worthy of investigation.

1.2.2 Potassium channel structure

Potassium channels have been investigated for decades and their structures are well known and have been used to name the channel subfamilies. As described above there are 3 different structural subfamilies according to the structure of the channel subunit (Fig. 1.1). The principal subunits co-assemble in the following ways. The 6 TM groups which include the K_V channel have both the N- and C-termini located intracellularly and the region (the P-loop) between the fifth and sixth transmembrane domains (S5 and S6) forms the ion conduction pathway. The functional channel of the first class is formed by the tetrameric association of these 6 TM and 1 pore subunits (Chandy et al., 1991; Gutman and Chandy, 1993). BK channel structure is described below (Fig. 1.4). The second class includes inward rectifiers, K_{ATP} channels and G protein-coupled channels (Doupnik et al., 1995). These channels also have two TM domains with intracellular N- and C-termini. The P loop between the 2 TM domains forms the pore, and the functional channel is a tetramer of subunits with 2 TM and the pore.

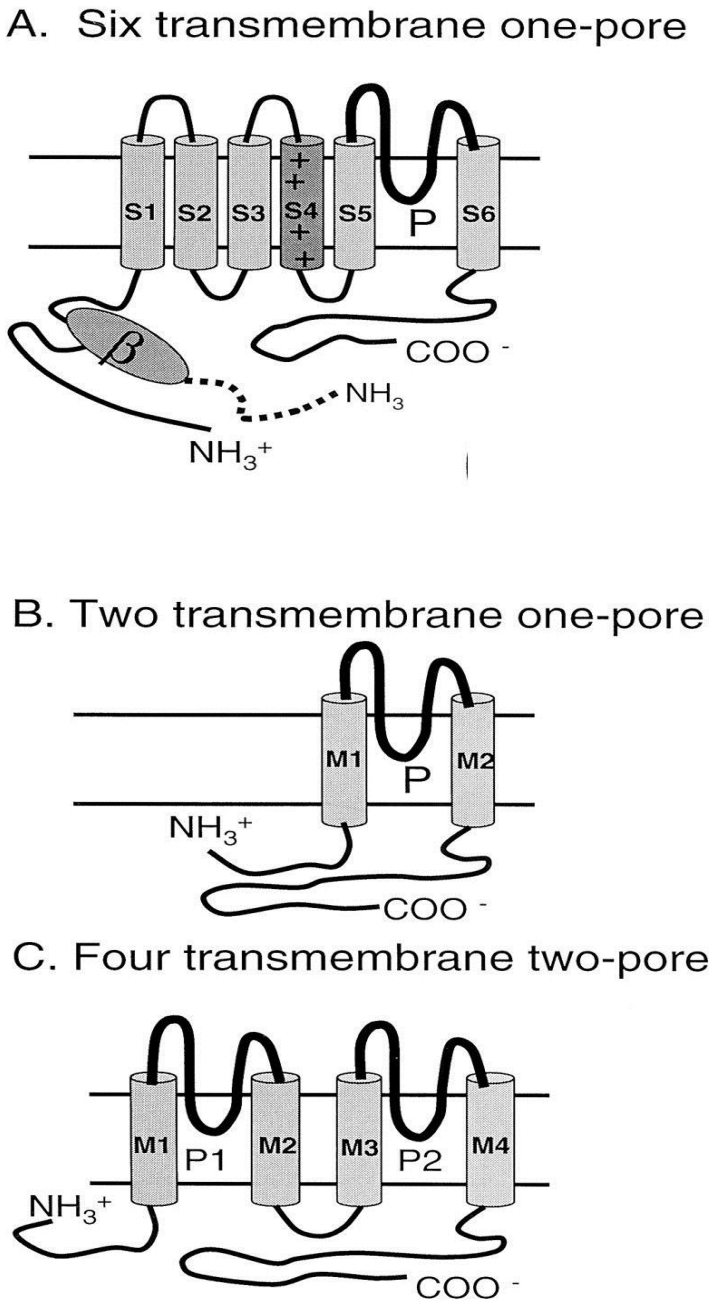

Fig 1.1 Three typical structures of potassium channel subunit. (A) 6 transmembrane and 1 pore subfamily. P-loop between S5 and S6 forms the ion pore and S4 acts as voltage-sensor. (B) 2 transmembrane and 1 pore subfamily. Ion pore is also formed by the loop between the 2 transmembrane domains. It has no voltage sensor so it is not a voltage-gated channel. (C) Four transmembrane and 2 pore subfamily. 2 loops (P1&P2) between the transmembrane domains form 2 ion pores in each monomer (these graphs were taken from Shieh et al., 2000).

The third class, the K_{2P} family, contains two subunits each with 2 TM domains and 1 pore region. These two subunits are linked in tandem, and the functional channel is a dimer of the subunits with 4 TM and the pore subunits. Another class of channel has a 6 TM and 1 pore segment linked in tandem to a 2 TM and 1 pore segment, and in this case the functional channel is formed from the dimeric association of the subunits with 8 TM and the pore. We can summarize these channels in a phylogenetic tree (Fig. 1.2) (Gutman et al., 2003). This gives some idea of the vast number of potassium channels possible.

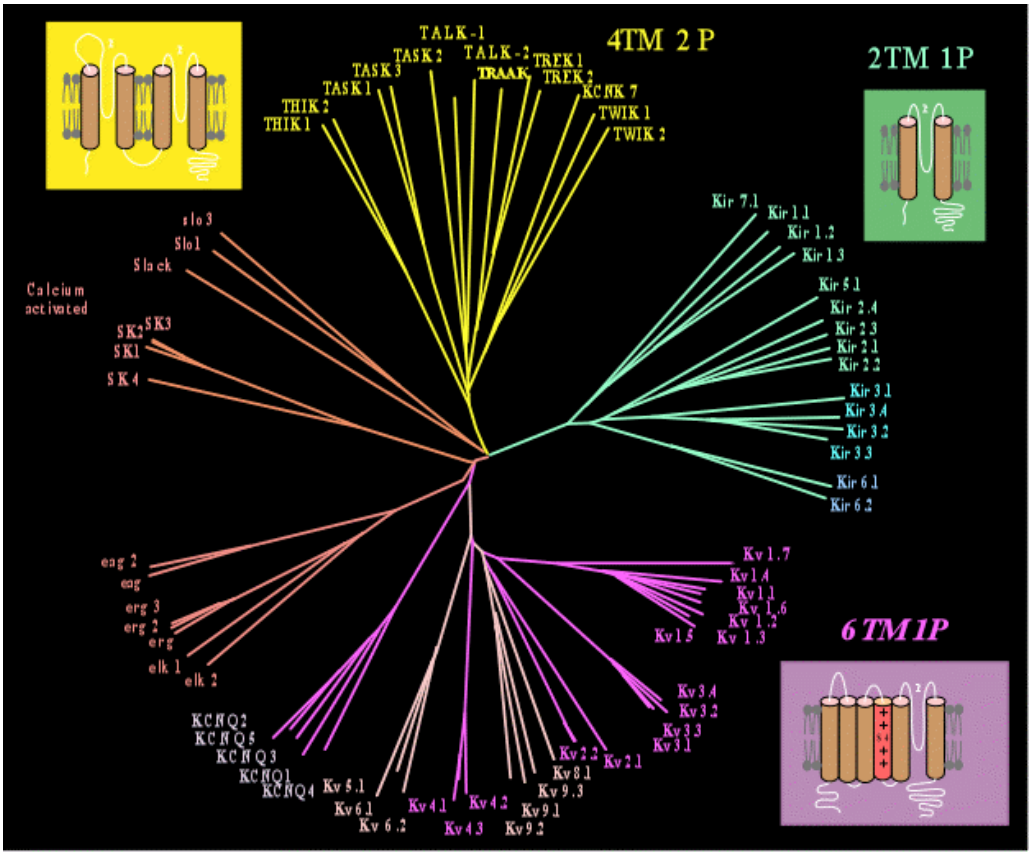

Fig 1.2 The unique family of potassium channels. The green lines indicate the 2 TM and 1 P subfamily including inwardly rectifying K channels (Kir), the purple lines indicate the 6 TM and 1 P subfamily including voltage-gated K channels (Kv), KQT-like channels (KCNQ) and Ca-activated channel (K_{Ca}) and the yellow lines indicate the 4 TM and 2 P subfamily (the graph was taken from http://www.ipmc.cnrs.fr/~duprat/ipmc/nomenclature.htm, created by Fabric Duprat, accessed date 15th June 2012).

1.2.3 Potassium channels: localization and functions

Ideas on potassium permeability and potassium channels were first published with reference to the resting membrane potential and action potential of nerve axons (Hodgkin and Huxley, 1945; Hodgkin and Huxley, 1952 and Hodgkin and Katz 1949). Now they are known in virtually all types of cells (both excitable and non-excitable cells) in all organisms. They play critical roles in many different biological tasks, but all potassium channels carry out a basic function that is the transmembrane translocation of K^+ ions. The opening of a potassium channel leads to K^+ movement from the intracellular to extracellular environments. It automatically results then in a negative change in the voltage across the cell membrane. Membrane repolarisation or hyperpolarisation occurs in different tissues for different reasons. Obviously, in excitable cells, such as nerve, muscle, hormone-secreting adrenal chromaffin and pancreatic β cells potassium channel activation is involved solely in membrane potential regulation. Equally potassium channel-related hyperpolarization of T and B cells is a pre-requisite for mitogenesis and proliferation in the immune response (DeCoursey et al., 1984; Chandy et al., 1984; Matteson et al., 1984 and Fukushima et al., 1984). But potassium channels are also expressed in other non-excitable cells. We already know that potassium channels play roles in the cellular recycling of K^+ ions required for the electrolyte balance affected by the renal epithelium (Giebisch, 1998; Palmer et al., 1994; Muto et al., 1999 and Wang et al., 1993). Potassium channels may also be crucial for tumour development and the growth of cancer cells (Skryma et al., 1994). Is this

related to a role in membrane potential control? Even in bacteria, potassium channels are found and have a presumed role in volume regulation and the maintenance of cell shape (Booth et al., 2003). For over almost three decades, potassium channel functions in lymphocytes and in cell proliferation were highlighted discoveries in the field of potassium channels in non-excitable cells and there have been a steady expansion of publications (Chandy et al., 2004). Fig1.3 indicates the rapid and steady expansion of publication in these two fields from 1970s till November 2003 (Chandy et al., 2004).

Over these years, cell proliferation studies show clearly that inhibition of K^+ channel expression or usage of specific potassium channel blockers may reduce cancer cell proliferation (Rybalchenko et al., 2001; Abdul et al., 2003 and Asher et al., 2011). Further investigation reveals that there is not only one type of potassium channel present in different cancer cells from prostate, colon, lung, breast and other tissues. A variety of K^+ channels are found in these tissues including Ca^{2+} -activated K^+ channels (including the intermediate-conductance and large-conductance Ca^{2+}-activated K^+ channels), Shaker-type voltage-gated K^+ channels, voltage-gated K^+ channels and 2P-domain K^+ channels.

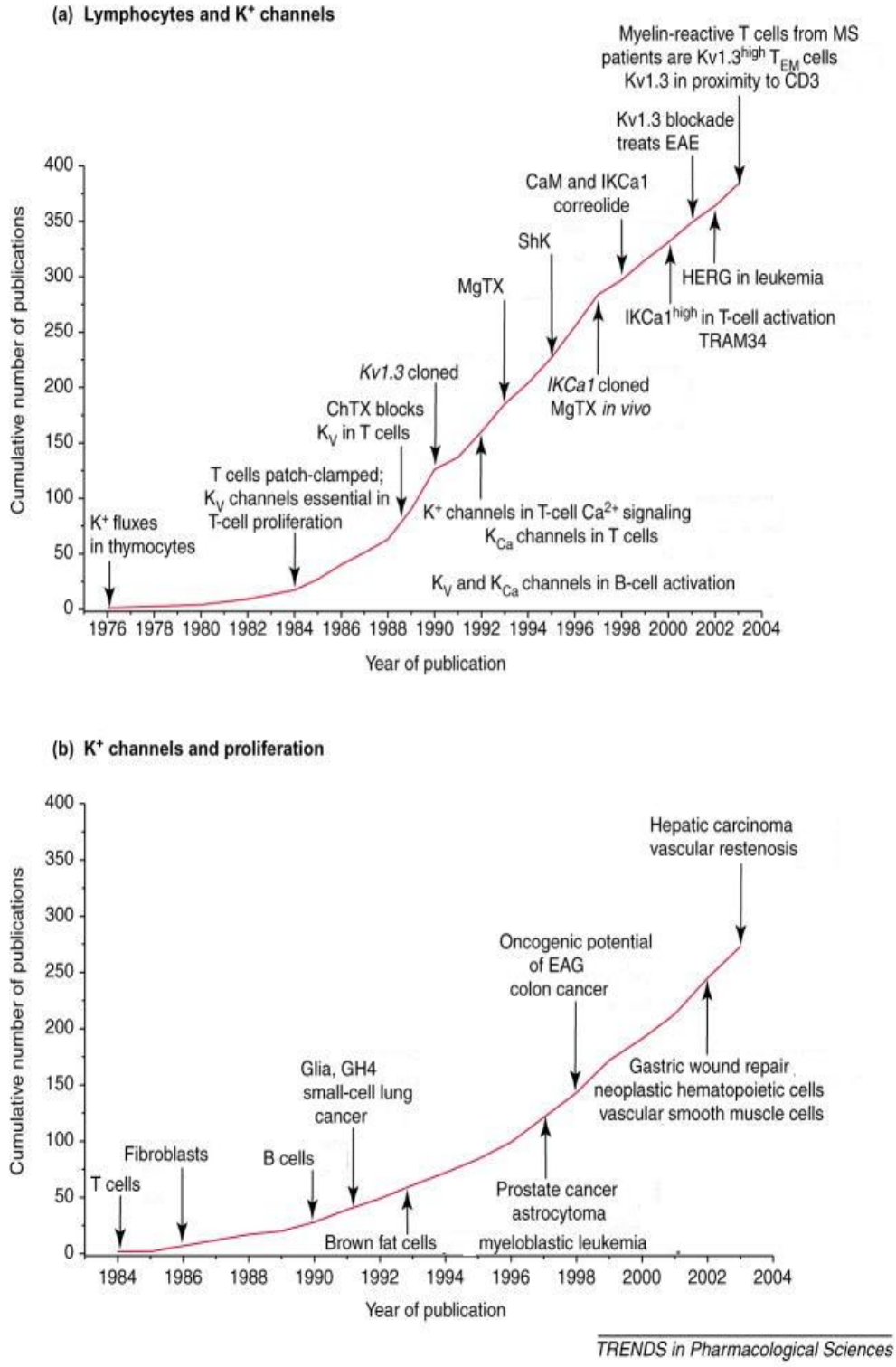

Fig 1.3 The numbers of publications within 20 years (1984-2004) on two subjects: (a) potassium channels and Lymphocytes, (b) potassium channel and proliferation (these graphs were taken from the article *K^+ channels as targets for specific immunomodulation* Chandy et al., 2004).

Voltage-gated potassium (Kv) channel functions in excitable tissues such as nerve and muscle cells of heart are clear. In the excitable cells, the membrane potential can depolarize to a level to activate Kv channels. In contrast, the mechanism underlying potassium channel regulation of cell proliferation is an unknown question. The cell membrane potential of non-excitable cells is presumably stable under most conditions. When cells divide the membrane is depolarised. Studies have revealed significantly that the cancer cell membrane potential is typically more depolarized compared to the membrane potential of terminally differentiated normal cells (O'Grady and Lee, 2005). For example, when carcinoma cells are bathed in serum-containing media, a depolarized membrane voltage is detected. The depolarized membrane voltage of carcinoma cells may result in activation of Kv channels. In contrast, no depolarized membrane voltage is detected when carcinoma cells are bathed in serum-free Ringer's solution (Kunzelmann, 2005). Since electrophysiological studies are continuously carried out on cells that are bathed in a serum-free solution, little is known about the membrane voltage of normal cells and cancer cells *in vivo*. Kv channels may not be active in serum-free culture solution. They are active *in vivo* due to the particular composition of phospholipid metabolites and other intracellular factors such as oxygen deprivation and the local acidosis. In general, roles of K_V channels in cancer cell growth could be related to a number of possible factors, but consideration of the membrane potential as the driving influence would appear to be a sound place to start.

Not only K_V channels but also Ca^{2+}-activated K^+ channels have been discovered in many cancer cells such as those of the prostate (Abdul and Hoosein 2002 and Parihar et al., 2003), the uterus (Suzuki et al., 2004), glioma (Basrai et al., 2002), the stomach (Elso et al., 2004), the pancreas (Jager et al., 2004), the pituitary gland (Czarnecki et al., 2003), the breast (Ouadid-Ahidouch et al., 2004) and the colorectum (Lastraioli et al., 2004). The investigations intriguingly demonstrate the expression of a K channel that modulates cell cycle. The enhanced density of intermediate-conductance Ca^{2+}-activated K^+ channel (IK) is detected in breast cancer (MCF-7) cells synchronized at the end of the G_1 and S phase when compared with early G_1 phase. High IK1 activity induces a more negative membrane potential of the cells at the end of G_1 phase (Ouadid-Ahidouch et al., 2004). This negative membrane potential may paradoxically induce Ca^{2+} inflexion hence support the high basal intracellular Ca^{2+} concentration in late G1 (Ouadid-Ahidouch et al., 2004). In addition, the large-conductance (BK) K^+ channels were detected expressing predominantly in the S phase of breast cancer cells. This leads to the evaluation of the impact of BK channel activation on proliferation currently (Bloch et al., 2007). In a recent study the expression of BK channels was found enhanced in prostate cancer cells. It was ascribed to be the genomic amplification of the KCNMA1 locus which encodes the principal α-subunit of the BK channel (Bloch et al., 2007). BK channel showed “a high activity in fast growing malignant prostate cancer cells, but little contribution to the conductance in cultured epithelial cells from benign prostate hyperplasia” in Bloch’s experiments (Bloch et al., 2007). In conclusion, convincing evidence

showed that Ca^{2+}-activated K^+ channels are involved in the proliferation of cancer cells, probably during late G1 and S phase. But it is unclear whether this applies only to cancer cells or to all other proliferating cells. Thus, studies on normal cells and tumour cells are necessary.

The Ca^{2+}-activated K^+ channels control proliferation of endothelial cell as well. The proliferative properties of Ca^{2+}-activated K^+ channels have been closely linked to their influence on both spatial and temporal aspects of intracellular Ca^{2+} levels in vascular smooth muscle and endothelial cells (Neylon, 2002). BK channels have been found playing key roles in endothelial cell proliferation and formation of atherosclerotic plaques (Kuhlmann et al., 2003). And endothelin-1 also induced human endothelial cell proliferation by activating BK channels (Kuhlmann et al., 2005).

1.2.4 Calcium-activated potassium channels

As indicated above, calcium-activated potassium channels (K_{Ca}) have key roles in cell proliferation which is an unusual but an important function of these ion channels. The following discussion deals with the principal properties of these channels reviewing their distinguishing features.

The K_{Ca} channel family can be divided into three groups based on their respective physiology, pharmacology and biophysical characteristics: The large conductance (100-300 pS) K_{Ca} group includes the $K_{Ca}1.1$ channel (Marty,

1981), the intermediate conductance (25-100 pS) consists of the $K_{Ca}3.1$ channel (Gardos, 1958; Ishii et al., 1997; Logsdon et al., 1997), and the small conductance (2-25 pS) group (Blatz and Magleby, 1986; Park, 1994) comprises the $K_{Ca}2.1$, $K_{Ca}2.2$ and $K_{Ca}2.3$ channels.

All K_{Ca} channels are activated in response to an increase in intracellular Ca^{2+} and $K_{Ca}1.1$ channel is the only one that can also be activated by membrane depolarization. The $K_{Ca}1.1$ channel also has a unique topology structure. Being different to the other K_{Ca} channels, it has 7 transmembrane domains with an extracellular N-terminus (Wallner et al., 1996), while all the other K_{Ca} channels are similar to the voltage-gated K^+ channels (six transmembrane domains with intracellular N- and C-termini). The functional channel of all the K_{Ca} family members is composed of four pore-forming subunits with an occasional auxiliary (β) subunit.

K_{Ca} channels are expressed in almost all cells where they integrate cellular metabolism with cellular electrical activity, contributing to various physiological functions. In general the key physiological functions of K_{Ca} channels include: $K_{Ca}1.1$ channel modulates smooth muscle tone and neurotransmitter release (Hewawasam et al., 2000 and Tanaka et al., 1998) K_{Ca} 2.1 channel modulates neuronal excitability (Ikeda et al., 1991) and K_{Ca} 3.1 modulates lymphocyte activation and epithelial cell secretion (Khanna et al., 1999; Amigorena et al., 1990 and Edwards, 1998).

1.2.4.1 SK and IK channels

$K_{Ca}2.1$ channel, the small conductance Ca^{2+}-activated K^+ channel (SK) subfamily contains three highly homologous members: $K_{Ca}2.1$, $K_{Ca}2.2$ and $K_{Ca}2.3$ (Kohler et al., 1996). As mentioned above, SK channels have a similar topology structure to the Kv channels but display only two positively charged amino acids at the S4 segment while Kv channels typically display seven. This difference may certainly contribute to the voltage insensitivity of the K_{Ca} channels. Therefore, SK channels are activated by increasing cytosolic Ca^{2+} rather than voltage (Stocker, 2004). In contrast, the SK channels are highly sensitive to intracellular Ca^{2+} (300-700 nM). This type of Ca^{2+}-dependent activation is achieved by the constitutive binding of the SK channels to calmodulin, a highly expressed Ca^{2+}-binding protein, via a calmodulin-binding domain situated at the cytoplasmic C-termini (Xia et al., 1998).

Several studies have detected that the SK channels are the only known targets of the bee venom toxin, Apamin. $K_{Ca}2.1$ is the least sensitive (IC_{50}=3.3~13 nM), $K_{Ca}2.2$ is the most sensitive (IC_{50}= 63 pM) and $K_{Ca}2.3$ shows intermediate sensitivity (IC_{50}= 2 nM) (Kohler et al., 1996). SK channels are highly distributed in the central nervous system (Stocker and Pedarzani, 2000). They are involved in the membrane potential regulation. Following an action potential, the membrane is hyperpolarized which is termed an afterhyperpolarization (AHP). Three types of AHP are distinguished, the fast (fAHP), the medium (mAHP) and the slow (sAHP). Investigations found SK

channels trigger the mAHP which means the SK channels are involved in the control of firing rate (the number of APs generated over a unit of time) and of the firing pattern (the way the APs are distributed over an interval of time) (Pedarzani et al., 2000 and Wolfart et al., 2001). In different neuronal populations, K_{Ca} channel operation may have different physiological consequences. For example, in midbrain dopaminergic neurons SK channel function impacts on dopamine secretion (Wolfart et al., 2001). SK channels are heavily expressed in the basal ganglia (in particular in the substantia nigra, pars compacta) and in the limbic system, suggesting that they may modulate motricity and emotional behaviour. SK channels may be a key target in the therapy of several pathological disorders which depend on function of these neurons, such as Parkinson's disease and schizophrenia (Liegeois et al., 2003).

The $K_{Ca}3.1$ (IK) channel is the member of the Ca^{2+}-dependent K^+ family with an intermediate conductance. It was the first Ca^{2+}-dependent K^+ channel to be detected in human erythrocytes and was known as the Gardos channel but it is still the least studied one (Gardos, 1958). The channel has the same basic topology of the K_{Ca} subfamily and also binds to calmodulin. This channel has a high sensitivity to intracellular Ca^{2+} (200-300 nM) (Hoffman et al., 2003). The IK channels are expressed mainly in the periphery, in cells of hematopoietic origin, colon and salivary glands. IK channels show different pharmacological properties to SK channels. Thus they are insensitive to apamin, but sensitive to the peptide toxins Charybdotoxin (that also blocks BK channels) and Maurotoxin (that also blocks Kv1.2). Since IK channels were first identified in

human erythrocytes channel function was investigated in the haematology arena first. In normal resting T-lymphocytes IK channels are expressed at a relatively low level. The voltage-dependent K^+ channel Kv1.3 is the main channel responsible for maintaining the cell membrane potential. However in activated T-lymphocytes the numbers of IK channels are markedly increased (Ghanshani et al., 2000). The IK channel activities are involved in T cell proliferation and differentiation into effector T cells. During cell growth there is a sustained Ca^{2+} entry that lasts for a few hours. The resulting high Ca^{2+} level would inhibit additional Ca^{2+} entry, but the opening of the IK channels causing efflux of K^+ would provide a hyperpolarization effect that helps the Ca^{2+} entry through steepening of the electrochemical gradient (Cahalan et al., 1997). Specific blockers of the IK channel prevent T-lymphocyte proliferation which is consistent with this presumed role for the IK channel (Chandy et al., 2001). Furthermore, recent studies revealed that in vivo blockage of the IK channel can be useful in pathological situations that involve excessive T-lymphocyte-mediated activation. This could be of clinical utility in T-lymphocyte-mediated autoimmune diseases such as multiple sclerosis and T-lymphocyte-mediated inflammation amongst others.

1.2.4.2 BK channel

$K_{Ca}1.1$ (BK) channel is the most intensively studied channel of the K_{Ca} subfamily. This type of channel can be easily detected for channel opening generates large unitary K^+ currents. The BK channel has a conductance of

100~300 pS (Toro et al., 2005), while other vertebrate K^+ channels have conductances ranging from 2 to 100 pS (Hille, 1992). Investigations reveal that there are two possible reasons for the large conductance: 1. The BK channel crystal structure shows two rings of negative charged glutamate on the inner pore-helix at the inner mouth of the channel (Nimigean et al., 2003 and Brelidze et al., 2003). 2. The BK channel has a larger internal vestibule and an internal mouth than other K channels. These are the conclusions reached from the following studies. Li and Aldrich (2004) showed that large quaternary ammonium compounds bind to the BK channel from the inside much quicker than to the Shaker channel (Li and Aldrich, 2004). Once these compounds were bound, the BK channel can close behind them trapping them, whilst the Shaker channel cannot (Li and Aldrich, 2004). In addition, Brelidze and Magleby (2005) found that the increased concentration of sucrose on the internal side of the BK channel reduced the channel conductance. BK channel's inner mouth is estimated based on the amount of sucrose needed to make the diffusion of K^+ from the bulk solution to the inner mouth of the channel rate limiting. The results showed that BK channel's internal mouth is twice as large (20 Å in diameter) as that of the Shaker channel (Webster et al., 2004; Brelidze and Magleby, 2005) and similar in size to the large-conductance (~200 pS) prokaryotic MthK channel (Jiang et al., 2002). Their large conductance leads to the fact that BK channels were among the first channels to be studied in detail at the single channel level with the patch-clamp technique.

BK channel is expressed in almost all cell types and it has extraordinary physiological functions. The BK channel was first described in Drosophila as the slowpoke channel and later identified in mouse and humans (Pallanck and Ganetzky, 1994). Surprisingly, although BK channels in different tissues have very different properties there is only one gene that has been identified corresponding to this type of channel. In addition, the $K_{Ca}1.1$ channel gene is extremely conserved among different species in mammals (Toro et al., 1998). Further studies revealed that there are regulatory subunits and alternative splicing in BK channel structure contributing to its diversity. The BK channel topology includes 4 α subunits and 4 auxiliary β subunits as shown in Fig 1.4. Four β subunits have been identified that consist of two transmembrane domains, an extracellular loop and cytoplasmic N- and C-termini, and have different expression patterns. As Fig 1.5 indicates, the β1 subunit (KCNMB1) was identified in smooth muscle and has high affinity for Charybdotoxin (CTX), a peptide blocker of BK and IK channels (Knaus, et al., 1995 and Orio, et al., 2002). The β2 subunit (KCNMB2) was detected in chromaffin cells and brain, the β3 subunit was identified in testis, pancreas and spleen. The β3 subunit associated BK channel shows rapid inactivation. The β4 subunit is expressed in the brain. In contrast to the β1 subunit this subunit decreases the BK channel sensitivity to peptide toxins but the channel is sensitive to the alkaloid, tetrandrine (Meera et al., 2000; Reinhart et al., 1991 and Wang and Lemos 1992). In general, the four regulatory subunits increase the sensitivity of the pore-forming α subunit to intracellular Ca^{2+} and voltage and can also change its pharmacological properties. In addition, they may act as binding

target for drugs. As mentioned above, alternative splicing of the α subunit, accounting for physiological differences, has also been identified in various tissues such as adrenal chromaffin cells, brain and human gliomas (Saito, et al., 1997; Tseng-Crank, et al., 1994 and Liu, et al., 2002). At least six sites for alternative splicing have been identified in the mouse BK transcript. Properties of the different splice variants are reflected in the Ca^{2+} sensitivity or slowed channel gating. In addition, BK channels are targets of cellular signaling pathways including protein phosphorylation, dephosphorylation, and are regulated by G-proteins and nitric oxide (Schubert and Nelson, 2001 and Scornik, et al., 1993). Protein phosphorylation has thus far received most attention and has been widely studied. Channel phosphorylation by protein kinase A (PKA) and protein kinase C (PKC) seems to stimulate channel activity in smooth muscle by altering the responsiveness of the channel to Ca^{2+} (Schubert and Nelson, 2001). Moreover, several proteins have been identified that can associate with the BK channel such as Syntaxin 1A, β2 adrenergic receptors and β-catenin (Ling et al., 2003; Liu et al., 2004 and Lesage, et al., 2004). Interestingly, the effects of these proteins on the BK channels include regulation of channel distribution in cells and / or current modulation.

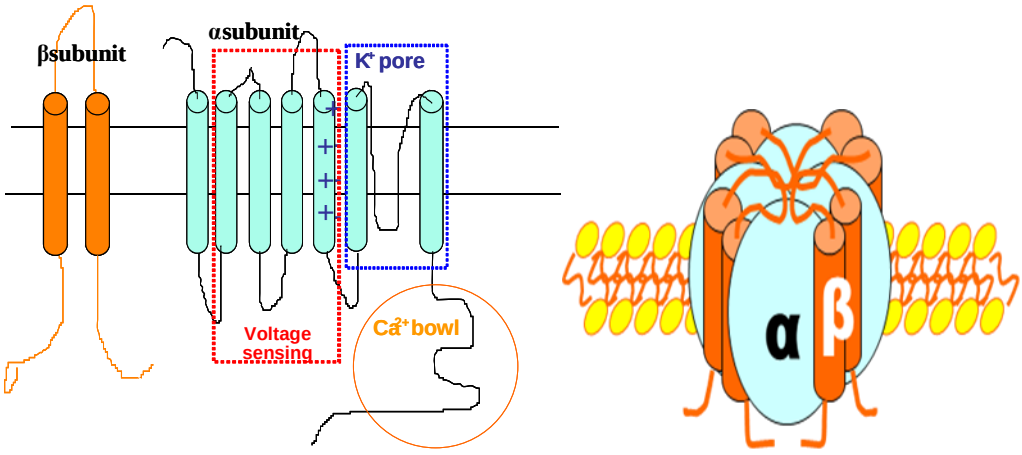

Fig 1.4 BK channel structure consists of the pore-forming α subunit and associated β subunit. The α subunit has 7 transmembrane domains (S0-S6) and thus is different from the other two types of Ca^{2+}-activated K channels. S1-4 are the voltage sensors and there are charged amino-acid in S4. As in the case of other Ca^{2+}-activated K channels, the loop between S5 and S6 forms the ion pore. The extracellular N-terminus binds the β subunit. β subunit has 2 transmembrane domains connected by a long loop. The N-terminus varies on different β subunits. 4 α subunits and 4 β subunits form the channel as shown on the right.

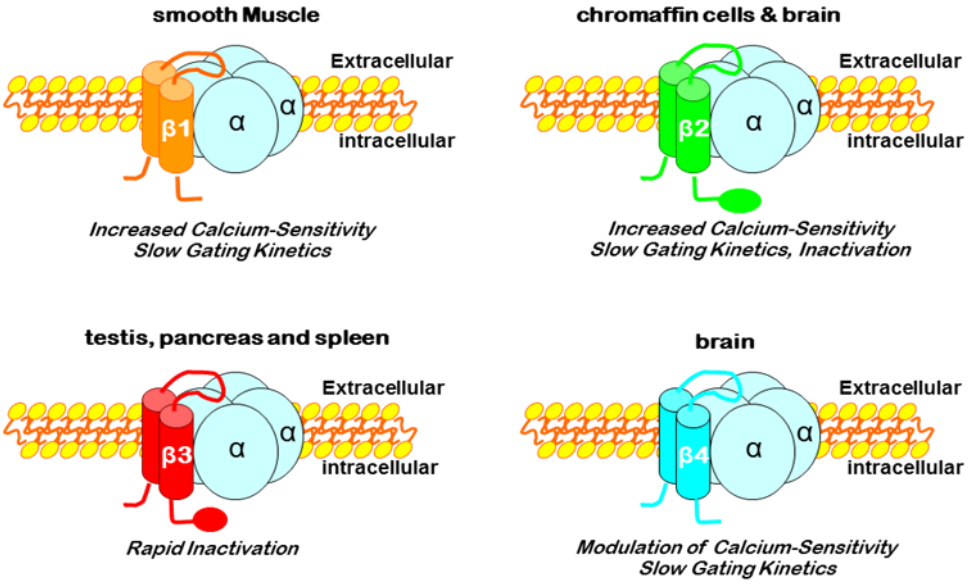

Fig 1.5 Four different β subunits were identified in different tissues. The properties of the BK channels associated with different β subunit vary as a consequence.

Given the complex modulation of BK channels, the output of the channel could influence several physiological functions in various tissues. Briefly, BK channels may be involved in all cellular properties relating to voltage or Ca^{2+} such as modulation of smooth muscular tone and Ca^{2+}-dependent neurotransmitter release (Hewawasam et al., 2000 and Tanaka et al., 1998). BK channels have been identified in a variety of smooth muscles including vascular, urinary bladder, uterine and others. In all smooth muscles, the channel appears to be β1 subunit coupled. Smooth muscle cells contract as a result of an increase in the intracellular Ca^{2+} concentration which activates the Ca^{2+}-calmodulin-dependent protein kinase. This kinase triggers a biochemical cascade resulting in muscular contraction. From the beginning, the intracellular Ca^{2+} increase is caused by the opening of voltage-dependent Ca^{2+} channels (VDCCs) in the plasma membrane or the opening of ryanodine-receptors in the sarcoplasmic reticulum. Membrane depolarization drives both of these events. Both a rise in intracellular Ca^{2+} and the membrane depolarization will activate the BK channel that respond with an efflux of K^{+} and an attendant hyperpolarization of the cell membrane potential. In return, this will close the membrane VDCCs. In this way, the activities of BK channels work as a negative feedback on contraction and induce muscle relaxation. Experiments have shown that the specific BK channel blocker, iberiotoxin induced membrane depolarization and vasoconstriction (Jaggar, et al., 1998). On the other hand, BK channel openers would relax vascular smooth muscle by inducing membrane hyperpolarization and closure of Ca^{2+} channels. According to other investigations (Wellman and Nelson, 2003 and Robertson, et al.,

1993), several endogenous vasodilators such as nitric oxide, atrial natriuretic factor, β adrenergic agonists relax vascular muscle directly or indirectly (via activation of PKA and/or PKG), by activating the BK channel. Studies with β subunit knockout mice demonstrated that the loss of β subunit produce hypertension and cardiac hypertrophy (Brenner, et al., 2000 and Pluger, et al., 2000). This may be because the Ca^{2+} sensitivity of the BK channel decreases when it loses the β subunit and can no longer respond normally to an intracellular Ca^{2+} increase. Moreover, Fernández-Fernández, J.M. and his team found a gain-of-function β variant which has a protective effect against human diastolic hypertension (Fernández-Fernández, et al., 2004). Interestingly this β variant can further increase the Ca^{2+} and voltage-sensitivity of the pore forming α subunit.

Another tissue where BK channels are widely expressed is the central nervous system. They are expressed non-uniformly in different parts of brain in various nerve cell types. In similar fashion to their function in smooth muscle, BK channels act as a feedback inhibitory mechanism in the brain. They initiate membrane repolarization and prevent further Ca^{2+} entry through VDCC in neurons so regulating neurotransmitter release. As a result, importantly BK channels inhibit excessive depolarization and Ca^{2+} entry in pathological situations such as ischaemia or epilepsy (Calderone, 2002).

Consequences of loss of function of BK channels in the body can be explored by investigating the characteristics of BK channel knockout ($BK^{-/-}$) mice. BK-α

subunit knockout mice apparently had a normal inner hair cell in the cochlea phenotype they progressively developed outer hair cell in the cochlea dysfunction and degeneration starting from 8 weeks (Ruttiger et al., 2004). These mice also showed cerebella ataxia with deficient motor co-ordination. They exhibited a range of motor dysfunctions including intention tremor, abnormal gait, shorter strides, irregular stepping, and decrease speed of swimming with more frequent floating. Furthermore, there was significantly reduction of the spontaneous firing of the Purkinje neurons in these animals (Sausbier et al., 2004). On the other hand, BK-β1 knockout mice have normal body and kidney weights and normal hearing function and cochlear structure. In these mice the bowel structure and colon function were observed different. They had loose fecal matter and a weaker structural integrity of colon than the normal animal. These changes may relate to the stronger colonic smooth muscle contractions, reduced reservoir, and water recovery functions of the colon. And all these could be due to the reduced Ca^{2+} sensitivity of BK channels lacking the β1-subunit, which could also resulted in K^+ excretion decreasing and increase in arterial tone and blood pressure in the knockout mice (Pluznick et al., 2003, 2005, Hagen et al., 2003, Brenner et al., 2000a, 2000b).

1.2.4.3 Pharmacological aspects

BK channel modulators are an efficient way to dissect this channel's function and a number were used in this Thesis. BK openers or BK activators are the

agents that cause BK channel activation. BK openers increase efflux of K^+ ions leading to hyperpolarization. Thus they decrease cell excitability in excitable cells or cause smooth muscle relaxation. Furthermore, these agents are potential therapeutic tools in diseases such as hypertension, coronary artery spasm, urinary incontinence, and neurological disorders. The BK openers include a large series of synthetic benzimidazolone derivatives, such as NS004 and NS1619, the biaryl amines, such as mefenamic and flufenamic acids, the biarylureas, such as NS1609, the pyridyl amines and the pimaric acids, such as isopimaric acid. It should be noted that some ligands also activate BK channels nonselectively, for example: fenamates, including niflumic, flufenamic, and mefenamic acids (Ottolia &Toro, 1994). They decrease the duration of channel long closed states leading to the enhanced channel activation in a variety of cells through a pathway which may be independent of their cyclooxygenase–prostaglandin mechanisms (Stumpff, et al., 2001).

Another series of compounds that regulate the BK channel are oestrogen receptor modulators. BK channel activation by 17-β estradiol contributes to its non-genomic effect (acute vasorelaxation) on the vasculature (Valverde et al., 1999). Similarly, BK channel can be activated by tamoxifen at therapeutic concentration which blocks volume-sensitive chloride, voltage-activated calcium, non-selective cation channels, and voltage-gated potassium channels (Dick et al., 2001). This is the possible mechanisms of the side effects of tamoxifen, such as QT prolongation and arrhythmias, where its deleterious actions on the above mentioned ion channels are unquestionably important

adverse side-effects of this ligand (Dick et al., 2001; He et al., 2003). Other studies in other tissues have reported an alteration in BK channel activity in response to various endogenous and exogenous compounds. For example, "2 - methoxyestradiol, an endogenous metabolite of 17ß-estradiol, inhibits the channel activity by decreasing the number of open and activated channels" (Chiang & Wu, 2001). The decrease of the amplitude of the outward potassium current in vascular endothelial cells was due to the inhibition of BK channel activity (Wu, 2003).

Many neurotransmitters, metabolites of arachidonic acid, and downstream effectors (e.g. cAMP and cGMP) regulate BK channel activity through signalling pathways that involve G-proteins and/or a balance between phosphorylation–dephosphorylation. For example, nitric oxide (NO) and NO donors relax various blood vessels by a direct increase in activation of BK channels (Bolotina et al., 1994; Mistry and Garland, 1998) or via cGMP-dependent protein kinase (PKG) (Carrier et al. 1997 and Robertson et al., 1993). PKG acts on BK channel activation directly by phosphorylating a serine residue (Ser1072) in the α-subunit of the channel (Fukao et al., 1999).

BK channel blockers have long been used as experimental tools to examine both structural characteristics (subunit composition) of the BK channels and their varied roles in various physiological conditions. These reagents include peptide toxins such as iberiotoxin (IbTX) and slotoxin, quaternary ammonium compounds such as tetraethyl ammonium (TEA) and tetrabutyl ammonium

(TBuA) and alkaloids such as tertrandrine and paxilline (Li & Aldrich, 2004). IbTX is one of the peptide toxins which selectively blocks BK channels. It binds to a site in the extracellular vestibule of the pore, thus occluding the external pore (Giangiacomo et al., 1992; Brayden & Nelson 1992). Investigations revealed that four residues of the extracellular loop of β1-subunit (L90, Y91, T93, and E94) located close to the external vestibule were important in generating the high affinity peptide toxin binding site in BK channels (Hanner et al., 1998). In this way, crucially the sensitivity of the channels to these peptide toxins depends on the type of the associated β subunits associated. Although quaternary ammonium compounds are not selective for BK channels, they decrease the channel activity by two ways: lodging in their inner pore and hastening the deactivation process of the channels during repolarization (Li & Aldrich, 2004). Paxilline, an indole alkaloid, is another selective blocker for BK channel. It decreases BK channel activity in rat aortic smooth muscle cells, in a manner similar to that of IbTX (Knaus et al., 1994; Tammaro et al., 2004). Tetrandrine, a quinoline alkaloid, also decreases the activity of BK channels in cultured endothelial cells. And the intracellular Ca^{2+} levels have no impact on tertrandrine's activity (Wu et al., 2000). In summary the regulators of BK channels are listed in Table1.2 below. And the following graphs indicate the structures of BK openers and blockers including a large series of synthetic benzimidazolone derivatives, such as NS004 and NS1619, the biarylureas, such as NS1608, the biaryl amines, such as mefenamic and flufenamic acids and the pyridyl amines, natural modulators like dihydrosoyasaponin-1 (dehydrosoyasaponin-1; DHS-1)

peptide toxins, such as Iberiotoxin and Slotoxin, tertrandrine and paxilline (Ghatta et al., 2006).

Blockers	Peptide toxins: iberiotoxin, charybdotoxin and slotoxin Non-peptide blockers: paxilline, penitrem and tetrandrine Non-specific: tetraethylammonium, tetrabutylammonium, clotrimazole and ruthenium red
Openers	NS004, NS1619, NS8 and NS1608 Flufenamic acid, mefenamic acid, niflumic acid Estradiol, dihydrosoyasaponin-I (DHS-I), maxikdiol and pimaric acid
Secondary messengers	cAMP, cGMP and calcium
Endogenous metabolites	Nitric oxide, arachidonic acid metabolites and 2-methoxy estradiol
others	pH, voltage, osidation reduction, glycosylation and phosphorylation

Table1.2 BK channel modulators include naturally-occurring blockers, synthetic inhibitors and blockers, marketed and/or investigational drugs, naturally-occurring openers and synthetic openers.

Structure of BK channel openers

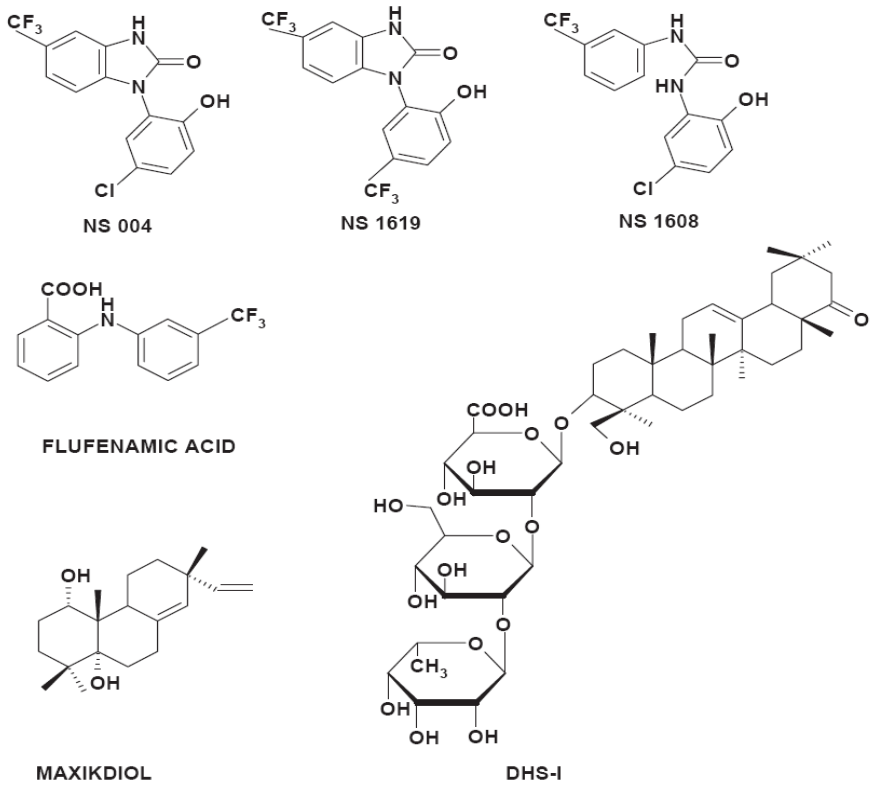

(From S. Ghatta et al. / Pharmacology & Therapeutics 110 (2006) 103–116)

Structure of BK channel blockers

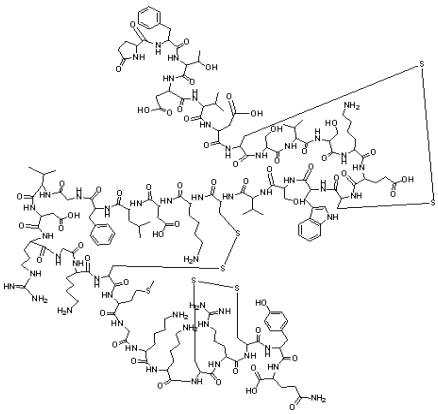

IBERIOTOXIN

(from *www.sigmaaldrich.com*)

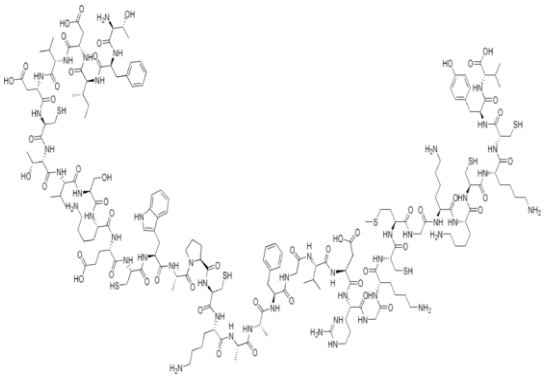

SLOTOXIN

(from Wikipedia)

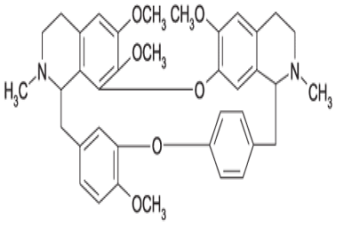

TETRANDRINE

(from Wikipedia)

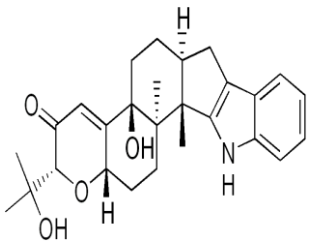

PAXILLINE

(from Wikipedia)

1.2.4.4 BK channel – therapeutic indications

BK channels are known to be expressed in almost all tissues in the body and over many years investigations have revealed that BK channels are involved in various (patho) physiological conditions. Such a ubiquitous distribution might raise questions about the possible selectivity of any drug design strategy based on a BK channel target. As indicated previously, in the cardiovascular system, BK channels are key players in controlling the vascular contraction. In vascular smooth muscle BK channels open in response to $[Ca^{2+}]i$ increase resulting

from either increased flux of Ca^{2+} into the cell through Ca^{2+} channels or by release of Ca^{2+} from internal stores (Jaggar et al., 2000) and elicit potassium efflux. The potassium efflux is also called spontaneous transient outward current (STOC) which leads to vascular smooth muscle relaxation by driving the membrane potential more negative. Hence the voltage-gated Ca^{2+} channels are closed so that no Ca^{2+} is supplied to initiate cell membrane depolarization and muscle contraction. In summary, BK channel activators may provide useful treatment of vascular dysfunction accompanied with various disorders. In the urinary system, under physiological conditions BK channels opening leads to hyperpolarization, which in turn regulates membrane potential and relaxes urinary bladder smooth muscle. Thus β-adrenergic activation of BK channels in urinary bladder smooth muscle may be useful for the treatment of the unstable bladder. In the nervous system, BK channel dysfunction is considered to be related to the neurological disorders. BK channels have been identified in the dendrites, axons, and synaptic terminals and are important players in controlling the excitability of neurones and influence neuronal signaling and neurotransmitter release. BMS-204352 is a specific brain penetrant BK channel opener which has shown beneficial effect in neuronal ischemia (Cheney et al., 2001; Gribkoff et al., 2001).

1.3 Bone

Bone is a dynamic tissue. In additional to providing structural support and protecting internal organs, it is a major storage depot for calcium, phosphorus

and other minerals. Bone growth begins as early as in embryogenesis. It keeps growing in length and width until skeletal maturity. It is then formed and renewed continuously throughout life, a process known as bone remodelling. Rates of remodelling in trabecular bone may be 5 to 10 times higher than in cortical bone throughout life. The entire skeleton is replaced in a healthy adult in a cycle of about 10 years. Bone remodelling occurs on the bone surface and a bone remodelling unit consists of a group of all linked cells of activation, resorption and formation (Parfitt et al., 2001). The cells eroding the bone to create small cavities are osteoclasts. The cells fill in the cavities with new bone are called bone-forming osteoblasts (Crockett et al., 2011). Bone remodelling is a natural way of restoring bones and keeping them healthy and deficiencies in this process result in conditions such as osteoporosis. Osteoporosis can affect people of any age and three million people in the UK have or are at risk of this disease. It places a growth burden on the NHS and hip fracture alone cost health and social services over 1.7 billion pounds a year. Fractures of wrist and spine are also common and can lead to pain, dependence and death in some case. So that it is important to make any improvement in the prevention, diagnosing and treatment of osteoporosis.

1.3.1 Bone formation and composition

The knowledge of bone morphology and structures at different levels provides the basis to understand the function of bone and the possible mechanism(s) of underlying diseases. First of all, at a microscopic level bone has two forms

according to the pattern of collagen forming the osteoid that are known as woven bone and lamellar bone. The features of these are listed in Table 1.3. Woven bone is an immature bone type and is found in the embryo and the newborn, in a fracture callus, and in the metaphyseal region of growing bone. Lamellar bone is therefore considered as mature bone. It appears 1 month after birth and by 1 year of age, it is actively replacing woven bone, as the latter is resorbed. There is still woven bone in adult animals as the vascular channels are located mainly in the woven bone in cortical bone. Woven bone and lamellar bone are observed in either trabecular or cortical bone, which are named according to their porosity and apparent density. As shown in Fig 1.6, trabecular bone looks spongy and cancellous so it has an extraordinarily high surface area for cellular activity. It is found principally at the metaphysis and epiphysis of long bones and in cuboid bones such as the vertebrae. Compact bone is found as the "envelope" bone which is dense and compact.

Table 1.3 comparison of woven and lamellar bone

Woven bone	**Lamellar bone**
coarse-fibered, no uniform of collagen fibre	many collagen fibers parallel to other fibres
high proportion of osteocytes and cells are randomly arranged	low proportion of osteocytes in concentric sheets
found in embryo, fracture callus, tumors, osteogenesis imperfect and pagetic bone	most normal bone is lamellar bone in mature animal

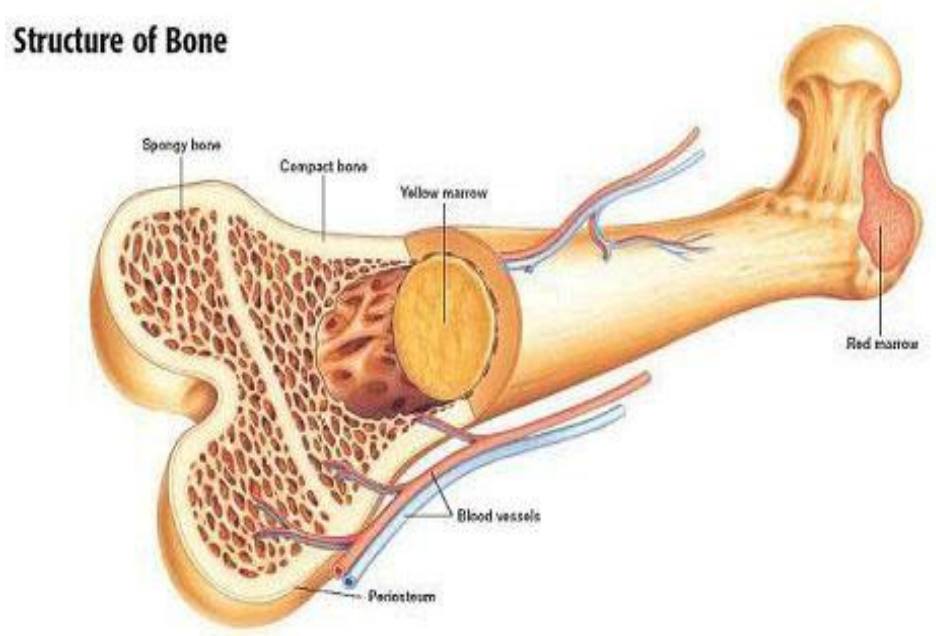

Fig 1.6 Compact bone is dense and on the surface of bone, while trabecular bone is spongy and fills the inner cavities of bone (the picture was taken from Mrs. Andersen's Science Pages, The Human Body. http://woostermiddle.stratfordk12.org/Content/The_Human_Body.asp accessed date 15th June 2012).

In childhood and adolescence, bone modelling is associated with growth and reshaping. In bone modelling, growth in length depends on proliferation and differentiation while growth in width and thickness is accomplished by formation of bone at the periosteal surface. In adults, bone remodelling constitutes the lifelong renewal process. It implies the continuous removal of bone and synthesis of new bone matrix and subsequent mineralization. These two processes involve three major types of bone cells: osteoclasts, osteoblasts and osteocytes (Parfitt et al., 2001). Osteoclasts are multinucleated cells of large size that degrade and reabsorb bone. This type of cell arises from the haemopoietic cells of the monocyte/macrophage lineage. Osteoclasts lie in regions of bone for reabsorption. Osteoblast is a type of bone forming cells. It is defined as a cell that produces osteoid, or bone matrix. Osteoblasts line the

surface of bone and follow osteoclasts in cutting cones. Osteocytes are osteoblasts encased in a mineralized matrix. They are the largest proportion of bone cells but seem, paradoxically perhaps, to have been paid the least attention. They are characterized by a high nucleus-to-cytoplasm ratio and contain fewer organelles.

As stated above bone forming and remodelling implies bone absorption and refilling. Osteoclasts reabsorb bone by isolating an area of bone from cell attachment, then reducing the pH of the local environment by producing hydrogen ions. Carbonic anhydrase provides the proton source for extracellular acidification by H^+-ATPase and the HCO_3^- source for the HCO_3^-/Cl^- exchanger (Roussellea and Heymann, 2001). The solubility of the apatite crystals is accelerated at low pH. After the movement of mineral, the organic components are hydrolyzed through acidic proteolytic digestion. Once the cavities are formed on the bone surface, the osteoblasts that follow lie on the new surface and are activated to lay down osteoid to refill the cavity and become incorporated into new bone. Once an osteoblast becomes surrounded by the bone matrix, it then becomes mineralized osteocyte (Crockett et al., 2011).

1.3.2 Osteoblasts

Since osteoblasts play key roles in bone forming and remodelling they have received much attention. Osteoblasts and osteocytes are of the same lineage i.e.

derived from mesenchymal cells. Mesenchymal cells in turn may lead to osteoblasts, chondrocytes, myoblasts and bone marrow stromal cells including adipocytes (Owen, 1988). The specific phenotype of the cell achieved depends on their maturation during differentiation. Mature osteoblasts for example are characterised as possessing high alkaline phosphatase (ALP) activity and the capacity to synthesize collagenous and noncollagenous bone matrix proteins including osteocalcin (Aubin and Liu, 1996).

Osteoblasts arise through the activity of osteoprogenitor cells which are mesenchymal cells located near all bony surfaces and within bone marrow. Mature osteoblasts secrete osteoid forming matrices and enzymes facilitateing mineral deposition within the matrices. Thus osteoblast cells constitute a lineage of highly differentiated cells: active osteoblasts (e.g. MG63 cell line), bone lining cells and osteocytes and they are represented by a distinctive morphology. Mature functional osteoblasts are metabolically active and dedicated to the process of bone matrix (osteoid) synthesis. In keeping with high proliferative capacity and marked differentiation, the active osteoblast exhibits a voluminous nucleus relative to other cell types and there is a large Golgi apparatus, rough endoplasmic reticulum and high mitochondria content. The abundant rough endoplasmic reticulum and Golgi apparatus is characteristic of cells that manufacture protein for either export or secretion. The matrix elements produced by osteoblasts include structural proteins, such as type I collagen; a variety of noncollagenous proteins, including osteocalcin and osteopontin, osteonectin, proteoglycans and regulatory factors, including

cytokines, growth factors, and prostaglandins (Aubin et al., 1993 and Aubin and Liu et al., 1996). In addition to the above synthetic products, osteoblasts produce neutral proteases, alkaline phosphatase, and other enzymes that degrade the extracellular matrix and prepare it for calcification. On other bone surfaces, where bone is not being actively formed, the osteoblasts appear elongated and flat and are relatively quiescent metabolically. Bone lining cells also have functions. In these cells histochemical studies have demonstrated that alkaline phosphatase is distributed over the outer surface of the cell membrane. Evidence suggests that these osteoblasts produce enzymes and enzyme-regulating proteins such as collagenase, collagenase inhibitor, and plasminogen activator, which are involved in the process of bone matrix degradation (Aubin et al., 1993).

In vitro, osteoblast function is affected by interleukins, insulin derived growth factor, platelet-derived growth factors and estrogen. This leads now to a discussion of investigations on the regulation of osteoblast function.

1.3.3 Regulatory factors in osteoblast function

First of all, it is well known that the hormones secreted by bone marrow cells and bone cells control the remodelling of bone. These hormones include estrogen and testosterone, and many other proteins. Recently, it has been discovered that in addition to parathyroid hormone (PTH), certain cytokines or proteins affect osteoblast behaviour. Hence the growth factors, the interleukins

(IL-1, IL-6, and IL-11), transforming growth factor-β (TGF-β) and tumor necrosis factor-α play key roles in controlling the activities of the osteoblasts (Pfeilschifter et al., 2002). Osteoblasts arise when the osteoprogenitor cells differentiate under the presence of growth factors such as fibroblast growth factor (FGF), platelet-derived growth factor (PDGF), TGF-β and bone morphogenetic proteins (BMPs). In addition, a novel growth factor secreted by the macrophage cells of the immune system was isolated and found to induce growth of bone cells.

The different kinds of specific receptor-effector interactions in osteoblasts are best illustrated by responses to PTH, prostaglandins, 1,25-dihydroxyvitamin D, and glucocorticoids. PTH and prostaglandins bind to cell surface-associated receptors and then activate intracellular second messenger pathways to achieve a cellular response. These mechanisms include both the adenylate cyclase/cyclic adenosine monophosphate pathway and the phosphoinositol-calcium pathway. In contrast, 1,25-dihydroxyvitamin D and glucocorticoids diffuse through the membrane, bind to cytosolic receptors, which then translocate to the nucleus of the cell and interact with nuclear DNA to modulate and regulate the transcription of DNA to messenger RNA. Recently, estrogen receptors were identified in osteoblasts and their functions are similar to other steroid hormone receptors.

In summary, osteoblasts which are one of the most important bone cells have important functions and complex regulatory mechanisms. In addition to

primary cells, many labs use cell lines to investigate how regulatory factors influence their function, and how these cells communicate and interact with each other. One aspect, as of yet poorly investigated, is the possible role of ion channels in the cellular process of osteoblast such as proliferation and differentiation (Russell, 2003 and Russell et al., 2006).

1.4 Potassium channels in bone cells

Ion channels in bone cells have been identified and considered as potential target for therapeutic agents for the treatment of osteoporosis and other bone disorders (Komarova et al., 2001). Recently, in osteoclasts numerous ion channels have been characterised such as K^+, Na^+ and Cl^- channels. The K^+ channels that have been identified in osteoclasts include an inward rectifier K^+ channel, a transient outward rectifier channel and two classes of Ca^{2+}-activated K^+ channels. These two types of Ca^{2+}-activated K^+ channels are the large and intermediate conductance channels. Functions of ion channels in osteoclasts were determined as setting the membrane potential, signal transduction and cell volume regulation (Komarova et al., 2001). A summary of the possible function and mechanisms of these ion channels is shown in Fig 1.7. BK channels are activated by elevation in internal Ca^{2+}. The resultant hyperpolarization of the osteoclast, it is argued, would augment Ca^{2+} influx, providing positive feedback (Wiltink et al., 1995). These channels represent potential molecular targets for the development of antiresorptive drugs.

Bone modelling and remodelling involves both osteoclast and osteoblast behaving normally as described above and ion channels in osteoblasts may also be important therapeutic targets of bone diseases. Indeed, the investigations of ion channels in osteoblasts started from the early 1980s with such considerations in mind. In 1982, Ferrier et al. revealed their discovery of low-frequency voltage noise in a mammalian bone cell clone (Ferrier et al., 1982).

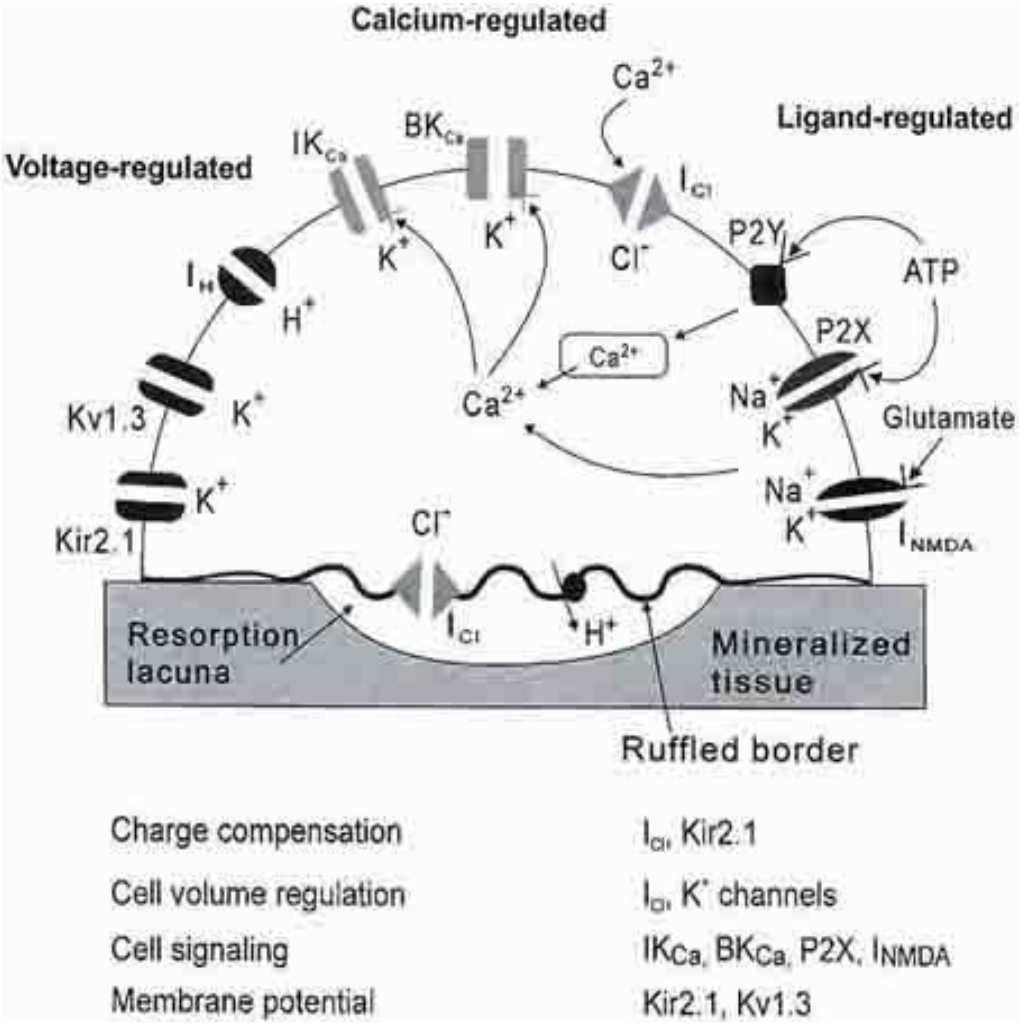

Fig 1.7 Diagram of ion channels revealed in mammalian osteoclasts. They are K channels: Kir2.1, K_V1.3, IK and BK channels, chloride channel (I_{Cl}), extracellular ligand-gated channels: P2X- nucleotide receptor nonselective cation channel; I_{NMDA}- glutamate receptor nonselective cation channel and P2Y G protein-coupled nucleotide receptor linked to mobilization of Ca2+ from intracellular stores. (This graph was taken from Komarova et al., 2001).

Then in 1984 a Ca^{2+}-activated K^+ conductance was confirmed in a clonal osteoblast-like cell line (Dixon et al., 1984). Within 10 years, investigations on the clonal osteoblast-like cell line osteoblast revealed that serum, 2-macroglobulin and parathyroid hormone regulate the cell membrane potential through the existing K channels. The big conductance Ca-activated K channel was identified in embryonic chick osteoblast by using molecular and electrophysiological approaches (Ravesloot et al., 1990). In the following years, different groups described various potassium channels in osteoblast-like MG63 cells (Moreau et al., 1997; Yellowley et al., 1998 and Rezzonic et al., 2002). Importantly, BK channels in MG63 cells are activated by the Prostaglandin E_2 which is an important mediator of bone response to growth factors, hormones, inflammation or mechanical strain. Furthermore, BK channels regulate the osteocalcin secretion of MG63 cells (Moreau et al., 1997). Established osteoblast-like cell lines like those described are useful models for the molecular and cellular study of osteoblasts. Primary osteoblasts differ substantially in their properties at different stages of development, whereas cloned cell lines from bone or bone tumors represent a particular stage of differentiation. At the time of commencing the work described in this Thesis no equivalent data exist for human primary osteoblasts.

Previous reports studying BK channels in osteoblast-like MG63 cells raised a number of unanswered questions and anomalies such as the channel subtypes and their specific functions. In this project, BK channels were investigated systematically in osteoblast-like cell lines and primary osteoblasts from human,

rat and mouse in an attempt to answer the questions: 1. What are the subtypes of BK channel and their subunits composition? (as see in Section 4) 2. What are the specific activation features of BK channel in these cells compared to what we knew in other cells such as nerve and muscle? And what are the specific responses to the well-known BK channel modulators? (as see in Section 5) 4. What are its contributions to the cell functions? (as see in Section 6)

SECTION 2: MATERIALS AND METHODS

2.1 Cell culture

In this project, three different osteoblast-like cell lines were investigated: human osteosarcoma MG63 and SaOS-2 cells, and mouse bone marrow-derived 7F2 cells. Four kinds of primary cells were also used. These were primary human osteoblasts (HOBs), primary mouse and rat osteoblasts and bone marrow cells (mesenchymal cells). In addition to these bone forming cells, a mouse osteocyte cell line (MLO-Y4) was also investigated. All these cells were cultured in an incubator (Nuaire DH autoflow) with 5% CO_2 and 95% air at 37˚C. All culture operations were done under sterile conditions in a laminar flow unit (Faster Ultrsafe 48). Since they are all adherent cells, trypsin was used to detach them, when there were confluent monolayers. Cells were washed with 37°C Dulbecco's Phosphate Buffer Solution (DPBS) (Invitrogen, UK) to rinse off calcium and magnesium salts present in the cell culture. 0.5 ml, 37°C (for 25 ml flask) trypsin (solution (0.025% trypsin IV, 0.2% EDTA) (Sigma-Aldrich, UK) was then added for 5 minutes. Cells were checked under a microscope to ensure they had properly detached from the culture surface before adding culture medium to inactivate the trypsin. All cells were

centrifuged at 500 *g* for 3 minutes and then the cell pellet was collected. Cells were either then seeded on to glass coverslips for patch-clamp studies, and into suitable cell culture plates for the cell number assays.

2.1.1 Human osteoblast-like cell lines

Two osteosarcoma-derived cell lines have been extensively used which are MG63 and SaOS-2 cells. The most pronounced difference between the two cell lines was that ALP activity in the SaOS-2 cells was 10-fold higher than in the MG63 cells. The proliferation rate of the MG63 cells was much higher than that of the SaOS-2 cells. SaOS-2 cells exhibit a more mature osteoblast phenotype, compared with that of MG63 cells (Shapira and Halabi, 2009).

MG63 cells are derived from the osteosarcoma of a 14 year old boy (Heremans et al., 1977). These cells were kindly supplied by Dr. B. A. J. Evans (School of Medicine, Cardiff University, Heath Park, Cardiff, CF14 4XN). Cells were cultured in complete Dulbecco's modified eagle medium (DMEM, from Invitrogen, UK) containing 1% penicillin-streptomycin solution (100 U/ml penicillin G sodium and 100 μg/ml streptomycin sulphate) (Invitrogen, UK) with 5% foetal bovine serum (FBS, from Invitrogen, UK) in 25 cm^2 flasks. Cell medium was changed twice a week, and cells were passaged (1:10) once a week. In this project, the passage number of MG63 cells was always below 34.

SaOS-2 cells were originally from the osteosarcoma of an 11 years old girl (Fogh et al., 1977). These cells were also kindly supplied by Dr. B. A. J. Evans.

The culture medium was the complete DMEM medium as described above. The medium was changed twice a week and cells were passaged (1:5) once a week. The passage number of SaOS-2 cells was always below 30.

2.1.2 Mouse osteoblast-like cell line

7F2 cells are osteoblasts originally derived from mouse bone marrow (Thompson et al., 1998). The cells were isolated from the p53-/- mouse femoral bone marrow and subsequently cloned. These cells were kindly supplied by Dr. B. A. J. Evans. The cells are mature osteoblasts as they express alkaline phosphatase, secrete type I collagen and osteocalcin, show a significant cyclic adenosine monophosphate response to parathyroid hormone and mineralize extensively. On the other hand, these osteoblast-like cells can be induced to undertake massive adipocyte transdifferentiation. This transdifferentiation is accompanied by the complete loss of expression of all osteoblastic markers except alkaline phosphatase. These observations indicate that some cells that have acquired all of the characteristics of mature osteoblasts can be diverted to the adipocyte pathway (Thompson, et al., 1998). These cells were cultured in alpha minimal essential medium (α-MEM) containing 10% FBS, 100 U/ml penicillin and 100 μg/ml streptomycin. The culture medium was changed twice a week and cells passaged (1:8) once a week, with the passage number always being less than 28.

2.1.3 Human primary osteoblasts

Primary human osteoblasts derived from the normal hipbone of a 64 year old Caucasian female (passage number 3 and 4) were obtained from PromoCell GmbH, and maintained as proliferating cultures using the recommended growth medium (PromoCell GmbH). PromoCell confirm that the cells are positive for osteocalcin by immunofluorescence.

2.1.4 Mouse/rat primary bone marrow cells and osteoblasts

Mouse/rat primary osteoblasts and bone marrow cells were from the mouse/rat femur or tibia. The culture medium was α-MEM with 10% FBS, 100 U/ml penicillin and 100 μg/ml streptomycin. As shown in Fig 2.1, the dissected bones were first rinsed with sterile DPBS several times at room temperature (RT). Then the bone was placed in a Petri dish and with the use of a scalpel and forceps the periosteum was removed. After this, one end (epiphyses) was cut off and discarded, and the remaining bone was placed in a 200 μl Eppendorf tube with 50 μl medium. This Eppendorf tube was centrifuged at 1000 rpm for 3 min at RT, and this resulted in a cell pellet (bone marrow cells) being deposited at the bottom of the tube. These bone marrow cells were resuspended in medium and seeded into 25 cm^2 flasks at a cellular density of 5 x 10^5 cells / ml. When the cells in flasks were confluent, they were trypsinised and seeded onto coverslips for patch-clamping.

The cortical bone from the remaining bone was washed with PBS in a Petri dish and cut into fragments of 1-3 mm. These fragments were washed in a new dish until they were white in colour. To initiate explant cultures, flasks were conditioned by preincubating with 2 ml medium for 30 minutes. Then (following Protocol 22.14 from "Culture of Animal Cells", Freshney, 2000) the preincubation medium was discarded from the flasks and 2.5 ml of fresh medium was added. 10 to 20 fragments of the bone were transferred into the flask with the aid of an inoculating loop and the explant pieces were distributed evenly. The flasks were left in the horizontal position in the incubator. After a week the outgrowth was checked under a microscope (Fig 2.2) and the medium was changed. To maintain these bone cell cultures, the medium was changed twice a week. Once again when the cells were fully confluent, they were trypsinised and seeded on to coverslips for patch-clamping.

2.1.5 Mouse osteocyte cell line (MLO-Y4)

MLO-Y4 cells had been originally obtained from Professor Lynda Bonewald, (University of Missouri-Kansas City, USA). These cells were kindly supplied by Dr. B. A. J. Evans. Cells were cultured in αMEM with 10% FBS, 100 U/ml penicillin, and 100 µg/ml streptomycin. Flasks were coated with collagen type I in order that cells maintained their osteocytic phenotype. Medium was changed every 2 days. Confluent cultures were harvested using trypsin and seeded on to cover slips coated with collagen type I to carry out electrophysiological experiments. Osteocytic phenotype was assessed by the

maintenance of dendritic morphology. Only cells showing dendritic phenotype were selected for recording.

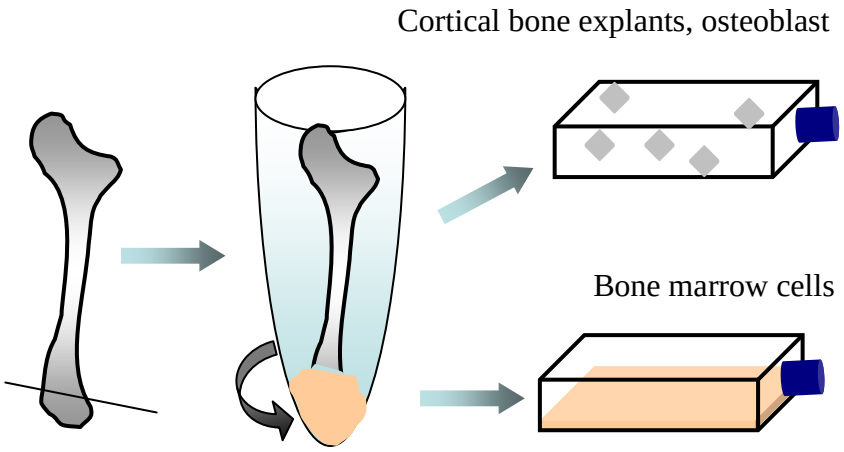

Fig. 2.1 Mouse/rat osteoblast and bone marrow cell preparation. After centrifugation bone marrow cells were at the bottom of the tube. These cells were resuspended in αMEM with 10% FBS and seeded into cell culture flasks. The cortical bone from the long bone was cut into small explants and seeded evenly in another flask.

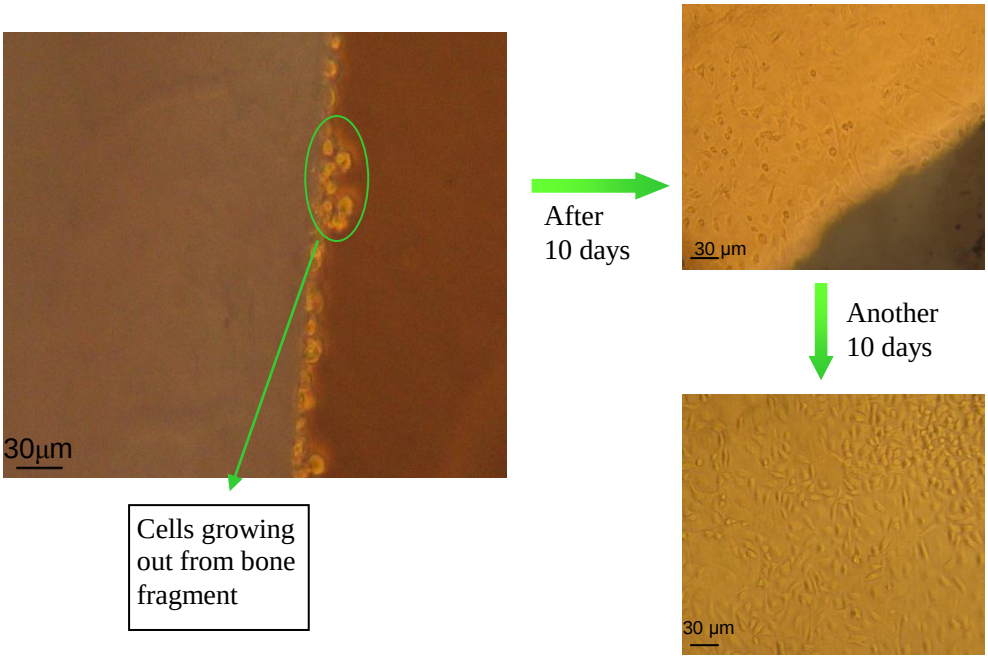

Fig 2.2 These images show bone cells growing out from cortical bone fragments. The fragments were cultured with αMEM with 10% FBS in 25cm^2 flasks. After a week, cells could be clearly seen growing out from explants. After another 20 days these cells were confluent.

2.2 Electrophysiology

Electrophysiological methods study the electrical properties of cells and tissues. Patch-clamping techniques are classical electrophysiological techniques and are extremely powerful in investigating the minute electrical signals, or currents, through ion channels in biological membranes. All the patch-clamping experiments were performed at room temperature.

2.2.1 Basic theory of patch-clamping and the equipment set up

In the 1970s Erwin Neher and Bert Sakmann (Neher and Sakmann, 1976) developed the patch-clamp method to record the current through single channels in the cell membrane. It was quickly adopted by numerous labs to study the electrophysiological properties of many cell types. It caused a revolutionary advance in many research areas in both cellular and molecular biology. Some key improvements such as the "giga seal" (a seal is formed between the cell membrane and the glass pipette with a resistance of >1 gigaohm (GΩ)) and the use of the various recording configurations permitted patch recording from both the cell surface membrane or cell-free membrane patches as well as "intracellular" whole-cell recordings (Hamill et al., 1981).

The electronic equipment or current to voltage amplifier records the transmembrane currents as a function of membrane voltage changes. To record effectively the pA currents that ion channels carry, both mechanical stability of all the components of the setup is crucial and electrical interference must be

kept minimal. Thus all the equipment (microscope, manipulators etc.) are set up on a vibration isolation table in a Faraday cage and all items were earthed appropriately (Fig 2.3).

Patch-clamp electrodes were pulled from 1.5 mm outside diameter, 0.86 mm inside diameter borosilicate glass capillaries (GC150-F10, Harvard Apparatus Ltd.) and fire-polished by a DMZ-Universal Puller. The fire-polished electrode had a tip diameter of approximately 1-2µm. The electrode was back filled with a fine silica microfill syringe needle (Harvard Apparatus). The resistances were typically 2-10 MΩ when filled with the High K (140) solution. The filling solutions for the electrodes are described in Section 2.5.

Cells to be patched were sub-cultured on coverslips (Ø 16 mm) in 6–well plates. When patched, these cells were usually subconfluent and not more than 6 days post-seeding in culture. The coverslip was transferred from the 6-well plate to a Perspex recording chamber with a glass bottom under sterile conditions in a laminar flow unit. A tiny bit of petroleum jelly were used to hold the coverslip in position. After washing the cells with the recording solution another 500 µl of this solution was added directly to the cells on the coverslip and this formed the bath solution. Then the recording chamber was positioned on the stage of a microscope (Microtech 200) in the Faraday cage. Recordings were made at room temperature, using an Axopatch 1D clamp amplifier (Axon Instruments). The electrode resistance was determined by Ohm's Law from the current amplitude in response to a 20 mV short duration pulse.

2.2.2 Different configurations of patch clamping

In Fig 2.4, the four different configurations of the patch-clamp method, all of which are used in this study, are shown. Cell-attached patches can be achieved by tightly sealing a glass microelectrode on to the plasma membrane of a cell. A giga-Ohm seal can be formed by slight negative pressure supplied by gentle suction through a syringe or by mouth (a). At this stage pulling back the electrode will result in an excised inside-out patch(c). Alternatively more suction or applying a negative potential will result in a whole-cell recording (b). Pulling back the electrode at this stage will result in an outside-out patch (d).

Single channel patch-clamping is a technique with a very high resolution. Conformational changes in one single native protein can be detected which trigger the opening or closing of one ion channel in real time. With the establishment of a tight seal between the glass electrode and the cell membrane, the current caused by the opening of the desired ion channel in a quasi-physiological environment can be recorded. If we compare the channel properties in cell- attached patches with the one in excised patches, any differences can be assumed to be related to cytosolic gating factors of the channel (e.g. ATP, polyamines, Ca^{2+} etc). In this way, we can investigate whether the channel can be regulated by any cytosolic messengers or not. On the other hand, since the ion channel is isolated from the bath solution, any modulators cannot access the channel directly. Only those modulators which are cell membrane permeable that regulate the channel activity directly or

through cytosolic second messengers can be tested in the cell-attached patch configuration.

In inside-out patch the cytosolic side of the cell membrane is exposed to the bathing solution. Regulators can therefore be applied directly to the intracellular binding sites. This configuration is preferred when studying how cytoplasmic events affect an ion channel. In this project, this configuration was used to identify the types of potassium channels and to investigate the modulators (both drugs and ions) binding to the channels from the intracellular site.

Outside-out patch is useful for recording the activity of the channel that requires application of a compound to the outside of the channel surface (Friday and Howard, 1991). This configuration was gives the opportunity to examine the properties of an ion channel when it is exposed to different solutions on the extracellular of the membrane. Specifically, it was used to investigate extracellular binding modulators.

With these techniques the external and internal ionic environment of the cells and channels can be controlled, thus providing comprehensive capabilities for testing the influence of various manipulations such as drug or toxin effects and composition changes. For example, the ionic composition on either side of the membrane or the channel can now be adjusted; toxins, transmitters and other agents can be applied easily, in defined concentrations, to either side of the membrane.

These isolated membranes and systems are suitable for the use of molecular and genetic techniques (Barondes et al., 1998). As a result, many physiological questions at the molecular level can now be answered. For example, determining exactly where in the channel molecule or subunit an antagonist or drug acts is now possible. Thus, using the powerful combination of electrophysiology and molecular biology, a definitive link between structure and function at the molecular level can be achieved.

The disadvantages of these models are principally derived from the isolation process itself. The membrane is isolated so that it lacks normal connections with other membrane domains; it may therefore be functioning differently than that normally seen in the living organism, and thus may provide answers not relevant to the native "real world." In addition, there is the danger that the "extracellular" and "intracellular" media used represent a totally artificial environment that would not be relevant to living cells *in vivo*. The lack of normally circulating agents such as steroids, hormones, plasma proteins could lead to drastic changes in the function of the channels under study.

The complementary whole-cell patching technique is necessary to examine the physiological roles of the required ion channel in the entire cell. It allows modifying the internal environment by using a patch-clamp pipette. The recording from a whole-cell patch gives an average response from all the channels in the cell membrane.

To investigate single ion channel electrophysiology the patch-clamp method remains the most powerful and versatile tool. It allows the unitary currents through single channels to be observed which is diagnostic of function. It still remains after over 30 years the method of choice allowing the recording of macroscopic whole-cell or microscopic single-channel currents flowing across biological membranes through ion channels. In this thesis all configurations were used and put to the test in a number of new cells.

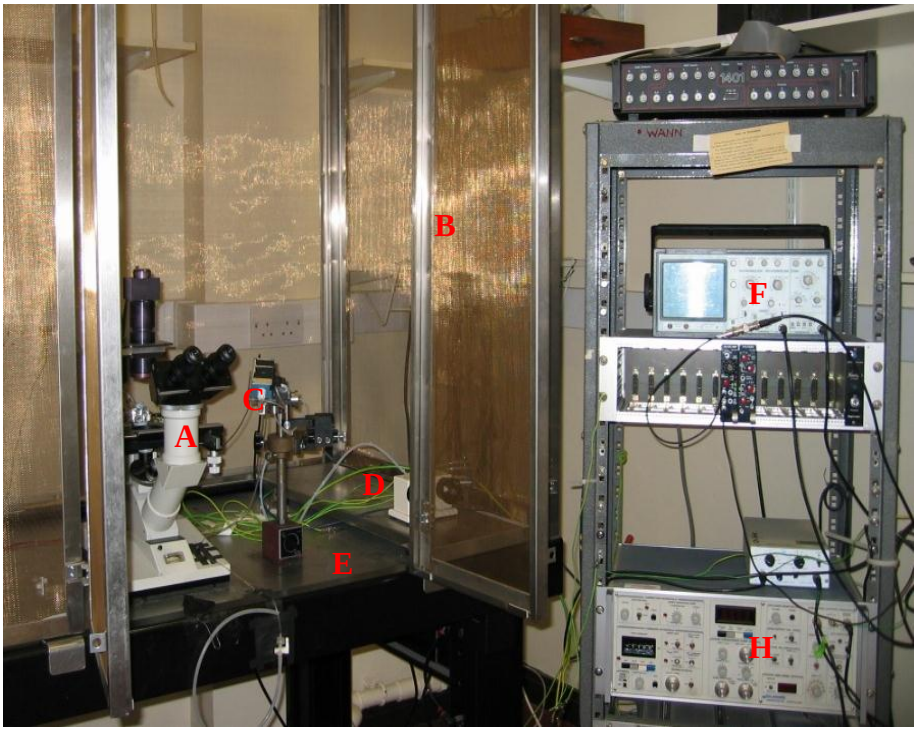

Fig 2.3 Patch clamp equipment**.** Coverslips with cells were positioned in a Perspex chamber with a glass bottom. The chamber was positioned on the microscope (A) in the Faraday cage (B). The amplifier carrying the electrode holder (C) was held by the Narishige hydraulic manipulator (D). All equipment was positioned on the anti-vibration table (E) and all items were earthed. The Axopatch amplifier (H) was connected to an oscilloscope (F) via a Neurolog amplifier (to deal with offsets and to provide additional gain) and to a Digidata A-D converter (the National Instruments (NDAQ-MX)) which in turn was interfaced with the computer.

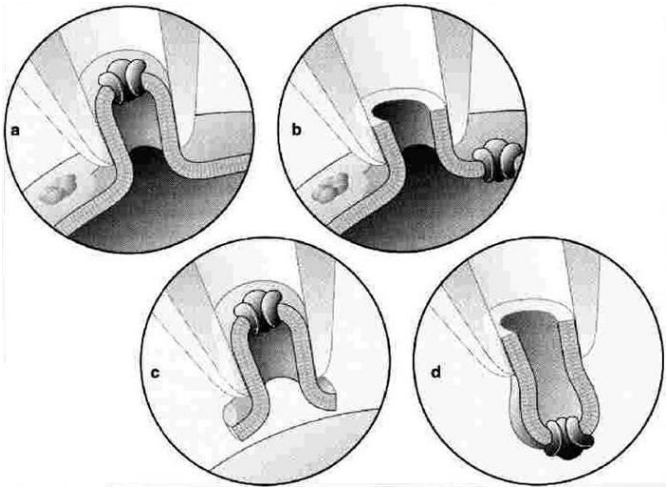

Fig 2.4 Four different configurations of patch-clamping: (a) cell-attached, (b) whole cell, (c) inside-out and (d) outside-out. From the various configurations we can obviously control and manipulate the solutions that the inside and outside of the cell membrane is facing.

2.2.3 Software and data analysis

The Strathclyde Electrophysiology Software (developed by John Dempster) was used throughout to record and analyse all single channel and whole cell data. Electrophysiology data recorder WinEDR (ver. 2.5) was used for the collection of single channel patch data and Electrophysiology data recorder WinWCP (ver.3.8.1) was used for the collection of whole cell patch data. To identify the smallest single channel currents, high resolution was necessary. Signals were often therefore filtered at 5 kHz (-3dB, four pole Bessel Filter) and digitized at 20 kHz by a 12-bit A-D converter (National Instruments (NDAQ-MX)). The variance of the noise of the current record was minimal (RMS noise between 0.6-0.8) and the signals were viewed using an oscilloscope during recording in addition to being displayed on the computer

screen. The duration of each single channel recording used for analysis was 30 seconds if not otherwise specified.

Initial analysis generated the histograms of all current distributions. These histograms, fitted with Gaussian functions to the closed and open peaks, indicated the unitary current through an ion channel at a given membrane potential. Plots of the unitary current taken from the Gaussian-Fit to the open peak vs potential (I-V) were used to determine the conductance of this channel. I-V plots were constructed using Origin 7 Statistic Software (OriginLab, USA). In addition, P_{open} (Po) values were generated either as a measure of the area under the curve of the amplitude histogram of the open peaks or from transition detection methods (using the 50% threshold). To quantify the results the Po versus voltage data were fitted to a single Boltzmann equation using Origin 7 Statistic Software.

Kinetic studies analyse the behaviour of a single channel in a patch, and are used to study the number and duration of events i.e. openings and closures of any single channel event, thus providing an insight into the gating behaviour of a single ion channel protein. Single opening and closures may be very brief (in the range of tens of μs), and often the random noise in the record will result in current fluctuations that can resemble these short duration single channel openings and closures. Heavy filtering of the data can prevent such occurrences, but this would decrease the quality of the data, resulting in short duration true channel openings and real closures being effectively “erased” from the recording. The level of filtering in the patch system will determine

whether or not the opening or closure can be clearly defined. These factors mean it is important when undertaking kinetic analysis of the record to determine the resolution of the method used (i.e.- the shortest measured time interval, known as the minimum resolvable event), which can be calculated when the level of electronic filtering during the process of recording, the digitisation rate of data for storage, plus any subsequent filtering prior to analysis are known. The effective cut-off frequency of the filters used throughout the recording and analysis must be determined using the following equation (Colquhoun, 1994):

$$1 / f_c^2 = 1 / f_1^2 + 1 / f_2^2 \ldots 1 / f_n^2$$

Where f_c is the sum of all the combined filters during recording, including that imposed by the recording system (f_1), the rate of digitisation (f_2) and (f_n) refers to any subsequent filters applied throughout analysis. For example if single-channel data were sampled or digitised at a frequency of 20 kHz on the patch-clamp amplifier and then filtered at 5 kHz, the final cut-off frequency would be 4.85 kHz, which would probably be acceptable for most applications (Walz et al., 2002).

By statistical analysis with Origin, each single channel recording was analysed to get information on: what is the current corresponding to the peak time points? What is the state of the channel at a specified time point? And what is the channel open probability? With this information plots of the unitary current against voltage (I-V curve) can be produced to get the unitary conductance of the channel. Plots of the Po against voltage provide data on the activation or

gating properties of the channel, specifically its voltage dependence i.e. position on the voltage axis and slope.

2.3 Cell number assays

Cell number assays (MTS) were carried out with MG63 cells in the presence and absence of various compounds. Cell viability assays were also undertaken.

2.3.1 Viability assay

The cells were seeded in 12-well plates with a density of 30,000 cells/well and incubated in the test medium at 37˚C in an atmosphere of 5% CO_2, 95% air. After the required incubation (followed photographing in some cases), cells were trypsinised and centrifuged at 1000 rpm for 5 min. After centrifugation the cells were resuspended in medium and 0.4% trypan blue dye in PBS. The dead cells were stained so that the live, unstained cells could be counted using a haemocytometer as shown in Fig 2.5.

Determination of the cell viability:

$$\frac{living\ cells}{total\ cells} \times 100\% = cell\ viability\,(\%)$$

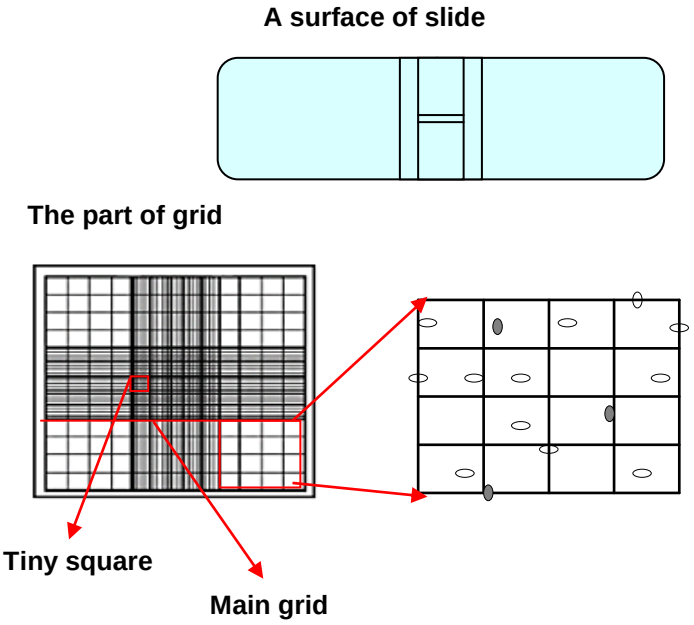

Fig 2.5 Viable cells counts. Cell suspension was mixed 1:1 in trypan blue and only non-viable cells stain. 10 µl cell suspensions were transferred to each chamber of a clean, dry haemocytometer. Cells were counted in each 1 mm^2 area. If cells were on the border outlining each square, only the cells on the top and left border of each square were counted.

2.3.2 MTS assay

The working principle of MTS assay is that MTS (3-(4, 5-dimethylthiazol-2-yl)-5-(3-carboxymethoxyphenyl)-2-(4-sulfophenyl)-2H-tetrazolium) is reduced by the mitochondrial dehydrogenase enzyme released by metabolically active cells. MTS is bioreduced into a colored formazan product which can be measured directly by a plate reader using absorption at 490 nm. The solution contains 300 µM electron coupling reagent (phenazine ethosulfate; PES) which has an enhanced chemical stability combining with MTS (1.90 mg/ml) to form a stable solution. In this project the CellTiter 96®AQ_{ueous} One Solution

Reagent (Promega, UK) was used, which contains 1.90 mg/ml MTS and 300 µM PES in PBS.

Confluent cells in 25 cm^2 flasks were trypsinised as previously described and counted. 100 µl cell suspensions containing 3,000 cells were added to each well of a 96-well plate evenly by using a multi-channel pipette (Eppedorf, UK). Cells were left at 37ºC, 5% CO_2, 95% air to settle over night and this point was considered as day 0. On day 1, 200 µl of complete DMEM with or without test compound was added to each well. If the compound was dissolved in DMSO or any other vehicle then the same concentration of DMSO or vehicle was used in the control wells. Otherwise complete DMEM medium was used as control. Cells were then cultured at 37ºC, 5% CO_2, 95% air for 96 hours before assessing cell numbers using the MTS assay. Each control and test condition used 10 replicates (i.e. 10 wells) in each assay, and each assay was repeated 3 times.

The MTS assays were performed by adding 20 µl of CellTiter 96®AQ_{ueous} One Solution Reagent directly to each subcultured cell well, incubating for 1 hour / 2 hours then recording the absorbance at 490nm with a Tecan® ELISA 96-well plate reader. The data were expressed as relative cell number, this being the optical density for each experimental group / optical density for the control group. The relative cell number was defined as:

$$relative\ cell\ number = \frac{Experimental\ group\ absorbance - background\ absorbance}{Control\ group\ absorbance - background\ absorbance}$$

2.4 Mineralisation assay

Since MG63 cells do not mineralise in culture, these experiments were performed with osteoblast-like SaOS2 cells and primary human osteoblasts maintained as described above. Cells were cultured in 6- and 12-well plates until almost confluent. They were then treated with culture medium containing L-ascorbic acid 2-phosphate (50µg / ml), β-glycerophosphate (2 mM) and dexamethasone (10^{-7}M), in the presence or absence of BK channel modulators. The media were changed twice weekly, and the cells were stained for calcium deposits within the mineralised matrix 3 – 4 weeks after the start of the assay. Briefly, experiments were terminated by fixing cell layers in formal saline (4.1% formaldehyde in PBS) for 15 minutes. Mineralised bone nodules were visualised by staining with alizarin red (1% solution in water) for 5 minutes, rinsed with 50% ethanol to remove excess stain, then dried in open air. The mineralisation density was analysed using Image Pro Plus version 6.1 (Media Cybernetics).

In addition to cell layers staining, protein concentration from mineralised cells was estimated by a Bio-Rad protein assay. An acid dye (coomassie® brilliant blue G-250) binding to the solubilised proteins extracted from cell lysate samples caused the absorbance of the dye shifting from 465 nm to 595 nm. The relative protein concentration can be calculated from the standard curve created from Bovine serum albumin (BSA, Sigma) stock solution.

2.5 Drugs and solutions

Non-selective potassium channel blockers, quaternary ammonium compounds (tetraethylammonium chloride, TEA; tetrabutylammonium chloride, TBuA; tetrapentylammonium chloride, TPeA and tetrahexylammonium chloride, THeA), the selective BK channel opener NS1619, raloxifene and tetrandrine were purchased from Sigma Chemical Co. Ltd (UK). The selective BK channel blockers iberiotoxin (IbTX), slotoxin and paxilline and the selective BK channel opener isopimaric acid were obtained from Alomone Laboratories (Caltag-medsystems Ltd., UK).

The compounds

Compounds	Doses	Stock	Storage Temperature
IbTX	10~100 nM	1mM (distilled H_2O) (electrophysiology) 1 mM (DMSO) (cell number assays)	-20°C
Slotoxin	10~100 nM	1mM (distilled H_2O) (electrophysiology) 1mM (DMSO) (cell number assays)	-20°C
TEA	300 µM~30 mM	1 M (distilled H_2O)	fresh made
Tetrandrine	5~90 µM	20 mM in DMSO	-20°C
Paxilline	10~60 µM	1M (distilled H_2O) (electrophysiology) 1M (DMSO) (cell number assays)	-20°C
Isopimaric acid	10~100 µM	1 M (distilled H_2O) (electrophysiology) 1 M (DMSO) (cell number assays)	-20°C

Solutions used in electrophysiology:

High K saline 1 contains (mM): 5 NaCl, 140 KCl, 1 $MgCl_2$, 1 $CaCl_2$, 10 HEPES, 11 EGTA, pH adjusted to 7.2 with KOH (free Ca^{2+} is 0.031 mM)

High K saline 2 contains (mM): 5 NaCl, 140 KCl, 1 $MgCl_2$, 1 $CaCl_2$, 10 HEPES, pH adjusted to 7.2 with KOH.

NaCl Locke contains (mM): 150 NaCl, 3 KCl, 2$MgCl_2$, 2$CaCl_2$, 10 HEPES, 10 Glucose and the pH adjusted to 7.4 with NaOH

2.6 RT-PCR

RT-PCR (Reverse transcription-polymerase chain reaction) is a technique in which an RNA strand is "reverse" transcribed into its DNA complement (cDNA), followed by amplification of the resulting DNA using a polymerase chain reaction (PCR). The exponential amplification via RT-PCR provides a highly sensitive technique, where any specific piece of DNA or RNA can be characterized, analyzed, and synthesized. PCR involves preparation of the sample, the master mix and the primers, followed by detection and analysis of the reaction products.

RNA was extracted from a chosen cell line by following the TRIZOL (Invitrogen, UK) isolation protocol. Any DNA present in the RNA preparation was removed using DNA-Free (Ambion, UK). The amount of RNA isolated was quantified by measuring the light absorbency at two distinct wavelengths of 260 nM (for RNA) and 280 nM (for DNA). The A_{260}/A_{280} nm absorption ratio was expected to be greater than 1.7.

In the RT reactions the Ambion RT System Kit® was used. AMV reverse transcriptase (AMV RT), an enzyme that catalyzes the polymerization of DNA using template RNA, was added in one reaction in which cDNA was produced. In a second reaction there was no AMV RT thus any DNA present would be due to contamination of the RNA preparation with genomic DNA. The cDNA samples were stored at -20˚C until used for PCR.

Five sets of primers were used. These primers were all located in the exons. One set was for the BK channel α-subunit (KCNMA) (Allard et al, 2000). The other pairs of primers were for the BK channel β1-subunit (KCNMB1) (Hartness et al, 2003), β2-subunit (KCNMB2), β3-subunit (KCNMB3) and β4-subunit (KCNMB4). All the primers were purchased from Invitrogen UK. Specificity was confirmed by BLAST analysis.

A few preliminary tests were run to determine the suitable conditions for the reactions. And then all the PCR reactions were run for forty cycles as follows:

95°C, 2 min → 94°C, 30sec → 55°C, 45sec → 72°C, 1min → 72°C, 1min

(94°C, 30sec → 55°C, 45sec → 72°C, 1min) × 40 cycles

All reactions products were visualized on 2% agarose gels by staining with ethidium bromide. A gel was made up of 2% agarose (Sigma, UK) in 1 X TAE buffer (40 mM Tris base, 1.14 mg/ml and 1 mM EDTA) with 1μl ethidium bromide (10mg/ml). Hyperladder IV (Bioline, UK) and cDNA samples were loaded into the gel wells. Under 100 V the samples ran on the gel for 25-45mins (depending on the size of the gel) before bands were visualized using a UV Gel Doc System and photographed.

2.7 Statistics

In this project all numerical data are expressed as means ± SD. Data from the MTS assays were tested for statistical significance with one-way ANOVA combined with Bonferroni using the Origin 7 statistics package. The statistical results of cell viability assays were produced by Student's t test using Origin 7. Data from electrophysiology experiments such as channel current (I), channel open probability (Po) were compared by Student's t test. A value of $p < 0.05$ was considered significant.

SECTION 3: ION CHANNEL SURVEY IN OSTEOBLAST AND OSTEOBLAST-LIKE CELLS

3.1 Introduction

Ion channels are cell membrane proteins that are widely expressed in all cells of all living organisms. It has previously been stated that "The electrical properties of ion channels distinguish us from stones" (Armstrong, 2003). Since Hodgkin and Huxley did their important pioneering work on analysing the passage of the electrical nerve impulse down the squid axon membrane (Hodgkin and Huxley, 1952), ion channels have been intensely studied. They have been cloned (Noda et al., 1984; Kamb et al., 1987; Tempel et al., 1987; Pongs et al., 1988), subtypes identified, the pore regions established (Hartmann et al., 1991; Yellen et al., 1991) and even the crystal structure at high resolution (~ 3 Å) of some channels has been determined (Doyle et al., 1998 and Jiang et al., 2003). These excellent and detailed studies have h elped build a picture of ion channel structure and function, have added to our knowledge of ion channel-related diseases and finally offered the prospect of new therapies.

3.1.1 **Potassium channels, a widely distributed class of ion channel**

Ion channels come in many different forms and can be classified by the species of ions which are permeant or can pass through. Hence there are K channels, Na channels, Ca channels, Cl channels and some non specific cation channels. Ion channels are also classified by the nature of their gating. Thus there are voltage-gated channels, ligand-gated channels and second messenger-regulated channels. Thus classification of ion channels requires knowledge of both the permeant species and the gating mechanism.

K channels, one subclass of ion channel, are in fact a large superfamily of membrane protein channels. They may be divided into four different types on the basis of their transmembrane topology and gating. Within each of these types the channels can be again subdivided into subtypes according to their conductance and / or regulatory factors. These are shown in Table 3.1 with their putative function.

Various types of K channels play fundamental roles in the regulation of membrane excitability. They are critical to diverse physiological process including neuronal signalling, smooth muscle contractility, hormone secretion and cell proliferation and are increasingly being identified as molecular targets in a number of pathophysiologic states. Consequently they continue to trigger considerable enthusiasm as drug targets (e.g. Shieh et al., 2000).

Table 3.1

Class	**Subclass**	**Putative Function**
Ca-activated, 6 / 7 transmembrane, 1 pore	• BK channel • IK channel • SK channel	Inhibit cell function following stimuli which increase intracellular Ca
Inwardly rectifying 2 transmembrane, 1 pore	• ROMK • GPCR regulated • ATP-sensitive	• Recycling and secretion of potassium • Mediate the inhibitory effect of many GPCRs • Close when ATP is high • Related to cell secretion
Tandem pore domain 4 transmembrane, 2 pore	• TWIK • TRAAK • TREK • TASK	• Contribute to the resting membrane potential
Voltage-gated 6 transmembrane, 1 pore	• hERG • KvLQT	• Action potential repolarization • Limit frequency of firing of action potentials

3.1.2 Potassium channels in inexcitable cells

K channels were first identified in excitable cells such as neurons, skeletal and cardiac muscle. In these cells K channels are key players in controlling the resting membrane potential and shaping the action potential (see Table 3.1). However many more recent studies show that K channels are not only a feature of these excitable cells but are also expressed in many inexcitable cells including fibroblasts (Gray et al., 1986), macrophages (Ahluwalia et al., 2004), blood cells (Decoursey et al., 1984; Amigorena et al., 1990), glial cells (Ramsdell et al., 1991), bone cells (Ferri et al., 1982 and Bertran, D'Alessio and Kotsias, 1995), epithelial cells (Iliev and Marino,1993) and even cancer cells (Pancrazio et al., 1991). The physiological properties and functions of potassium channels in these cells could be wide ranging as their existence in different tissues with varied functions suggests. For example, potassium channels play key roles in proliferation of cells of the immune system and tumour cells (Leonard et al., 1992; Wonderland et al., 1996). In addition, a putative role for these channels in apoptosis and proliferation in many cell types has been highlighted recently (Kunzelmann 2005; Burg et al., 2006 and Deng et al., 2007). Potassium channels in osteoclasts contribute to several important processes including proton transport and volume regulation (Weidema et al., 2000) and potassium channels in osteoblasts may be involved in secretion of important mediators of bone function (Moreau et al., 1996).

Both osteoclasts and osteoblasts are important cell types in bone and so one key question is: Do potassium channels have key roles to play in ensuring the integrity of bone? The hypothesis proposed here is that such channels may have a role in osteoblast function.

The aim of this work was to investigate systematically in a number of different osteoblast or osteoblast-like cells which potassium channels were present. To this end, patch-clamp studies in cell-attached patches or excised patches were carried out on the osteoblast-like cell lines MG63 and SaOS-2. Thus far no such equivalent data exist in human primary osteoblasts. A comparison was therefore made with primary osteoblasts from human, rat and mouse and some experiments were also done with osteocytes (MLO-Y4), adipocytes and HEK293 cells (transfected with the BK channel α subunit) as a further comparison.

3.2 Materials and methods

All experiments in this Chapter used only single channel patch-clamp methods to define which channels were present and active. The full methods are described in Section 2. The duration of the current records analysed were at least 30 seconds at any one potential.

Patch electrodes were filled with High K solutions 2 (as described in Section 2) and the cells were bathed in NaCl Locke. All solutions were filtered through

0.2 μm PVDF membrane 4 mm syringe filters (Whatman). The composition of these solutions and all compounds suppliers were given in Section 2.

In all cases, three thousands cells were seeded on to 16 mm diameter coverslips in 6 well plates. Cells were cultured at 37°C in a humidified atmosphere of 5% CO_2 and 95% air. To obtain comparable data, patch-clamp experiments were performed within 3 days after seeding and before cells were confluent.

Single channel recordings made at various membrane potentials were saved as digitised recordings using the electrophysiology software package, WinEDR (J. Dempster) and analysed in the conventional way. Hence, amplitude histograms were first created to reveal closed and open peaks and Gaussian fits made to compute unitary current and any other current peaks. The mean unitary currents from the Gaussian fits at various patch potentials were used to create the plots of unitary current versus voltage change (I-V). The distribution of current amplitudes gives a good approximation of the open probability (Po) of any channel. Additionally, this was occasionally obtained by carrying out transition state detection (50% threshold) and this provided estimates of mean channel open and closed times also. Such computations enabled plots of Po vs voltage (channel activity) to be generated. The above plots gave information on single channel conductance, ionic selectivity and channel activity.

The following Goldman-Hodgkin-Katz (G-H-K) equation (Goldman, 1943; Hodgkin and Katz, 1949; Frankenhauser, 1962; Binstock and Goldman, 1971 and Clay, 1991) was used to calculate the permeability ratio (P_K/P_{Na})

$$E = \frac{RT}{F} \ln \frac{P_K[K]_o + P_{Na}[Na]_o}{P_K[K]_i + P_{Na}[Na]_i}$$

where E is the reversal potential, R is the universal gas constant, T is temperature, F is Faraday's constant, and P_x is the permeability to the xth species of ion.

Quantification of results required curve fitting e.g. linear or polynomial fits, or in the case of the Po data, results were fitted by a single Boltzmann function:

$$P_o = \frac{1}{1 + \exp\left[\frac{V_{\frac{1}{2}} - V_m}{V_{slope}}\right]}$$

The statistical methods were described previously in Section 2. All data are expressed as mean ± SD

3.3 Results

Only phase bright cells in isolation were patched and the success rate at attaining giga seals (> 1GΩ) was usually above 50% unless it is specified.

Given the solutions used for patching (see above) the concentration gradients for Na^+ and K^+ were: in cell-attached patches $[K^+]_o = 140$ mM, $[Na^+]_o = 5$ mM;

$[K^+]_i$ = 150 mM (assumed), $[Na^+]_i$ = 5 mM (assumed) (Lodish et al., 2000); in inside-out patches $[K^+]_o$ = 140 mM, $[Na^+]_o$ = 5 mM; $[K^+]_i$ = 3 mM, $[Na^+]_i$ = 150 mM; in outside-out patches $[K^+]_o$ = 3 mM, $[Na^+]_o$ = 150 mM; $[K^+]_i$ = 140 mM, $[Na^+]_i$ = 5 mM. The movement of ions is determined by two opposing factors: the membrane electric potential difference and the ion concentration gradient. Once these two factors balance each other out the system (ion movement) reaches an equilibrium. If the membrane is permeable only to K^+ ions, then the measured electric potential difference across the membrane equals the potassium equilibrium potential in millivolts which is E_{revK}. The magnitude of E_{revK} can be calculated by the generalised Nernst equation:

$$E_{revK} = \frac{RT}{ZF} \ln \frac{[K]_o}{[K]_i}$$

R (the gas constant) = 1.987 cal/(degree · mol), or 8.314 joules/(degree · mol); T (the absolute temperature) = 293 K at 20 °C, Z (the valency) = +1, F (the Faraday constant) = 23,062 cal/(mol · V), or 96,479 coulombs/(mol · V). At room temperature (20°C) this Nernst equation reduces to

$$E_{revK} = 58 \log \frac{[K]_o}{[K]_i}$$

In cell-attached patches, since $[K_o]/[K_i] \approx 1$, then E_{revK} = 0 mV. Under these conditions we can distinguish cation from anion currents easily but from reversal potentials we cannot always distinguish potassium from non-selective cation channel openings in the cell-attached configuration. While in inside-out patches, the reverse potential from mean data of the experiments was 60mV and thus we can distinguish potassium channels from non-selective cation channels.

3.3.1 Channels in human osteoblast-like cells

Single channel recordings in cell-attached patches from human osteoblast-like cells (MG63 and SaOS-2 cells) showed a number of discrete current levels indicative of a number of channel openings. Channel openings often appeared at negative potentials (e.g. – 70 mV). The membrane potential was calculated as: membrane potential = - patch potential change required to minimise the rms noise i.e. at E_k or at 0 mV. On the basis of the unitary conductance, open probability, and mean open time; three different types of channels were identified in these cells. These channels were expressed with high density and very often they co-existed with smaller conductance channels opening alongside the largest conductance one.

In this section the two principal channels identified in MG63 cells are described. Visual inspection of the raw electrophysiological recordings (Fig 3.1) at depolarised potentials in a cell-attached patch indicated that the major openings were a large conductance channel. This channel opened on depolarisation with an open probability (Po) which increased with each depolarising step. The reversal potential was invariably close to 0 mV as predicted for a cation selective ion channel. This channel was observed in 116 cell-attached patches, and the channel conductance from the pooled current-voltage (I-V) plots was calculated to be 315 ± 45 pS (n=98) (for a single I-V example see Fig 3.2). The channel activation (Po-V) curve indicated that this

type of channel was strongly voltage-dependent with a $V_{½}$ typically of 90 mV, slope factor = 5.1 (see Fig 3.2). Another type of channel with smaller unitary conductance (67 ± 19 pS) was also readily identified in cell-attached patches. This type of channel was not however active in each individual patch. In fact the prevalence was around 9:1 in favour of the large conductance channel. A comparison of the two channels is summarised in Table 3.2. There are marked differences in parameters such as single channel conductance, channel open times and open probability. The large conductance channel was however more active and prevalent and therefore was easier to identify than the other type.

In some excised inside-out and outside-out patches these types of channels also co-existed in the same patch as shown in Fig 3.3. In excised patches in asymmetrical K^+ (3/140) the single channel conductance of the large conductance channel decreased to 151 ± 12 pS while the smaller one is 38 ± 7 pS in inside-out patches. The large conductance channel showed apparently shorter duration of the open state than the smaller conductance channel as shown in Fig 3.3 (A). In outside-out patches the mean large conductance is 124 ± 13 pS (n=24) and the small one is 34 ± 5 pS (n=3). The dependence of conductance on $[K^+]$ is indicative of the higher permeability of the channel for K^+. The reversal potential from the mean data of large conductance channel in excised inside-out patches was +60 mV, giving a P_K:P_{Na} ratio (calculated from the G-H-K equation) of 15:1.

Table 3.2

	Channel conductance	Open probability
Type I	315 ± 45 pS (cell-attached patch) 151 ± 12 pS (inside-out patch) 124 ± 13 pS (outside-out patch)	0.1 to ~ 0.9
Type II	67 ± 19 pS (cell-attached patch) 38 ± 7 pS (inside-out patch) 34 ± 5 pS (inside-out patch)	< 0.1

Importantly, the large conductance channel was also readily identified in SaOS-2 cells. Typical channel openings and the I-V plot constructed from raw data from a typical recording are shown in Fig 3.4. This plot showed a distinct "tailing off" of current when the membrane potential is over 100 mV. This is because the K channel is virtually impermeable to Na^+, which caused the I-V relationship to become asymptotic to the abscissa whenever there is internal Na^+ block of the channel. This is a notable feature of BK channel having been pointed out in other tissues (Yellen et. al., 1984 and Paul et al., 1998). The channel conductance was calculated to be 286 ± 17 pS (n=17) from pooled I-V plots from cell-attached patches.

3.3.2 Channels in human primary osteoblast (HOB)

Single channel recordings from HOB cells were carried out using the same protocol as in the case of MG63 cells. The success rate at attaining giga seals on HOB cells was lower than 30%. The channels detected in these HOB cells again interestingly can be divided into 3 major types according to single

channel conductance. Typical channel openings in a cell-attached patch from a HOB cell are shown in Fig 3.5. The slope conductances of the three types of channels, determined from the current–voltage (I-V) relationship (see e.g. Fig 3.6) were 233 pS, 139 pS and 69 pS. Different types of channels opened either alone or alongside another type in cell-attached recordings. Typically the large conductance channel opened first at depolarization (e.g. 20 mV, see Fig 3.6) and the large conductance channel was found in 9 out of 10 patches. The activity of the large conductance channel was voltage-dependent, activity increasing when the cell membrane was depolarised, although occasionally, the channel went into long closed periods. The Po versus voltage data are shown in Fig 3.7 indicating that the large conductance and intermediate conductance channels were both voltage-dependent, channel activity increasing steeply with depolarization (P_o varies between 0.01 and 0.9). In the case of the small conductance channel the Po did not however change with the patch potential, remaining at < 0.1 up to + 80 mV.

3.3.3 Channels in mouse primary osteoblast and bone marrow cells

The channels identified in cell-attached patches from mouse primary osteoblasts can be divided into 2 types. The major type was also the large (c.f. data above) conductance (221 ± 9 pS) one (n=5) (Fig 3.8). It was expressed and active in about 80% patches in this cell type. Data from an excised inside-out patch gave an extrapolated reversal potential of 53 mV. Thus this channel is selective to K^+ because P_K: P_{Na} ≈15:1(calculated as described above). The

activity and density of this channel was lower than that observed in MG63 cells and human primary osteoblasts (see e.g. activation plot in Fig 3.9). Mouse bone marrow cells are much smaller than the mouse primary osteoblasts. So that these bone marrow cells were almost impossible to be patched. Only 3 successful seals were achieved although there were no data recorded from them, because the seals were lost almost immediately.

3.3.4 Channels in mouse osteoblast-like cells (7F2)

7F2 cells retain some features of mesenchymal cells and as such can differentiate into adipocytes. These cells can be distinguished easily under the microscope, 7F2 cells being fibroblastic, whereas the adipocytes were on average larger, were flat and possessed bright lipid droplets. In the differentiation medium (as stated in Section 2) these two types of cells often co-existed on the same coverslip and could be patched sequentially.

Interestingly, although seals could be readily obtained, no single channel openings were detected in either cell-attached or excised patch recordings from the adipocytic cells (n=19).

The cell-attached patches on the differentiated 7F2 cells went to excised inside-out patches very easily so no cell-attached patch recordings were made from these cells. Single channel recordings revealed in inside-out patches the presence of a larger (154 ± 11 pS) and smaller (31 ± 7 pS) conductance

channel in the differentiated 7F2 cells. In I-V plots in Fig 3.10 are shown the openings of these two different channels in inside-out patches from two 7F2 cells. The straight line regression fits generate slope conductances of 41 pS and 125 pS for type I and type II respectively.

3.3.5 Channels in mouse osteocytes (MLO-Y4)

Mouse osteocyte-like cells (MLO-Y4) were grown on collagen type1 coated coverslips for all patch-clamp experiments. Only cells showing a dendritric phenotype were patched. A small conductance channel was recorded in 15 cell-attached patches and gave a mean single channel conductance of 51 ± 9 pS (n=12). Po of the channel showed no significant changes (between 0.6 ~ 0.7) when membrane potential changed from +80 mV to +160 mV (see e.g. Fig 3.11). No large conductance channel was detected from MLO-Y4 cells in either cell-attached or excised patches.

3.3.6 Channels in rat primary osteoblasts and bone marrow cells

Rat primary osteoblasts and bone marrow cells were obtained from two different *Sprague Dawley* rats. Although seals were easy to achieve, no channels were detected in cell-attached patches from either rat primary bone marrow cells or osteoblasts at either depolarised or hyperpolarised potentials (n=13). No channels were found in excised patches from these cell types either (n=11).

3.3.7 Potassium channels in HEK293-α cells

Transfected HEK293-α cells were seeded on to poly-lysine-coated cover slips and were patched 24 hours later. These cells were a homogeneous population or were 'purified' by transfection with BK channel hSlo subunit. Hence only the large conductance voltage-dependent channel was observed under the conditions of these experiments. In cell-attached patches the conductance was calculated to be 210 ± 31pS (n=12, see e.g. Fig 3.12A). The activity of the channel increased when the membrane is depolarised. Fig 3.12B showed that the potassium channel in HEK293-α cell was voltage-dependent, the channel activity increasing on depolarisation, the $V_{1/2}$ being 120 mV.

3.4 Discussion

A number of different cell types were investigated in this section, in some cases there were no published data available on the complement of channels present in such cell types and in some instances the cells themselves were also new to the laboratory. It was therefore first necessary to establish that they could be patched easily and to survey what channel (if any) they possessed. As it turned out, all cell types could be patched although some were easier than others e.g. MG63 cells. In particularly, HOB and MG63 cells were easy to patch and gave an over 50% successful rate of getting "giga-seal". On the other hand, primary osteoblasts from rat and mice were hard to patch because of their size and even when patched the seal was lost easily. So that it caused

difficulties to gain data from these cells. Whole-cell patch had been tried on MG63 and HOB cells but it was hardly to approach a successful stable whole-cell patch. It either lost the seal or went to out-side out patch.

The cells that have been investigated include human osteoblast-like cells (MG63 and SaOS-2), human primary osteoblasts (HOB), mouse osteoblast-like cells (7F2), rat and mouse primary osteoblasts and bone marrow cells, mouse osteocyte-like cells (MLO-Y4) and a BK channel hSlo subunit transfected cell line (HEK293). Both cell-attached and excised patches were studied and a summary of the principal conductances identified is given in Table 3.3. Reversal potentials and the dependence on $[K]_o$ indicated that at least some of these openings could be attributed to currents through K^+-selective channels. Hence in excised patches in asymmetrical K^+ it was shown that the reversal potentials of these detected channels were around 60 mV, giving a calculated $P_k/P_{Na} \approx 15$ from the G-H-K equation. Thus these large conductance channels are modestly selective for K^+ (as shown in figures 3.3., 3.8 and 3.10). Slope conductances, determined from the current-voltage (I-V) relationship, varied from 20 pS to 300 pS. In some cases (e.g. the large conductance) the channel activity increased with the depolarisation showing these channels to be voltage-dependent. Other channels which were voltage-independent might be K_{ATP} channels, which have a unitary conductance of around 50 pS. Previous work in this laboratory has shown the message for the principal subunits of K_{ATP} exists in MG63 cells plus the appropriate electrophysiology and pharmacology (Henney et al., 2006).

Table 3.3 **Type I** = Large conductance (>150pS)
Type II = Intermediate conductance (50 pS~150 pS)
Type III = Small conductance (<50 pS)
√ , indicates presence of channel; n.d. indicates not detected

	Voltage-dependent channel			Not voltage-dependent channel
	Type I	**Type II**	**Type III**	
MG63 cells	√	√	√	√
SaOS-2 cells	√	n.d.	n.d.	n.d.
HOB cells	√	√	√	√
Mouse primary osteoblasts	√	n.d.	n.d.	n.d.
Mouse primary bone marrow cells	n.d.	n.d.	n.d.	n.d.
7F2 cells	√	n.d.	n.d.	√
7F2 adipose cells	n.d.	n.d.	n.d.	n.d.
MLO-Y4 cells	n.d.	n.d.	n.d.	√
Rat primary osteoblasts	n.d.	n.d.	n.d.	n.d.
Rat primary bone marrow cells	n.d.	n.d.	n.d.	n.d.
HEK293-α cells	√			

Previous work identified K channels in MG63 cells (Wann et al., 2004) and has revealed a putative role in cell secretion (Moreau et al., 1997). Hence MG63 cells were used as positive control to detect BK channels in this part of work. Similarly, BK hSlo subunit transfected HEK293 cells acted as a positive control for the expression BK channel. On the contrary, mouse osteocyte-like cells (MLO-Y4) were introduced as a negative control for BK channel (Gu et al., 2001).

The large conductance channels may be distinguished from the other channels in that it shows wide expression and high activity in almost all of these cell types. This channel was therefore highlighted for further investigations.

3.4.1 Potassium channels in osteoblast-like cells

As indicated above, potassium channels have been described previously in human osteoblast-like cells (Moreau et al., 1997), and significantly it has been suggested that these potassium channels modulate the secretion of osteocalcin. In this section, a large and intermediate conductance, voltage-dependent channel and a smaller conductance, voltage-independent channel were also identified. Additionally, another human osteoblast-like cell which is more differentiated (SaOS2) was investigated. In this cell only the large conductance channel was identified in single channel recordings. Although MG63 and SaOS2 cells are both derived from osteosarcoma they have different characteristics such as that SaOS2 cells more closely resemble osteoblast cells by having the ability to mineralise. Hence different channels may be expressed in the different cells for their specific functions. Osteoblast-like cells from mouse (7F2) was also studied for the first time. These 7F2 cells can differentiate into adipocytes so both phenotypes were patched and interestingly the results revealed that the large conductance (potassium) channels in 7F2 cell were not active in the adipocytes. Thus, in 7F2 cells both large and small conductance channels were located in inside-out patches, whilst in the parallel experiments on adipocytes no channel openings were observed. Why such channels are lost en route to differentiation into adipocytes is a question for the future.

HEK-α cells are native HEK293 cell transfected with the BK channel α subunit (hslo) cDNA. Recordings from cell-attached patches in these cells showed openings of only the large conductance, voltage-dependent potassium channel. All the openings match the characteristics of typical BK channel openings such as large conductance (210 pS) and voltage-dependence. The position of the activation (Po) curve on the voltage axis in the cell-attached recordings (e.g. Fig 3.12) makes an interesting comparison to the Po data for native channels in for example MG63 cells, given that there is no β subunit present in the HEK293 cells which is known to influence activation parameters. This is discussed further in the Section 4. The results from patches in these two types of cells served as useful negative and positive controls and highlight the position of the osteoblast or osteoblast-like cells in terms of the expression of the large conductance K channel.

MG63 cells and SaOS-2 cells are osteoblast-like osteosarcoma cell lines. These cells display such osteoblastic characteristics as the production of cAMP, responsiveness to PTH and prostaglandin E2, 1,25-$(OH)_2D_3$ induced osteocalcin and alkaline phosphatase synthesis (Lajeunesse et al., 1990) . The large conductance channel was found in both these cell lines, but the question is how well do these cells "model" the real osteoblast? For this reason it was crucial and additionally interesting to survey the complement of channels in primary osteoblasts.

3.4.2 Channels in primary bone cells

Primary cells from human, rat and mouse were investigated. The recordings from human primary cells (HOB) showed three types of channels: large conductance and intermediate conductance, voltage-dependent channels and a small conductance, voltage-independent channel. The results reveal a large conductance channel in 90% patches, a higher prevalence than in MG63 cells (70%). while the intermediate and small conductance channels are present in less than 20% of the patches. What is clear therefore is that MG63 cells represent a good working model for HOB at least in respect of the operation of these channel conductances.

In addition to HOB cells, rat and mouse primary osteoblasts and bone marrow cells were investigated. Surprisingly, there were no channels detected in recordings from cell-attached patches of rat osteoblasts or bone marrow cells (n=13) whereas in contrast the large conductance voltage-dependent channel was present and active in mouse primary osteoblasts but not mouse bone marrow cells (see Table 3.2 and section 3.3.3). The studies on juvenile bone in BK- deficient ($BK^{-/-}$) female mice revealed no BK channels expressing in mouse osteoblasts (Sausbier et al., 2011). In the patch-clamp studies reported here a BK channel was detected in mouse cells that were presumed to be osteoblasts. The question is are these electrophysiological data here truly in disagreement with the data of Sausbier et al. (2011) who carried out no electrophysiology. Or rather does it reflect the different methods used and their

antibody studies were simply deficient in not being able to identify the BK channel structure present in mouse osteoblasts.

The large conductance potassium channels are thus prevalent and active in human and mouse primary cells as well as in human osteoblast-like cell lines. This suggested a function for this channel in these cell lines which may match that in primary cells in vivo. Hence, future work focuses (see Sections 4, 5 and 6) on the characterisation of this channel in either these primary cells or cell lines.

3.4.3 Channels in other cells surveyed

As a comparison, patch-clamp studies were carried out on cells which are neither primary osteoblast cells nor osteoblast-like cells such as the mouse osteocyte-like cell line (MLO-Y4) and also transfected HEK-α cells.

In MLO-Y4 cells only the small conductance, voltage-independent channel was observed. The large conductance, voltage-dependent potassium channel was not apparently active in any patches from this type of cell. This is consistent with the initial description of potassium channels found in MLO-Y4 cells by Gu et al. (Gu et al., 2001). They explored the presence of mRNA for the type 1 and 2 small conductance Ca^{2+}-activated potassium channels (SK) and sulphonylurea receptor SUR2, a subunit of glibenclamide-insensitive ATP-dependent K channels (KATP). The message for the large conductance, Ca^{2+}-

activated potassium channel was not detected in their experiments (Gu et al., 2001).

3.5 Conclusion

This section of work aimed to conduct a preliminary patch-clamp single channel survey on the expression of activities of channels in primary osteoblasts, primary bone marrow cells, osteoblast-like cells, osteocyte-like cells and DNA transfected HEK293 cells. Data from this survey gave initial fundamental and important information on the viability and suitability of cells along with the channel type, prevalence and activity in these cells. A large conductance (> 200 pS), voltage-dependent potassium channel (assumed to be BK) was observed in almost all cell types. BK channel is classically a voltage-dependent, Ca^{2+} - activated potassium channel with a large conductance. It is found in a wide variety of cells including nerve cells, muscle cells and endocrine cells. One report concludes that the BK channel may regulate MG63 cell secretion (Moreau et al., 1996). This laboratory has presented in preliminary form findings suggesting that BK channels express with high density and activity in both MG63 and SaOS-2 cells (Wann et al., 2004a and Wann et al., 2004b). Given that they are found in almost all the cells being investigated in this section, the BK channel was considered ideal for further investigation on its characteristics and more importantly possible function in osteoblast–like cells and primary osteoblasts.

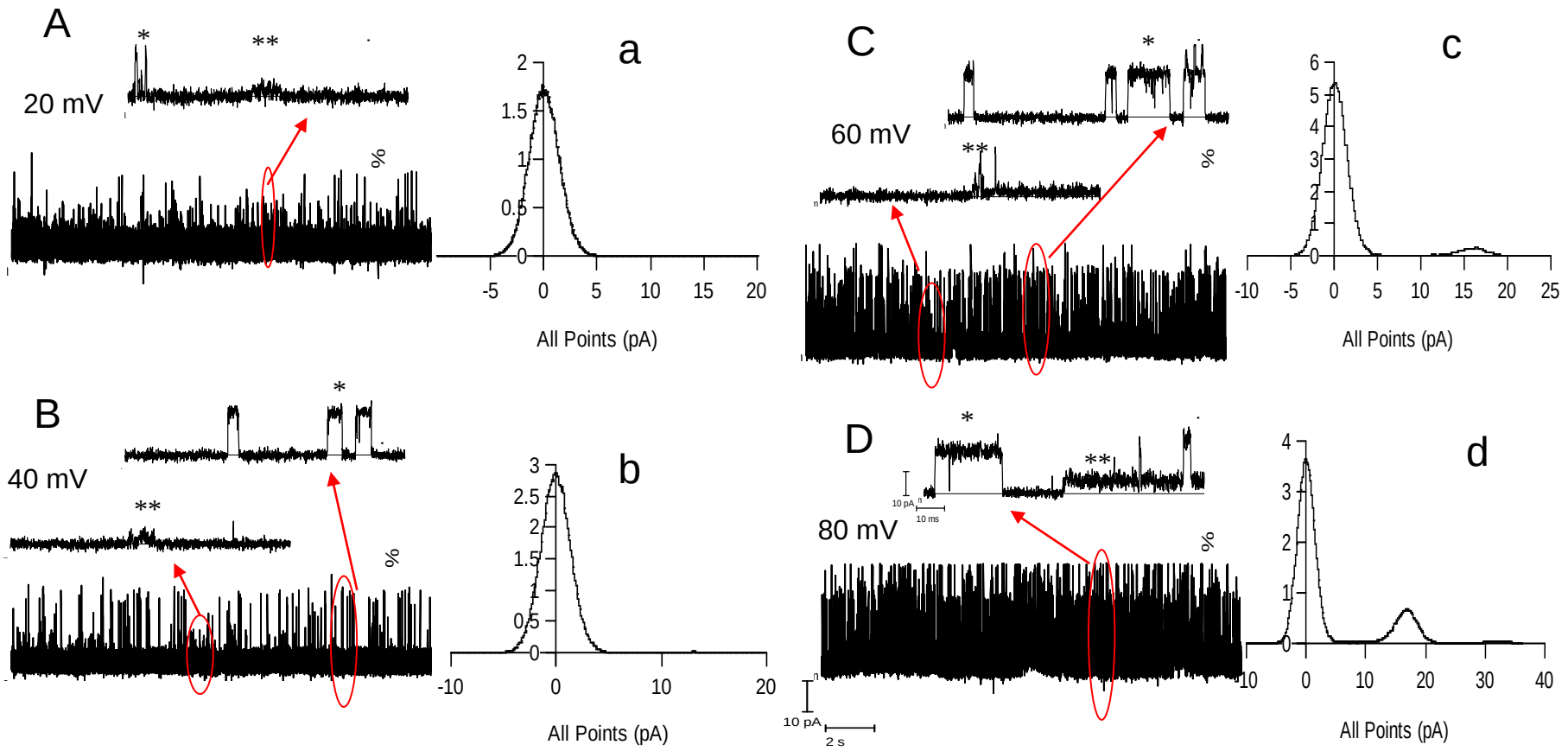

Fig 3.1 Channel openings recorded at various membrane potentials in a single cell-attached patch from an MG63 cell. The raw data in panels A, B, C and D show openings at assumed membrane potential of 20, 40, 60 and 80 mV from at least two types of channel. One type of opening is of large amplitude (e.g. >10 pA) and is of a modest duration. The other opening was on average much longer and was of smaller amplitude (unitary current < 5 pA). The amplitude histograms (a, b, c, and d) constructed from the raw data show very clearly these two channel types which are denoted by * and **. The two sets of caliberation bars in D refer to all of the panels. The "Bin Width" set up for histogram analysis is 0.2 pA and the "Bin number" is 500.

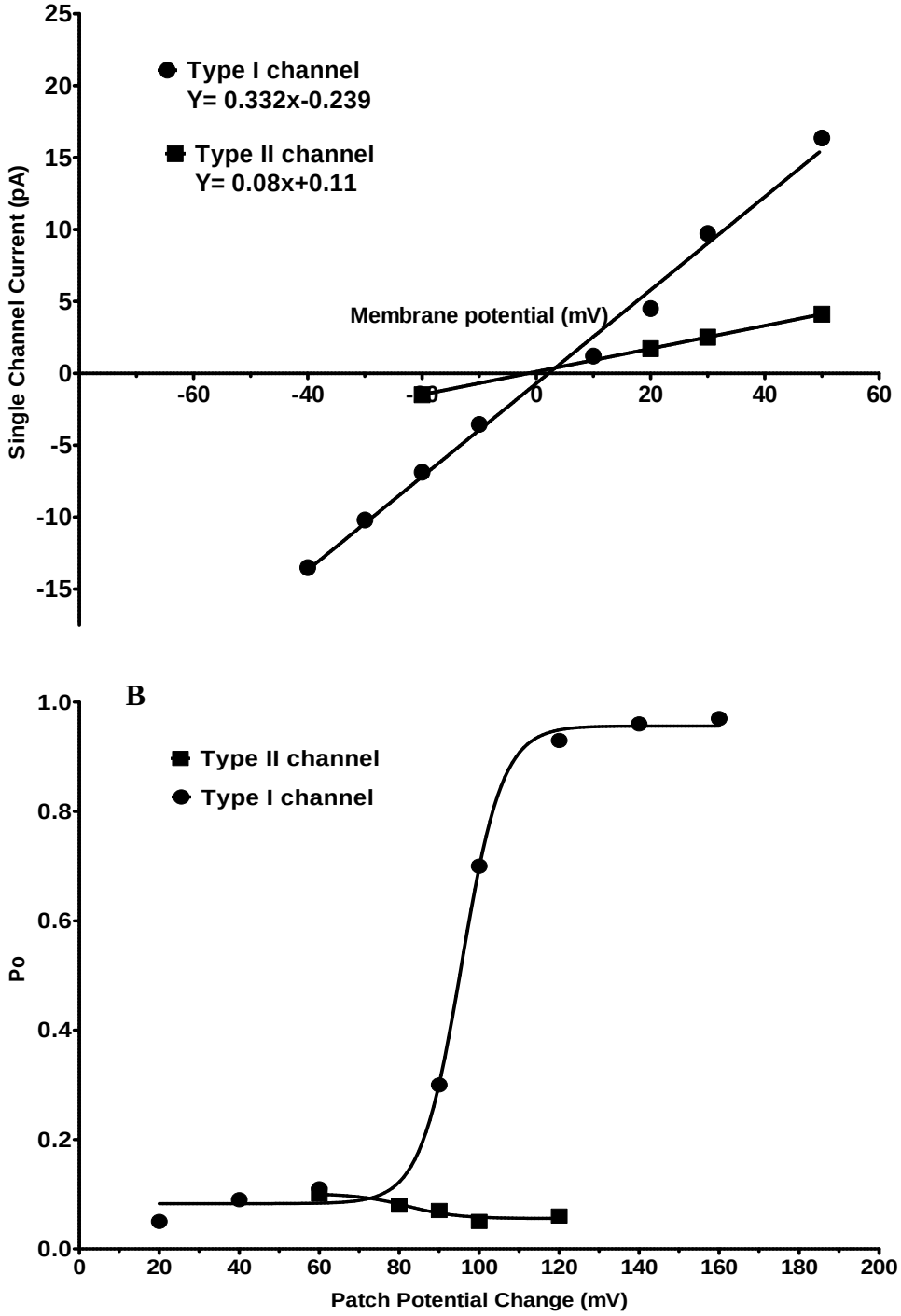

Fig 3.2 *I-V* plots from the openings of the 2 different channels (A) and the corresponding voltage- activation curves for these channels (B) in a single cell-attached patch from an MG63 cell. A) The straight line regression fits to the *I-V* plots yielded slope conductance of 332 pS for the type I, and 80 pS for the type II channel respectively. B) The Po versus voltage data for the type I channel were fitted by a Boltzmann function, giving a $V_{1/2} \approx 90$ mV, slope factor = 5.1. In the case of the type II channel, the Po was voltage-independent with a value lower than 0.1.

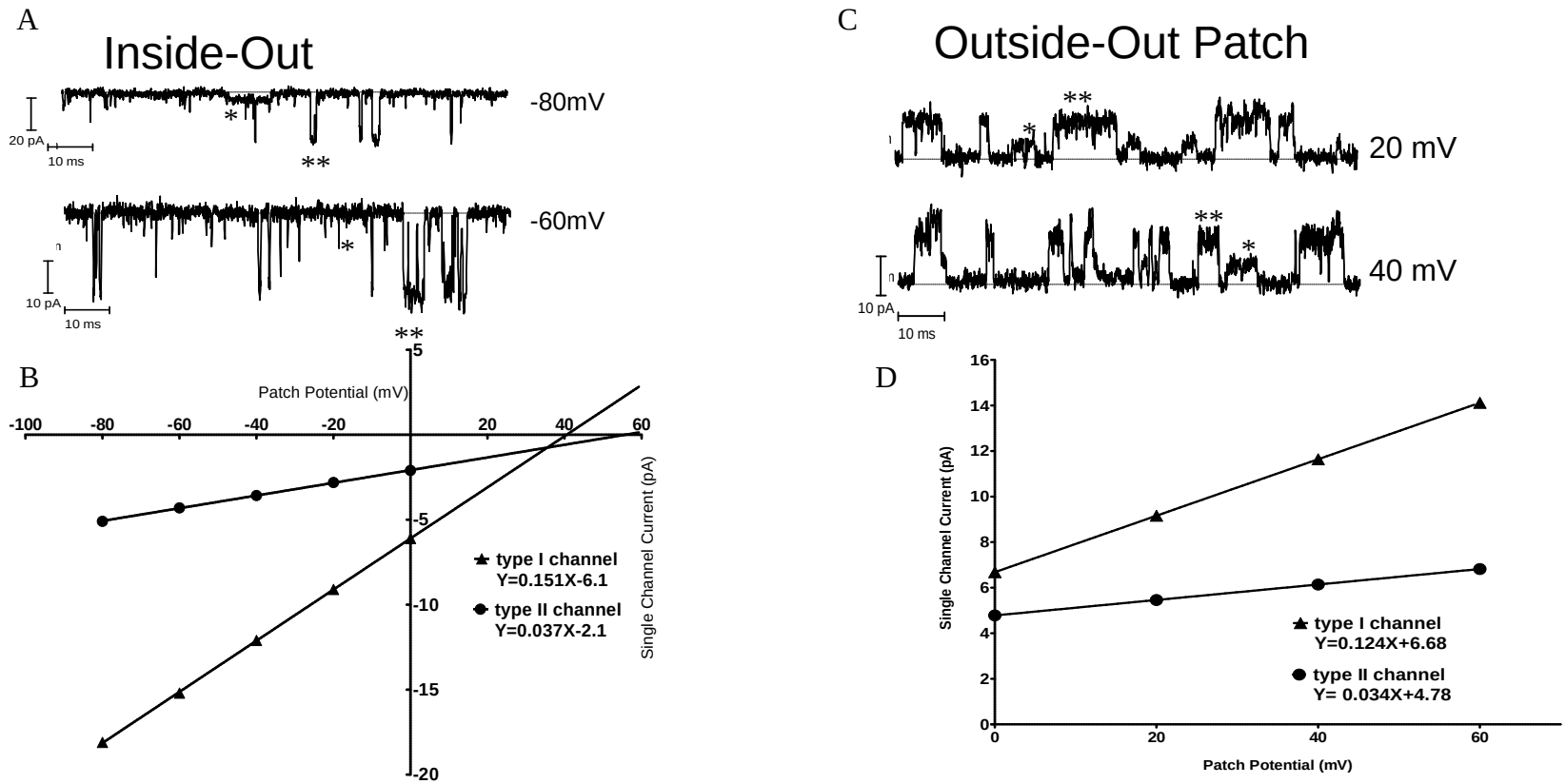

Fig 3.3 In MG63 cells small conductance channels were found alongside a large conductance channels in both inside-out and outside-out patches. Raw data (A) showed that in an inside-out patch two types of channel openings (denoted by asterisks) were recorded at -80 and -60 mV patch potential. As shown in (B), the plot of the single channel current against the patch potential gave values of conductances as 151 pS and 37 pS. The extrapolations indicate E_{rev}= 56 mV and 40 mV respectively. (C) and (D) show equivalent channel data in an outside-out patch. The conductances for the two channels here are 124 pS and 34 pS (see D).

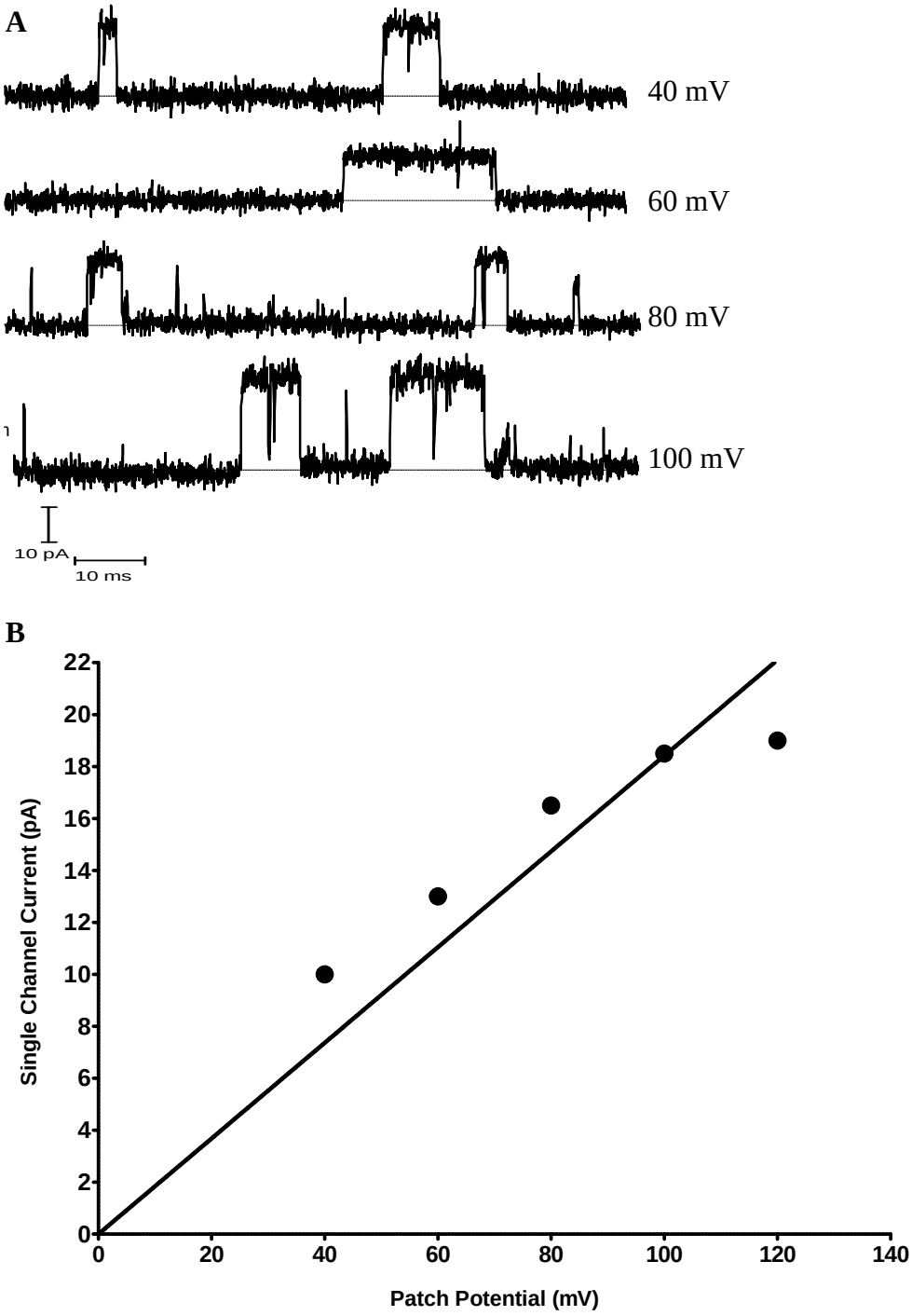

Fig 3.4 Channel openings recorded at various membrane potentials in a single cell-attached patch from an SaOS-2 cell (A) and *I-V* plot generated from these channel openings (B). (A) The raw data show that the large conductance channel opens at depolarized potentials (assumed membrane potentials 40, 60, 80 and 100 mV). (B) The linearity of the *I-V* plot between 0 and 80 mV membrane potential in symmetrical K^+ solution yielded the slope conductance of 219 pS.

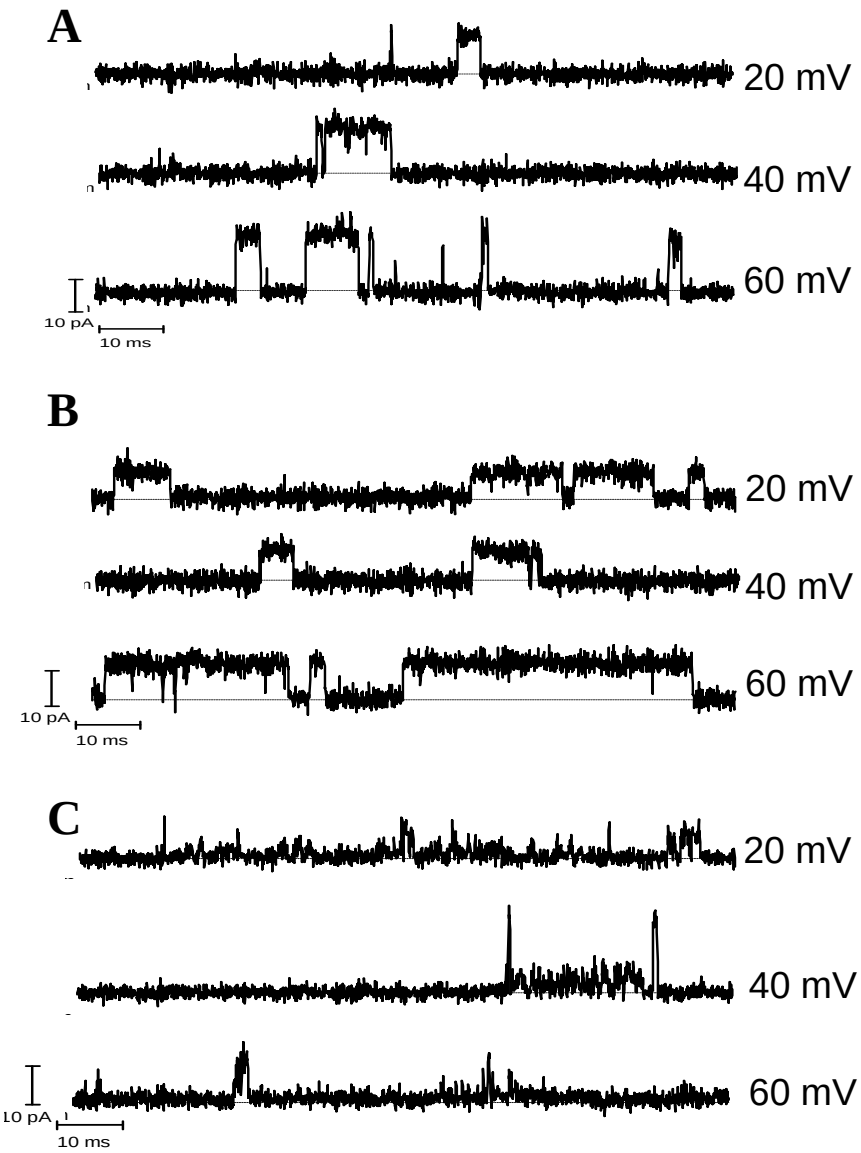

Fig 3.5 Sample traces of single channel current recorded in different cell-attached patches from HOB cells. A, B and C showed three different types of potassium channels which opened at depolarised potentials. Traces in (A) indicate the large conductance channel. (B) Shows recorded openings of an intermediate conductance channel, compared to the large conductance channel it shows longer open times on average. (C) A small conductance channel open alongsides the other two types of channel and its openings were hard to distinguish from the system noise.

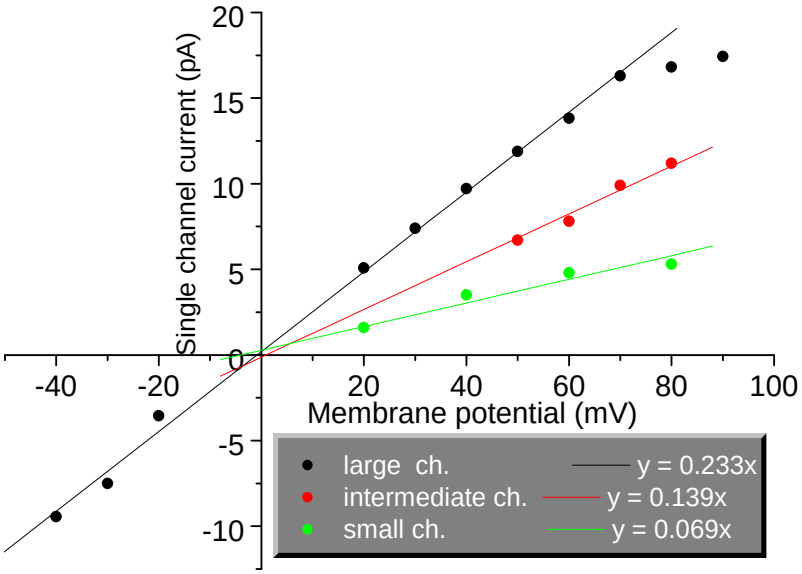

Fig 3.6 *I-V* plots from the 3 different channel openings. The straight line regression fits to the *I-V* plots yielded slope conductances of 233 pS for big conductance channel, 139 pS for intermediate conductance channel and 69 pS for the small conductance channel.

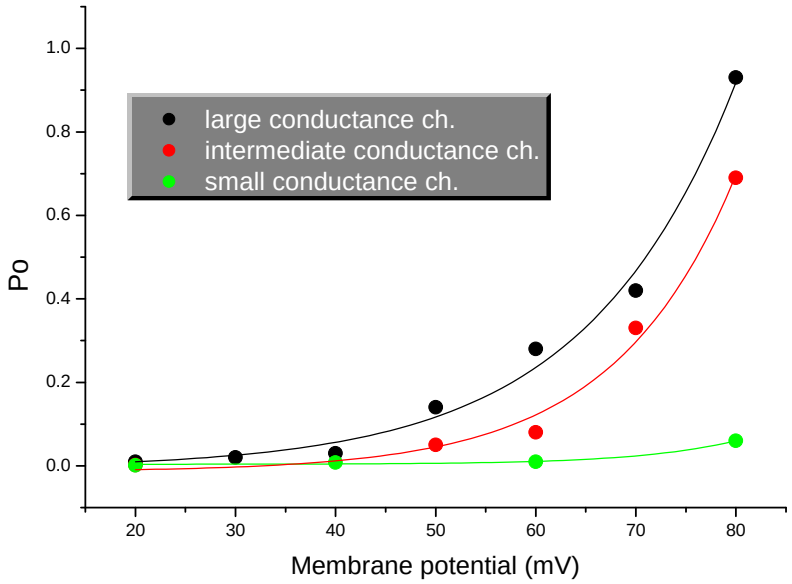

Fig 3.7 The corresponding voltage-activation curves for these channels in HOB cells. The large conductance and intermediate conductance channels are voltage-dependent, their open probability increasing with depolarised potentials (● and ●). The activity of the small conductance channel as a function of membrane potential is shown for comparison (●).

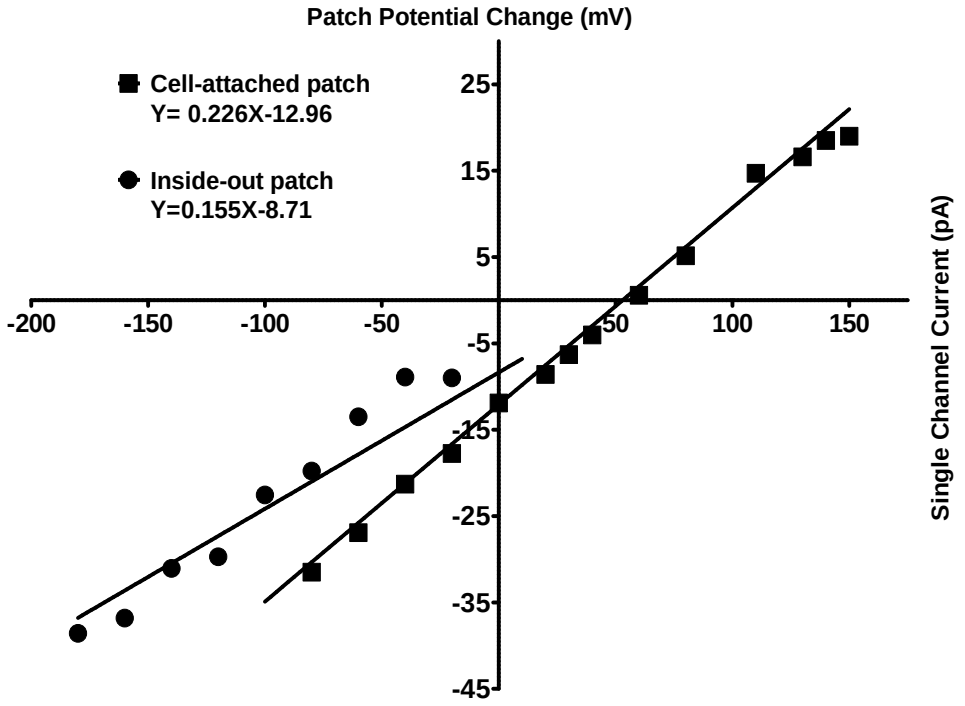

Fig 3.8 The large conductance channel is present in mouse primary bone cells in both cell-attached and inside-out patches. The current-voltage plot showed that in the cell-attached configuration the single channel conductance was 226 pS with a reversal potential around 50 mV depolarised to rest. The conductance was 155 pS in the inside- out patch reverse physiological gradient ($140K_o/3K_i$) with an extrapolated reversal potential of 53 mV

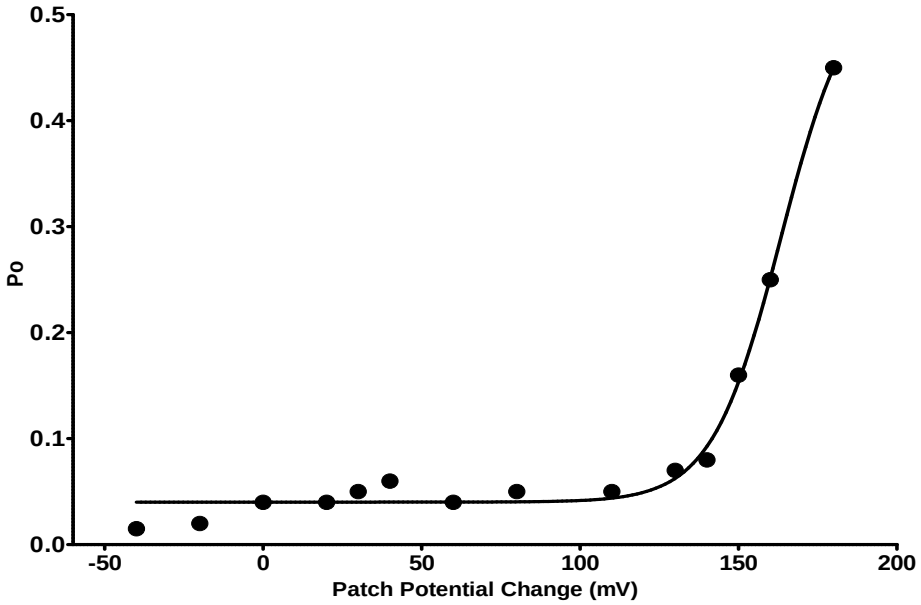

Fig 3.9 The relationship between the open probability of the large conductance channel and membrane potential in a cell-attached patch from a mouse primary bone cell. The $V_{1/2}$ was estimated at 163 mV, slope factor = 10.9.

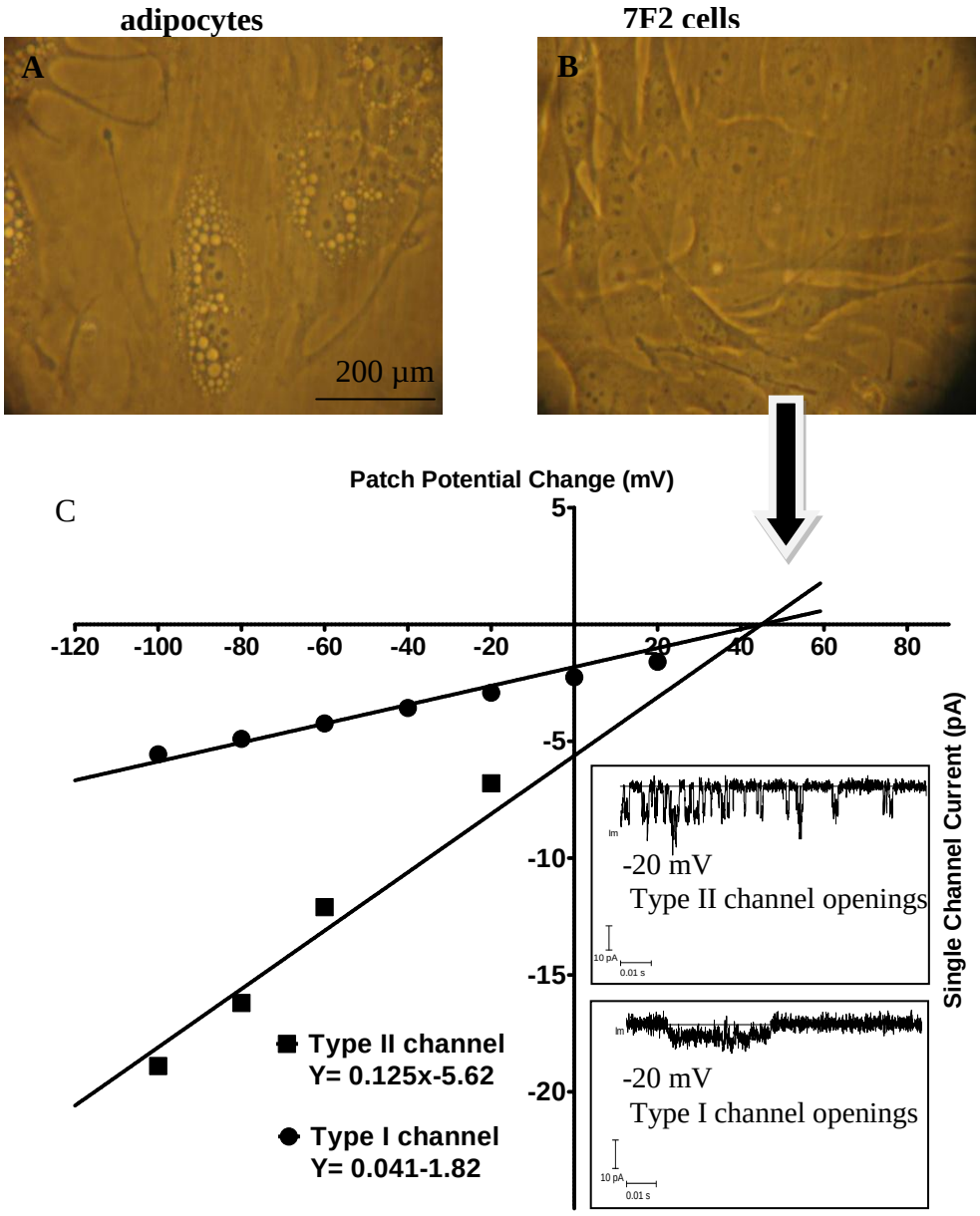

Fig 3.10 Two types of channels in inside-out patches from 2 7F2 cells. A) and B) show images of the adipocytes and 7F-2 cells respectively. C) The I/V plots yield conductances for the type I and type II channels of 41 pS and 125 pS respectively. The extrapolated reversal potentials were for type I and II of +44 mV in both cases. Insets show sample data at -20 mV for the two channel types.

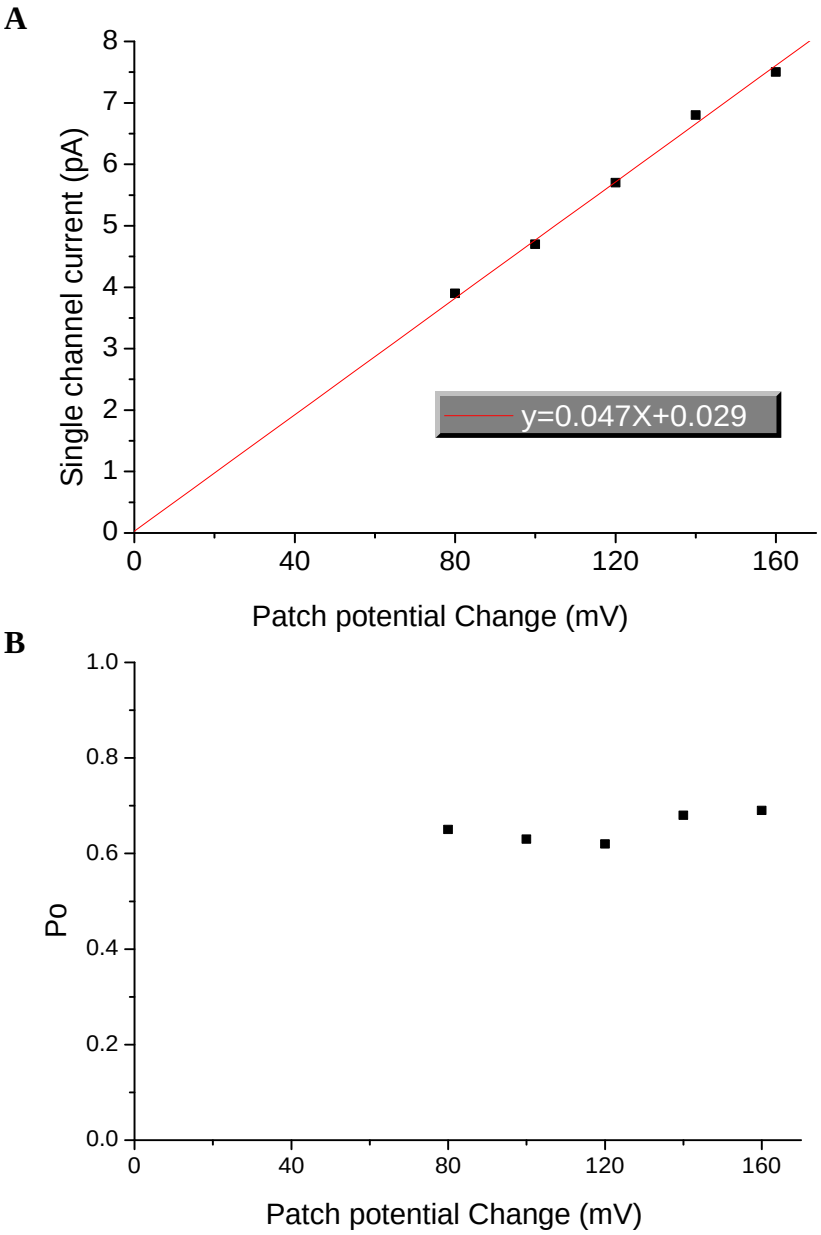

Fig 3.11 A small conductance channel is present and active in cell-attached patches from a MLO-Y4 cell. A) The *I-V* plot was linear and gave a slope conductance of 47 pS. B) The relationship between Po and membrane potential was constant (0.6- 0.7) between + 80 mV to + 160 mV.

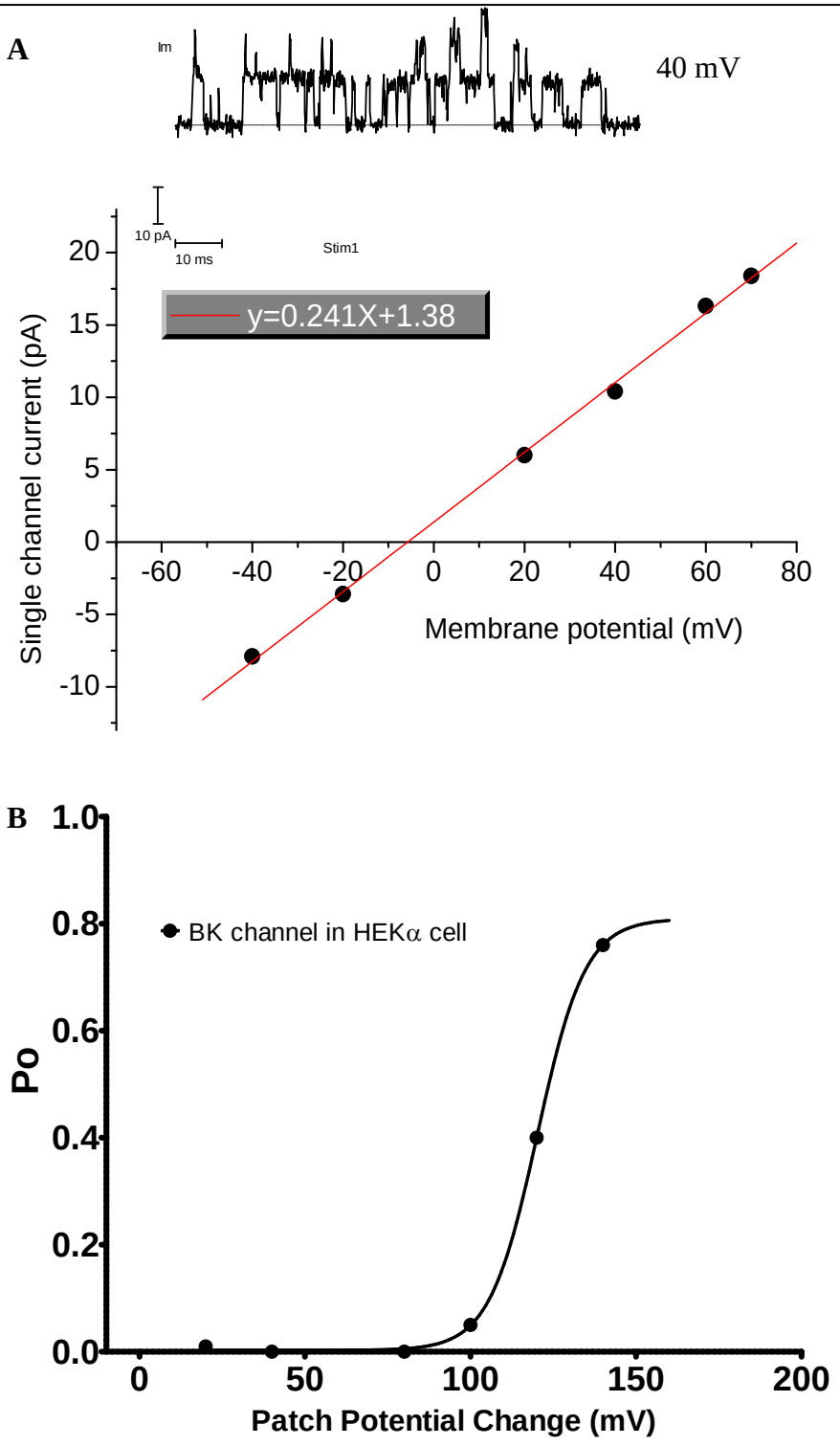

Fig 3.12 Cell-attached patches from HEK293-α cells possessed large conductance channels. A) The *I-V* plot was linear between -40 and +70 mV and yielded a slope conductance of 241 pS. B) Po – V plot shows that the channel activity increased markedly with depolarisation. The data were fitted by a Boltzmann equation, the $V_{1/2\ Po}$ being 120 mV, slope factor = 7.2.

SECTION 4: EXPRESSION AND ACTIVITY OF BK CHANNELS IN MG63 AND HOB CELLS

4.1 Introduction

The BK channel belongs to a Ca^{2+}-activated K^+ channel subfamily which is widely expressed in both excitable and inexcitable cells. It is easily identified because of its very large conductance and hence large unitary current (10 times of the other K^+ channels) when opened (Rothberg, 2004). The opening of BK channel results in a large efflux of K^+ ions which will cause a rapid powerful hyperpolarisation of the cell (Rothberg, 2004). This powerful current through the BK channel occurs in response to electrical depolarisation of the cell membrane and/or increased intracellular calcium (Rothberg, 2004). The dual regulation of BK channel means that these channels can regulate strongly the cell membrane potential over a broader range of physiological conditions comparing to other ion channels (Hille et al., 1992).

4.1.1 BK channel structure

Ca^{2+}-activated K^+ channel subunits have 6 or 7 transmembrane domains and a single pore domain. In contrast, to the other two Ca^{2+}-activated K^+ channels (IK and SK), the BK channel has additional hydrophobic segments resulting in an extra transmembrane domain at the N-terminus so that the pore-forming subunit (α-subunit) possesses 7 transmembrane domains. It has now been established that in addition to the pore forming α subunit, tissue specific accessory β subunits are expressed in different cell types. The native channel is suggested to be formed from 4 α-subunits in combination with associated 4 β-subunits. The extracellular loop of the β subunit lies near the mouth of the ion pore. This structure is describes as below.

The human α subunit (hSlo) is encoded by a single gene that is located in human chromosome 10. Seven transmembrane domains of α subunits are referred to as S0 to S6. In addition to the extra S0 domain, the BK channel has a long intracellular cytosolic C-terminus where at least one of the regulatory Ca^{2+}-binding domains resides (Schreiber and Salkoff, 1997). This sequence is also called the Ca^{2+} bowl which relates to the channel's sensitivity to intracellular Ca^{2+} changes. The hairpin loop between S5 and S6 forms the ion

pore. K channels are classified as "long pore channels" and all K channels have essentially the same pore constitution. Without exception, all K channels contain the same "signature sequence" TVGYG which provides carbonyl oxygens that form four K binding sites (Heginbotham et al., 1992 and Doyle et al., 1998). The S4 domain of the BK channel, like all voltage-gated (S4) channels acts as the voltage sensor. Recent studies have led to the suggestion that channel open time, unitary conductance, and voltage- dependence of BK channels are determined by the N-terminal core, whereas Ca^{2+} sensitivity of the channel appears to involve a region of several negatively charged residues at the C-terminal core (Knaus et al., 1995). Co-expression experiments of recombinant hSlo and the β-subunits of the BK channel indicate that the β-subunit shifted the mid-point of activation in the Po versus voltage curve (McManus et al., 1995). The β-subunit acts as the regulator and the structure is much simpler than α-subunit. It is formed by 4 exons spanning ~29 kb of human chromosome 5. The subunit is formed of two transmembrane domains with a highly glycosylated intracellular loop (ψ). Recently, genes encoding four types of β-subunit (β1-β4) have been discovered and characterized, and diversity is further enhanced by alternative splicing of the β3 mRNA (Wallner et al., 1996). The regulatory β subunit is associated with the extracellular N-terminus of α subunit. This structure can be summarised in the schematic below.

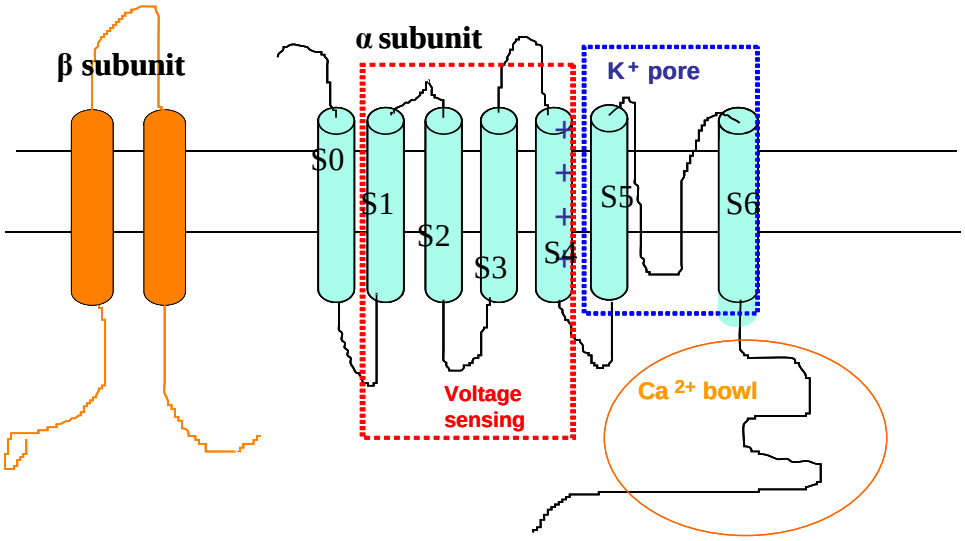

4.1.2 BK channel characteristics

Electrophysiologically BK channels are distinguished from other K channels on the basis of their large conductance and novel gating system. When $[Ca^{2+}]_i$<100 nM, BK channel is in a Ca-independent state which means that channel activity is mostly related to voltage. When $[Ca^{2+}]_i$ >100 nM, less electrical energy is required to open the channel (Toro et al., 1998). In addition, the BK channel sensitivity to Ca or voltage is regulated by the associated β subunits. 4 different tissue specific β subunits confer different functions e.g. the α+β1 combination has a low affinity for iberiotoxin (IbTX, a selective blocker for hslo). Channels comprised of β2 subunits inactive rapidly. The β3 subunit is found in pancreas and spleen cells. α+β3 constructs produce channels with activation properties similar to those of α subunit. The β4

subunit endows the channel with mixed characteristics. Brenner et al., (2005) report either up- or down- regulation of channel activity formed from co-expression of α and β4 at lower and higher Ca^{2+} concentrations respectively.

4.1.3 BK channel expression and function

BK channels are involved in various (patho)physiological conditions. In the cardiovascular system, BK channels are thought to be key players in ensuring normal vasomotor tone by regulating the excitation-contraction coupling process. The function of BK channels present in urinary bladder smooth muscle is to maintain the balance between contraction and relaxation of these cells. At present, BK channel dysfunction is also being considered as a cause for certain neurological disorders. BK channels are present in the dendrites, axons, and synaptic terminals and play an important role in controlling the excitability of neurons. They also influence neuronal signalling and neurotransmitter release. In skeletal muscle BK channels are responsible for the repolarisation of the action potential (Siemer and Grissmer, 1999). BK channels are also found in osteoclasts (e.g. Sausbier et al, 2011) and can be activated by the factors that elevate internal Ca^{2+}. This has been proposed to cause hyperpolarization of the osteoclast, which would decrease Ca^{2+} influx, giving rise to negative feedback (Wiltink et al., 1995). High density BK channels have also been identified in osteoblast-like MG63 cells (section 3 here and Wann et al., 2004). But precisely what type of BK channel i.e. the subunit composition is still unknown. In this section an attempt is made to

characterise the BK channel in osteoblast-like MG63 cells. The long term goal is to define its subunit composition and the hypothesis is that physiological parameters provide a clue to the type of β subunit present. Also the expression and properties of the BK channel in human primary osteoblasts is described for the first time.

4.2 Materials and methods

In this section both molecular biology (RT-PCR) and patch-clamp electrophysiology techniques were used to probe BK channel properties in both human osteoblast-like MG63 cells and primary human osteoblasts.

4.2.1 Cell culture

The culture conditions for human osteoblast-like MG63 cells and primary human osteoblasts were as described in Section 2.

4.2.2 RT-PCR

As described in Section 2, following the TRIZOL isolation protocol, RNA was extracted from MG63 (passage 27) and HOB cells. To quantify the amount of RNA, 2 µl RNA was mixed with 68 µl sterile water and the solution was transferred into a Quartz chamber. The light absorbency of the sample was

measured at 260 nm (for RNA) and 280 nm (for DNA). The reference number for RNA absorbency at 260 nm is 10 OD ≈ 40 µg/ml and the acceptable range of A_{260}/A_{280} is 1.8~2.

The Ambion RT System Kit® was used for reverse transcription reactions. Each 40 µl reaction mixture contained 2 µg RNA :

	Reaction	**Control**
1M $MgCl_2$	8 µl	8 µl
10x buffer	4 µl	4 µl
dNTP mix	4 µl	4 µl
RNAase	1 µl	1 µl
AMV RT	1.4 µl	/
Oligo dTprimer	2 µl	2 µl
RNA	2 µg	2 µg
Sterile H_2O	Top up to 40 µl	Top up to 40 µl

Controls were carried out without AMV RT. These reactions were run with the following programme: 42 ºC for 60 minutes followed by 99ºC for 5 minutes then soak at 4ºC. The cDNA samples were stored at -20 ºC till used for PCR.

Four sets of primers were used to run the PCR reactions. Primers for BK channel α- subunit (KCNMA) and β1-subunit (KCNMB1) were designed according to Allard et al. (2000) and Hartness et al. (2003). The other sets for BK β2-subunit (KCNMB2), β3-subunit (KCNMB3) and β4-subunit (KCNMB4) were designed as follows:

1. The National Centre for Biotechnology Information (NCBI) nucleotide database was searched for the BK channel β2, β3 and β4 subunit genetic sequences in the human genome.

2. The mRNA sequences obtained were copied into "source sequence box" of the Primer3 primer design software (Rozen and Skaletsky, 2000).
3. The selected paired primers were checked against the complete genetic sequence by using web-based Ensemble software (Hubbard et al., 2007). This step ensures the primers chosen are intron-spanning ones. Thus only mRNA (not genomic DNA) would be amplified during the PCR reaction cycles to yield products of the right size.
4. Finally, specificity was confirmed by BLAST analysis.

All the primers used in this project were purchased from Invitrogen (UK).

	Forward	**Reverse**
BK α subunit (KCNMA1)	5'-acgcaatctgcctcgcagagttg-3', 1640-1662	5'-catcatgacaggccttgcag-3', 2047-2028
BK β1 subunit (KCNMB1)	5'-ctgtaccacacggaggacact-3', 268-288	5'-gtagaggcgctggaataggac-3', 456-436
BK β2 subunit (KCNMB2)	5'-catgtccctggtgaatgttg-3', 465-484,	5'-ttgatccgttggatcctctc-3', 701-682
BK β3 subunit (KCNMB3)	5'-aacccccttttcatgcttct-3', 537-556	5'-tcttcctttgctcctcctca-3', 813-794
BK β4 subunit (KCNMB4)	5'-gttcgagtgcaccttcacct-3', 195-214	5'-taaatggctgggaaccaatc-3', 439-420

PCR reaction mixtures contained:

cDNA	1 µl
Primers	4 pmol each
GoTaq polymerase	0.625 U
$MgCl_2$	1.5mM
dNTPs	0.8mM
GoTaq reaction Buffer	12.5 µl

dNTPs were from Bioline Ltd. (London, UK) and all other reagents were from Promega. PCR cycling conditions were determined as following after 4 trials:

95°C for 2 min → 95 °C, 30 s →58 °C, 45 s →72 °C, 60 s →72 °C for 5 min

40 cycles

All reactions products were visualized on 2% agarose gels by staining with ethidium bromide. Negative controls (i.e. water blank and no RT product as a template) were performed in all PCR experiments.

4.2.3 Patch-clamp

Single-channel recordings were made from cell-attached and cell-free excised patches and segments of data analysed as described in Section 2 & 3. The passage number of MG63 cells was below than 34. The passage number of HOB cells was 3 and 4. The HOB cells were being patched first time in this laboratory. The successful rate of achieving seals was about 50% and these were usually acquired within 2 to 3 minutes.

4.3 Results

RT-PCR and the single channel electrophysiological studies in MG63 and HOB cells showed clearly the expression, the high density and the high activity of BK channels.

4.3.1 RT-PCR in MG63 and HOB cells

The messages for the BK channel α subunit (KCNMA1) and four β subunits (KCNMB1, 2, 3 and 4) were detected in MG63 cells by RT-PCR. Of considerable importance too was that the RT-PCR detected the messages for

the BK channel α subunit (KCNMA1), and only the β1 and β4 subunits in HOB cells. Fig 4.1 shows the bands of appropriate size for the BK channel subunits in the electrophoresis gels.

4.3.2 BK channels are functional in both MG63 and HOB cells

Since the PCR results demonstrated the existence of the messages for BK channel subunits in MG63 and HOB cells, it was anticipated that single-channel recording would reveal the presence of these BK channels in both cell types. This was indeed the case.

4.3.2.1 BK channels in MG63 cells

MG63 cells were relatively easy to patch and single channel recordings showed that in cell-attached patches the BK channel was densely expressed and active. Thus in about 80% of patches there was more than one opening in a single patch when recording with electrodes of resistances mostly 3-5 MΩ, tip diameter around 1 μm. Typical openings in a cell-attached patch from an MG63 are shown in Fig 4.2. As $[Ca^{2+}]$ actives BK channel, the high density of the BK channel in MG63 cells was clear when the $[Ca^{2+}]$ facing the inner mouth of channel was high as in excised inside-out patches in reverse physiological K^+ gradient (i.e. 1 mM Ca^{2+}). The amplitude histogram from a typical inside-out patch recording is shown in Fig. 4.3. Each current peak indicates one opening; hence there were a total of 3 openings. The maximum

number of openings was usually 3-4 although it could be higher in some patches. The unitary currents were derived from the distribution of all current amplitude histograms and plotted against the patch potential in I-V plots (Fig. 4.4). As described in section 3, the mean slope conductances for the BK channel in cell-attached, inside-out and outside-out patches were calculated to be 315 ± 45 pS (n = 98) in symmetrical K^+ (K_i/K_o =3/140) , 151 ± 12 pS (n = 6) and 124 ± 13 pS (n = 16) in asymmetrical K^+ (3/140). It should be noted that the inside-out data were obtained in a reverse physiological gradient. The success rate in maintaining patches in these configurations (for longer than several minutes) was 87 and 80 % for inside-out and outside-out configurations respectively. Channel open probabilities from cell-attached patches, computed from the areas under the open peaks, were plotted against the patch potential (Fig. 4.5A) and data fitted by a Boltzmann function. The channels were strongly voltage-dependent with a $V_{1/2}$ of 107 mV (n=3). The open probability of BK channels in excised inside-out patches in reverse physiological K^+ gradient was close to 1.0 over a wide range of negative patch potentials. Typical data are shown in Fig. 4.5B.

The kinetic states of the BK channel were also studied using the 50% transition detection method followed by plotting log-square distributions of open and closed times. Meaningful values for the open and closed time distributions were difficult to achieve because, as stated above, more than one channel was present in 80% of cases. However, Fig 4.6 was produced from a recording from an inside-out patch with only one channel at -60 mV. The open time

distributions were fitted with two exponentials giving two components of τ_{o1} = 3.804 ± 0.337 ms and τ_{o2} = 0.0924 ± 0.0177 ms. The closed time distribution was fitted in the same way and also gave τ_{ca} = 7.683 ± 1.307 ms and τ_{cb} = 0.0137 ± 0.00484 ms. This indicated that BK channel gating in MG63 cells leads to at least 2 distinct open and 2 distinct closed states.

The Ca^{2+}-dependence of the channel was clear from experiments where recording were made from outside-out patches where different High K solutions were used as filling solutions for the patch electrode. As expected channel activity increased with the $[Ca^{2+}]_i$. This effect was most obvious at positive potentials where the BK activity was almost 5 times higher with 1mM Ca^{2+} than with 30 nM Ca^{2+} (see Fig 4.7).

4.3.2.2 BK channels in primary human osteoblasts

Very little electrophysiology has previously been carried out on human primary osteoblasts. Single channel recordings from HOB cells revealed the prevalence and high activity of BK channels. BK channels were observed in 13 cell-attached patches. Fig 4.8 shows a typical example from a cell-attached patch showing BK channel openings at different patch potentials. The histogram from the all points distribution of current amplitudes revealed at least 3 active channels. Current-voltage data for this channel in cell-attached patches were fitted by a straight line yielding mean slope conductances of 268 pS (Fig 4.9A). The relationship between the open probability and voltage for the same four

patches was fitted by a Boltzmann function with a mean $V_{1/2}$ of 108 mV (see Fig 4.9B).

Recordings from inside-out patches revealed that BK channels in human primary osteoblasts in reverse physiological potassium were active, the Po being > 0.7 over a range of potentials (data not shown). This compares favourably with the high Po (~ 1.0) for the BK channel in the case of MG63 cells under the same conditions (Fig.4.10).

4.3.3 Conclusion

In this section the expression and characterisation of the large conductance channel, BK was studied. In summary, the results showed importantly that the BK channel was expressed in both MG63 cells and primary human osteoblasts (HOB). This is the first time the channel has been reported in HOB cells. The channel had all the hallmarks of large unitary conductance, $[Ca^{2+}]_i$ sensitivity and voltage-dependence.

4.4 Discussion

4.4.1 RT-PCR showing the expression β1 and β4 subunits

Although the BK channel has been identified in MG63 cells by others in addition to this laboratory (Moreau et al., 1997; Rezzzonico et al., 2002; Wann

et al., 2004), RT-PCR results in this section are the first evidence for the β1, 2, 3, and 4 subunits of BK channel in MG63 cells and the β1, 4 subunits and α subunit of BK channel in HOB cells. The β subunits are important players contributing greatly to the functional properties of the BK channel (e.g. Lu et al., 2006). Importantly, the β1 subunit is suggested to be the necessary associated β subunit for BK channel sensitivity to the estrogens (Valverde et al., 1999; De Wet et al., 2006), the estrogens activating the channel through a direct association with its subunits. Estrogen is of course considered an important regulator of osteoblast function and is used a therapeutic drug for some bone diseases such as osteoporosis. Estrogen replacement therapy contributes to the maintenance of skeletal mass which is related to the positive impact that it has on osteoblasts (Taranta et al., 2002). In addition to the classical estrogen receptor (ER), given the presence of the β subunit, BK channels might be another binding site for estrogen in osteoblasts, by analogy with other tissues. Hence in vascular smooth muscle there is thought to be a binding site for estrogen on the β1 subunit of the BK channel itself and it is argued that women in earlier life are less susceptible to cardiovascular disease as a consequence (Valverde et al., 1999). In conclusion, RT-PCR results show that the message for the BK channel β1 subunit exists in MG63 and HOB cells, so suggesting a possible route for estrogen enhancement of the BK channel in osteoblasts. Unfortunately here it was only possible to "activate" the BK channel with chronic exposure to estrogen so its action remains perhaps ambiguous.

The β4 subunit was first discovered in neuronal tissues and the co-expression of β4 subunit increase the voltage sensitivity of BK channel (Ha et al., 2004) left shifting the channel activity (P_o - V) curve. β4 subunit associated BK channels possess distinctive pharmacological characteristics such as apparently low sensitivity to the scorpion toxins. In summary, it can be concluded that the native BK channels in both MG63 and HOB possess both β1 and β4 subunits at least and that any properties of these channels should reflect that composition. Specifically, the pharmacology of the channel should be a function of the β subunit composition. Future experiments should consider examining the influence of channel subunit composition on biophysical properties of the channel, namely conduct a full channel lifetime analysis and examination of substate behaviour as a function of the β subunit composition.

4.4.2 Electrophysiological features of BK channels in MG63 and HOB cells

BK channel events in MG63 cells or HOB cells were easily detected in single channel patch-clamp recordings. BK channel opening results in such a large K^+ efflux and hence unitary current which increases with depolarisation (at least in cell-attached and outside-out patches), making it easy to distinguish in both cell-attached and excised patches. Another very important "hall mark" feature of the BK channel in these cells is the high activity. In terms of prevalence, it is also comparable to some excitable cells e.g. Xenopus motor nerve terminals (Sun et al., 2004). The high prevalence and activity make it compelling to argue a strong case for function in these cells. This is particularly true given

that, when activated, it contributes such a large fraction of the membrane current.

4.5 Conclusion

In 1996 the BK channel was reported for the first time in inexcitable osteosarcoma MG63 cells by Moreau et al. (1996). This section shows clearly that the BK channel is highly expressed in both MG63 cells and primary human osteoblasts. This raises further obvious questions such as: a) what are the pharmacological features of BK channels in these cells? b) what might be the possible function in addition to the modulation of osteocalcin secretion (Moreau et al., 1997). The pharmacological experiments and the cell based assays in the next sections (5 and 6) are an attempt to address and answer these questions.

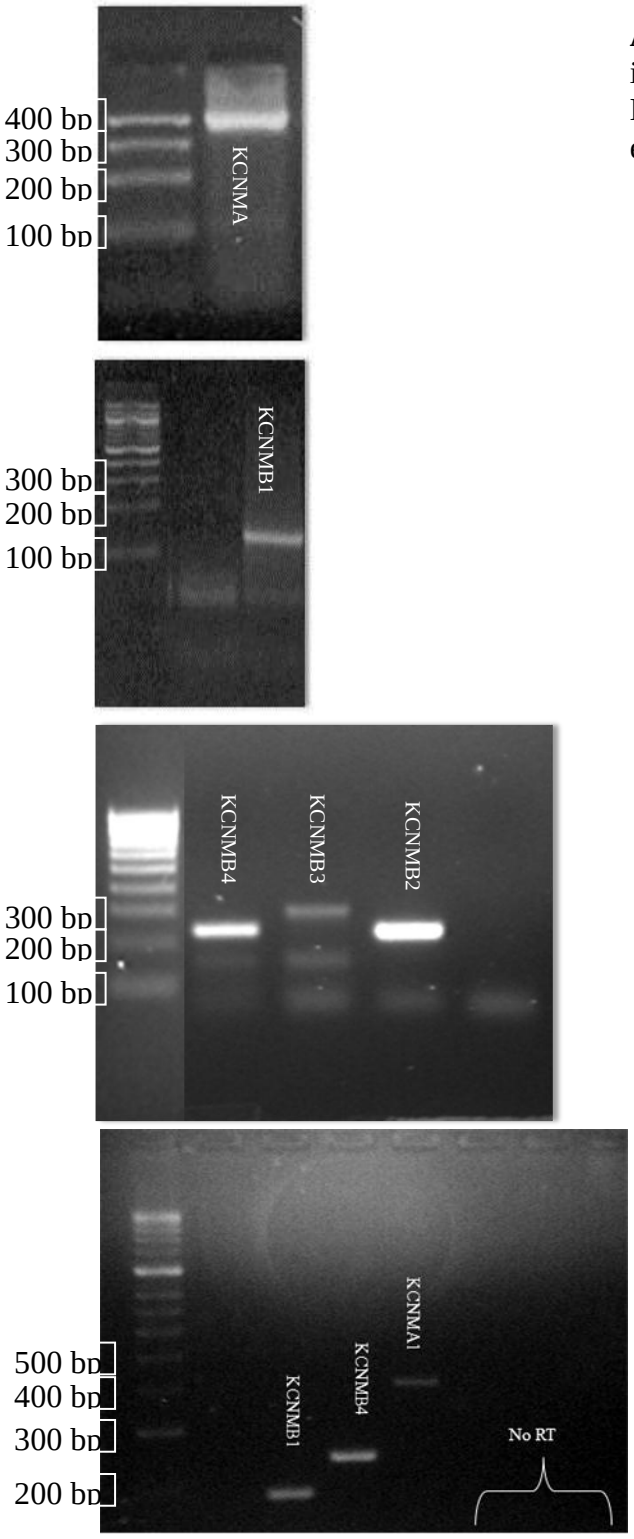

A The 407 bp size band indicates the α subunit of BK channel (KCNMA1) is expressed in MG63 cells.

B β1 subunit of BK channel (KCNMB1) is expressed in MG63 cells. The band size is 188 bp.

C Bands of 236 bp, 276 bp and 245 bp show that the BK channel in MG63 cells could contain in principle all β2 (KCNMB2), β3 (KCNMB3) and β4 (KCNMB4) subunits.

D Bands in gel demonstrate α subunit (KCNMA1, 407 bP), β1 subunit (KCNMB1, 188bp) and β4 subunit (KCNMB4, 245bp) message of BK channels in HOB cells.

Fig 4.1 Gel electrophoresis shows bands equivalent to the predicted size of the BK channel subunits. A, B and C) α, β1, β2, β3 and β4 in MG63 cells and D) α, β1 and β4 in HOB cells.

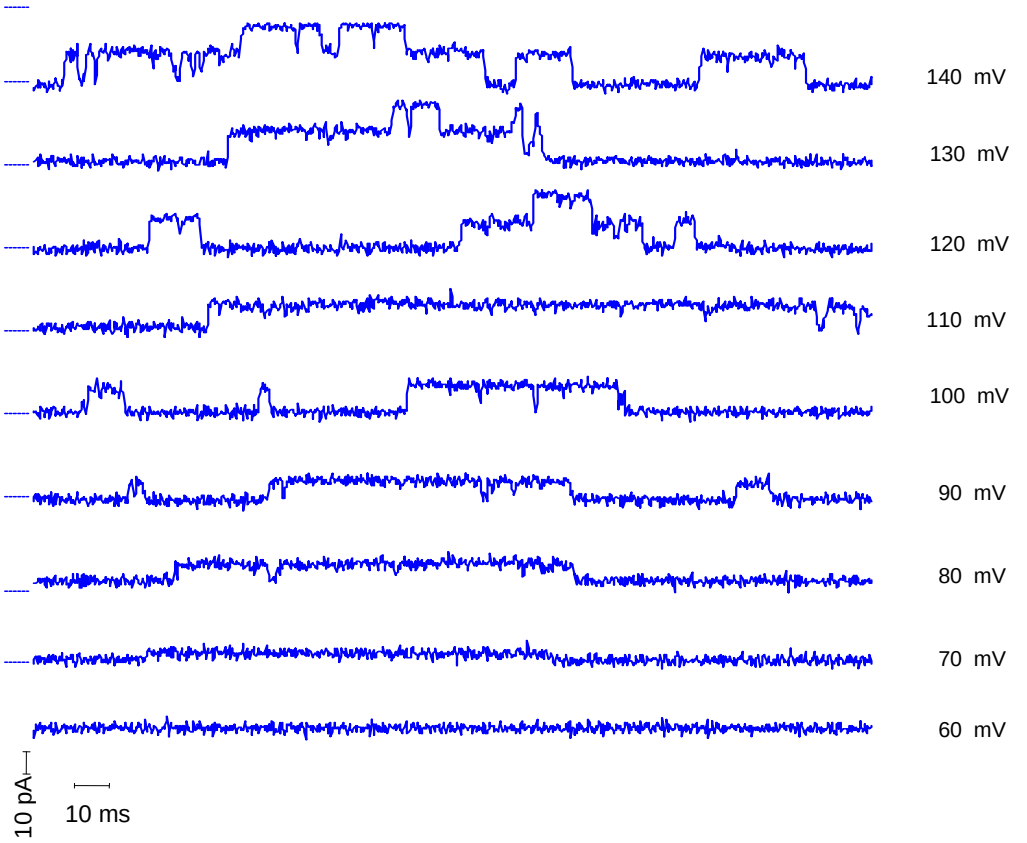

Fig.4.2 Channel openings in a cell-attached patch at a number of depolarised potentials from 60 mV to 140 mV. The dashed lines represent the closed state of the channel in this and all the subsequent figures.

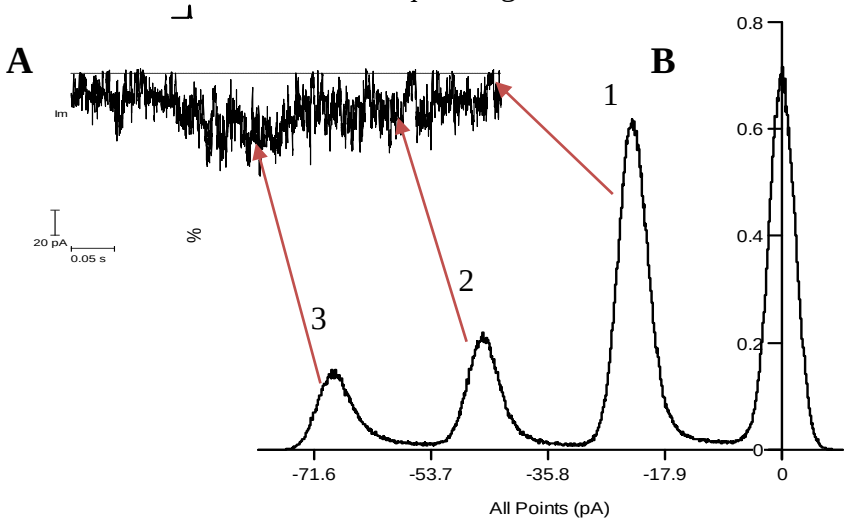

Fig.4.3 Raw multi-channel data in an inside-out patch in asymmetric K^+ gradient ($[K^+]i:[K^+]o$ = 3:140). The amplitude histogram constructed from these data is also shown. The patch potential was -80 mV. The four current peaks indicate that there were at least three channels present in this patch. The distance between each peak is 22 pA indicating that the unitary current at -80 mV is 22 pA.

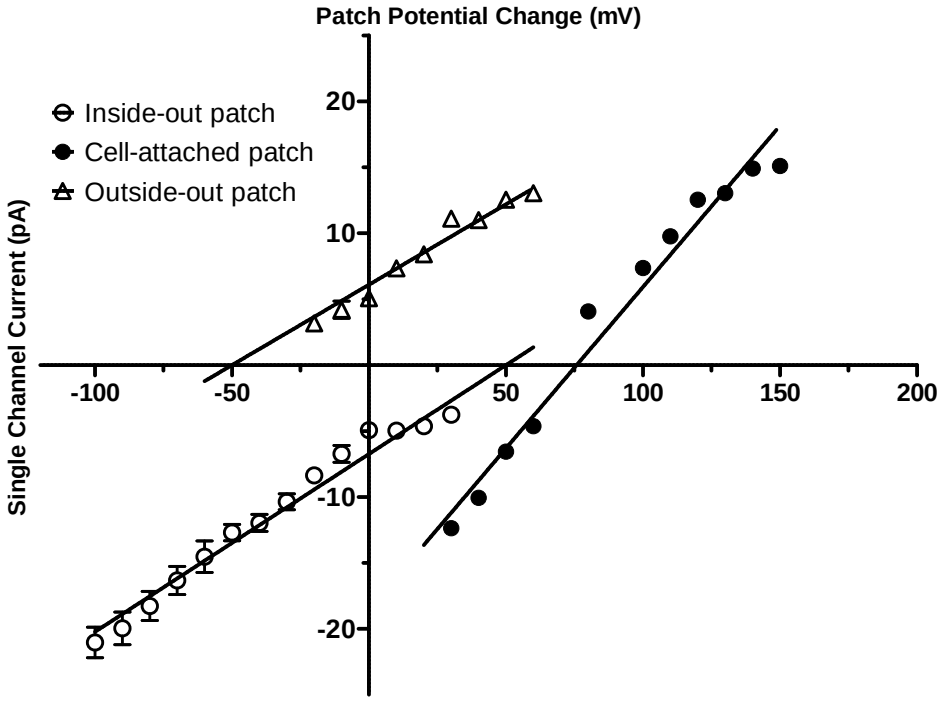

Fig 4.4 Current-voltage data for the BK channel in outside-out (Δ), cell-attached (●) and inside-out patches (○) from MG63 cells. Pooled data are shown for the excised patches and a single example for the cell-attached patch. Lines of best fit yielded conductances of 124 pS, n = 16 (Δ), 151 pS, n = 6 (○) and 315 pS (●). The reversal potential was 53 mV for the inside-out patch and –60 mV for the outside-out patch. The P_K / P_{Na} ratio calculated for the inside-out patch configuration from the G-H-K equation being 15/1. Note the characteristic tailing off of the unitary current values at positive potentials in the case of the cell-attached data.

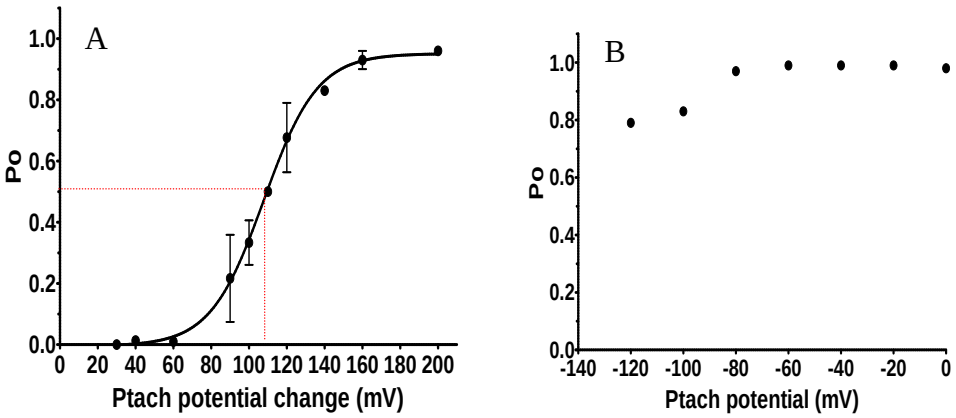

Fig 4.5 (A) The Po versus voltage data from cell-attached patches (n=3) were fitted by a Boltzmann function, giving a $V_{1/2}$ = 107 mV, slope factor =14.1 (B) Po versus voltage for a single inside-out patch in asymmetric K^+ reverse gradient. In the case of the inside-out patch the Po was constant at close to 1.0, from around -100 mV to 0 mV.

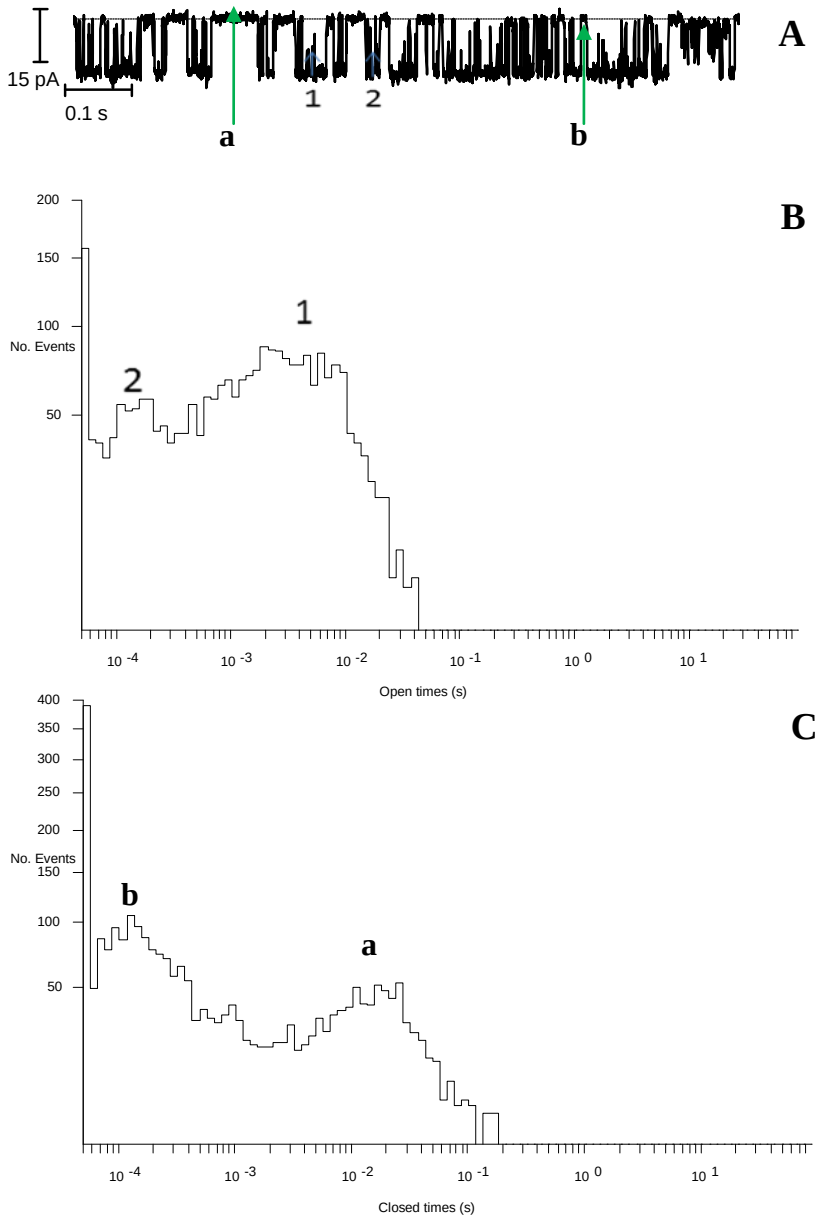

Fig. 4.6 A segment of single channel recording from an inside-out patch (-60 mV) from an MG63 cell show the BK channel displaying two types of openings. B) The dwell time exponential histogram for the open state generated from this record show both long and short openings. The histogram curves were fitted with 2 Exponentials to get long opening (1) τ_{o1} = 10.1 ms, short opening (2) τ_{o2} = 1.2 ms, C) the corresponding dwell time exponential histograms for the closed state showing long closure (a) τ_{ca} = 26.7 ms and short closure (b) τ_{cb} = 1.5 ms.

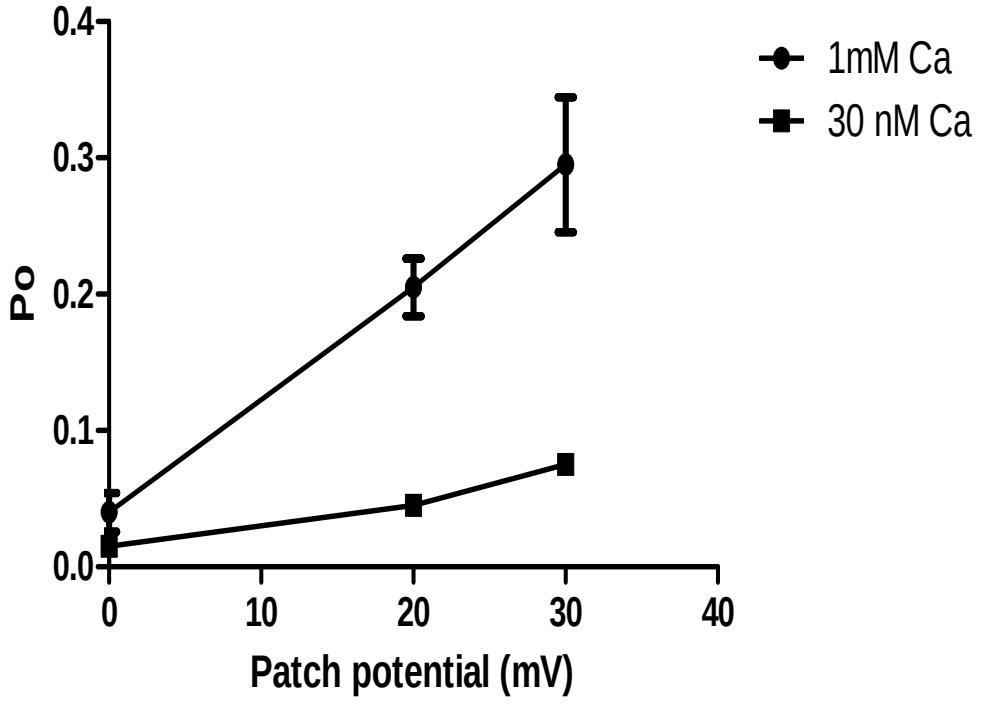

Fig 4.7 The Po from outside-out patches (n=2) in asymmetrical K (K_i : K_o = 140 : 3) at 0-30 mV. Po was consistently higher with 1 mM Ca^{2+} (c.f. 30 nM Ca^{2+}) in the electrode.

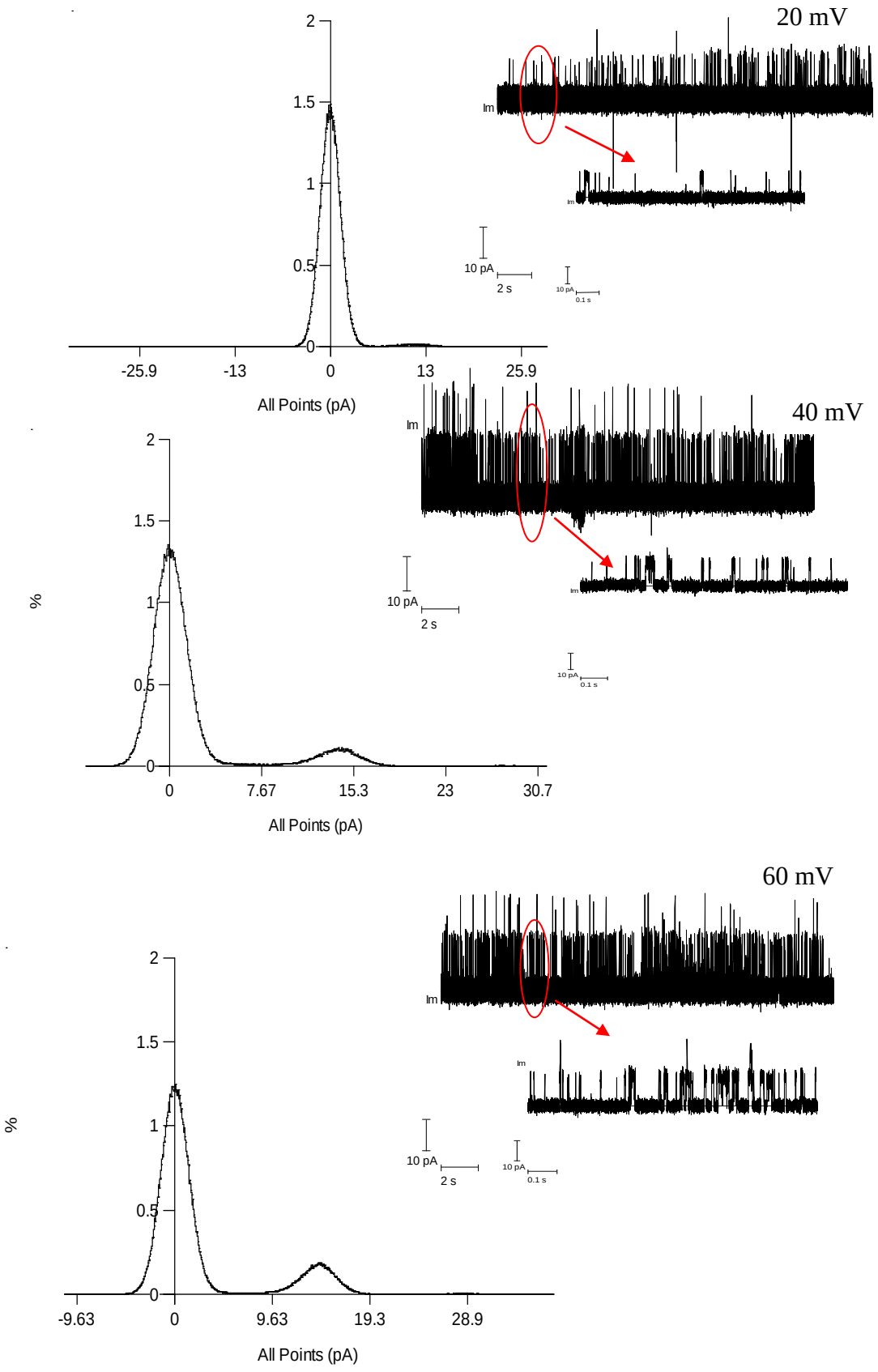
20 mV
Im
10 pA
2 s
10 pA
0.1 s
2
1.5
1
0.5
0
-25.9
-13
0
13
25.9
All Points (pA)
40 mV
Im
10 pA
2 s
10 pA
0.1 s
%
2
1.5
1
0.5
0
0
7.67
15.3
23
30.7
All Points (pA)
60 mV
Im
Im
10 pA
2 s
10 pA
0.1 s
%
2
1.5
1
0.5
0
-9.63
0
9.63
19.3
28.9
All Points (pA)

(continued)

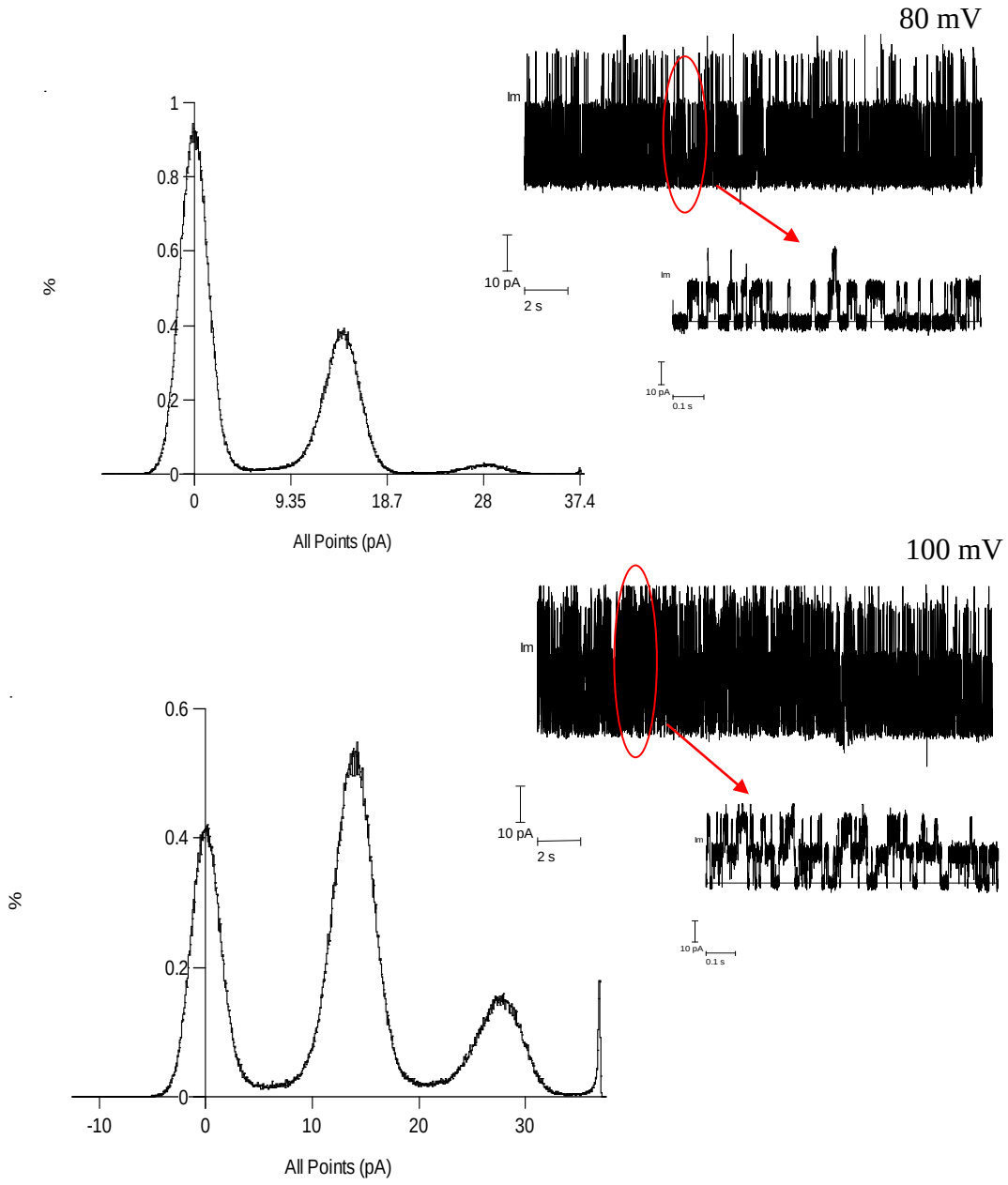

Fig. 4.8 Representative single-channel currents recorded at different potentials from 20 to 100 mV. The corresponded distribution of amplitude histograms clearly show the presence of multiple channels and the voltage dependence of the channel activity. In the histograms the first current peak on the left was considered to be the closed state and then the first opening, and second opening. The area under each peak indicates the percentage of events in that state. Hence, the histograms provide information that the "apparent" Po of this BK channel increased with the depolarised potential. The "Bin Width" for the histogram was set to 500.

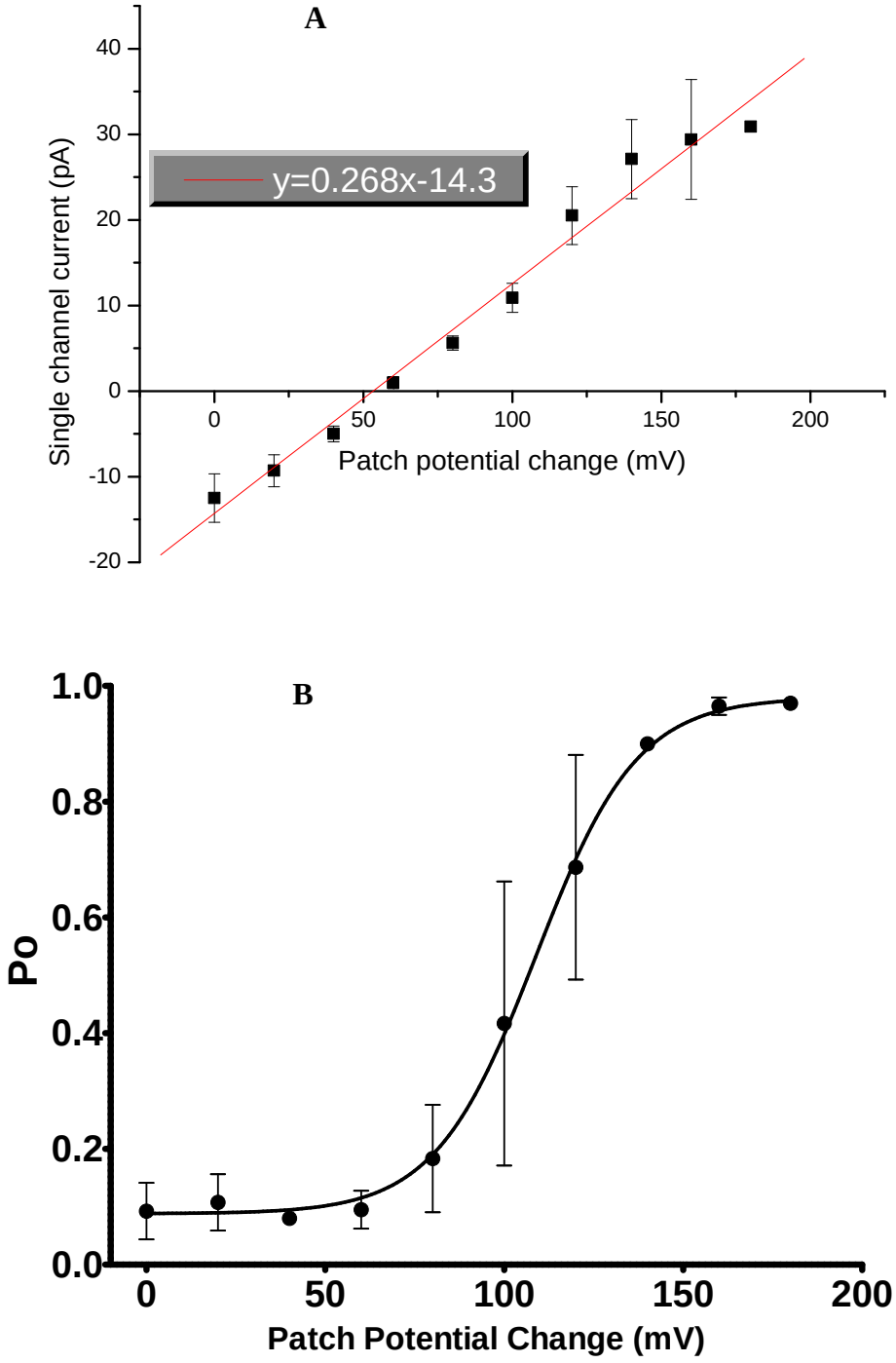

Fig 4.9 (A) The pooled current-voltage relationship for the data from 4 cell-attached patches from HOB cells are shown. The line of best fit yielded a unitary conductance of 268 pS. (B) The open probability of these channels is voltage-dependent, with a mean $V_{0.5}$ at about +108 mV (n = 4) depolarised from "rest", slope factor = 14.1.

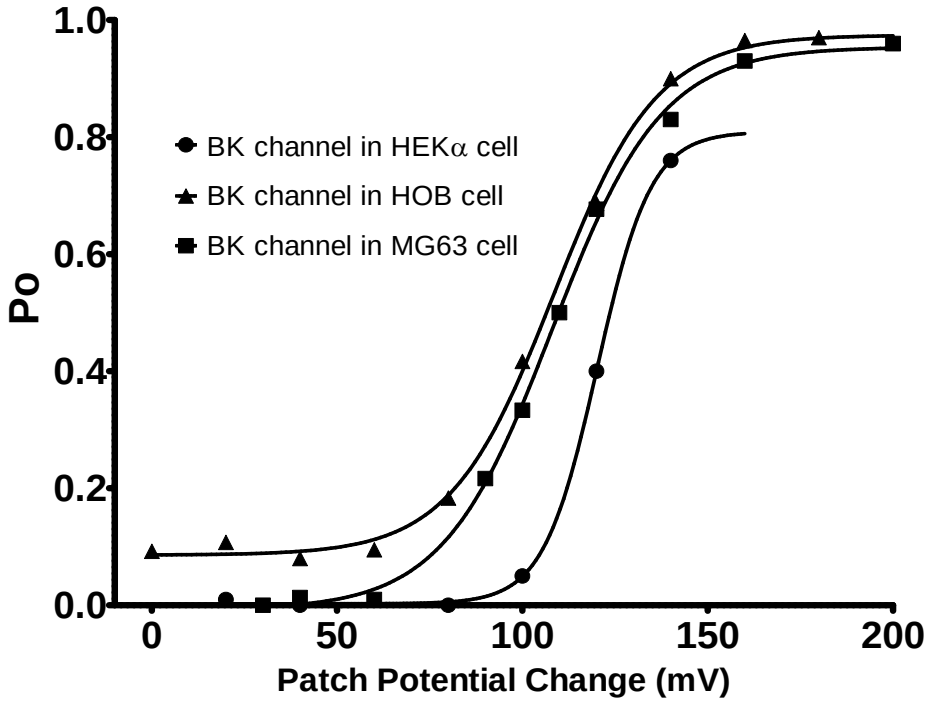

Fig 4.10 Po-V plots from cell-attached patches of MG63, HOB and HEK-α cells show that the BK channels in MG63 and HOB cells are more sensitive to voltage than in HEK-α cells. $V_{1/2}$ (MG63 cells, 108 mV, slope factor =14.7) ≈ $V_{1/2}$ (HOB cells, 108 mV, slope factor = 13.9) < $V_{1/2}$ (HEK-α cells, 120 mV, slope factor = 7.2): i.e. that the P_o = 0.5 value for BK channels in MG63 and HOB occurs at less depolarised potential than the BK channels in HEK-α cells.

SECTION 5: BK CHANNELS IN OSTEOBLASTS SHOW NEURONAL-TYPE FEATURES

5.1 Introduction

Although BK channels in excitable cells have been well investigated there is currently a lack of specific knowledge about this type of channel in non-excitable cells such as bone cells. In section 4, RT-PCR and electrophysiology work identified the existence of BK channels in both osteoblast-like cells and primary osteoblasts. The work in this section focuses on pharmacological characterization of this type of channel in these cells. First of all, on the basis of the literature, and the known expression of the subunits of BK channel described in section 4, a set of compounds was chosen for testing. The results define the pharmacological profile of BK channels in osteoblast-like cells and osteoblasts. These agents are now discussed briefly in turn.

5.1.1 BK channel regulators

5.1.1.1 Estrogen variable effects on BK channel

Estrogen, a hormone, is produced by the ovaries. Estrogen and its receptor modulators have been used in the treatment of breast cancer in postmenopausal women and breast or prostate cancer in men. In addition, estrogen with diet, calcium supplements, and exercise have been used to slow the progression of osteoporosis. The cell membrane BK channel is one such potential encouraging new target for estrogen. Both estrogen and Tamoxifen, a partial agonist of the estradiol receptor, have been shown to activate BK channels in both heterologous expression systems and smooth muscle cells, resulting in greater repolarizing current (Wellman et al., 1996; Darkow et al., 1997; Dimitropoulou et al., 2005). On the other hand, there are also reports about the negative effect of estrogen on BK channels. Valverde et al. (Valverde et al., 2001) showed that activation of BK channels by 17ß-estradiol occurs when the channel is associated with its accessory ß1 subunit. The mechanism entailed that estradiol-induced proteasomal degradation of the channel occurred after direct binding of oestrogen to the BK channel. The down-regulation can be elicited independently of classical nuclear estradiol receptors or the accessory ß1 subunit, but in the presence of ß1 subunits specific binding of estradiol to BK channels is increased significantly. The diagram below shows the roles of the β subunits in the regulation of the BK channel by 17ß-estradiol.

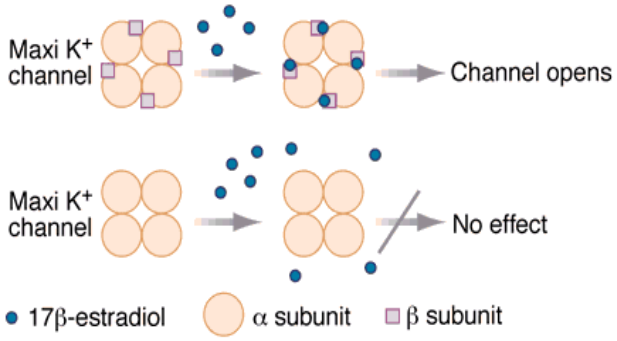

This diagram indicates that the specific binding the binding site for 17β-estradiol is on β subunit in BK channel.

5.1.1.2 Voltage-gated channel blockers, the quaternary ammonium acid family

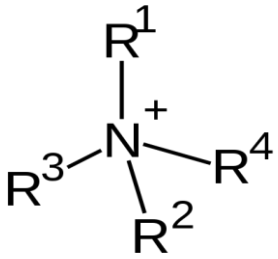

Tetraethylammonium (TEA) and other quaternary ammonium acids (QA) are potential blockers of potassium (K^+) channels and have been widely used as tools for determining the localization of the activation gate and the properties of the pore of several K^+ ion channels. These quaternary ammonium acids inhibit potassium channels by binding within the ion pore (Tan et al., 1999). Most K channels are inhibited by QA acids applied to either the intracellular or extracellular mouth of the channel. Extracellular QA acids show higher affinity than intracellular application. Mutation studies have shown that a specific amino acid located in the external loop determine the sensitivity to external TEA (Doyle et al., 1998; MacKinnon et al., 1990). BK channel α subunit (Slo) has the K^+-channel signature sequence location in the external mouth of the entryway as other four K^+ channels. Accordingly, in BK channels the quaternary ammonium acids may bind to the similar positions of the ion pore as in the case of other K^+ channels. The mechanism of QA block of BK channels has traditionally been

suggested as a 'foot-in-door' system. But Li and Aldrich (2004) modified the classic open channel-block mechanism and suggested that fast blockers do speed up the deactivation process, and blocked channels must close directly without unblocking first. This is shown in the Figure below:

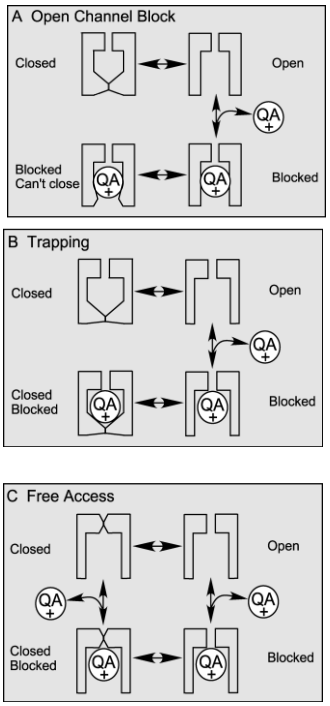

"Modification of the classical open-channel block mechanism of the block of BK channels by QA. (A) The classical open-channel block scheme, in which the blocked channel cannot close until it is unblocked first. (B) The "trapping" scheme, the channel can close with a bound blocker trapped inside. In this case, the blocker cannot enter or leave the channel when it is closed. (C) "Free access" scheme, in which the accessibility of the blocker to its binding site is not dependent on the conformation of the channel gate. Channels can be blocked or unblocked in either the open or the closed conformation. This mechanism can permit differences in binding affinity or kinetics between the closed and open conformation. The block may not thus be "independent" of gating" (these graphs and legend were taken from Li and Aldrich, 2004).

All data thus far indicate that the binding site for quaternary ammonium in BK channels is located in the ion pore which is formed by the loop between the S5 and S6 transmembrane domains of α subunit. All native BK channels are composed of 4 α subunits and associated β subunits. For example, native BK channels in human osteoblast-like MG63 cells, may comprise all four types of β subunits which certainly are expressed there. Our investigations are based on the hypothesis that the quaternary ammonium acids block BK channels in MG63 cells. The affinity and blockade kinetics will be related to the size of the molecules but not the associated β subunits.

5.1.1.3 Iberiotoxin belongs to the toxin peptide family

Peptides derived from the scorpion venoms are known to act as blockers of potassium channels. The peptides interact with the specific residues present in the outer vestibule of K^+ channels to physically occlude the pore. Among these 49 members of short-chain peptide toxins Charybdotoxin (ChTX), found in 1985, became the standard K^+ channel inhibitory peptide. Later Iberiotoxin (IbTX) and Slotoxin were identified as specific blockers of the BK channel. Their amino acid sequences share more than 75% homology in table below.

Sequence aligment of three scorpion toxins: charybdotoxin, iberiotoxin, slotoxin. The homologous amino acids were highlighted in red.

Charybdotoxin	QFTNVSCTTSKECWSVCQRLHNTSRGKCMNKKCRCYS
Iberiotoxin	QFTDVDCSVSKECWSVCKDLFGVDRGKCMGKKCRCYQ
Slotoxin	TFIDVDCTVSKECWAPCKAAFGVDRGKCMGKKCKCYV

The 3D, solution NMR structures of these peptides show a classic motif with three anti-parallel β-strands forming a β-sheet face on one side of the molecule and a helix on the other. The electrostatic isopotential at zero ionic strength shows clearly that the toxins have a surface that is positively charged (blue grid as shown below).

Predicted electrostatic isopotential of slotoxin, iberiotoxin and charybdotoxin. Red and blue represent negative and positive charged surfaces respectively.

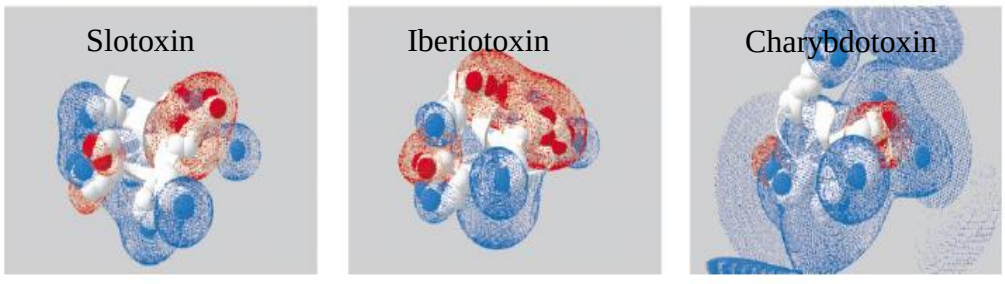

(the graphs were taken from Garcia-Valdes, et al., 2001)

The C-terminal domain of the scorpion toxins is positively charged. The positively charged sequence is considered to provide interaction region with the negatively charged pore region of BK channels, leading to channel blockade. Recently investigations provide the evidence that the peptide binding site is located in the external vestibule, near the channel pore. Peptides binding to the residues of the external domain cause physical occlusion of channel pore leading to inhibition of ion channel conductance. In addition, there are four residues of the extracellular loop of the β1-subunit situating close to the external vestibule and they are important in increasing the affinity ChTX binding site (Hanner et al., 1998). So as to the sensitivity of the channels to these peptide toxins depends on the regulatory β-subunits presenting in the cells (Ghatta et al., 2006). Specifically, Slotoxin can distinguish between the α, α+β1 and α+β4 complexes more efficiently than IbTX (Garcia-Valdes et al., 2001).

5.1.1.4 Alkaloid BK channel blockers: tetrandrine and paxilline

There are also non-peptide natural blockers such as paxilline and tetrandrine.

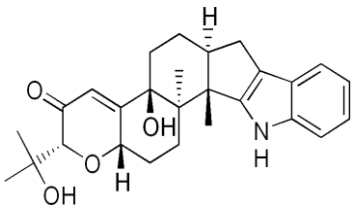

Paxilline, an indole alkaloid is from penicillium origin. It selectively blocks BK from the intracellular side. Its structure is as below. This compound is membrane permeable so it can be applied from either side,.

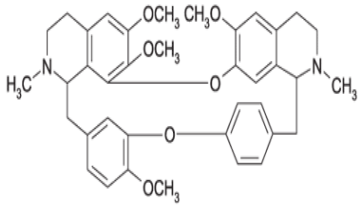

" Tetrandrine, a bisbenzyltetrahydroisoquinoline alkaloid extracted from the Chinese medicinal herb Radix stephania tetrandrae, is known to possess a wide spectrum of pharmacological activities" by Wu et al., 2000.

Throughout the past decades tetrandrine was recognized to possess anti-inflammatory, antiallergic, antioxidant, and antifibrogenetic activities. Additionally, it is capable of immunomodulation and inhibition of platelet aggregation. Recently, several studies have demonstrated that tetrandrine behaves like a calcium entry blocker. However, of interest here is the observation that tetrandrine inhibits scorpion toxin-insensitive BK channels present in rat neurohypophysial nerve terminals and expressed in Xenopus oocytes (Wang and Lemos, 1992). On the other hand, toxin-sensitive BK channels present in rat arterial smooth myocytes are not sensitive to tetrandrine (Wang and Lemos, 1995). However, recently, Wu et al. (2000) reported in a human endothelial cell line (HUV-EC-C) that toxin-sensitive BK channels can be blocked by tetrandrine also. Although at a given concentration of tetrandrine, the magnitude of any tetrandrine-induced inhibition of BK channels was increased as internal Ca^{2+} was elevated; the relationship between the inhibitory effect of tetrandrine and internal Ca^{2+} concentration is still not fully understood.

5.1.2 BK channel structure and sensitivity to the regulators

As described in section 4, the BK channel is composed of 4 α subunits and 4 β subunits. In contrast to the other voltage-gated potassium channels, the BK channel α subunit has an internal C-terminus and an external N-terminus which is the binding site of β subunit. The C-terminus is a long tail which is divided into 4 sequences (S7-S10) according to function which also distinguishes it from other voltage-gated potassium channels. The Ca^{2+} sensitivity of the channel appears to involve a region of several negatively charged residues at the C-terminal core (Knaus et al., 1995). The β-subunit acts as the regulator and the structure is much simpler than the α-subunit. The β1-subunit was first identified in bovine smooth muscle. Expression of the β1 subunit produces BK channels that are active at strong depolarization and high Ca^{2+} concentration. It also dictates the BK channel's response to 17β-estradiol and other estrogen receptor regulators. The α+β1 combination has low affinity for iberiotoxin (IbTX, a selective blocker for hslo). Channels comprised of β2 subunits inactive rapidly. The β3 subunit is found in pancreas and spleen cells. α+β3 constructs produce channels with activation properties similar to those of α subunit. The β4 subunit endows the channel with mixed characteristics. Brenner et al. reported upregulation and downregulation of channels formed from co-expression of α and β4 at lower and higher Ca^{2+} concentrations respectively (Brenner et al., 2005) . In addition, under normal experimental conditions these channels are not blocked by IbTX (100nM) or ChTX (1μM). In the brain BK channels have been distinguished on the basis of the effects of

PKA, and the sensitivity to these peptide scorpion toxins, ChTX and IbTX. Hence, channels that are toxin-sensitive, and where PKA usually increases activity, are referred to as type-I channels and in contrast channels that are toxin-resistant and where PKA decreases the activity of the channel are known as type-II channels (Reinhart et al., 1989,1991). Type II are found on nerve terminals and are sensitive to the alkaloid tetrandrine (Wang et al., 1992) and it has been proposed that co-assembly of the α subunit with a β4 subunit confers properties similar to the type II (Meera et al., 2000; Lippiat et al., 2003) and slows action potential repolarisation (Brenner et al., 2005).

In MG63 cells BK channel has been described variously as voltage-independent, with differing sensitivities to the peptide scorpion toxin blockers, ChTX and IbTX. Thus it has been reported to be both ChTX-sensitive (Moreau et al., 2005), or insensitive to both IbTX and ChTX (Rezzonico et al., 2002). In MG63 cells the BK channel is also reported as being insensitive to protein kinase A (PKA) which may be diagnostic in elucidating which subtype is present (Moreau et al., 1996). The gene for all 4 types of β subunits have been identified in MG63 cells and human primary osteoblasts (HOB) and the hypothesis tested here is that BK channels in MG63 or HoB cells would show the features of an α and β1 subunit combination. These channels would be sensitive to 17β-estrodiol and other estrogen receptor modulators. These channels might also be insensitive to toxin peptides.

5.2 Materials and methods

5.2.1 Cell culture

Cells were cultured under the same conditions as described in Section 2. To gain comparable results, cells were seeded on coverslips and were cultured for no more than 3 days before they were patched.

5.2.2 Test compounds and the perfusion system

11 compounds in total were tested in these experiments. These compounds were obtained and stored as described in Section 2. In each experiment, they were defrosted from aliquots and diluted to appropriate concentrations with NaCl Locke or High K solution according to the perfusion condition. All the solutions were filtered through a 20 μm filter before use.

Two different perfusion systems were tested.

1. **Continuous irrigation**

   As shown in Fig 5.1 NaCl Locke containing test compounds were applied through a tube to the bath chamber. At the same time, another syringe gently sucked away solution from the chamber gently. The added volume and sucked volume were kept the same (typically 600 μl). In this way, it was comparatively easy to control the test compound concentration. However in practice, this method of drug application caused the seal of the patch to become unstable to the extent that it was often lost relatively rapidly (5/6, n=6).

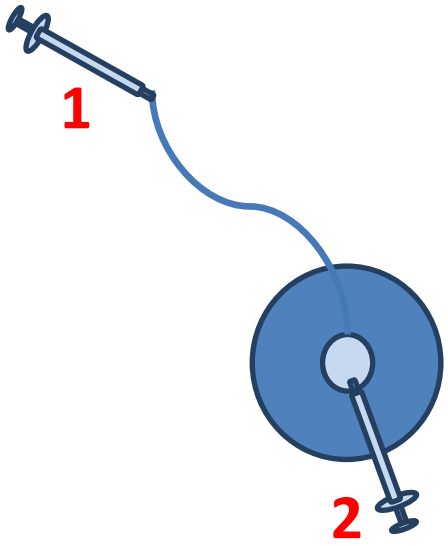

Fig 5.1 the supply solution containing test compounds was added to the recording chamber by means of a syringe. The total volume of exchanged solution is 600 µl which is 3 times the volume on coverslip. The final solution on the coverslip is assumed to contain the same concentration of compounds as in syringe 1 (as the labelling shows).

2. "Drop" method

To avoid the poor recording rate achieved using the above method, compounds were applied to the patch in one other way. In this case, 200 µl NaCl Locke was add onto the top of the coverslip in the chamber. Then at the appropriate time another 50 µl NaCl Locke containing a known concentration of compound was added. The final concentration was calculated as: $\text{final concentration} = \frac{\text{concentration in NaCl Locke (M)} \times 50\ \mu\text{l}}{250\ \mu\text{l}}$.

The recordings were taken after about 1 minute to allow an equilibrium concentration to be reached. This method had a minor effect on the stability of patch seals (2 from 10 attempt obtained). It was thus the method used to apply compounds to the patches in many of the experiments to be described.

Compounds were washed from the bath in the following way:

1. 220 µl bath solution was taken from the chamber by using a 1 ml syringe.

2. Another 220 µl fresh NaCl Locke was added.

Between tests of different concentrations of one compound there was one wash. The compounds were tested in concentration steps from low to high. The final wash repeated the above two steps twice. The reduced compound concentration was 1/70 of test concentration.

5.2.3 Configuration of patch clamping

Different configurations of patch clamping were chosen according to the binding sites of tested compounds. If the compound regulates BK channel from the intracellular side, inside-out patches or cell-attached patches were used. If the compound binds and is active from the external site then outside-out patches were deployed.

Each patch was recorded from in the control condition (drug-free NaCl Locke) at a range of patch potentials as control. Test compounds were tested over the same range of potentials and finally recordings were made over the same potentials after washout. Drugs were in contact with the cells for no more than 10 minutes and recordings made at each potential were typically 30 seconds. Recordings were analysed with WinEDR. All data are expressed as the mean ± SD.

5.3 Results

BK channel in either MG63 cells or primary human osteoblasts showed novel responses to the regulators outlined above. Firstly, BK channel in these cells was not highly sensitive to 17β-estradiol or other estrogen receptor regulators. 17β-estradiol (up to 30 μM) was applied to either outside-out (n=5) and inside-out patches (n=3). There was no significant increase in channel activity in patches in any either of these configurations. On the other hand, the BK channel was regularly detected and the effects of other regulators on channel activity is now described below. Ethanol has been shown to affect BK channel activity (Davies et al., 2003) hence perhaps it, as vehicle, is masking any action of estradiol. However, the cells were treated with 17β-estradiol for 48 hours and then patched, BK channel open probability were increased (data not shown).

5.3.1 TEA and the quaternary ammonium acids blocked BK channels in MG63 and HOB cells

As mentioned previously, quaternary ammonium acids are a family of classic potassium channel blockers that have been widely used as tools for determining the localization of the activation gate and the properties of the pore of several ion channels. In this study four compounds from the quaternary ammonium acid family: TEA, TBuA, TPeA and THeA were tested in outside-out patches at different concentrations and a marked difference in the affinity

to the BK channels was observed (Fig 5.2). TEA is the smallest molecule among these four quaternary ammonium acids. From the results it could be seen that both TEA and TBuA bind and unbind so rapidly to the channel that with the standard level of filtering used here (Fc = 5 kHz, -3 dB, four pole Bessel filter) it was not possible to detect faithfully the open and closed sojourns of the channel. Consequently a 'flickery' blockade was observed (Fig 5.3). The current histograms generated from these data indicate that the unitary current appeared to be smaller than the control value at the same patch potential. Unitary currents with TEA or TBuA treatment were plotted against compound concentration and the apparent reduction in unitary current was concentration-dependent (see Fig 5.4). THeA blocked BK channel by reducing channel open probability at the lowest concentrations tested (≤1 μM). Fig 5.5 shows typical raw data showing for THeA and TPeA in outside-out patches. Both compounds blocked the BK channel in a reversible fashion. From the raw data, the apparent unitary current and open probability (Po) were calculated and plotted against the compound concentration (Fig 5.6 A-D). These plots indicate that TEA and the other three quaternary ammonium acids blocked BK channels with an affinity related to the number of carbons (C-number) in the chain or the molecule size. Both TEA and TBuA affect the channel activity at a millimolar level, causing about a 20% decrease of channel Po at 1 mM. TPeA and THeA on the other hand affect the channel activity at a micromolar level, TPeA causing 70% blockade at 10 μM and THeA at an even lower concentration (3 μM) reducing the channel Po by 90%. The ED_{50} versus C-

number plot demonstrates a dramatic increase of affinity with the high C-number (Fig 5.6 E).

5.3.2 BK channels in MG63 and HOB cells were more sensitive to alkaloids than peptide toxins

The actions of alkaloids and peptide toxins were also tested in excised patches from MG63 cells. Tetrandrine (5-30 μM, n = 8) always and IbTX (5-60 nM, n = 5) sometimes (see below) blocked the BK channel (Fig 5.7 and Fig 5.8). The degree of block by tetrandrine was 42% (n = 2), 80% (n = 2), 85% (n =2) and 100% (n = 2) at 5, 10, 20 and 30 μM respectively and showed little voltage-dependence. The fractional inhibition by IbTX showed voltage-dependence (over 0-50 mV) that inhibition was higher at 0 mV than at more positive voltages. In five patches both blockers were tested sequentially and in this case all were sensitive to tetrandrine but only 2 were sensitive to IbTX (90 nM) (see Fig. 5.8). Furthermore, in this study 100 nM slotoxin showed no inhibition effect on BK channel opening in MG63 cells (n=9, data not shown). BK channels in MG63 cells were blocked by paxilline from the cytoplasmic side. As shown in Fig 5.9 the open probability was reduced by 30% with 10 μM paxilline at -60 mV (n=5). This effect could be washed out showing that the binding of paxilline to BK channels was reversible (data not shown).

The pharmacology of the BK channel in human primary osteoblasts was also examined in outside-out patches and was similar to that of the MG63 cells. The BK channel was blocked by external TEA (300 μM see Fig 5.10) was always

sensitive to 10-60 µM tetrandrine (n=7) (Fig5.11) and was blocked by IbTX (30-120 nM) in only some cases (3 of 6). Although not studied systematically, the BK channel in the primary cells was less sensitive to IbTX than that of the MG63 cells as shown in Fig. 5.12.

5.3.3 BK channel sensitivity to other regulators

One BK channel opener isopimaric acid was tested in outside-out patches. As shown in Fig 5.13 it enhanced the channel significantly by increasing the channel open probability by 34% at 10 uM (n=3) and a patch potential of 20 mV.

5.3.4 Summary

The principal findings in this section can be summarised as follows: BK channels in MG63 and HOB cells have a novel pharmacology and they are more like the phenotype in neurones than the ones in smooth muscles (Wang and Lemos, 1992). BK channels in MG63 and HOB cells can be blocked by quaternary ammonium acids, peptide toxins (IbTX) and alkaloids (tetrandrine and paxilline) but show different affinity for these compounds. BK channels were activated by the terpenoid opener, isopimaric acid.

5.4 Discussion

The novel pharmacological features of BK channels in MG63 and HOB cells must relate to their complex construction. Unlike the BK channels in smooth muscle or brain having single type of associate β subunit, BK channels in MG63 and HOB cells express all 4 types of β subunits. Since every single channel is composed of 4 β subunits there are 35 possibilities of the combinations of α and β subunit. Hence, BK channels in MG63 and HOB cells could potentially show extraordinary and mixed characteristics.

5.4.1 The β1 subunit and the BK channel sensitivity to estrogen

The β1 subunit of BK channels was detected by RT-PCR in both MG63 and HOB cells. But the BK channels in these cells did nevertheless not show the typical β1 subunit feature which is sensitivity to 17β-estradiol or other oestrogen receptor modulators. This can be explained in principle by De Wet's discovery on BK channels (De Wet et al., 2006). They report that 17β-estradial effects on the BK channel need at least three β1 subunits to be expressed out of the four present in the native channel. When there is more than one type of β subunit expressed the chances for four β1 subunits to be found in one channel complex is extremely low (< 1/35). The conclusion here is that there were a limited number of BK channels of that type present and hence there was little prospect of finding a BK channel that was sensitive to 17β-estradiol.

5.4.2 BK channel sensitivity to peptide toxins and alkaloids

Peptide toxins from scorpion are widely used as specific BK channel blockers in the research literature. The toxins have high affinity for the α subunit (Slo) and they interact with this α subunit via a biomolecular reaction. The toxins have a second biding site on the extracellular loop of the β subunit when BK channels express as an assembled α+β complex (Garcia-Valdes et al., 2001). Previous investigations revealed that β4 associated BK channels lose the sensitivity to the toxins (Lippiat et al., 2002). In the experiments in this section the BK channels in MG63 cells showed apparently low sensitivity to the peptide toxins. Only 40% of the detected BK channels were blocked by IbTX when the concentration was increased to 90 nM, while the IC_{50} of IbTX for the α subunit is 33 nM (Lippiat et al., 2002). In addition, almost no BK channel activity was blocked by 100 nM Slotoxin, (data not shown) which is extremely selective for the α subunit. The low affinity of the peptide toxin indicates that BK channels in MG63 and HOB cells have typical characteristics of α+β complex, especially α+β4.

In contrast to the low affinity for the peptide toxins, BK channels in MG63 and HOB cells have a high sensitivity to alkaloids such as tetrandrine and paxilline. Tetrandrine is not only a blocker of BK channels but also blocks voltage-gated Ca^{2+} channels and intracellular Ca^{2+} pumps. It is believed to induce effects on cell proliferation and cytotoxicity (Wang, Lemos and Ladecola, 2004). It blocks BK channels in neurohypophysial nerve endings (Wang and Lemos,

1995), vascular endothelial cells, pituitary tumor (GH3) cells (Wu et al., 2001) and glial tumor cells (Ransom et al., 2002). Being different to the peptide toxins, tetrandrine exerts stronger blocking effects on a BK channel that is coexpressed with β subunit than hSlo alone (Dworetzky et al., 1996). The high expression and high affinity of tetrandrine for BK channels in MG63 and HOB cells indicate that the BK channel when modulated could play a key role in these cells in proliferation, which will be discussed in Section 6.

5.4.3 BK channel react to the quaternary ammonium acids

TEA and other members of the quaternary ammonium acids are useful tools to probe functionally the pore region of K^+ channels. Armstrong and his colleagues carried out the first elegant studies on the blockage of squid axon K^+ channels by intracellular QA. Based on these studies they proposed some topological properties of K channel pores long before any relevant structural information about ion channels was available (Armstrong and Binstock, 1965; Armstrong, 1969 & 1971; Armstrong and Hille, 1972). In most previous investigations on BK channel in other tissues only TEA was used as a "generic" wide spectrum K^+ channel blocker. The other members of QA such as TBuA, TPeAa dn THeA effect on BK channels were seldom, if tested at all. The results in this section showed that BK channels in MG63 cells have affinity for the QA. TEA, TBuA blocked the BK channel at millimolar level and TPeA and THeA at the micromolar level. These concentrations are all much lower than the ones blocking potassium channels in squid giant axon

(Armstrong, 1972). This result indicated the higher affinity of BK channels to QA. According to the model (Fig. 5.14) created by Armstrong (Armstrong, 1975) accounting for inactivation of I_K of C_9 QA, this result may implicate the size of BK channel pore which is close to 8 Å.

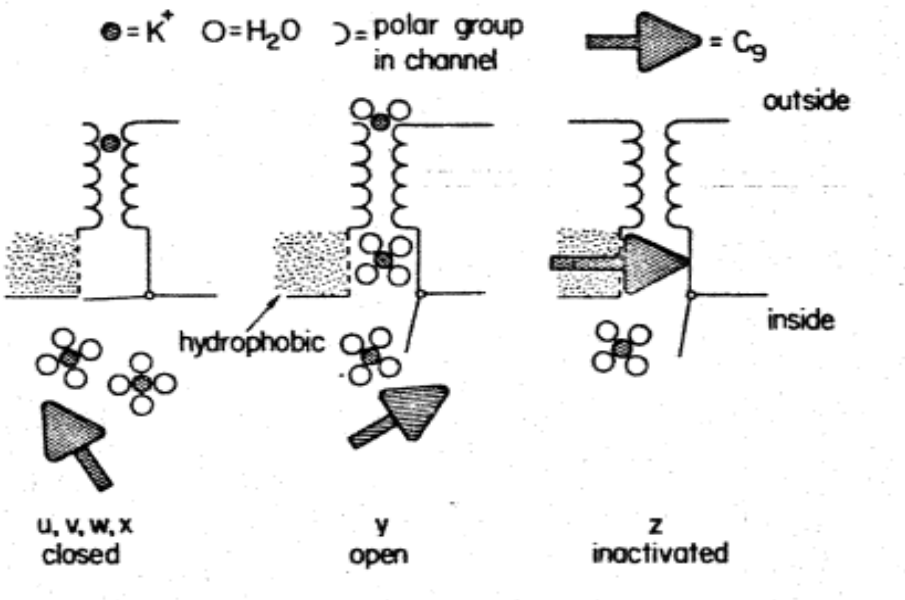

Fig.5.14 "A model to account for inactivation of I_K of C_9. When the K activation gate is closed, C_9 is not likely to be in the pores; but when the gates open, it may diffuse in at a rate dependent on its concentration in the axoplasm. The apolar nine carbon chain of C_9 binds to a hydrophobic group in the pore mouth, stabilizing the ion in blocking position." (this graph and the description of the model were both taken from Armstrong ,1975)

Additionally, QA apparently reduced channel unitary current which is different to the picture with other BK channel blockers. The question is whether these and related compounds are potential therapeutic drugs For example, 4-Aminopyridine (4-AP) which works as a relatively selective blocker of members of the Kv1 (Shaker, KCNA) family of voltage-activated K+ channels has been used clinically in Lambert-Eaton myasthenic syndrome and multiple sclerosis as it blocks potassium channels, prolonging action potentials duration

hence supporting secure nerve conduction and thereby increasing neurotransmitter release at the neuromuscular junction (Judge, 2006).

5.4.4 BK channels are activated by the opener isopimaric acid

Since BK channels in MG63 cells have high prevalence and activity the effect of channel openers were harder to investigate. However, we were still able to see the increase of channel open probability in some cases as shown above. This indicates that the BK channels in MG63 cells are conventional in being sensitive to isopimaric acid.

5.5 Conclusion

The systematic pharmacology studies on BK channels in MG63 and HOB cells not only provides the support for the BK channel existence in these cells but also indicates the possible functions of BK channel and further provides pointers to how to develop potential therapeutic drugs.

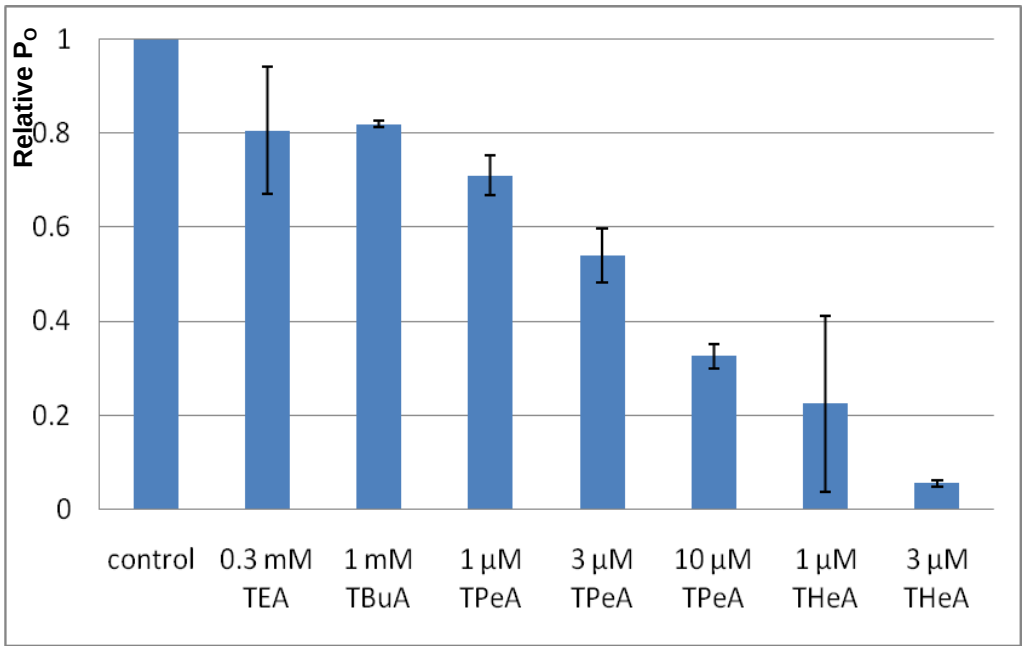

Fig 5.2. TEA, TBuA , TPeA and THeA blocked BK channels with different potencies. 0.3 mM TEA and 1 mM TBuA reduced channel open probability by about 10%. 0.001 mM and 0.01 mM TPeA caused a 20% and 70% reduction in Po respectively. THeA blocked BK channels at the lowest concentration of all four compounds, causing a 70% and 90 % reduction at 0.001 mM and 0.003 mM respectively.

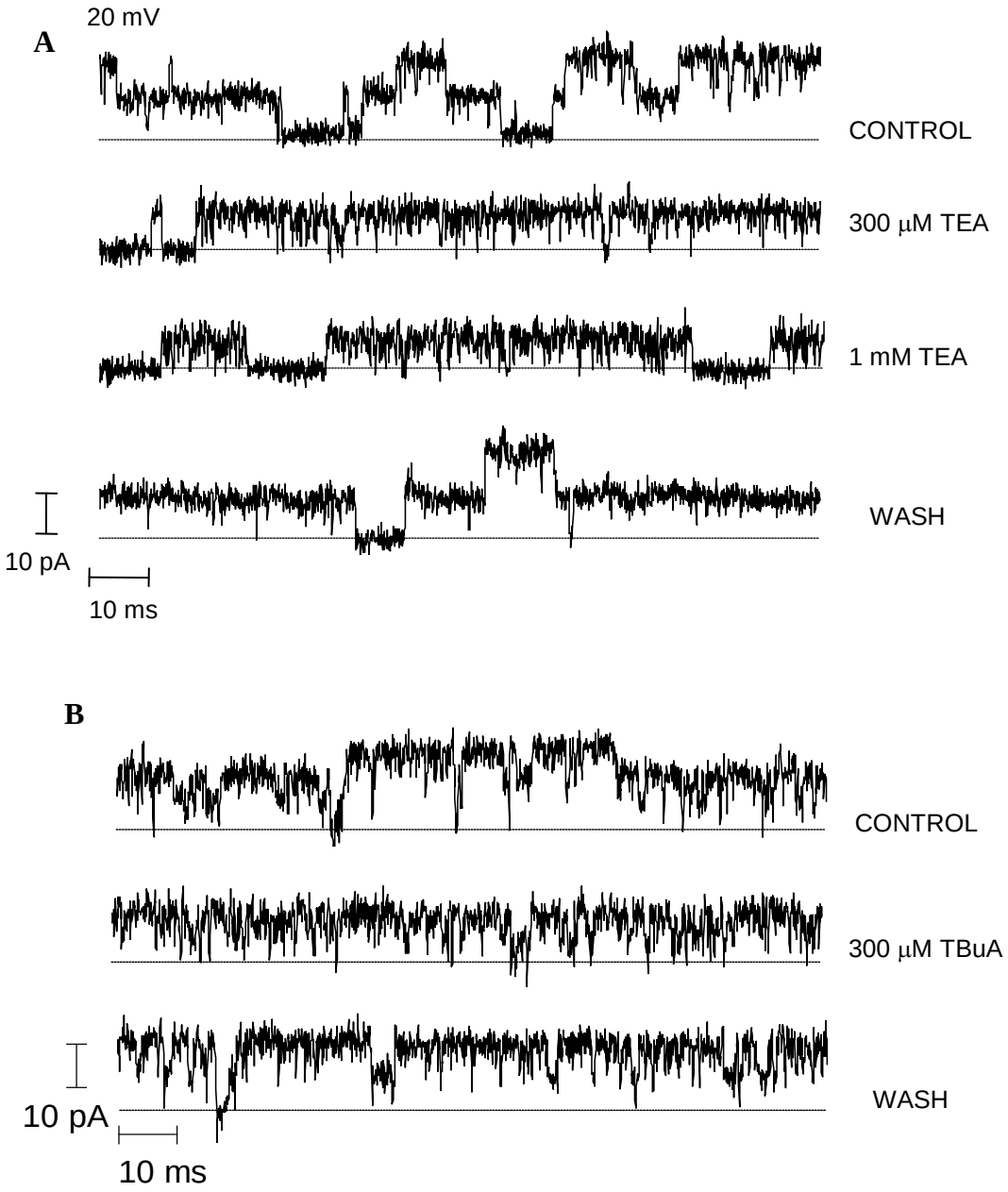

Fig 5.3 Raw data showing outside-out patches at 20 mV patch potential in asymmetric K (140/3). (A) External 0.3 mM and 1mM TEA caused 'flickery' block as well as an apparent decrease of Po. This was reversed on washout. (B) Blockade of the BK channel by external TBuA. 300 μM TBuA also produced channel 'flickery' openings which were reversed on washing.

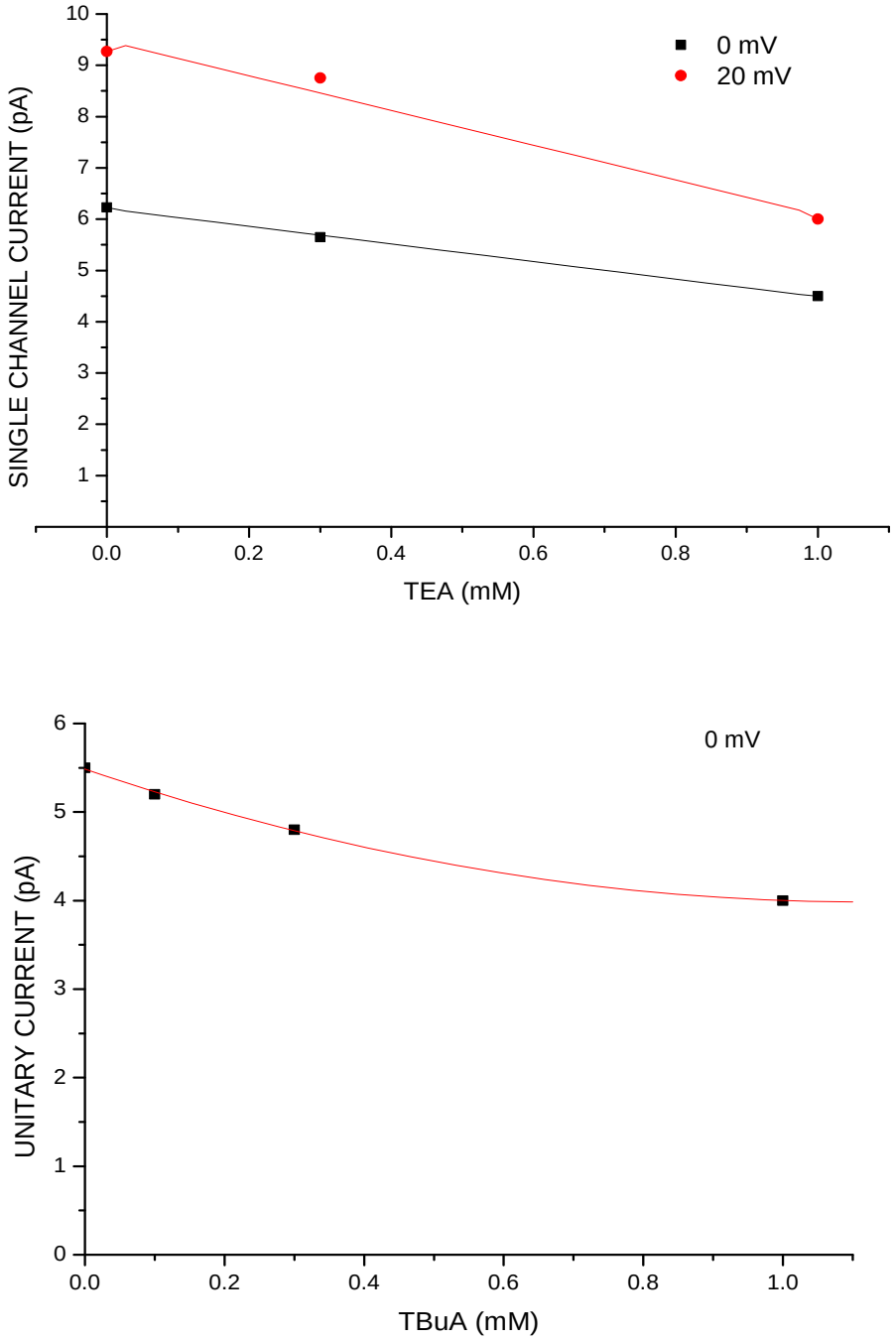

Fig 5.4 The BK channel unitary current appears to decrease as the concentration of external TEA or TBuA was increased. TBuA induced decrease of BK channel unitary current was comparable to that produced by TEA over the same concentration range (at 0 mV).

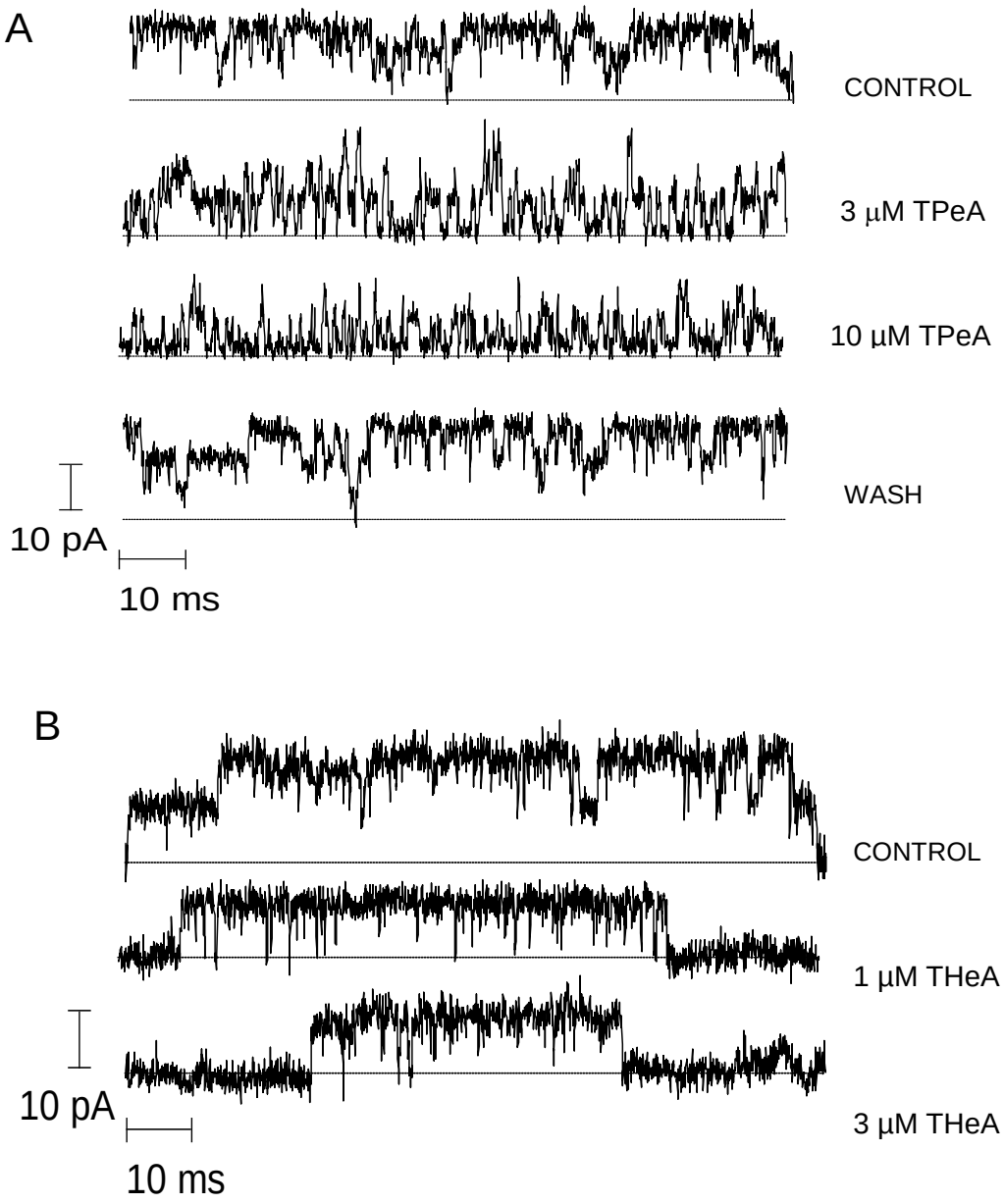

Fig 5.5 Typical data with external QA compounds in outside-out patches at 20 mV (A) TPeA reduced the BK channel open probability at 3 and 10 μM. (B) THeA showed similar effects on the channel at 1 and 3 μM.

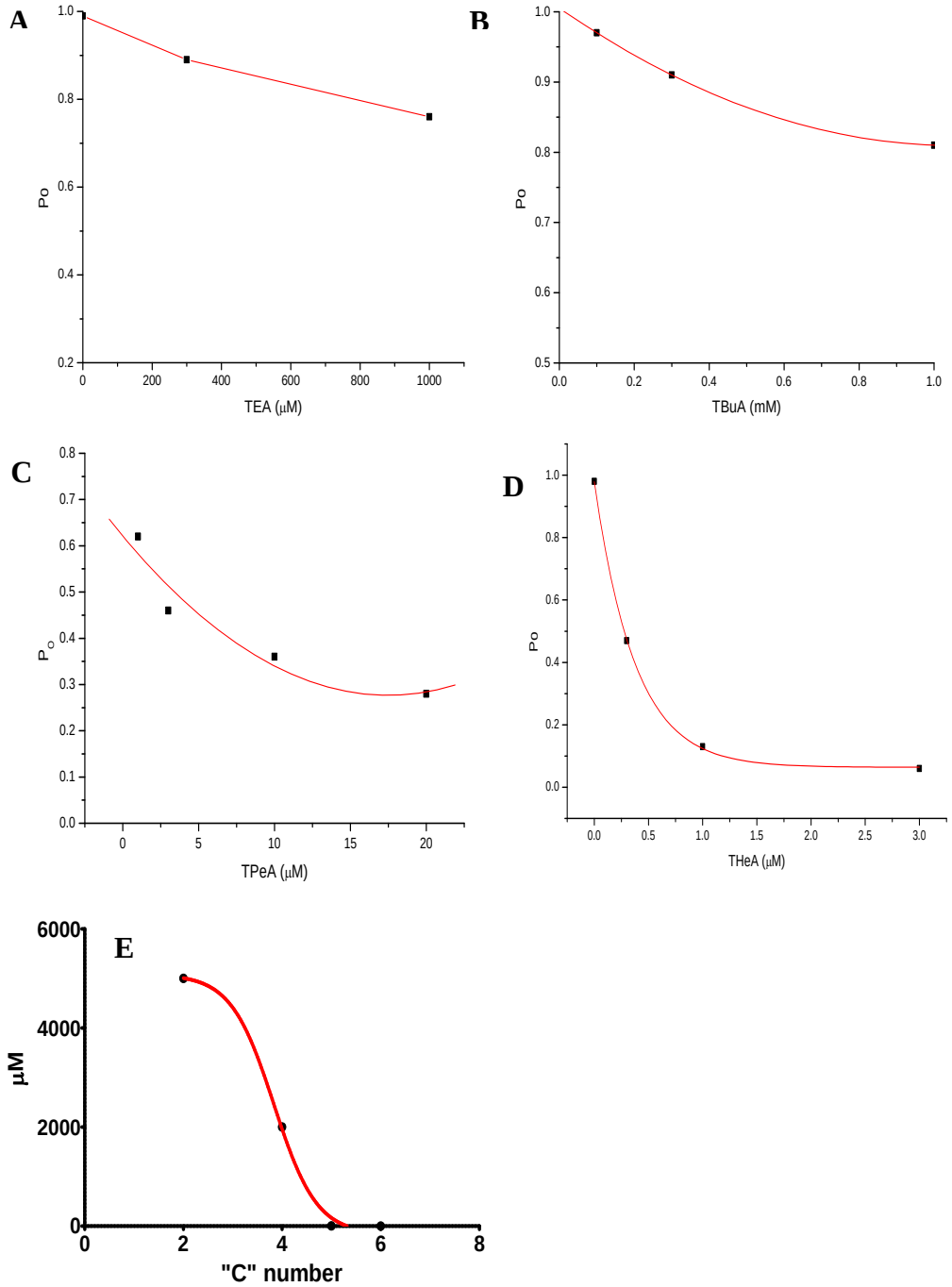

Fig 5.6 BK channel Po is reduced by TEA (A), TBuA (B), TPeA (C), THeA (D). TBuA blocked BK channels decreasing the channel open probability. The blockade at 1 mM was about 20%. TPeA decreased BK channel open probability (Po) at 1, 3, and 10 μM, in a concentration-dependent fashion. 10 μM TPeA caused 70% decrease of Po compared to control. BK channels were blocked by THeA at 0.5, 1, 3 μM. 3μM THeA decreased the channel open probability by 90%. The median effective doses (ED_{50}) decrease dramatically with high carbons number (C- number) in the molecules (E).

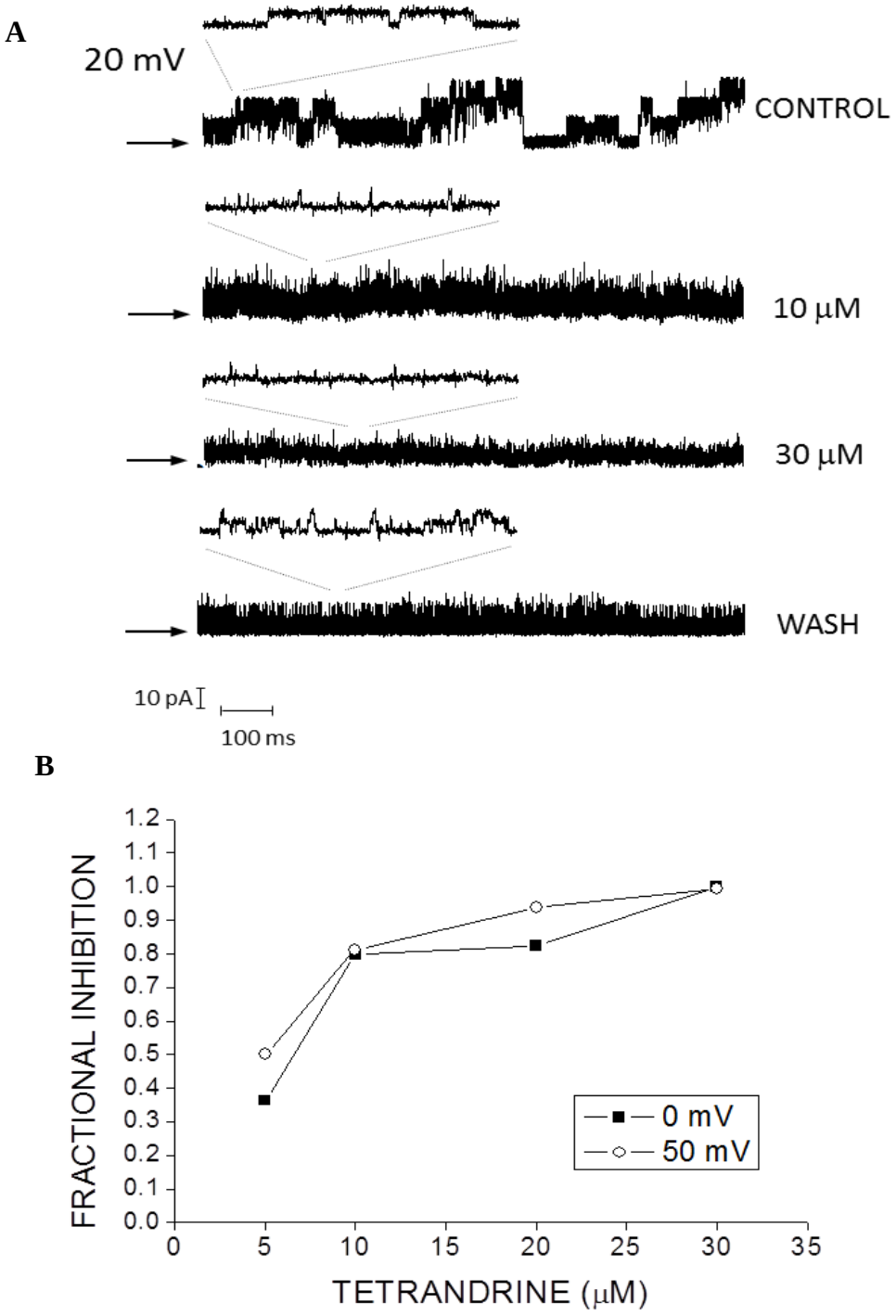

Fig 5.7 (A) The effects of the blocker tetrandrine on BK channel activity in an outside-out patch from an MG63 cell. The reversible block by 10 and 30 µM is shown for a patch potential of 20 mV. (B) The fractional inhibition of BK channels (calculated from the open probability values) by tetrandrine (5 - 30 µM) is shown for 0 and 50 mV patch potential in 2 outside-out patches. The degree of block by tetrandrine was not dependent on the patch potential over this range of values.

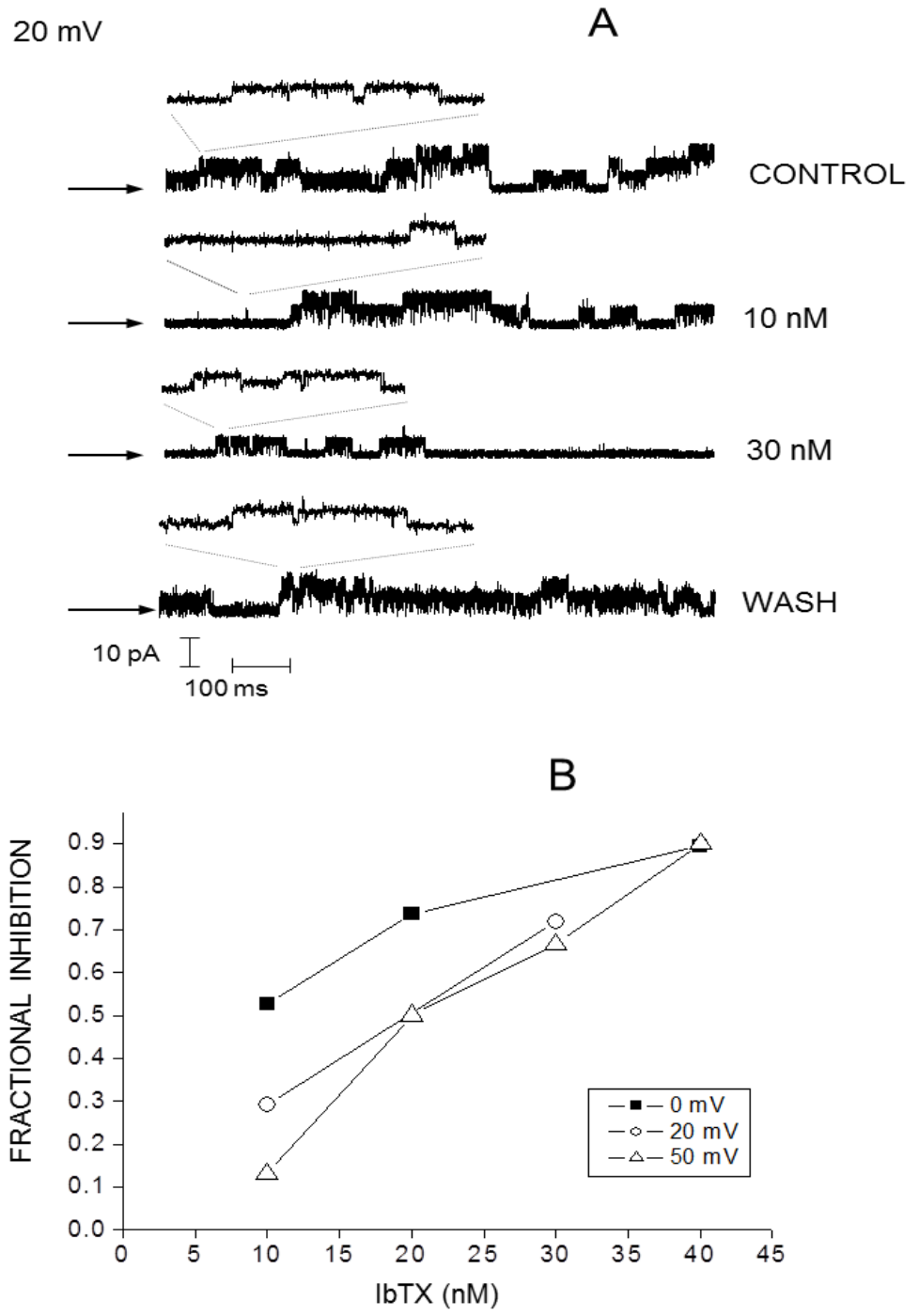

Fig 5.8 The effects of the scorpion toxin blocker IbTX on BK channel activity in outside-out patches from MG63 cells A) The reversible effect of 10 and 30 nM IbTX is shown in a 1s stretch of current record obtained from a single patch at +20 mV. B) The fractional inhibition of maxi channels (calculated from the open probability values) by IbTX (10 – 40 nM) is shown for patch potentials of 0, 20 and 50 mV in 3 outside-out patches. At concentrations below 30 nM the block by IbTX was patch potential-dependent being greatest at 0 mV at 10 nM.

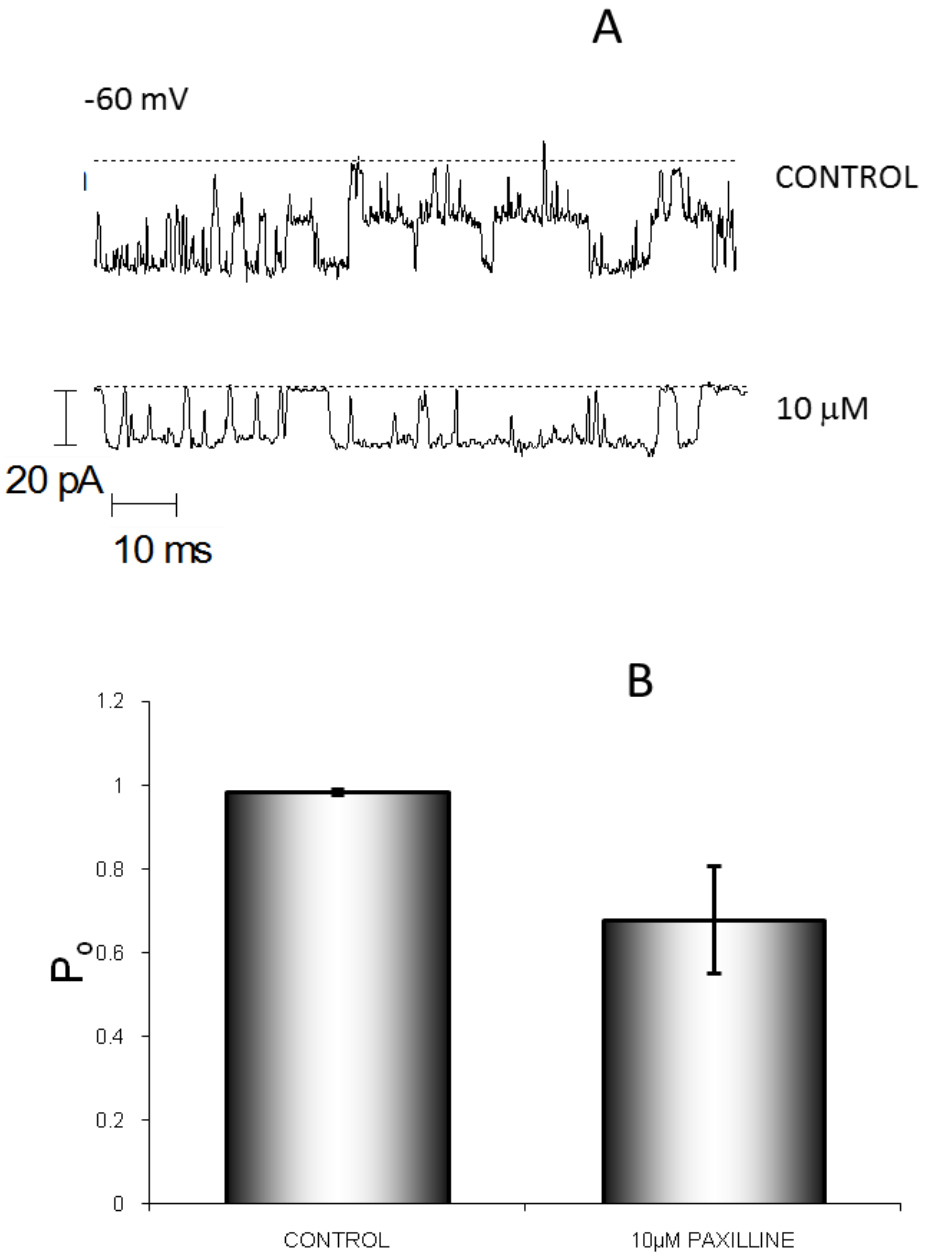

Fig 5.9 (A) The blockade of the BK channel by 10 µM paxilline in an excised inside-out patch from an MG63 cell at -60 mV (reverse physiological K gradient). (B) The pooled data from 5 experiments in patches from MG63 cells showing the mean decrease (30 %, $P < 0.05$) of open probability induced by 10 µM paxilline.

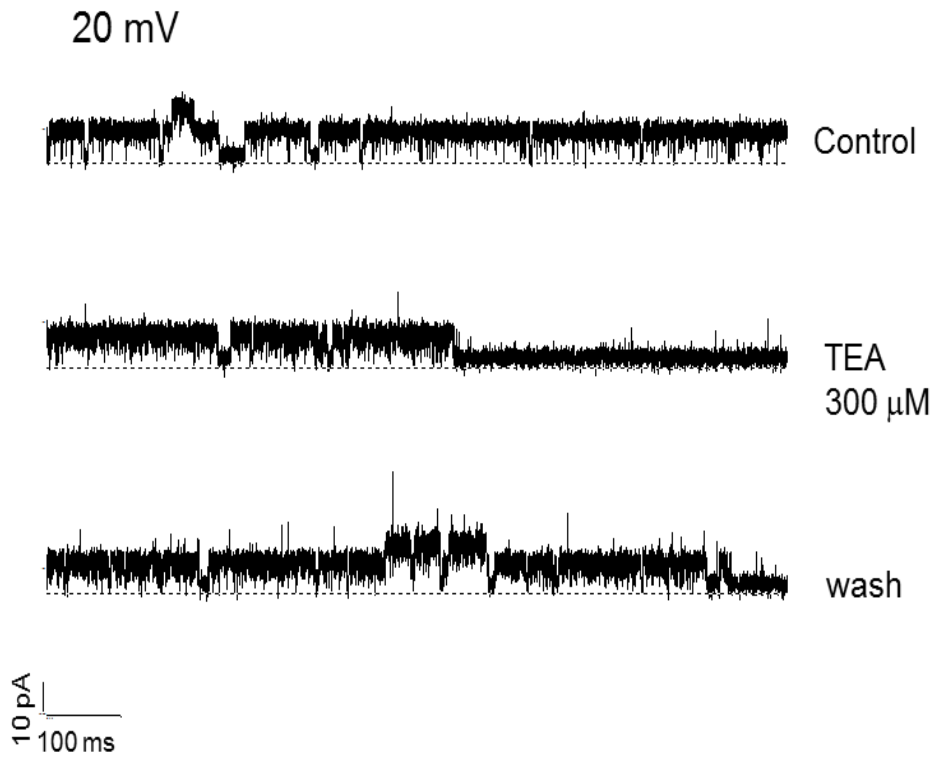

Fig 5.10 In an outside-out patch of human primary osteoblast at +20 mV 300 µM TEA blocked the BK channel showing both an apparent unitary current and Po reduction. This effect was reversible by washing out TEA from the outside of the patch.

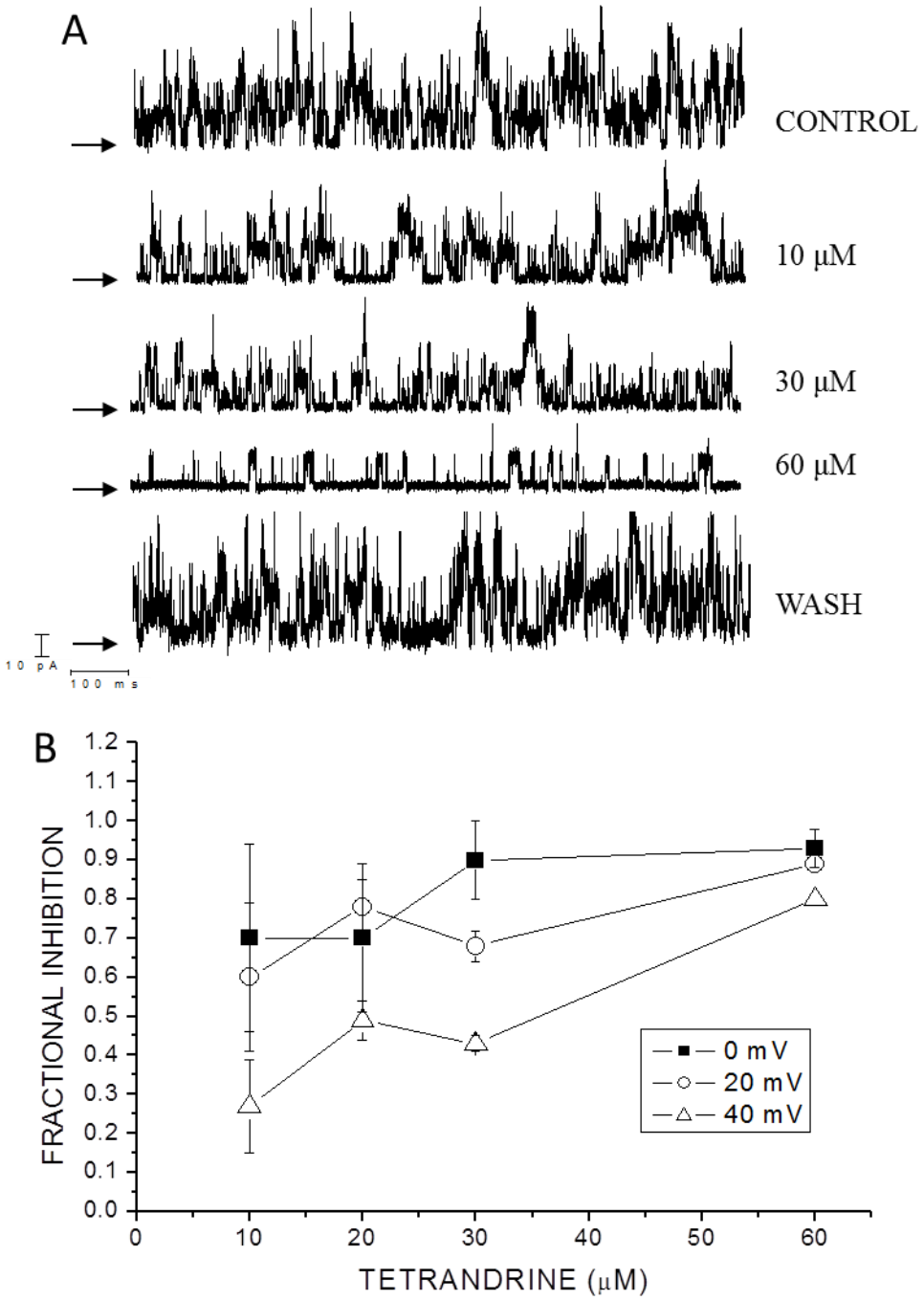

Fig 5.11 A) The reversible effect of 10, 30 and 60 µM tetrandrine is shown on a 1s stretch of current record from an outside-out patch.. The patch potential was 40 mV. B) The fractional inhibition of BK channels (calculated from the open probability values) by tetrandrine (10 – 60 µM) is shown at patch potentials of 0, 20 and 40 mV. Data are means from 7 outside-out patches.

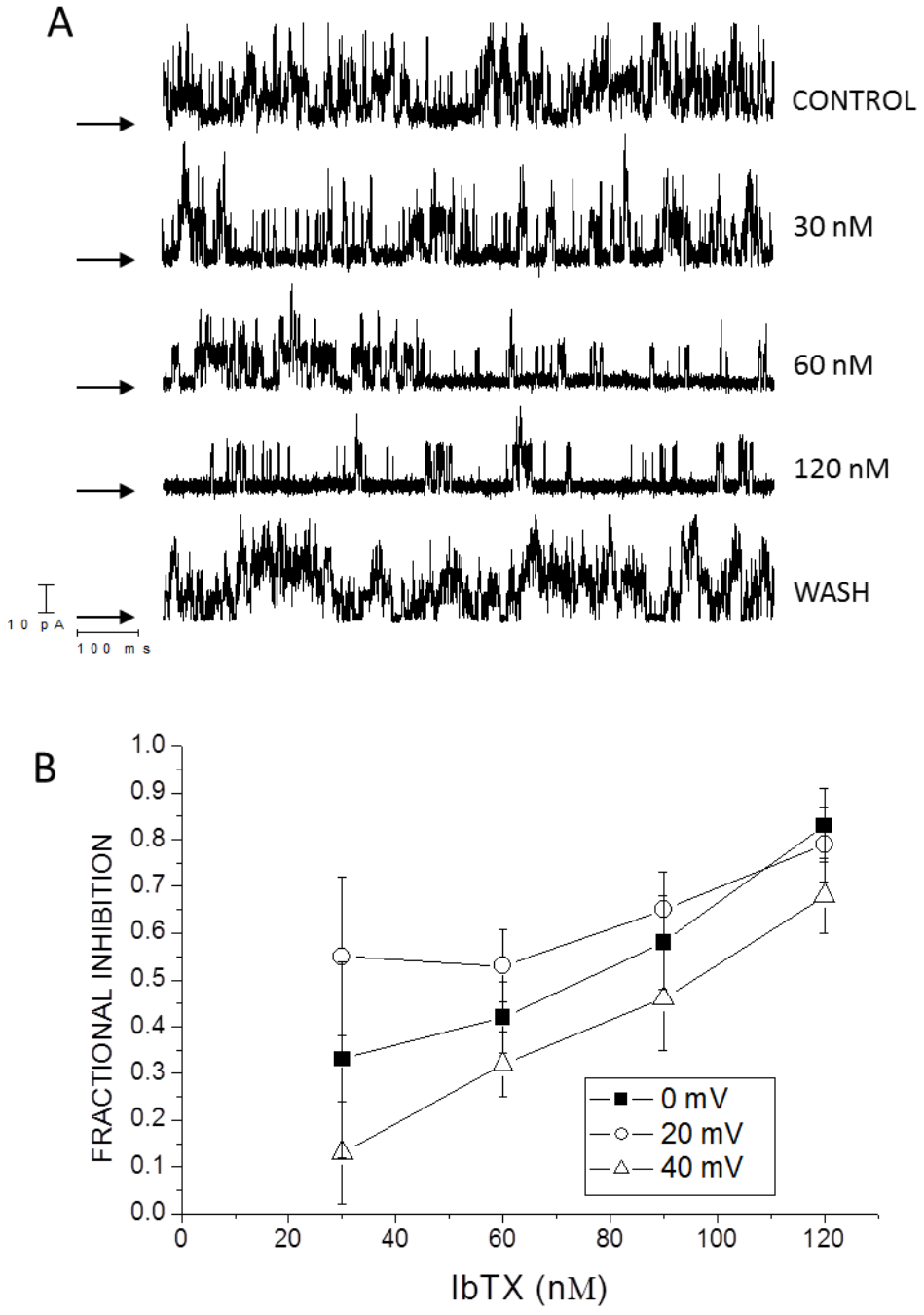

Fig 5.12 The reversible block by 30, 60 and 120 nM IbTX in an outside-out patch at 40 mV is shown in (A). The fractional inhibition of BK channels by IbTX (10 - 120 nM) calculated as a reduction in open probability value is shown at 0, 20 and 40 mV patch potential in 3 outside-out patches in (B).

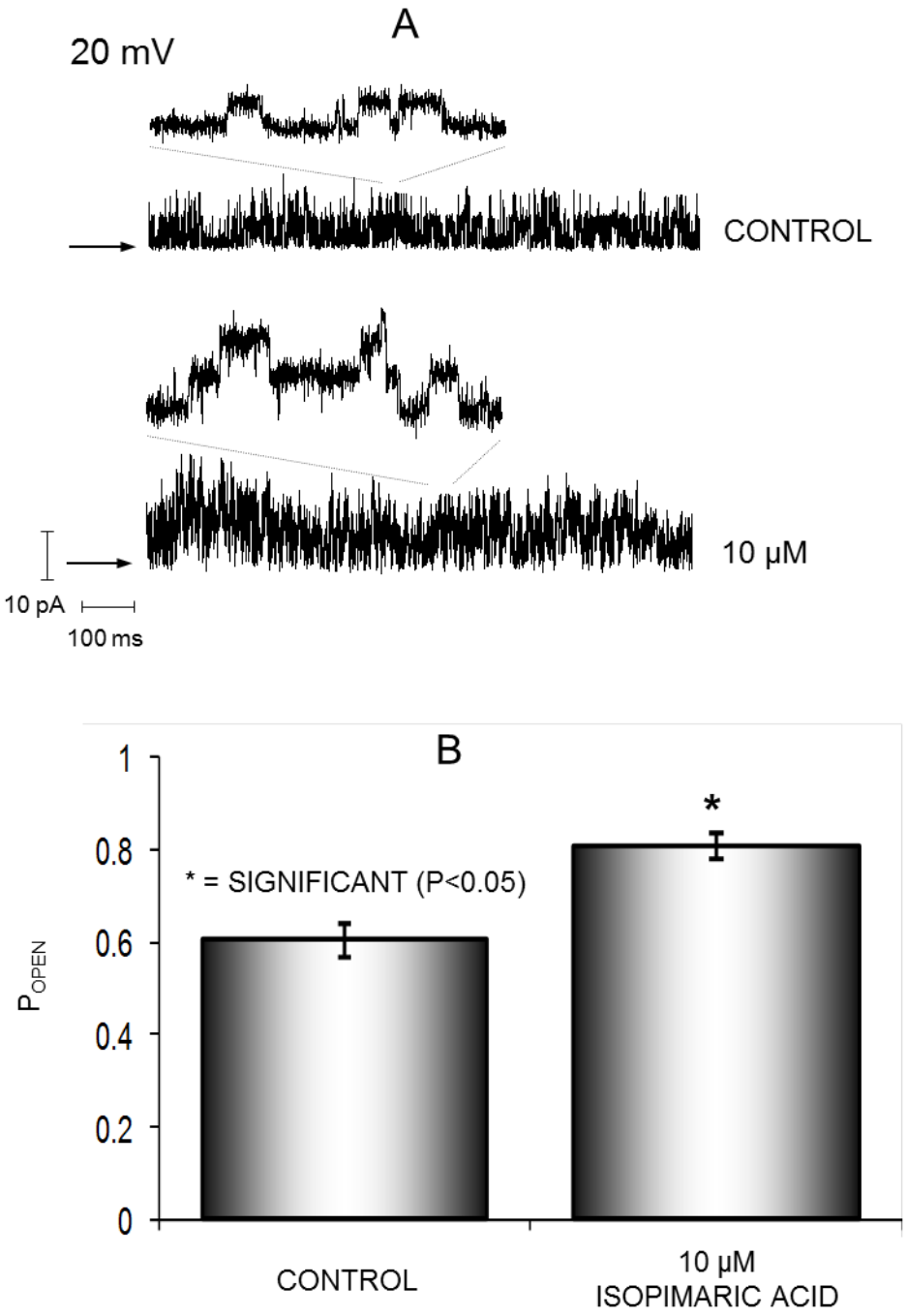

Fig 5.13 A) The activation of the BK channel by 10 µM isopimaric acid in an excised outside-out patch from an MG63 cell at 20 mV patch potential. B) The pooled data from 3 experiments in patches from MG63 cells showing the mean increase (34%) of open probability induced by 10 µM isopimaric acid.

SECTION 6: BK CHANNELS HAVE ROLES IN OSTEOBLAST CELL FUNCTION

6.1 Introduction

The most important function of osteoblasts in vivo is that they are able to proliferate and differentiate to form mineralized bones. The functions are correlated to various phenotypic makers such as high alkaline phosphatase (ALP) activity and synthesizing collagenous and noncollagenous bone matrix proteins including osteocalcin (Aubin and Liu et al., 1996). In earlier sections it was reported that BK channels are expressed with high density in both osteoblast-like cell lines (MG63 or SaOS2) and primary human osteoblasts. The channels were characteristically sensitive to the quaternary ammonium acids, and also peptide toxins and alkaloids. If the channels have important functions in these cells then these functions should be regulated by these channel modulators.

6.1.1 Osteoblasts in bone tissue

Firstly, we should ask what the functions of osteoblasts are and what is known of modulation by K channel ligands. As indicated previously there are three major types of bone cells. These are the osteoclast, the osteoblast and the osteocyte. The principal characteristics of osteoblast cells have been described in the Introduction to this Thesis (section 1) and they are recognised for their high capacity for proliferation and differentiation. As stated previously the latter process is modulated by the interleukins, insulin-derived growth factor, platelet-derived growth factor and estrogen (Guevremont et al., 2003) but to what extent other factors such as ion channel control impacts, is at present unknown. Here we only focus on the possible role of the BK channel.

6.1.2 Potassium channels and bone cell proliferation and mineralisation

The important role of K^+ channels in proliferation of cells of the immune system and tumour cells (Arcangeli et al., 1995) was perhaps to be expected. K^+ channels are major contributor in controlling membrane potential. And recently studies on tumour cell revealed that a transient hyperpolarization was required for the progression of the early G_1 phase of cell cycle (Wonderlin et al., 1996). Thus blockade of K^+ flux leading to depolarization, should delay proliferation by inhibition the transient hyperpolarization as described above.

The BK channel which has a large conductance will lead to a large amount of K^+ ion efflux during channel opening. Its impact is therefore greater than many other K channel types. This type of channel is consequently an important membrane potential regulator in the cells where it is expressed and is active. In conclusion, we might anticipate to see modulators of BK channel modify osteoblast cell growth and mineralisation in vitro.

6.2 Materials and methods

The contribution of BK channels to function in osteoblast-like cells was investigated in cell growth assays. MG63 cells were maintained in culture in the absence and presence of various BK channel modulators of differing specificity including TEA, IbTX, tetrandrine, paxilline and isopimaric acid.

6.2.1 Cell culture in growth assays

All cells were seeded in 6-well plates for Haemocytometer counting and in 96-well plates for the MTS assays. The protocol of performing these experiments is described as follows:

1. Confluent MG63 cells in 25 cm^2 flasks were trypsinised and counted.
2. Cells were suspended in complete DMEM medium at a concentration of 30,000 cells/ml.
3. A 2 ml cell suspension was used in each well of the 6-well plates, a 100 µl cell suspension was used in each well of the 96-well plates and

another 100 µl complete medium was added to make up a final 200 µl volume.

4. Cells in the plates were left at 37ºC, 5% CO_2, 95% air overnight and numbers then recorded as day 0.
5. Compounds to be tested were held in stock solutions in DMSO (filtered through 0.2 µm PVDF syringe filter, Whatman) and kept at -20 ºC, except TEA which was always dissolved in distilled water. Compounds were diluted to proper final concentrations in the complete DMEM medium.
6. Cells were checked that they were attached to the culture surface under a microscope after an overnight in culture. Only when the cells were completely attached, was the supernatant medium sucked out and discarded. 200 µl of medium containing compounds was added to each well.
7. If compounds were dissolved in DMSO then the same concentration of DMSO as the test group was used as the blank control. Otherwise complete DMEM medium was the blank control.
8. Cells were cultured at 37ºC, 5% CO_2, 95% air for 96 hours before being counted by either the Haemocytometer method or using the MTS assay.

6.2.2 Haemocytometer counting

After 96 hours in culture, cells were trypsinised and collected into a centrifuge tube. Cells from different wells but in the same treated group were collected

into one tube. After centrifugation, cells were resuspended in 2 ml DMEM medium. 50 µl cell suspensions were mixed with 50 µl 0.4 % Trypan blue dye. A cleaned haemocytometer was covered tightly by a piece of coverslip and care taken to ensure that the volume in a 1 mm^2 counting area is 1 µl (see section 2). 5 µl of cell solution in Trypan blue was added to each side of the counting area. The unstained live cells were counted using a haemocytometer. The relative cell number was determined as follows: the total cell count of each experimental group / total cell count of control group. Each experiment was repeated twice at different times and the final data were presented as the means ± SD.

6.2.3 MTS

The assays were performed by adding 20 µl of the MTS/PMS solution (20:1) (CellTiter 96 AQ_{ueous} One Solution Cell Proliferation Assay, Promega UK Ltd., UK) directly to each well, incubating for 1-2 hours then recording the absorbance at 490 nm with a Tecan® ELISA 96-well plate reader. The background absorbance was subtracted from the test absorbance values. Data were expressed as relative cell number as described in section 2. Each experiment was repeated 4 times. Data were presented as means ± SD (n=4).

6.2.4 Mineralization

Mineralisation staining

Because MG63 cells do not mineralise in culture, the mineralisation assays were performed with SaOS2 cells. Cells were seeded into 6- or 12-well plates, and maintained in culture until almost confluent. They were then treated with culture medium containing L-ascorbic acid 2-phosphate (50 μg/ml), β-glycerophosphate (2 mM) and dexamethasone (10^{-7}M), in the presence or absence of TPeA (3 μM) and THeA (0.3 μM). The media were changed twice weekly, and the cells were stained for calcium deposits within the mineralised matrix 2 weeks after the assay started. Briefly, experiments were terminated by fixing cell layers in formal saline for 15 minutes. Mineralised bone nodules were visualised by staining with alizarin red (1% solution in water) for 5 minutes, rinsed with 50% ethanol to remove excess stain, then air-dried.

Protein estimation experiment

The cells were treated with 100% methanol and solubilised in 0.5 M sodium hydroxide. Bio- Rad protein assay was used to determine total concentration of solubilised protein in cell lysate samples. The dye binds to proteins giving differential colour change in response to various concentrations of protein. The relative protein concentration measurement can then be estimated by reading absorbance measurements from a standard curve obtained.

6.2.5 Data analysis

Data on cell numbers were analysed by Excel and Origin7. Statistical significance ($p<0.05$) was calculated by using one-way ANOVA as described in section 2.

6.3 Results

In this study, BK channel blockers such as QAs, paxilline and tertrandrine interestingly showed dual-effects on MG63 cell growth. They caused an increase of MG63 cell numbers at low concentrations and a decrease of cell numbers at high concentrations. In addition, QAs affected SaOS2 cells mineralisation as cells cultured with the THeA and TPeA showed lower Alizarin Red S staining and lower protein concentrations.

6.3.1 MTS assay

Firstly, a standard curve for the MTS assay was performed by estimating the absorbance (OD) of different numbers of cells after 1, 2, and 3 hours incubation with dye. Fig. 6.1 showed that after 1 hour incubation gave better linear relation between OD and cell number than the other two incubation condition. Hence, all the MTS assay data were collected after one hour of incubation and using the cell numbers that fall in the linear range of the standard curve to reduce error.

The effects of BK channel blockers on MG63 cell numbers after 96 hours were then examined. Interestingly, both TEA and tetrandrine had a dual effect on growth (Figs. 6.2 and 6.3), significantly increasing cell numbers ($p<0.05$) at low concentrations ($\leq$ 3 mM and 3 μM respectively), but decreasing cell numbers at concentrations of $\geq$ 10 mM and 10 μM respectively (n=4) ($p<0.05$).

These stimulatory effects of TEA and tetrandrine occurred at concentrations of these agents equivalent to those required to achieve BK channel blockade (see e.g. inset in Fig. 6.2). Paxilline like the other modulators also showed this trend, stimulating cell numbers at low concentration, and inhibiting at high concentrations (n=2) (Fig. 6.3). TBuA, TPeA and THeA, three of the quaternary ammonium acids, produced similar effects on MG63 cell growth. TBuA produced an increase of MG63 cell number at a concentration ≤500 μM (Fig. 6.4). TPeA produced a dramatic increase of MG63 cell numbers at the concentration of 3 μM. And THeA produced an increase of MG63 cell numbers at the concentration of 0.3 μM. However these increases were only present over a very narrow concentration range, since the cell numbers dropped down at 10 μM TPeA and 1 μM THeA respectively (Fig. 6.5 and Fig.6.6). Neither IbTX (300 nM, n = 5) nor slotoxin (300 nM, n = 3) had any significant effect on cell numbers (Fig. 6.7).

To test whether blockade of a BK channel was the principal mechanism by which the stimulation was achieved, MG63 cells were grown in the presence of TEA and a BK channel opener, isopimaric acid. Importantly, the increase in cell numbers by TEA could be prevented by the BK channel opener, 50 μM isopimaric acid. Meanwhile, 50 μM isopimaric acid showed no effect on MG63 cell numbers in the same assay (Fig. 6.8).

6.3.2 Haemocytometer counting

MG63 cell numbers were increased at low concentrations and decreased at high concentrations in the case of both TEA and tetrandrine in repeat haemocytometer counting experiments (Fig. 6.9). The inhibition of the stimulatory effect of TEA by isopimaric was also confirmed in repeat growth assays (n=4).

We have also carried out viability measurements with Trypan blue using blockers over a full range of concentrations. In summary, low concentrations of blockers (TEA and tetrandrine) that increase cell numbers do not increase the percentage of dead cells, whereas higher concentrations of blockers (i.e. 10-30 mM TEA and 10 µM tetrandrine) increase significantly the number of dead cells. These was confirmed by checking cell morphology under a microscope and pictures taken of representative cells are shown in Fig. 6.10.

6.3.3 Mineralisation

SaOS2 cells were cultured in the presence of 3 µM TPeA or 0.3 µM THeA for 2 weeks then were stained with Alizarin Red S. The amount of staining indicated that both 3 µM TPeA and 0.3 µM THeA treated cells produced lower mineralisation than control (Fig. 6.11). The protein concentrations from lysate cells treated with THeA (0.3 µM) was lower than cells treated with TPeA (3 µM) and were both significantly lower than control (Fig. 6.12).

6.4 Discussion

Experiments in this section investigated the possible function of BK channels in the growth of osteoblasts and osteoblasts-like cells. A range of BK channel modulators were used to treat cells in culture followed by the measurement of cell number and cell viability. The results indicated a possible role in determining growth for BK channels in osteoblasts.

In summary, in the growth assays the BK blockers QAs and tetrandrine caused cell numbers to increase at low, and to decrease, at higher concentrations. The stimulatory effect of TEA was shown to be blocked by the BK channel opener isopimaric acid. The compelling conclusion is that TEA stimulates MG63 cell growth by modulating BK channels in these cells. Importantly, these quaternary ammonium acids (3 μM TPeA and 0.3 μM THeA) also decreased the SaOS2 cell mineralisation in culture.

6.4.1 Peptide toxins showed no effects on MG63 cells growth

Cell growth assays on MG63 cells with IbTX were described above and showed little effect of the toxin. Indeed such experiments have been conducted by three different investigators in this laboratory and all results proved negative, unlike what was found previously by other investigators using glioma cells (Ransom et al., 2000 and Weaver et al., 2006). However, this is in keeping with the fact that peptide toxins showed low affinity for the BK

channels in MG63 cells as described in Section 5. In cell growth assays, IbTX and slotoxin showed almost no effect on MG63 cell growth suggesting no obvious link between one class of BK channel (type I) and cell growth. On the other hand, in the pharmacological characterisation of BK channels described above in MG63 cells these channels were more sensitive to alkaloids and TEA than the toxins. Correspondingly, both TEA and tetrandrine showed obvious and interesting effects on MG63 cell growth.

6.4.2 TEA and other quaternary ammonium acids

Results from Section 5 revealed that TEA and other 3 QAs (TBuA, TPeA and THeA) blocked BK channels in MG63 cells at different concentrations. In short the longer the chain length, the greater the potency of blocker. These compounds also regulate MG63 cell growth as described in this section with the longer chain blockers being more potent. Although TEA has been reported to down-regulate cell growth in human gliomas (Weaver et al., 2004) no effects of other QAs in the literature have been reported before. The work reported here revealed these QAs (TEA, TBuA and TPeA) cause a cell number increase at apparently low concentrations, while decreasing at high concentrations. The compounds at high concentrations caused cell death as the dead cell numbers clearly increased in the haemocytometer counting experiments. TPeA showed a very narrow window between the concentrations causing a cell number increase (3 μM) and a decrease ($\geq$ 10 μM).

TPeA and THeA caused a decrease of SaOS2 cell mineralisation at the concentrations (3 and 0.3 µM, respectively) that cause an increase of cell growth. According to Steinand and Lian (1993) (see graph on the right), there are three distinct development periods of osteoblasts, including: proliferation, ECM maturation and mineralisation (illustrated in the diagram shown on the right). They also pointed out that cell proliferation and mineralisation are associated with different genes. The genes related to cell cycle are down regulated at the end of proliferation period meanwhile the genes relating to ECM maturation and differentiation are up regulated. When the cells were stimulated for growth, in this stage the differentiation associated genes might be inhibited.

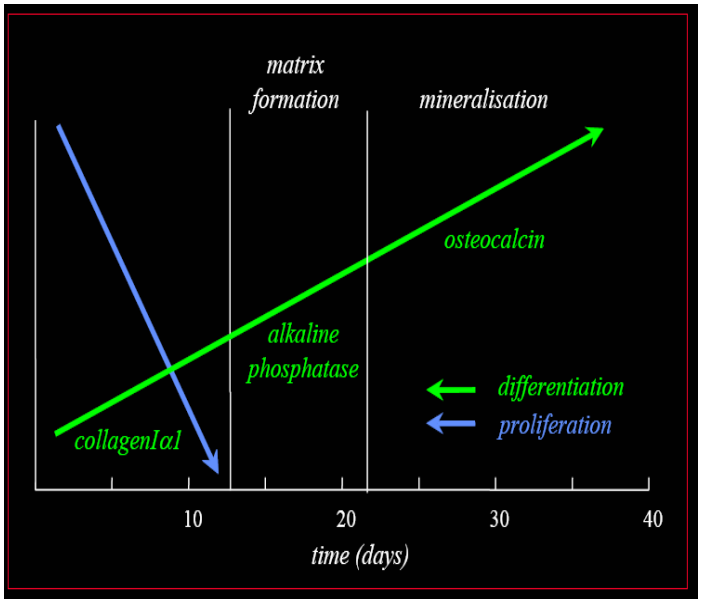

6.4.3 Alkaloids increase and decrease MG63 cell numbers

The key question here is why this alkaloid has a dual effect on cell numbers depending on the concentration tested. Could the increase in cell number be due to the reduced apoptosis which would follow any reduction of K efflux? (see Burg et *al.* 2006). Does this then dominate at low concentrations of

tetrandrine? As for the effects of higher concentrations, tetrandrine has previously been reported as a potential inhibitor of tumour cell proliferation (Wang et al., 2004). There are two possible tetrandrine-targeted signalling pathways where putative anti-cancer effects have been described. One is that the BK channel blockage leads to the depolarization of cell membrane which could activate P53 and P21 expression. P21 is a key inhibitor of cyclin D-cyclin-dependent kinases (CDK) complex and the phosphorylation of its target triggers cell proliferation. Hence P21 expression will inhibit cell proliferation. In addition, P53 may trigger cell apoptosis. Perhaps this is the dominant process at higher concentrations. In the cell growth assays with MG63 cells dual effects were observed: cell number increasing with lower than 3 μM tetrandrine and declining with high tetrandrine (≥ 10μM) in culture. This result would indicate that tetrandrine at low concentrations regulates cell growth through different mechanisms in tumour and osteoblast-like cells.

6.4.4 Experimental design

The MTS assay is a convenient way to investigate any changes of cell number but it is not able to distinguish between modified proliferation or altered apoptosis. The cell viability assay and consideration of the morphology of the cells would help. Hence, viability assays were carried out and cells were photographed under a microscope as described in Fig. 6.10. MG63 cell numbers in the experiments with 10 and 30 mM TEA decreased within 4 days incubation and dead cell number increased as shown in the pictures. These

results together indicate that 10 mM TEA or higher is toxic to MG63 cells and causes cell death. But from these experiments it is not possible to determine whether the cell death is caused by apoptosis or necrosis. Further experiments could be carried out to find out the underlying reasons for the changes in cell number. For example, the cells could be labelled with carboxyfluorescein diacetate succinimidyl ester (CFSE, Invitrogen). After culturing with BK channel modulators, cells would need to be run through flow cytometry to identify both the proliferated and dead populations.

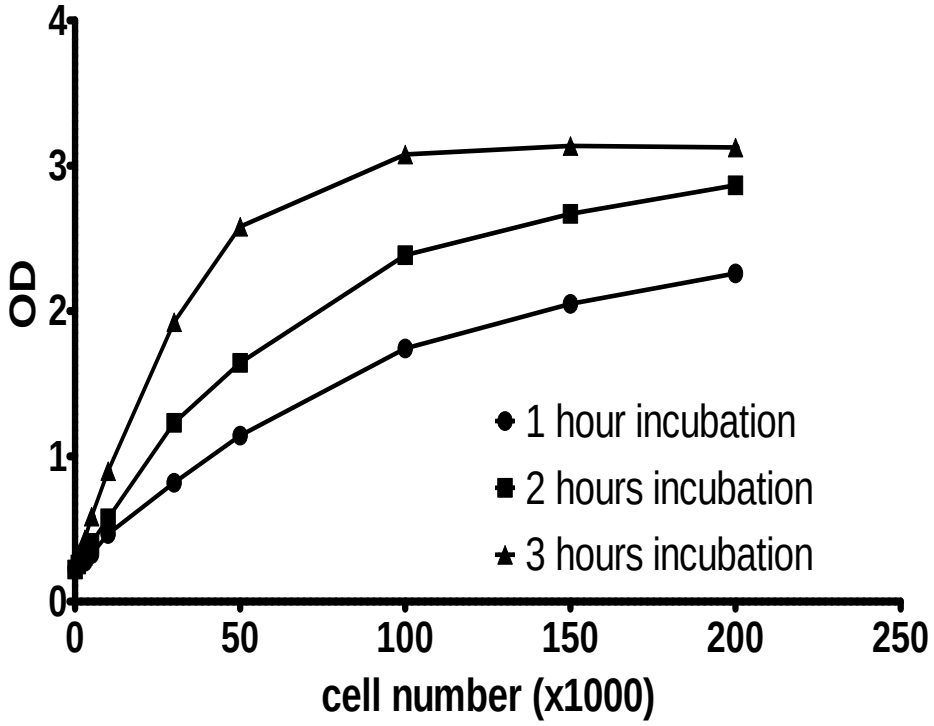

Fig 6.1 Standard curve of MG63 cells absorbance at 490 nm versus cell number. The absorbance was obtained after incubation of MG63 cells with CellTiter96®AQ_{ueous} for 1, 2 and 3 hours. And after 1 hour incubation, the absorbance showed better linear relation with cell numbers than the other two incubation time.

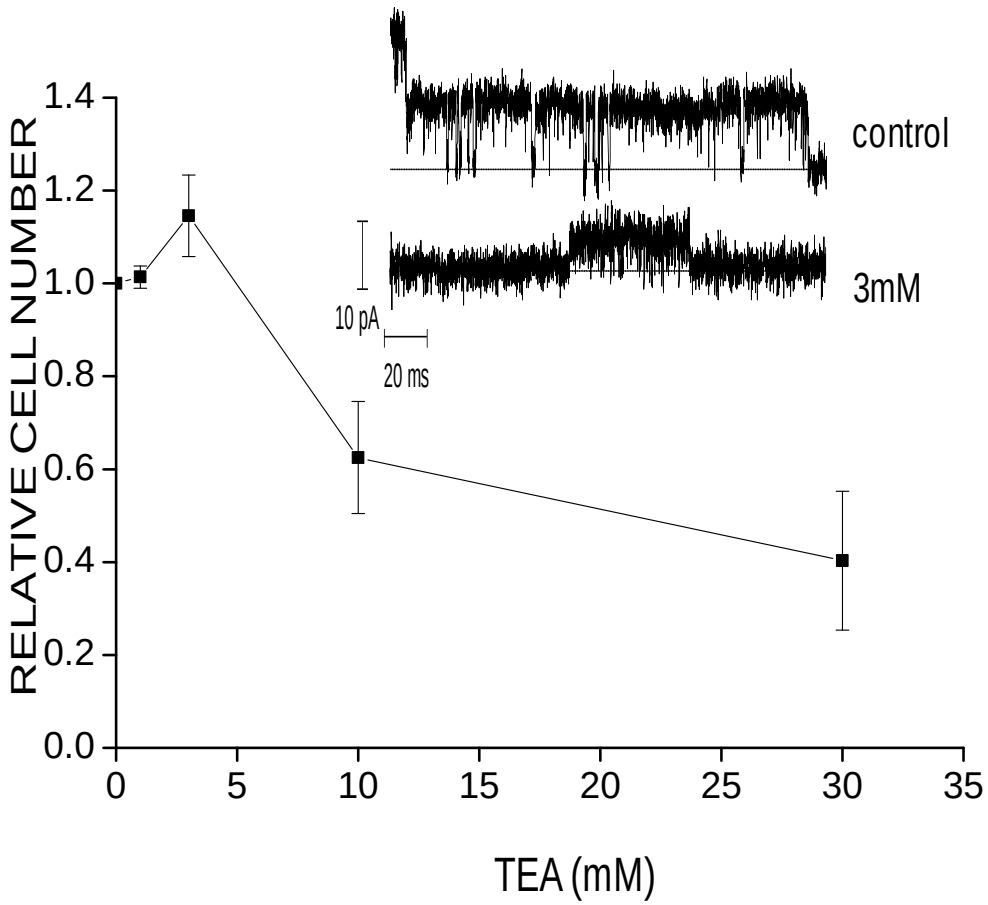

Fig 6.2 The relationship between MG63 cell numbers and TEA concentration (1-30 mM) determined by the MTS assay. The points are the means of 4 determinations after 4 days. There is a significant ($P<0.05$) increase and decrease in cell numbers at low and high concentrations of TEA respectively. The inset shows the effect of 3 mM external TEA on BK channel activity in an excised outside-out patch.

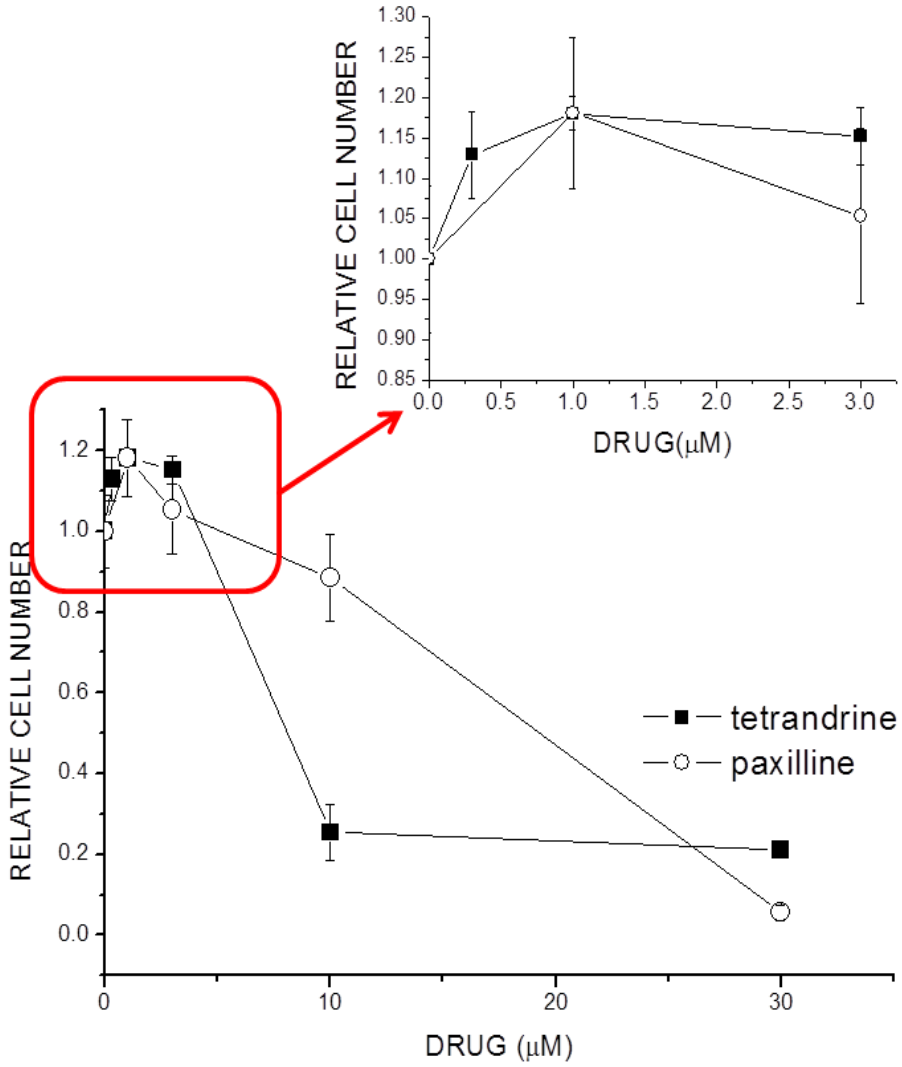

Fig 6.3 The relationship between MG63 cell numbers and tetrandrine concentration (300 nM to 30 μM) and paxilline (300 nM to 30 μM). The tetrandrine data are the means of 4 determinations after 4 days. There is a significant ($P<0.05$) increase and decrease in cell numbers at low and high concentrations of tetrandrine. Paxilline regulated MG63 cell number in a similar manner to tetrandrine. It also produced a significant increase at 300 nM from the pooled data from 2 experiments.

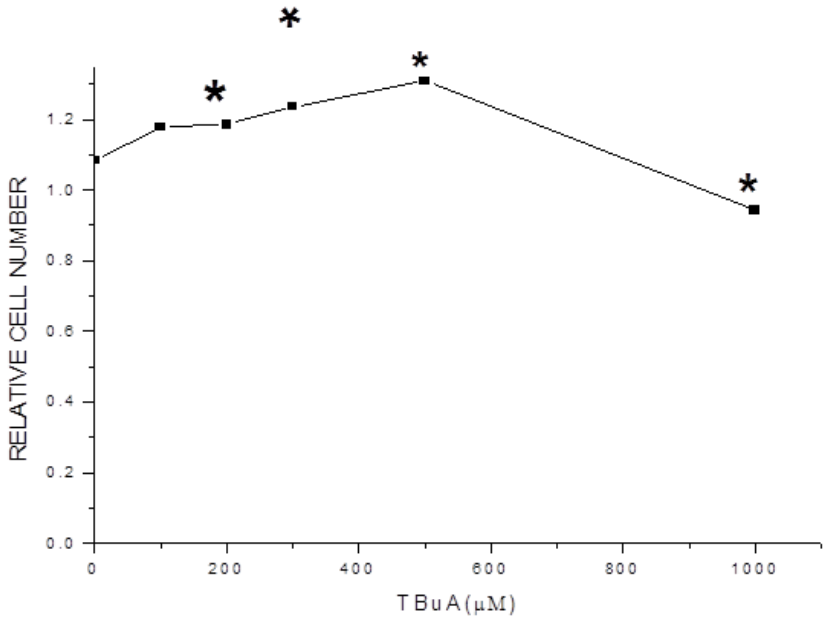

Fig 6.4 The relationship between MG63 cell number and concentration of TBuA determined by MTS assay. There were significant increases in relative cell number with TBuA ≤ 500 μM and a decrease at 1 mM.

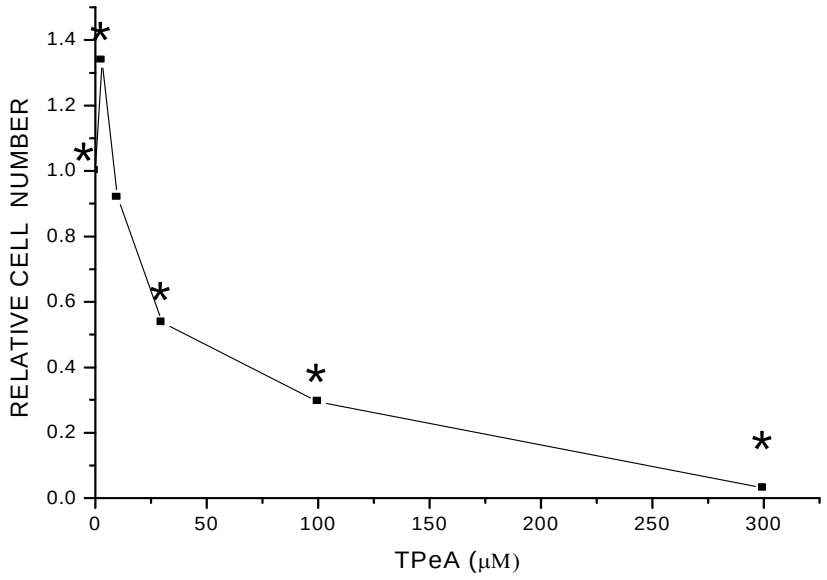

Fig 6.5 The changes in relative cell numbers with TPeA treatment determined by MTS assay. There is a significant increase at 3 μM, and cell numbers decreased at 10, 30, 100 and 300 μM. The insert is the amplification of the cell number at 3 μM TPeA.

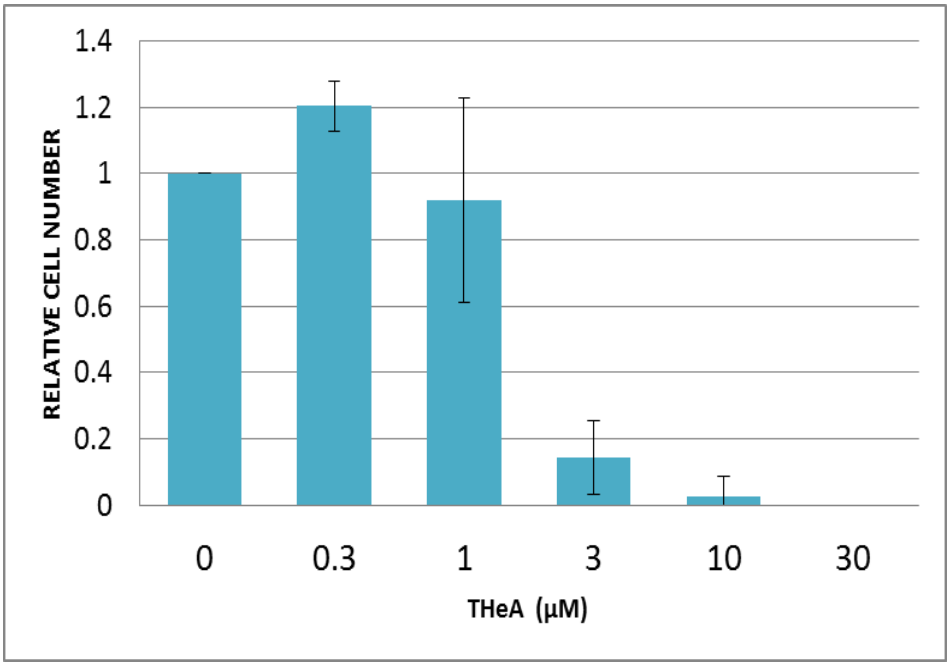

Fig 6.6 The changes in relative cell number with THeA treatment determined by MTS assay. There is a significant increase at 0.3µM, but cell numbers decreased at 1, 3, 10 and 30 µM.

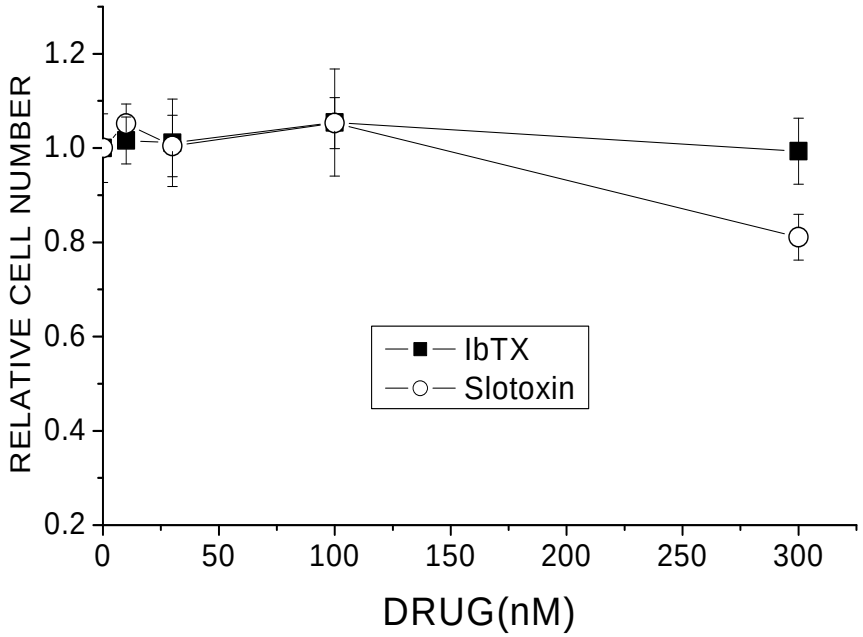

Fig 6.7 The relationship between MG63 cell numbers and IbTX (1-300 nM) and Slotoxin (1-300 nM) determined by the MTS assay. In the case of IbTX the points are the means of 5 determinations and 3 in the case of Slotoxin after 4 days. There is no significant difference in cell numbers over the whole concentration range for either blocker.

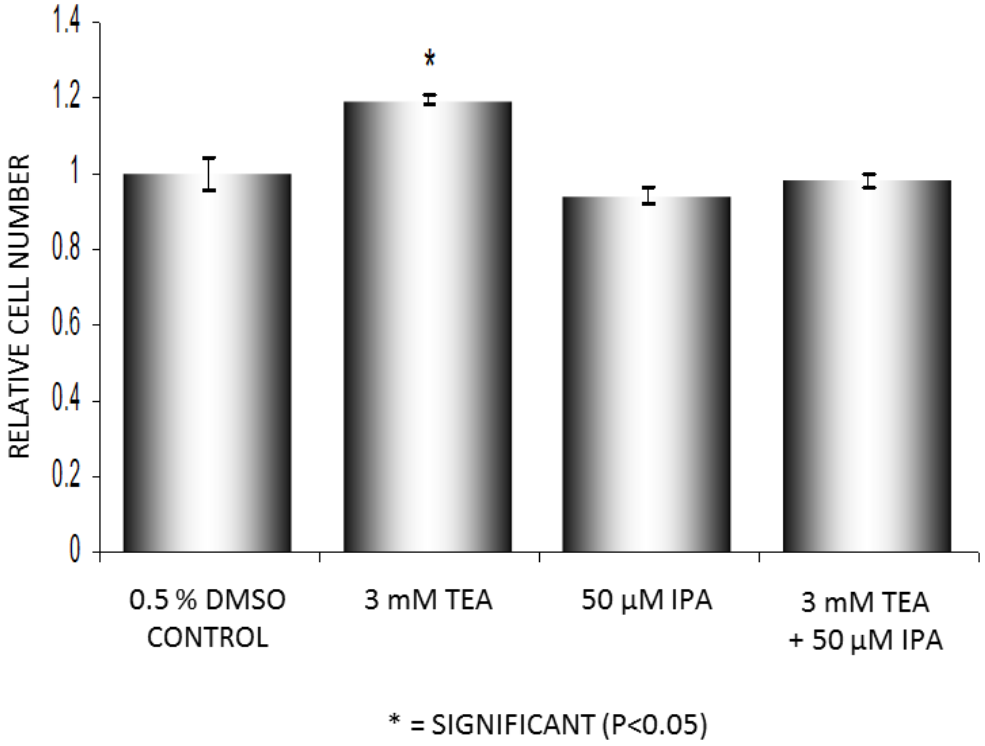

Fig 6.8 The effects of both TEA and isopimaric acid either alone or in combination, on MG63 cell numbers after 4 days. TEA alone increased significantly ($p < 0.05$, $n = 3$) cell numbers. Isopimaric acid alone (50 µM) did not affect cell numbers but blocked the effects of TEA.

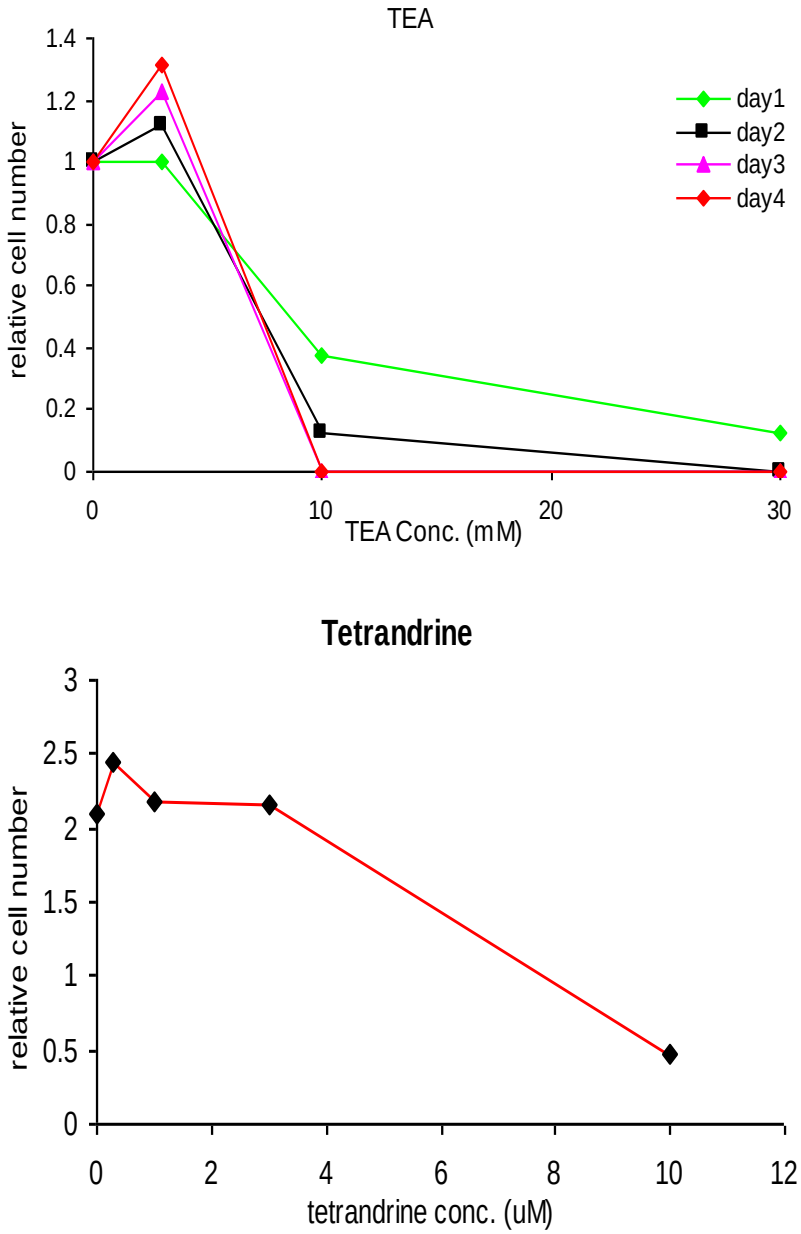

Fig 6.9 Haemocytometer counting confirmed the concentration and time-dependent biphasic effect of both blockers TEA and concentration-dependence of tetrandrine as indicated using the MTS assay. For example, 3mM TEA stimulated MG63 cell growth as the cell number increased (depending on culture days) while 10 and 30 mM TEA seemed to cause cell death rather than just inhibiting cell growth, sinceon day 3 and day 4 the relative cells numbers were close to 0.

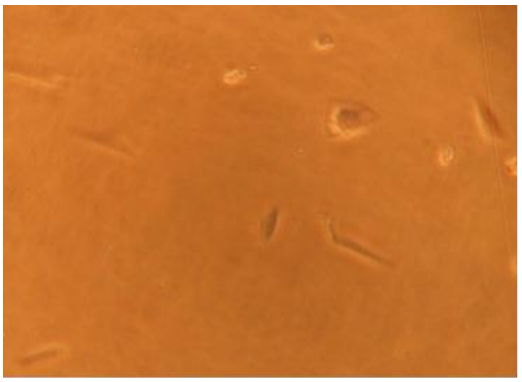

1 mM TEA Day 0.5

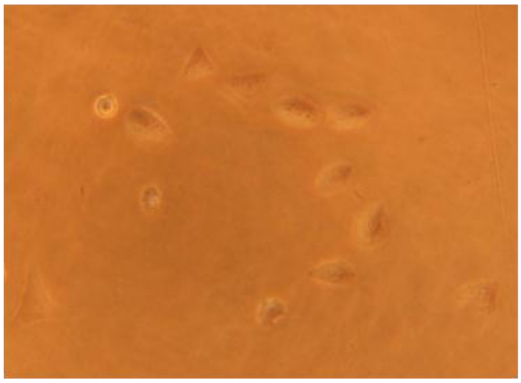

3 mM TEA Day 0.5

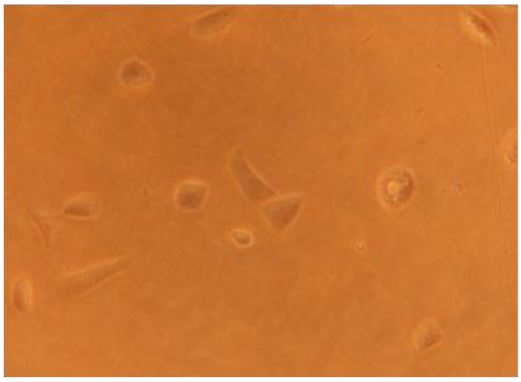

10 mM TEA Day 0.5

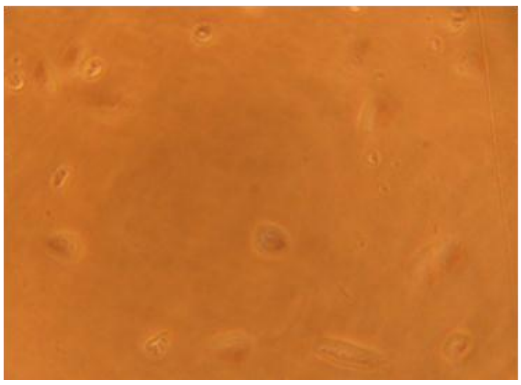

30 mM TEA Day 0.5

(continued)

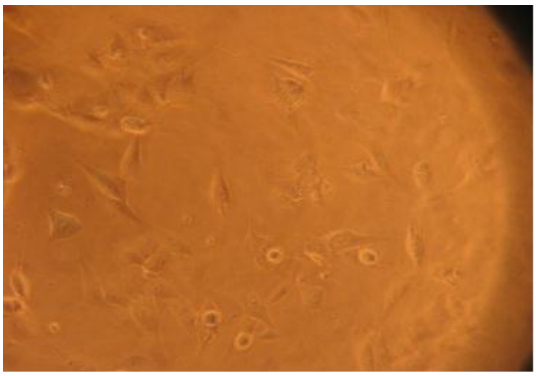

1 mM TEA Day 1

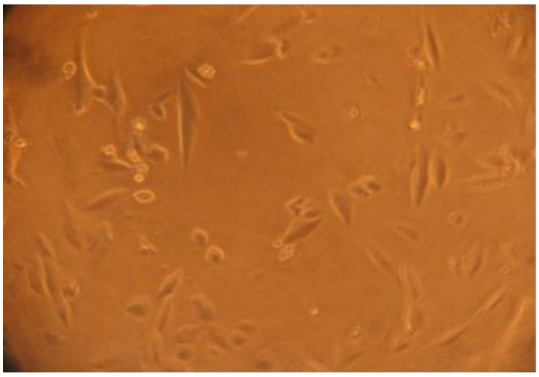

3 mM TEA Day 1

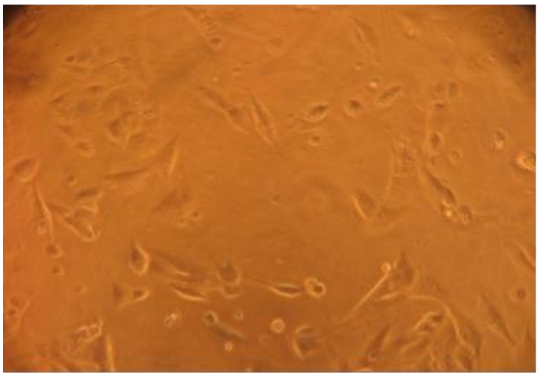

10 mM TEA Day 1

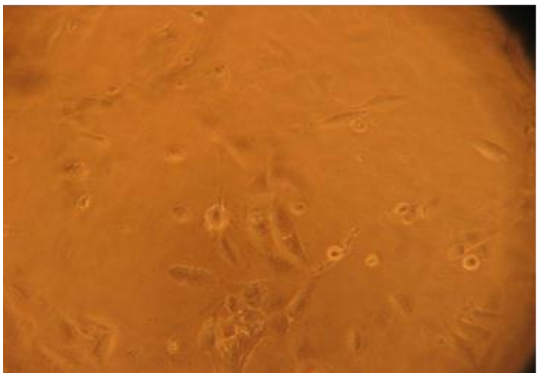

30 mM TEA Day 1

(continued)

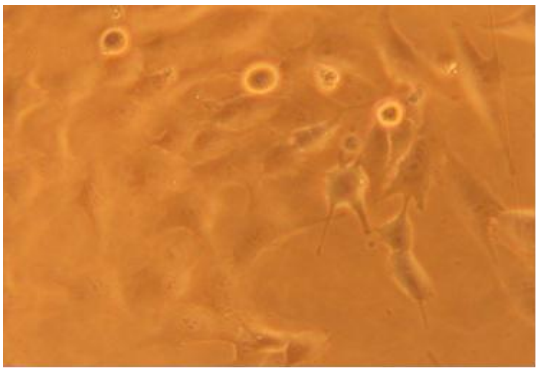

1 mM TEA Day 2

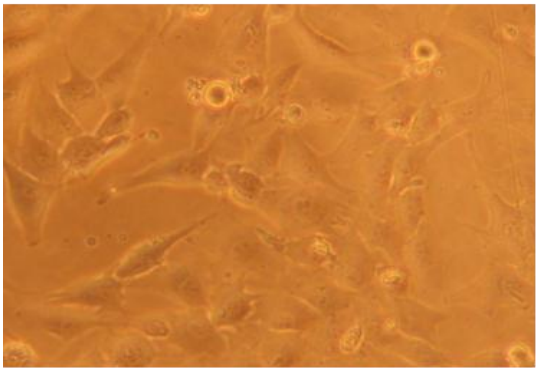

3 mM TEA Day 2

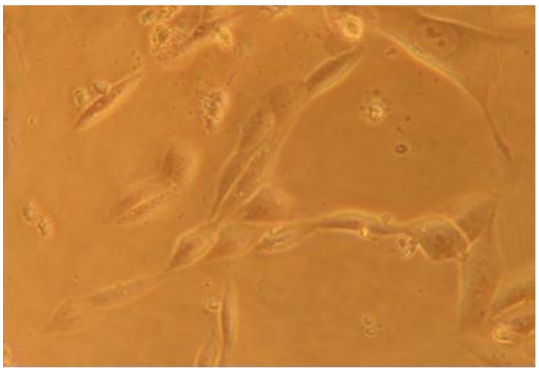

10 mM TEA Day 2

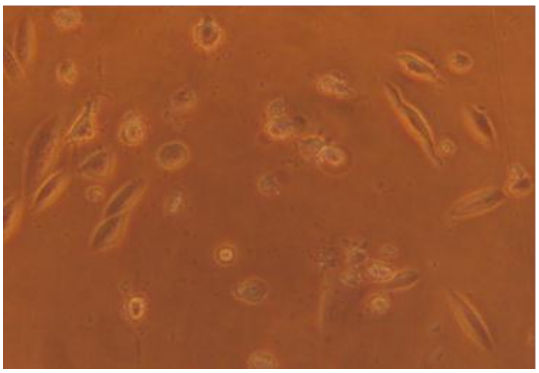

30 mM TEA Day 2

(continued)

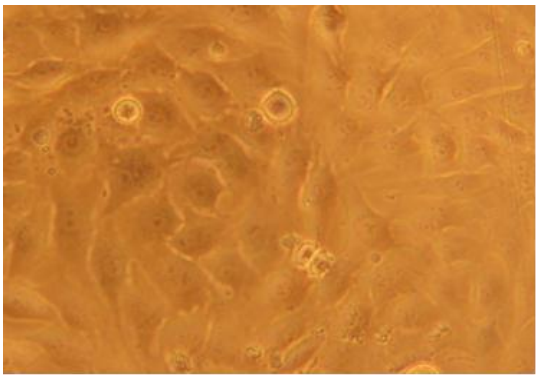

1 mM TEA Day 3

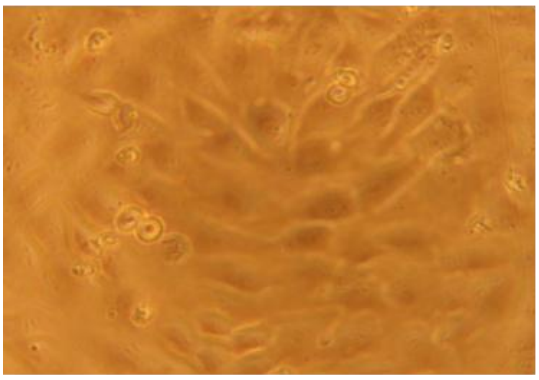

3 mM TEA Day 3

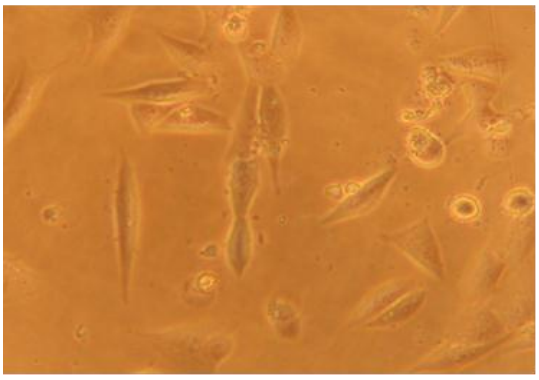

10 mM TEA Day 3

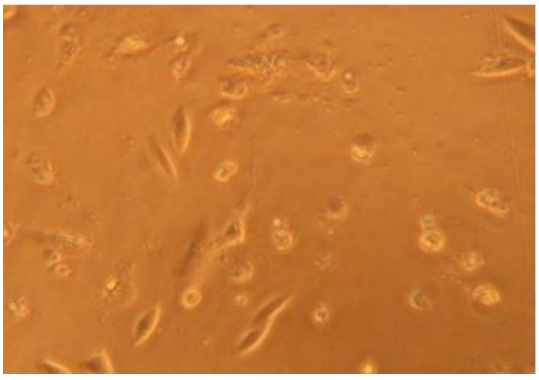

30 mM TEA Day 3

(continued)

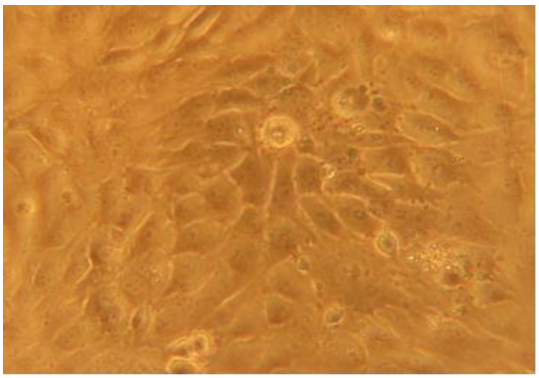

1 mM TEA Day 4

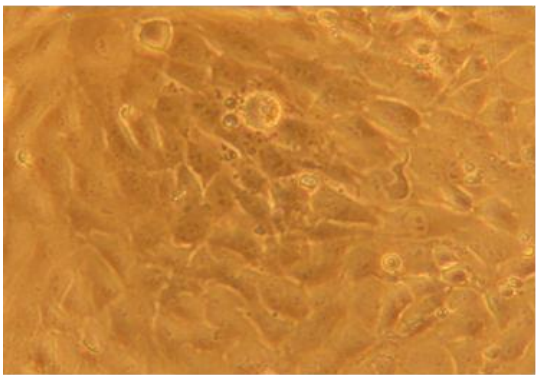

3 mM TEA Day 4

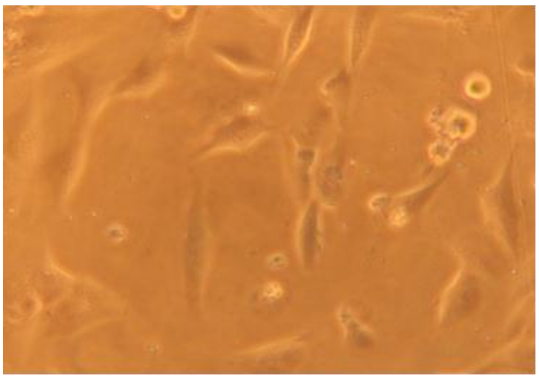

10 mM TEA Day 4

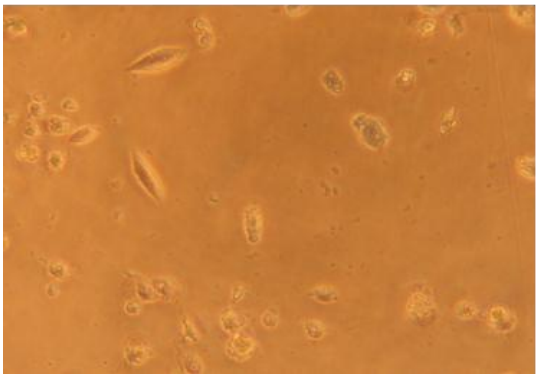

30 mM TEA Day 4

Fig. 6.10 MG63 cell growth with TEA in culture medium were evaluated microscopically. Pictures of cells cultured with 1, 3, 10 and 30 mM TEA at day 0.5, 1, 2, 3 and 4. All images were taken at x200.

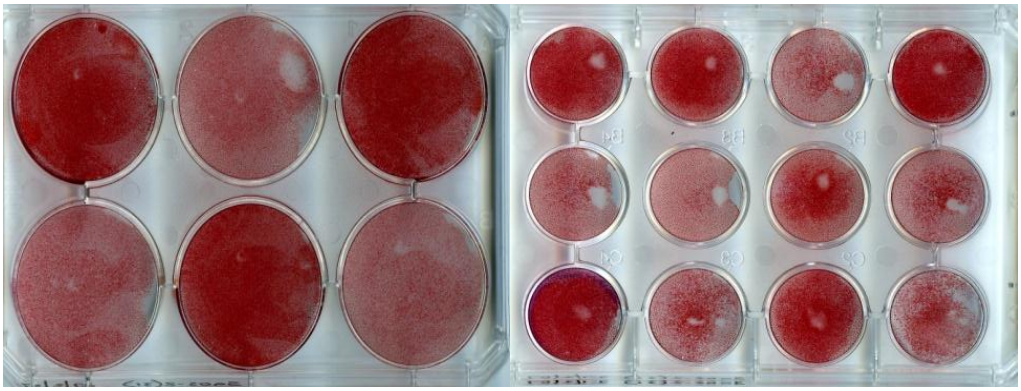

Fig. 6.11 Pictures showing the Alizarin Red S staining of SaOS2 cells after 2 weeks culture with 3 µM TPeA, 0.3 µM THeA and DMEM. Both 3 µM TPeA and 0.3 µM THeA showed weaker staining than DMEM control which indicates a decrease of cell mineralisation.

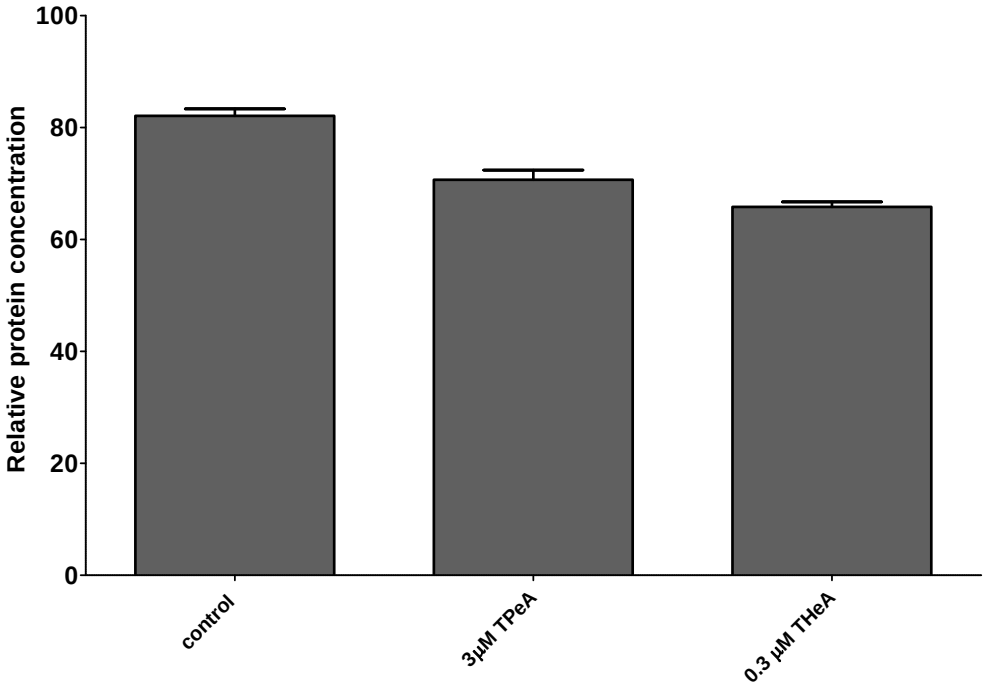

Fig. 6.12 Comparison of the relative protein concentrations of 3 µM TPeA or 0.3 µM THeA treated cells to DMEM control. After 2 weeks in culture 3 µM TPeA or 0.3 µM THeA decreased the protein concentration in SaOS2 cells significantly with P=0.03 and P=0.003, respectively.

SECTION 7: DISCUSSION

7.1 Summary

Data from this project systematically characterized the BK channels in human osteoblast and osteoblast-like cells. The principal findings in this project can be summarised as follows:

- BK channel was observed with high prevalence and activity in all these following cell types: primary osteoblasts, primary bone marrow cells, osteoblast-like cells, osteocyte-like cells and BK channel DNA transfected HEK293 cells. RT-PCR results show that the message for the BK channel α subunit (KCNMA1) and all the β subunits (KCNMB1-4) in MG63 cells and human primary osteoblasts is present.
- This type of potassium channel, whose P_K/P_{Na} estimated in excised inside-out patches in asymmetric K is 15/1, is voltage-dependent and has a mean conductance of over 200 pS in symmetrical 140 K. The BK channels in human primary osteoblast and osteoblast-like MG63 cells showed high activity with an open probability (Po) > 0.7 over a range of potentials from inside-out patches.

- BK channels in human osteoblasts and osteoblast-like cells showed apparently higher affinity to the alkaloid acid (tetrandrine) than to peptide toxins (IbTX).
- Importantly the BK channel was functional since BK channel blockers such as QAs and tetrandrine modulated osteoblast and osteoblast-like cell proliferation and mineralisation. Consistent with the view that the BK channel is the target, TEA effects on cell proliferation were inhibited by the BK channel opener, isopimaric acid. In addition both THeA and TPeA had an effect on osteoblast differentiation, decreasing $SaOS_2$ cell mineralisation capacity in vitro.

7.2 BK channels in osteoblasts may have novel characteristics

It could be argued that features of the BK channel in osteoblasts are novel in some respects. For example the channel is potentially comprised of β1 subunits yet lacks the required sensitivity to estrogens which one might hope for. The published data suggest variable effects of oestrogen on post-menopausal women. These results indicate the existence of complex estradiol-signaling mechanisms, mediated by plasma membrane proteins (i.e. non-genomic) rather than the classic intracellular receptor. The bone cell membrane BK channel is one such potential target for oestrogen. Both oestrogen and Tamoxifen, a partial agonist of the estradiol receptor, have been shown to activate BK channels in both heterologous expression systems and smooth muscle cells, resulting in greater repolarizing current (Wellman et al., 1996; Darkow et al.,

1997). Interestingly, Valverde et al. (Valverde et al., 1998) showed that activation of BK channels by 17ß-estradiol occurs when the channel is associated with its accessory ß1 subunit. This observation has led to the intriguing hypothesis that ß1 subunit directly binds estradiol and enhances channel activity by an unidentified mechanism. However, 2-Methoxyestradiol, an endogenous and active metabolite of 17β-estradiol, inhibits the BK channel in cultured vascular endothelial cells (Chiang et al., 2000). In 2003 Korovkina reported that exposure to 17ß-estradiol induced both a decrease in BK channel current and a down regulation of channel protein expression in heterologous systems (HEK293 cells). The presence of the ß1 subunit did not alter channel expression, and its expression was inhibited by estradiol. The mechanism the investigation implicated was that estradiol induced proteasomal degradation of the channel after direct binding of oestrogen to the BK channel. This down-regulation can be elicited independently of classical nuclear estradiol receptors or the accessory ß1 subunit, but in the presence of ß1 subunits specific binding of estradiol to BK channels is increased significantly. In the experiments reported in chapter 5, acute 17β-estradiol exposure did not alter the open current of BK channel and even decreased the Po in these experiments. If however the cells were treated with 17β-estradiol for 48 hours (data not shown) and then patched, the channels were activated. The open probability was increased in two experiments. It may be that 17β-estradiol modulated BK channel through other messengers or by binding to the channel β1-subunit although the slow development of the activation would then need to be explained. The β1 subunit of BK channels was detected by RT-PCR in both

MG63 cells and primary osteoblasts. But the BK channels in these cells do not show the typical β1 subunit feature, that is the requisite sensitivity to 17β-estradiol or other oestrogen receptor modulators. This could be partly explained by De Wet's discovery on BK channels (De Wet et al 2006). These authors report that the BK channel's sensitivity to 17β-estradiol needs at least 3 β1 subunits to be expressed in one native channel. When there is more than one type of possible β subunit (i.e.4) the chance for all 4 β1 subunits to be present in one channel is extremely low (< 1/35). Perhaps for this reason alone, acute application of 17β-estradiol did not cause a simple up- or down- regulation of BK channel activity.

The voltage-dependence of activation and the pharmacology of the BK channel can provide clues to the BK channel subunit composition. The characteristics the BK channel showed in the voltage-dependence of activation suggested a channel comprised of subunits β1 / β4 + α. However, the pharmacological results do not support this exactly. The presence of a β4 subunit normally confers insensitivity to IbTX. The novel feature here is that the osteoblast BK channel can always be blocked by tetrandrine but in some cases it can be blocked by both IbTX and tetrandrine. The pharmacology is only partially diagnostic of the subunit composition and more characterisation of the channel and quantitative PCR will provide further clues to the precise make up of the native channel. On the other hand, by analysing wild-type and BK-deficient ($BK^{-/-}$) mice using *in vitro* and *in vivo* assays, the different functional

characteristics of these β subunits have been to some extent defined. (Sausbier et al., 2005; Prossmann et al., 2009).

7.3 BK channel modulators and MG63 cell growth

Osteoblasts are dynamic cells undergoing proliferation and secretion and are also also targets of various regulators. These regulators could work through receptors on the membrane, or regulate cell function through other membrane proteins such as ion channels. The extent to which they work on the BK channel depends on its precise characteristics. It appears from this project, that the single channel conductance of the BK channel and its dependence on external K^+ is similar to other tissues. We believe that it is unamibiguously the BK channel despite reservations that have just been published in 2011 (see Sausbier et al. 2011). The ionic selectivity as determined in an excised patch is perhaps lower than has been previously reported however (Wann and Richards, 1994; Chapman *et al.* 2007). Although the BK channel subunits were identified, the relative amount of each subunit and the subunit composition of naïve channel were not determined. As indicated above the voltage-dependence of activation and the pharmacology of the BK channel can however provide clues to the subunit composition. The position of the activation on the voltage axis is suggestive of a channel comprised of subunits β1 / β4 +α (Lippiat *et al.* 2003; Chapman *et al.* 2007) which coincides partly with the recent the data of Hirukawa et al. (Hirukawa et al., 2008) showing that the principal β subunits of BK channels expressed in primary human osteoblasts derived from ulnar

periosteum were β3 and β4. This conclusion would however be at odds with the pharmacological picture in these cells. The presence of a β4 subunit normally confers resistance to IbTX (Meera *et al*. 2000). The novel feature here is that the osteoblast BK channel can in some cases be blocked by both the peptide toxin IbTX and the alkaloid tetrandrine.

In this study, quaternary ammonium acids seem to have a high impact on modulating the BK channels in osteoblasts and osteoblast-like cells. BK channels in patch-clamp were completely blocked by 3 mM TEA and at this concentration TEA caused a significant increase of MG63 cell growth. Other concentrations over 3 mM such as 10 and 30 mM TEA decreased the MG63 cell growth. This might suggest that TEA concentrations above 3 mM affect MG63 cell growth but this is not related to BK channels. On the other hand, these conflicting concentrations may be due to the experiments' sensitivity and condition. In the patch-clamp studies we were examining the effect of an acute exposure (tens of seconds - 1 minute) to the blocker on channel activity in excised patches (cell-free without intracellular machinery) at room temperature of 20-25° C, whereas the effects on whole cell growth were carried out in populations of cells over 96 hours at 37° C. The dual effect of TEA and tetrandrine in the growth assays is however interesting, although at present difficult to explain. That the cell increase caused by TEA could be inhibited by isopimaric acid is compelling evidence that the BK channel plays a key role in this case. One obvious question is whether the decrease in cell number at higher concentrations is also sensitive to isopimaric acid. Our mineralization

data with SaOS2 cells show that K channel blockade by quaternary ammonium acids have a negative impact on this process. These data are perhaps to be expected, given that the concentrations tested increased cell number and this may be achieved by a reduction in differentiation as described previously (section 6.4.2). It is interesting to note that such arguments cannot be easily invoked to explain the action of TEA on mineralisation in human primary osteoblasts which we have described (Henney et al., 2009).

Cell number is clearly an output of both proliferative capacity and apoptosis. Regulation of cell number could be related to changes in both, or either, proliferation and apoptosis. In this study, the changes of cell numbers at low and higher concentrations of BK channel blockers could be in principle due to the fact that the effects of the blockers on either proliferation or apoptosis is dominant at a particular concentration. Hence at low concentrations modulators augment proliferation predominantly, and high concentrations they enhance apoptotic process. Previous studies have demonstrated the links between activation of K^+ channels to both proliferation and apoptosis (Burg et al., 2006). The contribution of the BK channel to apoptosis could readily be tested in future work. Our results with low concentrations of blockers may due to that BK channel blockade stimulates MG63 cell growth by decreasing apoptosis. In addition, there are a number of reports which link membrane potential to progression through the cell cycle. The current view is that the antiproliferative effect in many cells of agents like K^+ channel blockers stems from the depolarisation they produce (Chandy et al., 2004). Such depolarisation would

occur with these blockers in the cells that the BK channel makes a significant contribution to the resting membrane potential. Nevertheless, significantly, blockade of K^+ channels also reduces apoptosis perhaps by increasing cell volume, and in contrast activation of K^+ channels increases apoptosis presumably through enhanced K^+ efflux and in turn reduced cell volume. Blockers like TEA and tetrandrine increase cell numbers in proliferation assay. This may indicate that the overriding effect at these concentrations is to reduce apoptosis. But one caveat is that neither QA nor tetrandrine are specific BK channel blockers. For example tetrandrine blocks L-type Ca channels in smooth muscle cells (e.g. Wu *et al.* 1997) and this may contribute to tetradrine-induced reduction in growth or enhanced apoptosis in the cells studied here. However, we have shown that the L-type Ca channel blocker dihydropyridine nifedipine or R/L/PQ or T-type Ca channel blockers such as the toxins SNX-482, FS-2, ω-agatoxin and kurtotoxin) have no effect on MG63 cell growth (unpublished observations). The second conclusion is that the IbTX-insensitive subtype of BK channel modulates growth of these cells be IbTX itself had no effect over a wide concentration range. Whether this BK channel is equivalent to the neuronal type of BK channel remains to be investigated further.

Does this mean that depolarisation occurs with these blockers? That would only occur if the BK channel makes a significant contribution to the resting membrane potential. As indicated above membrane potential has been linked to progression through the cell cycle. If the antiproliferative effect in many cells of K^+ channel blockers arises from the depolarisation the produce (Chandy *et*

al. 2004; Kunzelmann, 2005), then channel blockers that affect cell growth by regulation of the BK channel might be a useful future strategy to adopt. The prospects are particularly encouraging here as there are a number of ligands specific for BK channels (Imaizumi *et al.* 2002; Wu, 2003) and drug design strategies where K^+ channels are targets are already well developed.

7.4 Techniques and experiment design

Investigations of cell membrane ion channels typically use many scientific techniques including electrophysiology "patch clamp", RT-PCR, pharmacology, western-blotting and immunohistochemistry. In this project, target cells were patched for channel survey. Once the high prevalence and activity K channel was observed, RT-PCR was used to confirm the putative channel type and the RNA message for constituent subunits. Meanwhile, electrophysiology and pharmacological properties were investigated by patch-clamp along with functional assays on target cells. All these methods have their respective advantages and disadvantages so that the hope is that the combination of these techniques help us better firm up our conclusions.

7.4.1 Cell culture

Both osteoblast and osteoblast-like cells are adherent cells in culture providing stability, and to obtain comparable results only isolated single adherent cells were chosen. MG63 cells in culture displayed a rapid increase in cell density in

the centre of the culture surface and after 3 days cells were too confluent to be patched. This is the reason that all patch clamp work was carried out on freshly seeded cells within 3 days.

On the other hand, mouse primary bone cells did not grow easily. It took over 2 weeks for the cells to grow out from the bone fragments, and only after 6 weeks were cells confluent in the culture flask. Transfering these cells on to cover slip caused the loss of over than 50% of cell. Some cells died after they were trypsinised and typically more than 30% cells did not attach to the culture surface of the coverslip 24 hours after seeding. To achieve a higher percentage of surviving cells, pieces of bone fragments were cultured on cover slips. After 4 weeks culture, few cells were growing out from bone. There was hardly any further growth after 6 weeks. These cover-slips were kept in 6 well plates rather than in a culture flask. Medium was changed twice a week with half of the well volume to avoid the floating of the cover-slip. With this procedure there was still not much improvement in the viable cell number. The low achievable cell number actually limited the work on mouse primary bone cells.

7.4.2 Patch successful rate and seal formation

To gain repeatable results, a high success rate in achieving seals is the key factor. This success depends on the cell's condition, the operator and the experimental environment. First of all, fibroblastic shaped cells were chosen. On a typical cell culture cover slip, round and oval shaped MG63 cells were evenly distributed along with the fibroblastic shaped cells. But for some reason

"giga seals" were hard to obtain on these round cells. These cells did not appear to be unhealthy cells (e.g. very granular). It may be that the MG63 cells become rounded or elliptical as they are preparing to divide and perhaps this renders them unsuitable in some way for patch clamping. Since the majority of the cells were fibroblastic shaped, the lack of data from round and elliptical cells was inconvenient but acceptable. In typical experiment, the presence of BK channel modulators in the pipette was found to reduce the success rate. This was found with both blockers and openers. If the openers' binding sites were on the external domain they could active BK channel causing K efflux and changes of the membrane potential. Could this unstable membrane potential cause the low success rate of attaining "giga seals"? Conversely, blockers binding to external domains of the BK channel blocked BK channels in the patch. So, even when there were giga seals, the channel presence was hard to determine. For these reasons, all drugs were applied after successful seals were achieved as described in Section 5.

7.4.3 Cell growth assays

In this project, MTS assays and cell viability assay (trypan blue staining) were used to measures the effects of BK channels modulators on primary human osteoblasts and MG63 cells growth. In the MTS assay we have a convenient way to investigate any changes of cells number, but it does not reveal the real underlying cause. Are cells killed, is proliferation affected or is apoptosis

modified or a combination of these? The cell viability assays helped in a small way to answer these questions.

7.5 Future work

Due to the time constraints of this project only a hint of the possible role of the BK channels in osteoblast function has been gleaned. Further investigations to be carried out should attempt to answer the following important questions.

7.5.1 The composition of BK channel subunits in osteoblast

In this project, RT-PCR indicated that all of the β subunits are expressed in these cells (KCNMB1-4), but the relative amount of each is unknown, and at present the precise subunit composition of the native channel is uncertain. It has been shown that the β1-subunit increased the apparent Ca^{2+} sensitivity by increasing open probability and shifting half-activation voltages to significantly more negative potentials (McManus et al., 1995; Knaus et al., 1994; Dworetzky et al., 1996; Cox and Aldrich, 2000; Nimigean and Magleby, 1999). To define the native subunit composition q-PCR, Western-blot and fluorescence micrograph are potential analytical techniques to be utilised in the future. Firstly, q-PCR monitors the fluorescence emitted during reactions as an indicator of amplicon production at each PCR cycle (in real time) as opposed to the endpoint detection. In compare to RT-PCR it has the advantages: 1) it is not influenced by non-specific amplification. 2) amplification can be monitored

real-time. 3) no post-PCR processing of products (high throughput, low contamination risk). 4) detection is capable down to a 2-fold change. 5) confirmation of specific amplification by melting point analysis. 6) it is most specific, sensitive and reproducible. Clearly q-PCR results will provide the information on the ratio of all native BK channel subunits in osteoblast. Based on this, west-blotting and fluorescence could indicate the subunit composition and also the location of these subunits. In some case BK channel have been shown to co-express with subtypes of Ca^{2+} channel. Hence the BK channels isolated from rat brain are assembled into macromolecular complexes with the voltage-gated calcium channels Cav1.2 (L-type), Cav2.1 (P/Q-type), and Cav2.2 (N-type). Heterologously expressed BK-Cav complexes then essentially reconstitute a functional "Ca^{2+} nanodomain" and Ca^{2+} influx through the Ca^{2+} channel would activate BK in the physiological voltage range with rapid kinetics. The BK-Cav channel complexes have been considered to represent a molecular unit producing an effective and precisely timed hyperpolarization of the membrane potential in response to local Ca^{2+} influx (Berkefeld et al., 2006). Perhaps this kind of unit is only relevant to fast switching of events, in cells such as neurones.

Voltage-gated Ca^{2+} channel subunits have been identified in osteoblast by previous work (Barry, 2000). Hence the BK channels in osteoblasts membranes have the opportunity to form complexes with voltage-gated calcium channels. The question is what advantage does that provide in the context of bone cell function? In addition to immunohistochemistry, whole-cell patch is one other

tool to capture the expression of the complex. Whole-cell patch recording measures the total macroscopic current through the whole cell membrane detecting with the appropriate pharmacology both Ca^{2+} currents and the BK current, and may be required if expression of individual channels was low or the channel were too non uniformly distributed in the plasma membrane.

7.5.2 Apoptosis and proliferation

Cell number is clearly a function of both proliferative capacity and apoptotic mechanisms in MG63 cells, both of which processes may be sensitive to BK channel blockers, as stated above. K^+ channels have been linked previously to both proliferation and apoptosis and the contribution of the BK channel to apoptosis should be tested in future work. There are different types of assays available now such as the caspase assay which assesses apoptosis based on caspase function or TUNEL and DNA fragmentation Assays which can detect the cleaved 180-200 bp DNA increments during cell apoptosis.

7.6 Concluding statement

In short the experiments here are of fundamental importance to bone physiology but also may have implications for therapeutic approaches to bone disease. Much remains to be clarified, and many unanswered questions need to be resolved. Ion channel work in the bone arena is still a relatively new field with there being plenty of scope for future study. This Thesis has only helped

opened the door on what should be a fruitful and interesting research area ripe for exploitation.

References

Abdul M, Santo A, Hoosein N. (2003) Activity of potassium channel-blockers in breast cancer. *Anticancer Res*. 23 (4): 3347-51.

Abdul M., Hoosein N. (2002). Expression and activity of potassium ion channels in human prostate cancer. *Cancer Lett*. 186:99–105.

Ahluwalia, J., Tinker A., Clapp LH., Duchen MR, Abramov AY, Pope S., Muriel Nobles M., Segal A.W (2004). The large-conductance Ca2+-activated K+ channel is essential for innate immunity. *Nature*, 427, 853-858.

Amigorena S, Choquet D, Teillaud JL, Korn H and Fridman WH. (1990). Ion channels and B cell mitogenesis. *Mol Immunol* 27:1259–1268.

Armstrong A.M. (2003) Voltage-gated potassium channels. *Sci. STKE* 24 (188) p. re10.

Asher V, Warren A, Shaw R, Sowter H, Bali A and Khan R (2011) The role of Eag and HERG channel in cell proliferation and apoptotic cell death in SK-OV-3 ovarian cancer cell line. *Cancer Cell International* 2011, 11:6

Aubin, JE. and Liu, F. (1996). The osteoblast lineage. *In Principles of Bone Biology (ed. J. P. Bilezikian L. G. Raisz and G. A. Rodan),* pp. 51-67. San Diego: Academic Press.

Aubin, JE., Turksen, K. and Heersche, JNM. (1993). Osteoblastic cell lineage. *In Cellular and Molecular Biology of Bone (ed. M. Noda*), pp.1 -45. New York: Academic Press.

Barry ELR. (2000) Expression of mRNAs for the α_1 subunit of voltage-gated calcium channels in human osteoblast-Like cell lines and in normal human osteoblasts. *Calcified Tissue International.* 66(2): 145-150.

Basrai, D., Kraft, R., Bollensdorff, C., Liebmann, L., Benndorf, K., Patt, S. (2002). BK channel blockers inhibit potassium- induced proliferation of human astrocytoma cells. *Neuroreport* 13:403–407.

Beeton C. (2001). Selective blockade of T lymphocyte K^+ channels ameliorates experimental autoimmune encephalomyelitis, a model for multiple sclerosis. *Proc Natl Acad Sci U S A.* 98:13942–13947.

Berkefeld, H., Sailer CA., Bildl W., Rohde V., Thumfart JO., Eble S., Klugbauer N., Reisinger E., Oliver D., Knaus HG., Schulte U. and Fakler B. (2006). BK_{Ca}-Cav channel complexes mediate rapid and localized Ca2+-activated K+ signaling. *Science* 314(5799): 615-620.

Bertran GC, D'Alessio C and Kotsias BA (1995) Ion channels in non excitable cells. *Medicines*. 55 (5) Pt 1: 449-456

Binstock L, Goldman L. (1971) Rectification in instantaneous potassium current–voltage relations in Myxicola giant axons. *J. Physiol* 217: 517–531.

Blatz, AL. and Magleby, KL. (1986). Single apamin-blocked Ca-activated K^+ channels of small conductance in cultured rat skeletal muscle. *Nature* 323, 718– 720.

Bloch M, Ousingsawat J, Simon R, Schraml P, Gasser TC. *(*2007). KCNMA1 gene amplification promotes tumor cell proliferation in human prostate cancer. *Oncogene* 26:2525–2534.

Bolotina VM, Najibi S, Palacino JJ, Pagano PJ, Cohen RA (1994). Nitric oxide directly activates calcium-dependent potassium channels in vascular smooth muscle. *Nature*.368:850–853.

Booth IR, Edwards MD, and Miller S. (2003) Bacterial ion channels. *Biochemistry* 42: 10045-10053

Brayden, JE., and Nelson, MT. (1992). Regulation of arterial tone by activation of calcium-dependent potassium channels. *Science*, 256, 532–535.

Brelidze, TI., and Magleby KL. (2005). Probing the geometry of the inner vestibule of BK channels with sugars. *J. Gen. Physiol.* 126:105–121.

Brelidze, TI., Niu X, and Magleby K.L (2003). A ring of eight conserved negatively charged amino acids doubles the conductance of BK channels and prevents inward rectification. *Proc. Natl. Acad. Sci. USA.* 100:9017–9022.

Brenner R, Jegla TJ, Wickenden A, Liu Y, Aldrich RW (2000a) Cloning and functional characterization of novel large conductance calcium-activated potassium channel β subunits, hKCNMB3 and hKCNMB4. *J Biol Chem* 275: 6453– 6461.

Brenner R, Perez GJ, Bonev AD, Eckman DM, Kosek JC, Wiler SW, Patterson AJ, Nelson MT, Aldrich RW (2000b) Vasoregulation by the beta1 subunit of the calcium-activated potassium channel. *Nature* 407: 870–876.

Burg ED, Remillard CV and Yuan JXJ. (2006). K^+ channels in apoptosis. *J Membr Biol* 209, 1-18.

Cahalan, M.D. and Lepple-Wienhues A. (1997) Ion channels in lymphocyte function: Editorial. *Cellular Physiology and Biochemistry* 7: 133-134.

Calderone V. (2002) Large-conductance, Ca^{2+}-activated K^+ channels: function, pharmacology and drugs. *Curr Med Chem.* 9:1385–1395.

Candia S, Garcia ML, and Latorre R (1992) Mode of action of iberiotoxin, a potent blocker of the large conductance Ca^{2+}-activated K^+ channel. *Biophys J* 63, 583-590.

Carrier GO, Fuchs LC, Winecoff AP, Giulumian AD, White RE (1997). Nitrovasodilators relax mesenteric microvessels by cGMP-induced stimulation of Ca-activated K channels. *American Journal of Physiology*.273:H76–84.

Chandy KG (1984). Voltage-gated potassium channels are required for human T lymphocyte activation. *J Exp Med.* 160:369–385.

Chandy KG, Cahalan M, Pennington M, Norton RS, Wulff H, and Gutman GA (2001) Potassium channels in T lymphocytes: toxins to therapeutic immunosuppressants. *Toxicon* 39:1269–1276.

Chandy KG, Wulff H, Beeton C, Pennington M, Gutman GA and Cahalan MD (2004) K^+ channels as targets for specific immunomodulation. *TIPS* 25, 280-289.

Chapman H., Piggott C., Andrews PW., and Wann KT. (2007). Characterisation of large-conductance calcium-activated potassium channels (BK_{Ca}) in human NT2-N cells. *Brain Research*, 1129, 15-25.

Chavassieux, P., Serre CM., Vergnaud P., Delmas PD., Meunier PJ. (1993). In vitro evaluation of dose-effects of ethanol on human osteoblastic cells. *Bone Miner* 22(2): 95-103.

Cheney JA, Weisser JD, Bareyre FM, Laurer HL, Saatman KE, Raghupathi R, Gribkoff VK, Starrett JE Jr, and McIntosh TK. (2001) The maxi-K channel opener BMS-204352 attenuates regional cerebral edema and neurologic moto impairment after experimental brain injury. *J Cereb Blood Flow Metab* 21: 396–403.

Chiang HT, Wu SN (2001). Inhibition of large-conductance calcium-activated potassium channel by 2-methoxyestradiol in cultured vascular endothelial (HUV-EC-C) cells. *J Membr Biol* 182: 203–212.

Clay J.R (1991) A paradox concerning ion permeation of the delayed rectifier potassium ion channel in squid giant axons. *J. Physiol* 444: 499–511.

Cox DH, Cui J, Aldrich RW. (1997). Separation of gating properties from permeation and block in mslo large conductance Ca-activated K^+ channels. *Journal of General Physiology*.109(5):633–646.

Cox, DH. and Aldrich RW. (2000). Role of the beta1 subunit in large-conductance Ca^{2+}-activated K channel gating energetics. Mechanisms of enhanced Ca^{2+} sensitivity. *J Gen Physiol* 116(3): 411-432.

Crockett JC, Rogers MJ, Coxon FP, Hocking LJ, Helfrich MH (2011) Bone remodelling at a glance. *J Cell Sci.* 1;124(7):991-8.

Curley, M. and Morrison JJ. (2004). "Analysis of Maxi-K alpha subunit splice variants in human myometrium." *Reprod Biol Endocrinol* 2(1): 67.

Czarnecki, A., Dufy-Barbe, L., Huet, S., Odessa, M.F., Bresson-Bepoldin., L. (2003). Potassiumchannel expression level is dependent on the proliferation state in the GH3 pituitary cell line. *Am. J. Physiol Cell Physiol* 284:C1054–C1064.

Darkow, D.J., Lu L. (1997). Estrogen relaxation of coronary artery smooth muscle is mediated by nitric oxide and cGMP. *Am J Physiol* 272: H2765-2773.

Davies AG, Pierce-Shimomura JT, Kim H, VanHoven MK, Thiele TR, Bonci A, Bargmann CI, McIntire SL. (2003) A central role of the BK potassium channel in behavioral responses to ethanol in C. elegans. *Cell* 12;115(6):655-66.

Davies JH, Evans BA, Jenney ME, and Gregory JW (2002) In vitro effects of combination chemotherapy on osteoblasts: implications for osteopenia in childhood malignancy. *Bone* 31, 319-26.

De Wet, H., Allen M., Holmes C., Stobbart M., Lippiat JD., Callaghan R. (2006). Modulation of the BK channel by estrogens: examination at single channel level. *Mol Membr Biol* 23(5): 420-429.

DeCoursey TE. (1984). Voltage-gated K^+ channels in human T lymphocytes: a role in mitogenesis? *Nature* 307:465–468.

Deng XL, Lau CP, Lai K, Cheung KF, Lau GK and Li GR (2007) Cell cycle-dependent expression of potassium channels and cell proliferation in rat mesenchymal stem cells from bone marrow. *Cell Prolif* 40, 656-670.

Diamond, T., Stiel D, Luzner M., Wilkinson M., Posen S. (1989). Ethanol reduces bone formation and may cause osteoporosis. *Am J Med* 86(3): 282-288.

Dick GM, Rossow CF, Smirnov S, Horowitz B, and Sanders KM (2001). Tamoxifen activates smooth muscle BK channels through the regulatory $\beta 1$ subunit. *J Biol Chem* 276: 34594-34599.

Dixon, SJ., Aubin JE, and Dainty J. (1984) Electrophysiology of a clonal osteoblast-like cell line: evidence for the existence of a Ca2+-activated K+ conductance. *J. Membr. Biol.* 80:49–58.

Doyle, DA., Morais J., Pfuetzner RA., Kuo A, Gulbis JM., Cohen SL., Chait B. T., and MacKinnon R. (1998) The structure of the potassium channel: molecular basis of K+ conduction and selectivity. *Science.* 280:69–77.

Duncan RL and Hruska KA. (1994). Chronic, intermittent loading alters mechanosensitive channel characteristics in osteoblast-like cells. *Am J Physiol* 267, F909-F916.

Dworetzky, SI., Boissard CG. Lum-Ragan JT., McKay MC., Post-Munson DJ., Trojnacki JT., Chang CP., Gribkoff VK.(1996). Phenotypic alteration of a human BK (hSlo) channel by hSlobeta subunit coexpression: changes in blocker sensitivity, activation/relaxation and inactivation kinetics, and protein kinase A modulation. *J Neurosci* 16(15): 4543-4550.

DworetzkySI, Trojnacki JT, and Gribkoff VK. (1994). Cloning and expression of a human large-conductance calcium-activated potassium channel. *Brain Res* 27: 189–193.

Dyer, S. A., Buckendahl P. and Sampson HW. (1998). Alcohol consumption inhibits osteoblastic cell proliferation and activity in vivo. *Alcohol* 16(4): 337-341.

Edwards G (1998) Potassium channel modulation: What next? *Curr Res Ion Channel Modulators* 3:163–164.

Elso C.M., Lu X., Culiat C.T., Rutledge J.C., Cacheiro N.L., Generoso W.M., Stubbs L.J. (2004). Heightened susceptibility to chronic gastritis, hyperplasia and metaplasia in Kcnq1 mutant mice. *Hum. Mol. Genet*. 13:2813–2821.

Evans BA, Elford C, Pexa A, Francis K, Hughes AC, Deussen A, and Ham J (2006) Human osteoblast precursors produce extracellular adenosine, which modulates their secretion of IL-6 and osteoprotegerin. *J Bone Miner Res* 21, 228-236.

Fernandez-Fernandez JM, Tomas M, Vazquez E, Orio P, Latorre R, Senti M, Marrugat J, Valverde MA (2004). Gain-of-function mutation in the KCNMB1 potassium channel subunit is associated with low prevalence of diastolic hypertension. *J Clin Invest.*113:1032–9.

Ferrier, J., Dixon, J., Illeman, A., Dillon, E. and Smith, I. (1982), Low-frequency voltage noise in a mammalian bone cell clone. *Journal of Cellular Physiology* 113(2) 267-272.

Frankenhauser B (1962). Potassium permeability in myelinated nerve fibers of Xenopus laevis *J. Physiol* 160: 54–61.

Friday, K. E. and Howard GA. (1991). Ethanol inhibits human bone cell proliferation and function in vitro. *Metabolism* 40(6): 562-565.

Fukao M, Mason HS, Britton FC, Kenyon JL, Horowitz B, Keef KD. (1999). Cyclic GMP-dependent protein kinase activates cloned BKCa channels expressed in mammalian cells by direct phosphorylation at serine 1072. *J Biol Chem.* 274:10927–10935.

Fukushima Y., Hagiwara S. and Henkart M. (1984) Potassium current in clonal cytotoxic T lymphocytes from the mouse. *J Physiol.* 351:645–656.

Garcia-Valdes J, Zamudio FZ, Toro L, and Possani LD *(*2001*)* Slotoxin, alphaKTx1.11, a new scorpion peptide blocker of MaxiK channels that differentiates between alpha and alpha+beta (beta1 or beta4) complexes. *FEBS Lett* 505: 369-*373.*

Gardos, G. (1958). The function of calcium in the potassium permeability of human erythrocytes. *Biochim Biophys Acta* 30, 653– 654.

Gavaler, JS. and Van Thiel DH. (1992). Hormonal status of postmenopausal women with alcohol-induced cirrhosis: further findings and a review of the literature. *Hepatology* 16(2): 312-319.

Ghanshani S, Wulff H, Miller MJ, Rohm H, Neben A, Gutman GA, Cahalan MD, and Chandy KG (2000). Up-regulation of the IKCa1 potassium channel during T-cell activation. *J Biol Chem* 275:37137–37149.

Ghatta S, Nimmagadda D, Xu X, and O'Rourke ST (2006) Large-conductance, calcium-activated potassium channels: structural and functional implications. *Pharmacol Ther* 110: 103-116.

Giangiacomo, KM., Garrcia-calvo, M., Knaus HG., Mullmann, TJ., Garcia ML., Mcmanus, O. (1995*).* Functional reconstitution of the large conductance, calcium-activated potassium channel purified from bovine aortic smooth muscle. *Biochemistry,* 34, 15849–15862.

Giebisch G (1998) Renal potassium transport: mechanisms and regulation. *AJP-Renal Physiol* 274: 5 F817-F833

Goldman D.E (1943) Potential, impedance, and rectification in membranes *J. Gen. Physiol* 27 37–60.

Goldstein SA, Bockenhauer D, O'Kelly I, and Zilberberg N. (2001). Potassium leak channels and the KCNK family of two-P-domain subunits. *Nat Rev Neurosci* 2: 175–184.

Goldstein SA, Price LA, Rosenthal DN, and Pausch MH. (1996). ORK1, a potassium-selective leak channel with two pore domains cloned from *Drosophila melanogaster* by expression in *Saccharomyces cerevisiae*. *Proc Natl Acad Sci USA* 93: 13256–13261.

Gribkoff VK, Starrett JE Jr, Dworetzky SI, Hewawasam P, Boissard CG, Cook DA, Frantz SW, Herman K, Hibbard JR, Huston K, Johnson G., Krishnan BS., Kinney GG., Lombardo LA., Meanwell NA., Molinoff PB., Mayers RA., Moon SL, Ortiz A., Rakor l., Pieschl RL., Post-Munson DJ., Signor LJ., Srinivas N., Taber MT., Thalody G., Trojnacki JT., Wiener H., Yeleswaran K., Yeola SW. (2001) Targeting acute ischemic stroke with a calcium sensitive opener of Maxi-K potassium channels. *Nat Med* 7: 471–477.

Gu Y and Publicover SJ (2000). Expression of functional metabotropic glutamate receptors in primary cultured rat osteoblasts. *J Biol Chem* 275, 34252-34259.

Gu Y, Genever PG, Skerry TM, and Publicover SJ (2002) The NMDA type glutamate receptors expressed by primary rat osteoblasts have the same electrophysiological characteristics as neuronal receptors. *Calcif Tissue Int* 70, 194-203.

Guevremont, M., Martel-Pelletier J. Massicotte F., Tardif G., Pelletier JP., Ranger P., Lajeunesse D., Reboul P. (2003). Human adult chondrocytes express hepatocyte growth factor (HGF) isoforms but not HgF: potential implication of osteoblasts on the presence of HGF in cartilage. *J Bone Miner Res* 18(6): 1073-81.

Hagen BM, Bayguinov O, Sanders KM.(2003). Beta 1-subunits are required for regulation of coupling between Ca^{2+} transients and Ca^{2+}-activated K+ (BK) channels by protein kinase C. *Am J Physiol Cell Physiol* 285:C1270–C1280.

Hamill, O. P., A. Marty, Neher E, Sakmann B, Sigworth FJ. (1981). Improved patch-clamp techniques for high-resolution current recording from cells and cell-free membrane patches. *Pflugers Arch* 391(2): 85-100.

Hanner, M., R. Vianna-Jorge, A. Kamassah, W.A. Schmalhofer, H.G. Knaus, G.J. Kaczorowski, and M.L. Garcia. 1998. The β subunit of the high conductance calcium-activated potassium channel. Identification of residues involved in charybdotoxin binding. *J. Biol. Chem.* 273:16289–16296.

Harbour ME, Gegory JW, Jenkins HR, and Evans BAJ (2000). Proliferative response of different human osteoblast-like cell models to proinflammatory cytokines. *Pediatr Res* 48, 163-168.

Hattori T, Maehashi H, Miyazawa T, and Naito M (2001) Potentiation by Stannous Chloride of Calcium Entry into Osteoblastic MC3T3-E1 Cells Through Voltage-Dependent L-Type Calcium Channels. *Cell Calcium* 30, 67-72.

He J, Kargacin ME, Kargacin GJ, and Ward CA (2003) Tamoxifen inhibits Na^+ and K^+ currents in rat ventricular myocytes. *Am J Physiol Heart Circ Physiol* 285:H661–H668.

Henney, N.C., Li, B., Evans, B. A. J., Hall, E.J. and Wann, K.T. (2006) Potassium channel subunits in human osteoblast-like cells. *J. Bone Miner. Res.* 21, 7, 1169.

Hewawasam P, Gribkoff VK, Dworetzky SI, Ortiz AA, Kinney GG, Boissard CG, Post-Munson DJ, Trojnacki JT, Huston K, Signor LJ, Lombardo LL, Reid SA, Hibbard JR, Myers RA, Moon SL, Wiener HL, Thalody G, Yeleswaram K, Pajor LM, Knipe JO, Meanwell NA, Johnson G, Molinoff PB, Starrett JE and Gao Q (2000) Discovery of openers of large-conductance, calcium activated potassium (maxi-K) channels: A new approach to stroke neuroprotection (Abstract). 219th ACS National Meeting, March 25–29, San Francisco, CA.

Hille, B. (1992) *Ion channels of excitable membranes (third ed.1992). Sunderland, Mass: Sinauer Associates.* ISBN 0-87893-321-2.

Hodgkin A.L, Katz B. (1949). The effect of sodium ions on the electrical activity of the giant axon of the squid. *J. Physiol* 108: 37–77

Hoebertz A, Arnett TR, and Burnstock G. (2003). Regulation of bone resorption and formation in purines and pyrimidines. *TIPS* 24, 290-297.

Hoffman, J.F., W. Joiner, K. Nehrke, O. Potapova, K. Foye, and A. Wickrema. (2003). The hSK4 (KCNN4) isoform is the Ca^{2+}-activated K^{+} channel (Gardos channel) in human red blood cells. *Proc. Natl. Acad. Sci. USA.* 100:7366–7371.

HoK, Nichols CG, Lederer WJ, Lytton J, Vassilev PM, Kanazirska MV, and Hebert SC. (1993) Cloning and expression of an inwardly rectifying ATP-regulated potassium channel. *Nature* 362: 31–38.

Holbrook, T. L. and Barrett-Connor E. (1993). A prospective study of alcohol consumption and bone mineral density. *BMJ* 306(6891): 1506-1509.

Huang Y, Rane SG (1994) Potassium channel induction by the Ras/Raf signal transduction cascade. *J Biol Chem* 269:31183–31189.

Hughes S, Magnay J, Foreman M, Publicover SJ, Dobson JP, and El Haj AJ (2006) Expression of the mechanosensitive 2PK+ channel TREK-1 in human osteoblasts. *J Cell Physiol* 206, 738-748.

Ikeda M, Dewar D and McCulloch J (1991) Selective reduction of [125I] apamin binding sites in Alzheimer hippocampus: A quantitative autoradiographic study. *Brain Res* 567:51–56.

Iliev IG and Marino AA (1993) Potassium channels in epithelial cells. *Cell Mol. Biol. Res.* 39(6):601-11.

Imaizumi Y, Sakamoto K, Yamada A, Hotta A, Ohya S, Muraki K, Uchiyama M, Ohwada, T (2002) Molecular basis of pimarane compounds as novel activators of large-conductance Ca^{2+}-activated K^+ channel α-subunit. *Mol Pharmacol* 62 (4), 836-46.

Ishii, TM., Silvia, C., Hirschberg, B., Bond, CT, Adelman, JP., & Maylie, J. (1997). A human intermediate conductance calcium-activated potassium channel. *Proc Natl Acad Sci USA* 94, 11651– 11656.

Jager H., Dreker T., Buck A., Giehl K., Gress T., Grissmer S. (2004). Blockage of intermediate-conductance Ca2+-activated K+ channels inhibit human pancreatic cancer cell growth in vitro. *Mol. Pharmacol.* 65:630–638.

Jaggar JH, Nelson MT (2000). Differential regulation of Ca^{2+} sparks and Ca^{2+} waves by UTP in rat cerebral artery smooth muscle cells. *Am J Physiol.* 279:C1528–C1539.

Jiang Y, Lee A, Chen J, Ruta V, Cadene M, Chait BT, MacKinnon R (2003). X-ray structure of a voltage-dependent K+ channel. *Nature* 423 (6935): 33–41.

Jiang, Y., A. Lee, J. Chen, M. Cadene, B.T. Chait, and R. MacKinnon. (2002). Crystal structure and mechanism of a calcium-gated potassium channel. *Nature.* 417:515–522.

Jiang, Y., Lee A., Chen J., Cadene M., Chait B. T., and MacKinnon R. (2002) The open pore conformation of potassium channels. *Nature* 417:523–526.

Jørgensen NR, Henriksen Z, Brot C, Eriksen EF, Sorensen OH, Civitelli R, and Steinberg TH (2000). Human osteoblastic cells propagate intracellular calcium signals by two different mechanisms. *J Bone Miner Res* 15, 1024-1032.

Judge S, Bever C (2006). "Potassium channel blockers in multiple sclerosis: neuronal Kv channels and effects of symptomatic treatment". *Pharmacol. Ther.* 111 (1): 224–59.

Kartsogiannis, V. and Ng KW. (2004). Cell lines and primary cell cultures in the study of bone cell biology. *Mol Cell Endocrinol* 228(1-2): 79-102.

Khanna R, Chang MC, Joiner WJ, Kaczmarek LK and Schlichter LC (1999) hSK4/hIK1, a calmodulin-binding KCa channel in human T lymphocytes. Roles in proliferation and volume regulation. *J Biol Chem* 274:14838–14849.

Klein, R. F., Fausti KA. And Carlos AS. (1996). Ethanol inhibits human osteoblastic cell proliferation. *Alcohol Clin Exp Res* 20(3): 572-578.

Knaus HG, McManus OB, Lee SH, Schmalhofer WA, Garcia-Calvo M, Helms LM, Sanchez M, Giangiacomo K, Reuben JP, Smith AB 3rd, (1994)

Tremorgenic indole alkaloids potently inhibit smooth muscle high-conductance calcium-activated potassium channels. *Biochemistry* 33: 5819-5828.

Knaus, HG., Eberhart, A., KochRO., Munujos P., Schmalhofer WA., Warmke JW., Kaczorowski GJ., Garcia ML. (1995). Characterization of tissue-expressed alpha subunits of the high conductance Ca-activated K channel. J *Biol Chem* 270(38): 22434-9.

Kohler M, Hirschberg B, Bond CT, Kinzie JM, Marrion NV, Maylie J, and Adelman JP.(1996). Small-conductance, calcium-activated potassium channels from mammalian brain. *Science* 273: 1709–1714.

Komarova SV, Dixon SJ, Sims SM (2001) Osteoclast ion channels: potential targets for antiresorptive drugs. *Curr. Pharm. Des*. 7: 637-654.

KuboY, Baldwin TJ, Jan YN, and Jan LY. (1993). Primary structure and functional expression of a mouse inward rectifier potassium channel. *Nature* 362: 127–133.

Kuhlmann C.R., Schafer M., Li F., Sawamura T., Tillmanns H., Waldecker B., Wiecha J. (2003). Modulation of endothelial Ca(2+)-activated K(+) channels by oxidized LDL and its contribution to endothelial proliferation. *Cardiovasc. Res* 60:626–634.

Kuhlmann C.R., Wu Y., Li F., Munz B.M., Tillmanns H., Waldecker B., Wiecha J. (2004). bFGF activates endothelial Ca2+-activated K+ channels involving G-proteins and tyrosine kinases. *Vascul. Pharmacol*. 41:181–186.

Kuhlmann CR, Gast C, Li F, Schäfer M, Tillmanns H, Waldecker B, Wiecha J. (2004). Cerivastatin activates endothelial calcium-activated potassium channels and thereby modulates endothelial nitric oxide production and cell proliferation. *J Am Soc Nephrol*. 15(4):868-75.

Kuhlmann CR, Most AK, Li F, Münz BM, Schaefer CA, Walther S, Raedle-Hurst T, Waldecker B, Piper HM, Tillmanns H, Wiecha J. (2005). Endothelin-1-induced proliferation of human endothelial cells depends on activation of K+ channels and Ca+ influx. *Acta Physiol Scand.* 183(2):161-9.

Kunzelmann K (2005). Ion channels and cancer. *J Membr Biol* 205,159-173.
Laitinen, K. and Valimaki M. (1991). Alcohol and bone. *Calcif Tissue Int* 49 Suppl: S70-73.

Laitinen, K., Lamberg-Allardt C, Tunninen R., Karonen SL., Ylikahri R., Valimaki M. (1991). Effects of 3 weeks' moderate alcohol intake on bone and mineral metabolism in normal men. *Bone Miner* 13(2): 139-151.

Lajeunesse D., Frondoza C., Schoffield B., Sacktor B. (1990) Osteocalcin secretion by the human osteosarcoma cell line MG-63. *J. Bone Miner. Res*. 5(9): 915.

Lastraioli E., Guasti L., Crociani O., Polvani S., Hofmann G., Witchel H., Bencini L., Calistri M., Messerini L., Scatizzi M., Moretti R., Wanke E., Olivotto M., Mugnai G., Arcangeli A. (2004). herg1 gene and HERG1 protein are overexpressed in colorectal cancers and regulate cell invasion of tumor cells. *Cancer Res.* 64:606–611.

Lehenkari P, Parikka V, Rautiala TJ, Weckstrom M, Dahllund J, Harkonen PL, and Vaanaanen, HK (2003). The effects of tamoxifen and toremifene on bone cells involve changes in plasma membrane ion conductance. *J Bone Miner Res* 18, 473-481.

Leonard RJ, Garcia ML, Slaughter RS, and Reuben JP (1992). Selective blockers of voltage-gated K^+ channels depolarise human T-lymphocytes: mechanism of the antiproliferative effect. *Proc Nat Acad Sci USA* 89, 10094-10098.

Lesage F and Lazdunski M. (2000). Molecular and functional properties of two-pore-domain potassium channels. *Am J Physiol Renal Physiol* 279: F793–F801.

Lesage F, Guillemare E, Fink M, Duprat F, Lazdunski M, Romey G, and Barhanin J. (1996). TWIK-1, a ubiquitous human weakly inward rectifying K^+ channel with a novel structure. *EMBO J* 15: 1004–1011.

Lesage, F., Hibino, H., and Hudspeth, A. J. (2004). Association of beta-catenin with the alpha-subunit of neuronal large-conductance Ca^{2+}-activated K^+ channels. *Proc. Natl. Acad. Sci. USA* 101, 671-675.

Li GR, Deng XL, Sun H, Chung SSM, Tse HF, and Lau CP (2006). Ion channels in mesenchymal stem cells from rat bone marrow. *Stem Cells* 24, 1519-1528.

Li GR, Sun H, Deng X, and Lau C-P (2005). Characterisation of ionic currents in human mesenchymal stem cells from bone marrow. *Stem Cells* 23, 371-382.

Li, W., and R.W. Aldrich. (2004). Unique inner pore properties of BK channels revealed by quaternary ammonium block. *J. Gen. Physiol.* 124:43–57.

Liegeois JF., Mercier F., Graulich A., Graulich-Lorge F., Scuvee-Moreau J., Seutin V. (20003). Modulation of small conductance calcium-activated potassium (SK) channels: a new challenge in medicinal chemistry. *Curr. Med. Chem.* 10:625–647.

Ling, S., Sheng, J. Z., Braun, J. E., and Braun, A. P. (2003). Syntaxin 1A co-associates with native rat brain and cloned large conductance, calcium-activated potassium channels in situ. *J. Physiol.* 553, 65-81.

Lippiat JD, Standen NB, Harrow ID, Phillips SC, and Davies NW (2003). Properties of BK_{Ca} channels formed by bicistronic expression of hSloα and β1-4 subunits on HEK293 cells. *J Membr Biol* 192:141-148.

Liu X, Chang Y, Reinhart PH, Sontheimer H, Chang Y. (2002). Cloning and characterization of glioma BK, a novel BK channel isoform highly expressed in human glioma cells. *J Neurosci.* 22:1840–1849.

Liu, G., Shi, J., Yang, L., Cao, L., Park, SM., Cui, J., and Marx, SO. (2004). Assembly of a Ca^{2+}-dependent BK channel signaling complex by binding to beta2 adrenergic receptor. *EMBO J.* 23: 2196-2205.

Logsdon, NJ., Kang, J., Togo, JA., Christian, EP., and Aiyar, J. (1997). A novel gene, hKCa4, encodes the calcium-activated potassium channel in human T lymphocytes. *J Biol Chem* 272: 32723– 32726.

Marty, A. (1981). Ca-dependent K channels with large unitary conductance in chromaffin cell membranes. *Nature* 291: 497–500.

Matteson DR, Deutsch C. (1984). K^+ channels in T lymphocytes: a patch clamp study using monoclonal antibody adhesion. *Nature* 307:468–471.

McManus, OB., Helms LM, Pallanck l., Ganetzky B., Swanson R., Leonard., RJ. (1995). Functional role of the beta subunit of high conductance calcium-activated potassium channels. *Neuron* 14(3): 645-650.

Meera P, Wallner M, and Toro L. (2000). A neuronal β subunit (KCNMB4) makes the large conductance, voltage- and Ca^{2+}-activated K^+ channel resistant to charybdotoxin and iberiotoxin. *Proc Nat Acad Sci USA* 97, 5562-5567.

Miller, C. (2003). A charged view of voltage-gated ion channels. N*ature Structural Biology* 10(6): 422-424.

Mistry DK, Garland CJ (1998). Nitric oxide (NO)-induced activation of large conductance Ca^{2+}-dependent K^+ channels (BK_{Ca}) in smooth muscle cells isolated from the rat mesenteric artery. *British Journal of Pharmacology.*124:1131–1140.

Moreau R, Aubin R, Lapointe JY, Lajeunesse D (1997). Pharmacological and biochemical evidence for the regulation of osteocalcin secretion by potassium channels in human osteoblast-like MG63 cells. *J Bone Miner Res* 12: 1984-1992.

Moreau R, Hurst AM, Lapointe JY, and Lajeunesse D. (1996). Activation of maxi-K channels by parathyroid hormone and prostaglandin E2 in human osteoblast bone cells. *J Membr Biol* 150: 175-84.

MutoS, Asano Y, Seldin D, and Giebisch G. (1999). Basolateral Na^+ pump modulates apical Na^+ and K^+ conductances in rabbit cortical collecting ducts. *Am J Physiol Renal Physiol* 276: F143–F158.

Neylon C.B. (2002). Potassium channels and vascular proliferation. *Vascul. Pharmacol*. 38:35–41.

Nimigean, C.M., J.S. Chappie, and C. Miller. (2003). Electrostatic tuning of ion conductance in potassium channels. *Biochemistry.* 42:9263–9268.

Nimigean, CM. and Magleby KL. (1999). The beta subunit increases the Ca2+ sensitivity of large conductance Ca2+-activated potassium channels by retaining the gating in the bursting states. *J Gen Physiol* 113(3): 425-440.

O'Grady, S.M., Lee, S.Y. (2005). Molecular diversity and function of voltage-gated (Kv) potassium channels in epithelial cells. *Int. J Biochem Cell Biol* 37:1578–1594.

OriasM, Velazquez H, Tung F, Lee G, and Desir GV. (1997). Cloning and localization of a double-pore K channel, KCNK1: exclusive expression in distal nephron segments. *Am J Physiol Renal Physiol* 273: F663–F666.

Orio, P., Rojas P., Ferreira G. and Latorre R. (2002). New disguises for an old channel: MaxiK channel beta-subunits. *News Physiol Sci* 17: 156-61.

Orriss IR, Knight GE, Ranasinghe S, Burnstock G, and Arnett TR (2006). Osteoblast responses to nucleotides increase during differentiation. *Bone* 39, 300-309.

Ottolia M, Toro L. (1994) Potentiation of large conductance KCa channels by niflumic, flufenamic, and mefenamic acids. *Biophys J.* 67:2272–2279.

Ouadid-Ahidouch H., Roudbaraki M., Delcourt P., Ahidouch A., Joury N., Prevarskaya N. (2004). Functional and molecular identification of intermediate-conductance Ca-activated K channels in breast cancer cells: association with cell cycle progression. *Am. J Physiol Cell Physiol* 287:C125–C134.

Pallanck, L., and B. Ganetzky. (1994). Cloning and characterization of human and mouse homologs of the *Drosophila* calcium-activated potassium channel gene, slowpoke. *Hum. Mol. Genet.* 3:1239–1243.

PalmerLG, Antonian L, and Frindt G. (1994). Regulation of apical K and Na channels and Na/K pumps in rat cortical collecting tubule by dietary K. *J Gen Physiol* 104: 693–710.

Papazian DM, Schwarz TL, Tempel BL, Jan YN, Jan LY (1987) Cloning of genomic and complementary DNA from Shaker, a putative potassium channel gene from Drosophila. *Science* 1987, 237:749-753.

Pardo LA, Camino DD., Sanchez A., Alves F., Bruggemann A., Beckh S., Stuhmer W. (1999). Oncogenic potential of EAG K channels. *EMBO J.* 18:5540–5547.

Parfitt AM. (2001) Skeletal heterogeneity and the purposes of bone remodelling: implications for the understanding of osteoporosis. In: Marcus R, Zfeldman D, Kelsey J, eds. Osteoporosis. San Diego, CA: Academic Press 2001: 433–444.

Parihar A.S., Coghlan M.J., Gopalakrishnan M., Shieh C.C. (2003). Effects of intermediate-conductance $Ca(^{2+})$-activated $K(^{+})$ channel modulators on human prostate cancer cell proliferation. *Eur. J Pharmacol*. 471:157–164.

Park, Y. B. (1994). Ion selectivity and gating of small conductance $Ca(^{2+})$-activated K+ channels in cultured rat adrenal chromaffin cells. *J Physiol* 481(Pt 3), 555– 570.

Pedarzani P., Kulik A., Muller M., Ballanyi K., Stocker M. *(*2000). Molecular determinants of Ca^{2+}-dependent K^{+} channel function in rat dorsal vagal neurones. *J. Physiol. (Lond.)* 527:283–290.

Peng, TC., Lian JB, Hirsch PF., Kusy RP.(1991). Lower serum osteocalcin in ethanol-fed rats. *J Bone Miner Res* 6(2): 107-115.

Pfeilschifter J, Köditz R, Pfohl M, Schatz H (2002). Changes in proinflammatory cytokine activity after menopause. *Endocr Rev* 23 : 90–119.

Pluger S, Faulhaber J, Furstenau M, Lohn M, Waldschutz R, Gollasch M, Haller H, Luft FC, Ehmke H, Pongs O. (2000) Mice with disrupted BK channel β1 subunit gene feature abnormal Ca spark/STOC coupling and elevated blood pressure. *Circ Res* 87:E53–E60.

Pluznick JL, Wei P, Carmines PK, Sansom SC. (2003) Renal fluid and electrolyte handling in BKCa-beta1$^{-/-}$ mice. *Am J Physiol Renal Physiol* 284: F1274–F1279.

Pluznick JL, Wei P, Grimm PR, Sansom SC. (2005). BK-β1 subunit: immunolocalization in the mammalian connecting tubule and its role in the kaliuretic response to volume expansion. *Am J Physiol Renal Physiol.* 288:F846–F854.

Purohit, V. (1998). Moderate alcohol consumption and estrogen levels in postmenopausal women: a review. *Alcohol Clin Exp Res* 22(5): 994-997.

Ramsdell JS. (1991). Voltage-dependent calcium channels regulate GH4 pituitary cell proliferation at two stages of the cell cycle. *J Cell Physiol.* 146:197–206.

Ravesloot JH, van Houten RJ, Ypey DL, and Nijweide PJ (1990). Identification of Ca^{2+}-activated K^{+} channels in cells of embryonic chick osteoblast cultures. J *Bone Miner Res* 5: 1201-10.

Reinhart PH, Chung S, and Levitan I.B (1989). A family of calcium-dependent potassium channels from rat brain. *Neuron* 2:1031-41.

Reinhart PH, Chung S, Martin Brautigan DL, and Levitan IB (1991). Modulation of calcium-activated potassium channels from rat brain by protein kinase A and phosphatase 2A. *J Neurosci* 11: 1627-1635.

Rezzonico R, Cayatte C, Bourget-Ponzio I, Romey G, Belhacene N, Loubat A, Rocchi S, van Obberghen E, Girault J-A, Rossi B, and Schmid-Antomarchi H (2003). Focal adhesion kinase $pp125^{KK}$ interacts with the large conductance calcium-activated hSlo potassium channel in human osteoblasts: potential role in mechanotransduction. *J Bone Miner Res* 18: 1863-1871.

Rezzonico R, Schmid-Alliana A, Romey G, Bourget-Ponzio I, Breuil V, Breittmayer V, Tartare-Deckert S, Rossi B, and Schmid-Antomarchi H (2002). Prostaglandin E_2 induces interaction between hSlo potassium channel and Syk tyrosine kinase in osteosarcoma. *J Bone Miner Res* 17: 869-878.

Richter C, and Ferrier J (1991) Continuously active sodium channels in osteoblastic ROS 17/2.8 cells. *Bone and Mineral* 15: 57-71.

Robertson BE, Schubert R, Hescheler J, Nelson MT (1993). cGMP-dependent protein kinase activates Ca-activated K channels in cerebral artery smooth muscle cells. *Am J Physiol.* 265:C299–303.

Roger S., Potier M., Vandier C., Le Guennec J.Y., Besson P. (2004). Description and role in proliferation of iberiotoxin-sensitive currents in different human mammary epithelial normal and cancerous cells. *Biochim. Biophys Acta* 1667:190–199.

Roussellea A V, Heymann D (2001) Osteoclastic acidification pathways during bone resorption. *Bone* 30(4):533-540.

Russell RG (2003). Pathogenesis of osteoporosis. (In: *Rheumatology*. Hochberg MC, Silman AJ, Smolen SJ, Weinblatt ME, Weisman MH, editor. Mosby) New York. pp. 2075–2147.

Russell RG, Espina B, Hulley P (2006). Bone biology and the pathogenesis of osteoporosis. *Curr Opin Rheumatol.*18(Suppl1):S3–S10.

Ruttiger L, Sausbier M, Zimmermann U, Winter H, Braig C, Engel J, Knirsch M, Arntz C, Langer P, Hirt B, Mu¨ller M, Kopschall I, Pfister M, Munkner S, Rohbock K, Pfaff I, Rusch A, Ruth P, Knipper M (2004) Deletion of the Ca-activated potassium (BK) β-subunit but not the BK_1-subunit leads to progressive hearing loss. *Proc Natl Acad Sci USA* 101: 12922–12927.

Rybalchenko V, Prevarskaya N, Van Coppenolle F, Legrand G, Lemonnier L, Le Bourhis X, Skryma R. (2001) Verapamil inhibits proliferation of LNCaP human prostate cancer cells influencing K+ channel gating. *Mol Pharmacol.* 59(6):1376-87.

Saito M, Nelson C, Salkoff L, Lingle CJ (1997). A cysteine-rich domain defined by a novel exon in a Slo variant in rat adrenal chromaffin cells and PC12 cells. *J Biol Chem* 272:11710–11717

Sampson, H. W. (1998). Alcohol's harmful effects on bone. *Alcohol Health Res World* 22(3): 190-4.

Sampson, HW., Hebert VA., Booe HL and Champney TH (1998). Effect of alcohol consumption on adult and aged bone: composition, morphology, and hormone levels of a rat animal model. *Alcohol Clin Exp Res* 22(8): 1746-1753.

Sausbier U, Dullin C, Missbach-Guentner J, Kabagema C, Flockerzie K, Kuscher GM, Stuehmer W, Neuhuber W, Ruth P, Alves F, Sausbier M.,(2011). Osteopenia Due to enhanced cathepsin K release by BK channel ablation in osteoclasts. *PLoS ONE:* 6 e21168.

Sausbier, M., Hu, H., Arntz, C., Feil, S., Kamm, S., Adelsberger, H., Sausbier, U., Sailer, C. A., Feil, R., Hofmann, F., *et al.* (2004) Cerebellar ataxia and Purkinje cell dysfunction caused by Ca2+-activated K+ channel deficiency. *Proc. Natl. Acad. Sci. USA* 101, 9474–9478.

Schnitzler, C. M. and Solomon L. (1984). Bone changes after alcohol abuse. *S Afr Med J* 66(19): 730-734.

Schubert R, Nelson MT. *(*2001). Protein kinases: tuners of the BKCa channel in smooth muscle. *Trends Pharmacol Sci.*22:505–512.

Scornik FS, Codina J, Birnbaumer L, Toro L.(1993). Modulation of coronary smooth muscle K_{Ca} channels by $G_{s\alpha}$ independent of phosphorylation by protein kinase A. *American Journal of Physiology.* 265:C708–713.

Shieh, C. C., M. Coghlan (2000). Potassium channels: molecular defects, diseases, and therapeutic opportunities. *Pharmacol Rev* 52(4): 557-94.

Siemer, C. and S. Grissmer (1999). MaxiK channels: Molecular structure, function, and tissue distribution. *Perspectives in Drug Discovery and Design* 16: 155-165.

Skryma RN, Prevarskaya NB., Dufy-Barbe L., Odessa MF., Audin J. and Dufy B. (1997). Potassium conductance in the androgen-sensitive prostate cancer cell line, LNCaP: involvement in cell proliferation. *Prostate.* 33:112–122.

Stein GS, Lian JB. Molecular mechanisms mediating proliferation/differentiation interrelationships during progressive development of the osteoblast phenotype. Endocr Rev. 1993;14:424–442.

Steinert M, and Grissmer S (1997). Novel Activation Stimulus of Chloride Channels by Potassium in Human Osteoblasts and Human Leukaemic T-Lymphocytes. *J Physiol* 500: 653-660.

Stocker M, Pedarzani P. (2000). Differential distribution of three Ca^{2+}-activated K^+ channel subunits, SK1, SK2, and SK3, in the adult rat central nervous system. *Mol Cell Neurosci.*15:476–493.

Stocker M. (2004) Ca^{2+}-activated K^+ channels: molecular determinants and function of the SK family. *Nat. Rev. Neurosci*. 5:758-770.

Stumpff F, Strauss O, Boxberger M, Wiederholt M. Characterization of maxi-K-channel in bovine trabecular meshwork and their activation by cyclic guanosine monophosphate. *Invest Ophthalmol Vis Sci* 1997; 38:1883–1892.

Suzuki T., Takimoto K. (2004). Selective expression of HERG and Kv2 channels influences proliferation of uterine cancer cells. *Int. J Oncol*. 25:153–159.

Tammaro P, Smith AL, Hutchings SR, and Smirnov SV (2004) Pharmacological evidence for a key role of voltage-gated K+ channels in the function of rat aortic smooth muscle cells. *Br J Pharmacol* 143: 303-317.

Tanaka M, Sasaki Y, Hukui T, Kyotani J, Hayashi S, Hamada K, Kimura Y, Ukai Y, Kitano M and Kimura K (1998). A novel pyrrole derivative, NS-8, activates the Ca21-sensitive K1 channels and suppresses micturition reflex in rats. *J Urol* 159 (suppl):21.

Toro L, Wallner M, Meera P, Tanaka Y. Maxi-Kca, (1998). A unique member of the voltage-gated K channel superfamily. *News Physiol Sci.* 13:112–7.

Toro L, Alioua A, Lu R, Garcia-Valdes J, Zarei MM, Nishimaru K, Eghbali M, and Stefani E. (2005) Ca^{2+}-activated voltage dependent K^+ channels. In: *Ion Channels in the Pulmonary Vasculature. Lung Biology in Health and Disease.* Vol 197. J. X.-J. Yuan, ed. Taylor and Francis Group. Boca Raton, FL. Chapter 12, pp. 237-256.

Tseng-Crank J, Foster CD, Krause JD, Mertz R, Godinot N, Di Chiara TJ, and Reinhart PH (1994). Cloning, expression and distribution of functionally distinct Ca^{2+}-activated K^{+} channel isoforms from human brain. *Neuron* 13: 315-1330.

Valverde, M.A., P. Rojas, J. Amigo, D. Cosmelli, P. Orio, M.I. Bahamonde, G.E. Mann, C. Vergara, and R. Latorre. (1999). Acute activation of Maxi-K channels (hSlo) by estradiol binding to the β subunit. *Science.* 285:1929–1931.

Wallner, M., Meera, P., and Toro, L. (1996) Determinant for beta-subunit regulation in high-conductance voltage-activated and Ca(2+)-sensitive K+ channels: an additional transmembrane region at the N terminus. *Proc Natl Acad Sci U S A* 93: 14922– 14927.

Walz W. (2002) Patch-Clamp Analysis advanced techniques. *Neuromethods*. 38.

Wang G, and Lemos JR (1992). Tetrandrine blocks a slow, large-conductance, Ca^{2+}-activated potassium channel besides inhibiting a non-inactivating Ca^{2+} current in isolated nerve terminals of the rat neurohypophysis. *Pflügers Arch* 421: 558-565.

Wang G., Lemos J R., Ladecola C. (2004) Herbal alkaloid tetrandrine: from an ion channel blocker to inhibitor of tumor proliferation. *TIPS.* 25 (3): 120-123.

Wang WH, Geibel J, and Giebisch G. (1993). Mechanism of apical K^{+} channel modulation in principal renal tubule cells. Effect of inhibition of basolateral Na^{+}-K^{+}-ATPase. *J Gen Physiol* 101: 673–694.

Wang, G. and J. R. Lemos (1995). Tetrandrine: a new ligand to block voltage-dependent Ca2+ and Ca(+)-activated K+ channels. *Life Sci* 56(5): 295-306.

Wann KT, Henney N, Prajerová I, Boolaky UV, and Evans BAJ (2004). Single channels in human osteoblast-like cells. *J Physiol* 555P, PC59.

Wann KT, Henney N, Prajerová I, Boolaky UV, and Evans BAJ (2004b). Human osteoblast-like cells have high density maxi-K channels. *J Bone Miner Res* 19:1051.

Wann KT, Henney N, Prajerová I, Boolaky UV, Evans BAJ (2004a) Single channels in human osteoblast-like cells. *J Physiol* 555P*:* PC59.

Wann, KT and Richards, CD (1994). Properties of single calcium-activated potassium channels of large conductance in rat hippocampal neurons in culture. *Eur J Neurosci* 6: 607-617.

Webster SM, Del Camino D, Dekker JP, Yellen G (2004) Intracellular gate opening inShaker K+ channels defined by high-affinity metal bridges. *Nature* 428:864–868.

Wellman GC & Nelson MT (2003). Signaling between SR and plasma membrane in smooth muscle: sparks and the activation of Ca2+-sensitive ion channels. *Call Calcium* 34, 211–229.

Wellman, GC., Bonev AD. Nelon MT., Brayden JE. (1996). Gender differences in coronary artery diameter involve estrogen, nitric oxide, and Ca(2+)-dependent K+ channels. *Circ Res* 79(5): 1024-1030.

Weskamp M, Seidl W, and Grissmer S (2000). Characterisation of the increase in $[Ca^{2+}]_i$ during hypotonic shock and the involvement of Ca^{2+}-activated K^+ Channels in the regulatory volume decrease in human osteoblast-like cells. *J Membr Biol* 178: 11-20.

Wiltink, A., Nijweide PJ., Scheenen WJ., Ypey DL., Van Duijn B. (1995). Cell membrane stretch in osteoclasts triggers a self-reinforcing Ca2+ entry pathway. *Pflugers Arch* 429(5): 663-71.

Wolfart J., Neuhoff H., Franz O., Roeper J. (2001). Differential expression of the small-conductance, calcium-activated potassium channel SK3 is critical for pacemaker control in dopaminergic midbrain neurons. *J. Neurosci.*21:3443–3456.

Wolfram Kuhlmann C.R., Wiebke L.D., Schaefer C.A., Kerstin M.A., Backenkohler U., Neumann T., Tillmanns H., Erdogan A. (2004). Lysophosphatidylcholine-induced modulation of Ca^{2+}-activated K^+channels contributes to ROS-dependent proliferation of cultured human endothelial cells. *J Mol. Cell Cardiol*. 36:675–682

Wonderlin WF, and Strobl JS (1996). Potassium channels, proliferation and G1 progression. *J Membr Biol* 154: 91-107.

Wu SN (2003). Large conductance Ca^{2+}-activated K^+ channels: physiological role and pharmacology. *Curr Med Chem* 10: 649-661.

Wu, SN, Hwang, TL, Jan, CR, and Tseng, CJ. (1997). Ionic mechanisms of tetrandrine in cultured rat aortic smooth muscle cells. *Eur J Pharm* 327(2), 233-238.

Wu, SN., Li, HF. Lo YC. (2000) Characterization of tetrandrine-induced inhibition of large-conductance calcium-activated potassium channels in a human endothelial cell line (HUV-EC-C). *J Pharmacol Exp Ther* 292(1): 188-95.

Xia XM, Fakler B, Rivard A, Wayman G, Johnson-Pais T, Keen JE (1998). Mechanism of calcium gating in small-conductance calcium-activated potassium channels. *Nature* 395:503–507.

Yao X, Kwan HY. (1999). Activity of voltage-gated K^+ channels is associated with cell proliferation and Ca^{2+} influx in carcinoma cells of colon cancer. *Life Sci.* 65:55–62.

Yellen, G. (1984). Ionic permeation and blockade in Ca2+-activated K+ channels of bovine chromaffin cells. *J Gen Physiol* 84(2): 157-86.

Yellowley CE, Hancox JC, Skerry TM, and Levi AJ. (1998). Whole-cell membrane currents from human osteoblast-like cells. *Calcif Tissue Int* 62: 122-132.

Zanello LP, and Norman A (2006). 1α, $25(OH)_2$ Vitamin D_3 actions on ion channels in osteoblasts. *Steroids* 71: 291-297.

Zhou, Y., Morais-Cabral J. H., Kaufman A., and MacKinnon R. (2001). Chemistry of ion coordination and hydration revealed by a K+ channel-Fab complex at 2.0 A resolution. *Nature.* 414:43–48.